

Compensatory eye movements in mice

Compensatoire oogbewegingen van muizen

Proefschrift

ter verkrijging van de graad van doctor aan de
Erasmus Universiteit Rotterdam
op gezag van de Rector Magnificus
Prof.dr.ir. J.H. van Bommel
en volgens besluit van het College voor Promoties.

De openbare verdediging zal plaatsvinden op
woensdag 11 september 2002 om 13:45 uur
door

Adriaan Martijn van Alphen

Geboren te Delft.

Promotiecomissie

Promotor: Prof.dr. C.I. de Zeeuw

Overige leden: Prof.dr. J. Voogd
Prof.dr. P.A. Sillevius Smitt
Dr. M.A. Frens

Copromotor: Dr. J.S. Stahl

TABLE OF CONTENTS

H1 Introduction

1.1 Considerations on genetic techniques	7
1.2 Differences between mice and man	9
1.3 Compensatory ocular reflexes	11
1.3.1 Vestibulo-Ocular Reflex	11
1.3.2 VOR adaptation	14
1.3.3 Optokinetic Reflex	21
1.3.4 OKR adaptation	22
1.4 Contribution of this thesis	23

H2 Characterization of compensatory ocular reflexes in C57BL/6 mice

2.1 The dynamic characteristics of the mouse horizontal vestibulo-ocular and optokinetic response	37
2.2 A comparison of video and magnetic search coil recordings of mouse eye movements	55

H3 Use of eye movement recordings in the evaluation of peripheral vestibular pathology

3.1 Circling behavior in the Ecl-mouse is caused by lateral semicircular canal defects	75
3.2 Origin of vestibular dysfunction in Usher syndrome type 1B	91

H4 Cerebellar contribution to plasticity in the oculomotor system

4.1 Motor performance and motor learning in Lurcher mice	107
4.2 Cerebellar LTD facilitates but is not essential for long-term adaptation of the vestibulo ocular reflex	121
4.3 Vestibular compensation does not rely on LTD of the parallel fiber to Purkinje cell synapse	133

H5 General discussion

5.1 Technical considerations	150
5.2 The use of eye movement recordings as a tool to assess vestibular function	151
5.3 Plasticity in the oculomotor system	151
5.3.1 VOR adaptation	152
5.3.2 Vestibular compensation	153
5.3.3 OKR adaptation	154

Summary	159
Samenvatting	161
List of Publications	165
Curriculum Vitae	167
Dankwoord	169

CHAPTER 1
GENERAL INTRODUCTION

Introduction

This thesis will address the generation of compensatory eye movements in naturally mutated or genetically modified mice. The reason for generating compensatory eye movements is solely related to the requirements for good vision. In a subject moving through its environment the projection of visual surround would slip across the retina and retinal slip of more than only a few degrees per second would cause blurring of the projected image and reduce visual acuity (Westheimer and McKee, 1975). Compensatory eye movements are therefore generated to assure that visual projections on the retina remain at approximately the same retinal coordinates, thereby preserving a stable image despite perturbations due to self-generated or imposed movement of the head.

Because of its relative simplicity the oculomotor system, which encompasses the entire transformation from sensory input to the generation of compensatory eye movements, has served as a particularly useful model for physiologists who try to understand how the brain controls movement. The repertoire of possible movements in the oculomotor system is limited to those of the eyeball in its socket, which constitutes a single joint on which three pairs of extra-ocular muscles exert their force. Each pair of muscles affects movement around one of three orthogonal rotational axes and due to a fairly constant mechanical load on the eye muscles no stretch reflex is needed. This relative simplicity of the oculomotor system and the fact that both behavioral output and sensory input can be readily measured makes it amenable to detailed quantitative analysis.

Analysis of the oculomotor system may be of particular interest for cerebellar physiologists. A phylogenetically older part of the cerebellum, called the vestibulo cerebellum, is intimately involved in control of compensatory ocular reflexes. In view of the extremely regular anatomical organization throughout the cerebellar cortex (Eccles et al., 1967), it is believed that the cerebellum may perform a general computation, which is similar for all its target systems (Marr, 1968; Albus, 1971). Understanding cerebellar contribution to the control of eye movements may therefore lead to a more general comprehension of cerebellar role in other forms of motor behavior.

Ito (1984) recognized the use of three different experimental approaches in his effort to understand cerebellar function. 1) Dissection of the system to reveal the underlying structure, i.e. the anatomical organization of the system. 2) Correlation of neuronal activity to features of sensory input or behavioral output. Such correlation of activity revealed how information is coded in the brain. 3) Destruction of neuronal tissue to understand what functional role had been played by the damaged area. In his work Ito already comments on the need for improved techniques to make more refined lesions. In recent years the field of genetics has added such a refined technique to the existing repertoire by introducing the possibility of genetically altering single proteins. The combination of novel genetic techniques and existing physiological methodology may enlighten our understanding of how neurons process information and hence how sensory to motor transformation is achieved in the brain. The present work tries to apply this genetic technique to the oculomotor system by describing the effect of certain genetic mutations and interventions on oculomotor behavior of mice.

1.1 Considerations on genetic techniques

Current genetic techniques often attempt to investigate gene function by creating transgenic or knockout mice. In transgenic animals artificial DNA is introduced into a fertilized oocyte. Incorporation of the introduced DNA into the genome will lead to expression of the transgene in the adult animal. Although this technique is feasible in different species (Brink et al., 2000; Fan et al., 2001) application is largely limited to mice, because of their short gestation time and the availability of inbred strains that are genetically well characterized. The generation of a 'null' mutant or 'knockout' animals means that a targeted gene is completely deleted from the genome. The protein that this gene coded for will therefore no longer be expressed in any cell of the mutant animal. Knocking out a gene may cause functional or behavioral changes that could reveal, under certain assumptions, the contribution of that gene in a normal animal.

When working with genetically manipulated animals, the realization of several caveats is important for accurate interpretation of the data. Clearly a 'null' mutant or transgenic organism does not only suffer the influence of the deleted or altered gene product but might also possess a number of developmental, physiological or behavioral alterations that attempt to compensate for or are secondary to the genetic intervention. One may therefore expect physiological changes that are not necessarily indicative for the function of the targeted gene. A combined effort from different disciplines is therefore necessary to tease out differential effects that are due to the gene in question. Fortunately, genetic techniques have become more specific both spatially and temporally and it is possible to disrupt gene-function not in all cells of the organism but only in selective cell types and sometimes even at controlled moments in time. Such specificity has become possible through the discovery of growing numbers of tissue specific enhancers. Enhancers are sequences of DNA that control transcription of a gene and therefore expression of its protein. Many genes are expressed selectively in the central nervous system and expression of some of these genes is limited to certain neuronal subtypes. For instance the L7 protein is almost exclusively expressed in cerebellar Purkinje cells (Oberdick et al., 1990). Hence the L7-promotor/enhancer will be selectively activated in Purkinje cells. By introducing a gene of choice, coupled to the L7 promotor/enhancer, into the genome, this gene will be selectively expressed in Purkinje neurons of the cerebellum (Oberdick et al., 1990; De Zeeuw et al., 1998). Unfortunately, the effect of the transgene will be present during development starting from the moment the promotor is normally switched on by the cell. Any developmental changes caused by introduction of the transgene may be interesting in their own right but if one wants to assess involvement of the targeted protein in signal processing of the adult brain developmental aberrations will obviously hamper a straight forward interpretation. Developmental considerations will be less of a problem if the promotor switches on relatively late in development, like the L7 gene (E15), but more accurate control of gene expression would obviously be preferable. Such control has recently become possible with the use of inducible gene promotors like the tetracycline-controlled transactivator system. In this particular system the administration of tetracycline or one of its analogues typically acts to inhibit expression of a transgene (Gossen and Bujard, 1992; Malleret et al., 2001) but can also be made to activate it (Gossen et al., 1995; Mansuy et al., 1998). Such a system coupled to a cell specific promotor would allow accurate spatial and temporal control of gene expression. An important added advantage of temporal control

of gene expression is the fact that statistical analysis can be performed in paired fashion, i.e. before and after the gene was switched on, thereby greatly improving statistical power of the experiment.

The genetic background of animals in control and experimental groups deserves some special attention because it may have repercussions for interpretation of ones findings. Many different strains of mice are available and it is obvious that evaluation of experimental results should be with respect to animals of the same strain. Animals from the same litter that do not carry or are heterozygous for the altered gene are therefore often used as control animals. Using littermate animals has the added advantage that aside from genetic considerations, environmental influences during life are close to the same in control and experimental group. However, even with the use of littermates for controls, problems can arise when there is polymorphism in the genetic background of the animals. Polymorphism arises because donor strains from which embryonic stem cells were obtained for gene targeting were different from the strain that was subsequently used to create F2 generation offspring. The main reason to use a different strain for breeding than was used to obtain embryonic stem cells lies with the fact that strains used for the production of embryonic stem cells, e.g. 129 strain, often perform very poorly in all sorts of behavioral tasks (Crowley et al., 1997; Balogh et al., 1999; Dockstader and van der Kooy, 2001). The use of such mixed F2 generation offspring warrants three important considerations. Although genetic background may percentage-wise be equal in all offspring the heritage of individual genes is quite different from animal to animal. Control animals therefore differ from their genetically altered littermates in many more than just the single, targeted gene. Second the polymorphic background may have consequences for the expression of any effect due to the target gene. When for instance deletion of gene α may lead to activation of gene β and gene β is coded by either allele b (from stem cell) or B (from the breeding strain), then the phenotypical presentation of deleting gene α may depend on whether allele b or B was present. Both above considerations will fortunately not lead to systematic differences between control and experimental animals because the distribution of alleles is randomly assigned. They will lead to a larger variation within each statistical group and thus make a differential phenotype due to the genetic alteration harder to detect. The problem can be easily overcome by increasing the number of animals measured to compensate for the reduced statistical power of the test. However, the number of animals needed to prove small differences between groups can become impractically large. Rather than increasing the number of tested animals it may be more advantageous to reduce the genetic variation by continued breeding of the animals with the animals of the desired background. Unfortunately mice would be for 99% genetically identical after 12 backcrosses, which is about two years work (Festing, 1992).

A more serious complication, which arises when the background of embryonic stem cells is different from the background used for breeding, is referred to as genetic linkage. Although by sufficient back crossing with the desired strain animals become more identical with each cross, the genomic area surrounding the targeted gene will contain DNA from the original stem cell. This flanking DNA is likely to contain several genes and when stem cells were obtained from a 129-background these genes may possess a substantial number of mutations (Lathe, 1996). Selection of mutant mice thus not only leads to selection of the targeted gene but also to selection of these genes

flanking the targeted one. It is difficult to control for the effect of genetic linkage other than to use the same strain for breeding as one has obtained stem cells from. Alternatives to control for the problem of genetic linkage do however exist.

When the mutant concerns a 'null' mutation, it is possible to create a so-called 'rescue' mouse. A 'rescue' is a 'null' mutant in which the missing gene is reintroduced into the genome as a transgene to restore expression of the missing protein. If substitution of the protein in the 'null' mutant leads to recovery from the phenotype, it is a strong argument that the phenotype was due to the primary alteration and not to any of the above mentioned concerns. In case of a transgenic mouse the technique of creating a rescue is impossible since no gene had been deleted. However, the creation of different lines of transgenic animals solves the problem. When a transgene is introduced into the genome its insertion site is randomly determined. Repeating the process in several times in different oocytes will lead to insertion of the transgene at different sites in each attempt. When the phenotype of all strains is identical it must be caused by the introduced transgene, since the genes flanking the insertion site are obviously different in each strain. Another solution is possible when a genetic marker is available close to the target genomic region. Control animals could then be selected to possess the genomic marker but not the genetic alteration. Selection of the marker would ensure that control animals possess the same genomic region flanking the target locus as do experimental animals but without the genetic alteration. Hypothetically, one could even use gene targeting techniques to insert such a marker next to the gene of interest without disrupting its function, thus creating a 'knock-in' mouse (Gerlai, 1996). A third option that will not suffer from this problem of genetic linkage is again the use of aforementioned inducible genetic techniques, which would allow the experimenter to evaluate contribution of the gene within one animal and thus with an identical genetic background.

1.2 Differences between mice and man

The human retina contains a specialized central region, called the fovea, in which photoreceptors are densely packed and which covers about 1° of the visual field. The organization of the fovea permits vision with high spatial resolution. High resolution would be useless however, unless the fovea could be directed to areas of interest in the visual world. In humans five types of eye movement systems therefore exist that put the fovea on target and keep it there (Leigh and Zee, 1991). Saccadic eye movements shift the fovea rapidly to a target in the periphery. Smooth pursuit eye movements keep the fovea locked on target when it moves across space. Vergence movements change the angle between the eyes to place a visual target on the fovea of both eyes. Vestibulo-ocular eye movements (VOR) stabilize the full visual field on the retina by generating eye movements that compensate for perturbations of the head. Optokinetic eye movements (OKR) also serve to stabilize the full visual field but are driven by visual motion. Of these reflexes the first three are meant to link a visual target to the fovea while the latter two are meant to prevent external perturbations, which are generally caused by movement of the animal through its environment, from causing retinal slip and therefore diminishing visual acuity (Westheimer and McKee, 1975).

Considerable anatomical differences exist between the murine and human eye. These differences lead to less stringent requirements for the mouse oculomotor system

than for the human system. Apart from the diameter of a mouse eye, which is approximately an order of magnitude smaller, the distribution of photoreceptor cells across the retina is different. Contrary to human retina, rod receptor cells are distributed almost homogeneously across the mouse retina. Rods are interspersed with cone type photoreceptors, which are distributed in a centro-peripheral gradient that decreases in density from ± 5000 cells/mm² centrally to 1000 cells/mm² in the periphery (Juliusson et al., 1994; Szél et al., 2000). This centro-peripheral organization of cone type photoreceptors is mimicked by a distribution of retinal ganglion cells (Dräger and Olsen, 1981), which provide the output from the retina to the brain. A qualitatively similar distribution of retinal ganglion cells has been found in several other species including hamster, rat and rabbit (Tiao and Blakemore, 1976; Fukuda, 1977; Provis, 1979). In the rabbit organization of retinal ganglion cells differs slightly from that in mouse or rat in that radial distribution of retinal ganglion cells is more ellipsoid with a long axis in the nasal temporal direction, creating what is known as the 'visual streak' (Hughes, 1971; Vaney and Hughes, 1976). Although spatial distribution of cone receptor cells and ganglion cells resembles an area centralis, this specialization is nowhere near as advanced as that of primates or cats and hence the mouse is referred to as an afoveate animal.

The absence of a fovea reduces the need for highly accurate, goal directed eye movements like smooth pursuit or saccades. This is nicely reflected in the eye movements of rabbits, which have only a limited response to targets that move across a stationary background (Collewijn, 1981) and scarcely show reorienting gaze shifts when the head is fixed (Collewijn, 1977; Fuller, 1980). Ocular vergence movements have been observed when it concerns the acquisition of food in a freely moving rabbit (Zuidam and Collewijn, 1979) or in combination with compensatory ocular reflexes (Maruta et al., 2001; Rodriguez et al., 2001). The persistence of rudimentary forms of these three types of eye movements (pursuit, saccades, and vergence) despite an absent fovea may be related to requirements for binocular vision. Reorienting eye-head saccades may direct a target to the binocular retinal zone and for a correct correspondence between the retinal projections of each eye an appropriate vergence movement may be required. Limited pursuit capabilities may serve to keep the binocular zone locked to the target. In contrast to saccade, vergence or pursuit movements, compensatory ocular reflexes are easily elicited in afoveate animals. Because of the robustness of VOR and OKR they are often considered to be basic oculomotor reflexes on which more accurate systems required for voluntary gaze control are superimposed. Surgical destruction of cerebral input to the oculomotor system in primates eliminated voluntary eye movements and indeed revealed optokinetic eye movements that were qualitatively similar to those of afoveate animals (Zee et al., 1987).

In the mouse full body rotation in the dark or rotation of a full field visual scene clearly elicits compensatory eye movements (Mitchiner et al., 1976; Balkema et al., 1981; Balkema et al., 1984) and the oculomotor system of this animal can therefore be used as a model control system to study brain function. With the use of gene-targeting techniques neural signal processing can be delicately altered and quantitative analysis of OKR and VOR may prove ideal to accurately quantify the effects of genetic intervention at a behavioral level.

1.3 Compensatory ocular reflexes

To generate compensatory ocular reflexes, the brain interprets information obtained from the retina and labyrinth and translates this information into appropriate command signals to drive the eye muscles and keep retinal slip to a minimum. We aim to use genetic techniques to elucidate how the brain achieves this task, by altering gene expression in neurons that are involved in oculomotor processing. In these mutant mice we hope to find changes in the input/output relation of oculomotor reflexes that will allow us to deduce selective contribution of the part interfered with. An at least superficial understanding of what subsystems are involved in oculomotor processing is therefore required to interpret or even discern alterations in compensatory reflexes due to selective mutations.

1.3.1 Vestibulo-Ocular Reflex

VOR generates eye movements in response to movement of the head. Signals related to head movement are derived from the labyrinth. The labyrinth is made up of several cavities inside the petrosal bone, which build the scaffold for the epithelial semicircular ducts, referred to as membranous Labyrinth. Specialized areas in the membranous labyrinth contain receptor cells that translate movement into neuronal signals. The vestibular organ includes two types of transducers: the semicircular canals and otolith organs. Three semi circular canals detect head angular acceleration while two otolith organs behave as linear accelerometers measuring gravito-inertial force. Detection of linear and angular acceleration is analogous and is achieved by specialized cells, called hair cells. Hair cells are anatomically polarized and made up of a basilar and apical membrane. The apical side of the hair cell is differentiated into stereocilia and a single kinocilium. All stereocilia are located to one side of the kinocilium. They vary in length with the longest cilia close to the kinocilium and progressively smaller ones at larger distances from the kinocilium. Anatomical polarization of the cilia has functional implications because movement of the stereocilia towards the kinocilium leads to an increase in neuro-transmitter release at the basilar side of the hair cell while movement away from the kinocilium reduces the amount of transmitter release.

Hair cells that are sensitive to linear acceleration are located in the maculae of utricle and saccule. The cilia of these macular hair cells extend into a membrane, which is embedded with calcium-carbonate crystals, called the otolithic membrane. Linear acceleration due to translational movement or reorientation of the head with respect to gravity leads to displacement of the otolithic membrane relative to the hair cells and will cause a deviation of cilia. Hair cells that detect angular acceleration are located at the base of the semicircular canal where this structure widens into the ampulla. Hair cells are located within the crista ampullaris and their cilia are embedded in a gelatinous membrane called cupula, which spans the inside of the ampulla. Angular acceleration of the head will lead to movement of endolymph relative to the canal wall and will cause a deviation of the cupular membrane. Deviation of the cupular membrane will in turn cause a deviation in cilia and will depending on the direction of movement either excite or inhibit hair cells.

The relation between angular acceleration and deflection of the cupula was found to depend on inertia and viscosity of the endolymphatic fluid and on elastic properties of the cupular membrane. These mechanical properties made the semicircular canals respond as a low-pass filter with respect to angular acceleration (Steinhausen, 1933; Fernandez and Goldberg, 1971; Precht, 1978). The response of the canals was largely governed by two time-constants, which were roughly estimated to be 6 and 0.003 sec in humans and monkey (Wilson and Melvill Jones, 1979). However, a single pole low-pass filter with an average time constant between 2 and 4 sec described vestibular afferent activity in the bandwidth from 0.01 to 1 Hz accurately enough in the rat (Curthoys, 1982). Depending on the frequency content of the stimulus and the average time constant of primary afferents in a species, deflection of the cupula and thus neuronal discharge rate will not reflect angular head acceleration, but rather be proportional to angular velocity of the head making the system respond as a high-pass filter with respect to stimulus velocity. The mechanical properties of the canal are therefore said to constitute a step of mathematical integration from angular head acceleration to head velocity within a limited frequency bandwidth (Skavenski and Robinson, 1973).

Velocity to position neural integrator

The eyes are moved by neural commands that code both eye velocity and eye position. This combination of eye velocity and position coding in the command to the extra ocular muscles is necessary to compensate for restrictions imposed on the eye movements by mechanical properties of orbital tissues (Robinson, 1964; Robinson, 1965; Zuber, 1968). Mechanical properties of the orbit include viscous drag of the eyeball, which slows it down, and elastic forces of connective tissue, which pull the eye to a null position in the orbit where all passive and active forces balance out. To generate the position command needed to drive the eye muscles, velocity encoded output from the semi-circular canals requires additional processing in the form of a second step of integration (Carpenter, 1972; Skavenski and Robinson, 1973). The neural network that provides additional integration for control of horizontal eye movements is located in the nucleus prepositus hypoglossi and adjacent vestibular nucleus (Cannon and Robinson, 1987; Cheron and Godaux, 1987; Kaneko, 1992; Mettens et al., 1994), while the interstitial nucleus of Cajal serves the same role for vertical and torsional eye movements (Crawford et al., 1991; Fukushima et al., 1992). Integration of pre-motor velocity signals by these neural systems is not perfect, meaning that the velocity-to-position neural integrator is inherently leaky. Leakiness of the integrator can be shown as a slow exponential drift of the eye from an acquired eccentric position back to its null position when a subject is placed in the dark. In healthy human subjects this exponential drift of the eye is governed by a time constant of 20 sec, meaning that after 20 seconds the eye has drifted 63% of the distance from its eccentric position back to the null position (Becker and Klein, 1973). Similar values for the time constant of neural integration have also been found for cat and monkey (Robinson, 1974; Cannon and Robinson, 1987). Although the basic circuitry for neuronal integration is located in the brainstem, cerebellar function is required for optimal performance. Lesions of the cerebellum lead to a reduction of integrator time constant from 20 sec to 3 sec in the cat (Cannon and Robinson, 1987) and the cerebellar cortical network seems to improve function of an inherently leaky

integrator by increasing its time constant (Westheimer and Blair, 1973; Robinson, 1974; Westheimer and Blair, 1974; Zee et al., 1981). The flocculus was implicated as the cerebellar area that contributed to neural integration because lesion of this area caused post-saccadic drift and impaired gaze holding in cat, monkey and rat (Takemori and Cohen, 1974; Zee et al., 1981; Hess et al., 1988). However, recordings from vestibular neurons in the rabbit that discriminated between those neurons that received input from the flocculus and those neurons that did not, revealed no higher sensitivity of floccular target neurons to eye position rendering it unlikely that the flocculus was an important conduit for the neural integrator in the rabbit (De Zeeuw et al., 1995; Stahl and Simpson, 1995).

The time constant that determines leakiness of the neural integrator is probably not fixed but can be modified to suit requirements for accurate vision (Tiliket et al., 1994; Kramer et al., 1995). In a special training paradigm using sinusoidal vestibular stimuli Tiliket et al. (1994) were able to specifically change the phase of the eye movement with respect to head movement in human subjects. Secondary to changes in VOR phase, gaze-holding ability in these subjects had been altered and a post-saccadic drift was observed. Depending on whether training was aimed at inducing a phase lag or a phase lead post-saccadic drift was directed either centrifugally or centripetally. It was hypothesized that changes in VOR phase were achieved by changing the time constant of the neural velocity to position integrator. Since the neural velocity to position integrator is common for all eye movements (Godaux and Cheron, 1993; Chu and Kaneko, 1995), concomitant changes were observed in the aftermath of saccades.

Velocity storage

Investigating the VOR of the cat and monkey revealed that given the time constant of the semi-circular canals (Fernandez and Goldberg, 1971) and the assumption of a perfect neural integrator, phase of VOR output in response to sinusoidal vestibular stimulation could not be accurately predicted (Skavenski and Robinson, 1973; Robinson, 1976). In addition decay of eye velocity in response to a step in head velocity and recordings from secondary vestibular neurons indicated a dominant time constant for the VOR that was much larger than expected based on measurement from primary canal afferents (Buettner et al., 1978; Precht, 1978; Raphan et al., 1979). An additional neural mechanism had to be present that could store the canal signal and provide an output related to head velocity when such a signal could no longer be reliably obtained from the primary afferents. The mechanism was labeled 'velocity storage' (Skavenski and Robinson, 1973; Cohen et al., 1977) and served to increase the apparent time constant of the semicircular canals from 6 sec to 18 seconds in the monkey (Raphan et al., 1979) and from 4 to 15 sec in the cat (Robinson, 1976). Like the velocity to position integrator the velocity storage network is shared between optokinetic and vestibular reflexes (Raphan et al., 1979; Demer and Robinson, 1983). Its output had actually already been recognized long ago in the form of 'optokinetic after nystagmus' (OKAN) (Ter Braak, 1936). OKAN is described as a persistence and gradual decrease of nystagmus when a stimulus, consisting of constant velocity, full field visual motion, is suddenly replaced by darkness. Some problems arose with the interpretation of velocity storage when it was investigated in the rabbit (Winterson et al., 1979; Collewijn et al., 1980). First, when the overall time constant of

the rabbit VOR was estimated from the gain and phase relation to sinusoidal stimuli at different frequencies, it was found to be around 3 sec (Collewijn et al., 1980). Such a value was very close to what could be expected for the canal time constant, meaning that velocity storage did not contribute to the rabbit VOR when it is elicited by sinusoidal stimuli. However, in response to steps in head velocity clear post- and per-rotatory nystagmus were observed the time course of which was considerably longer than that predicted from a 3 sec time constant. In addition, OKAN was readily elicited by constant velocity optokinetic stimulation, confirming the existence of storage in the rabbit (Winterson et al., 1979; Collewijn et al., 1980). Velocity storage in the rabbit proved to be of a linear rather than an exponential nature and upon closer examination of data obtained in cats and monkey Collewijn reached the conclusion that in these other animals velocity storage also often deviates from an exponential time-course (Collewijn, 1981). Despite this deviation of the velocity storage element from being a mathematically linear operator it is still considered as such, to simplify systematic analysis of the oculomotor system (Cohen et al., 1992).

The anatomical substrate for the velocity storage network is likely situated in the vestibular nucleus in regions of the superior vestibular nucleus and rostral areas of the medial vestibular nucleus (Uemura and Cohen, 1972, 1973; Waespe and Henn, 1977a, b; Reisine and Raphan, 1992). The cerebellar nodulus contributes to proper function of the storage mechanism by controlling its time constant, since lesions of the nodulus cause an increase in the time it takes to discharge the storage mechanism (Igarashi et al., 1975; Takemori and Suzuki, 1977; Hasegawa et al., 1994). Control of the nodulus over the velocity storage time constant proved to be adaptive (Waespe et al., 1983; Cohen et al., 1992) and repeated exposure to steps in head velocity, low frequency sinusoidal rotation or repeatedly eliciting OKAN resulted in a reduction of the velocity storage time constant (Baloh et al., 1982; Schmid and Jeannerod, 1985; Cohen et al., 1992; Dow and Anastasio, 1999). This adaptive mechanism was labeled 'habituation'. Habituation appears different from VOR adaptation (described below) since lesions of the cerebellar nodulus prevented habituation from occurring and abolished a previous habituation of the VOR (Cohen et al., 1992) while such lesions had no effect on adaptation of VOR gain (Nagao, 1983; Cohen et al., 1992).

1.3.2 VOR adaptation

The VOR functions without the benefit of immediate feedback, which means that the eye movements that this reflex generates are not sensed by the vestibular organs that provide its input. Due to its open-loop design control of the VOR is rendered sensitive to changes in its internal parameters, which can upset calibration of the reflex. It was early realized that for the VOR to maintain accuracy throughout life it should possess a mechanism through which it could remain properly calibrated. Vision provides that calibrating mechanism. Vision directly contributes to accuracy of the VOR by adding a visually driven eye movement command to the vestibular driven command. This combination of vestibular and optokinetic reflexes is labeled visually enhanced VOR (VVOR) and provides a more accurate oculomotor response over a wider range of stimulus properties than either of the two reflexes separately. In addition, VOR circuitry possesses a measure of plasticity that allows its internal parameters to be tuned by vision to appropriately scale

eye movement output to head movement input. Such long-term modifications to the VOR can be experimentally achieved by altering visual feedback that accompanies head rotation. Visual feedback can be altered by placing reversing prisms (Jones and Davies, 1976; Robinson, 1976; Mandl et al., 1981) or magnifying/reducing lenses (Miles and Eighmy, 1980; Collewijn et al., 1983) in front of the eyes, or by pairing imposed body rotation with motion of an optokinetic pattern (Ito et al., 1979; Harrison et al., 1986). After exposing the subject to the altered visual feedback the underlying vestibular reflex, when tested separately in the dark, will have changed in the proper direction to compensate for the altered visual input. When a subject is fitted with miniaturizing lenses gain of the VOR will decrease, compensating for the fact that visual motion associated with head movement has become slower than normal.

The use of forced vestibular rotation to modify VOR revealed that VOR adaptation was frequency specific. Training a subject at a single stimulus frequency induced changes in VOR gain that were largest at the stimulus frequency used for training (Collewijn and Grootendorst, 1979; Lisberger et al., 1983; Schairer and Bennett, 1986b; Khater et al., 1990). It therefore appears that VOR adaptation does not simply reflect a global change in parameters of the VOR, like changing a central gain element, but involves the storage and retrieval of a specific movement pattern that is derived from visual input (Collewijn, 1979).

Flocculus hypothesis

VOR adaptation reflects a form of associative learning, which in a more general form is often referred to as motor learning. Maintenance of the learned behavior requires the memory trace to be stored somewhere and for motor learning the cerebellum has been implicated to serve that role. Based on its anatomical connectivity the cerebellar flocculus is a good candidate to provide a site for memory storage in the VOR (Fig. 1). Mossy fiber input to the flocculus pathways arises largely from the vestibular nucleus (Langer et al., 1985; Voogd et al., 1996), while climbing fibers to the flocculus are known to carry visual signals (Maekawa and Simpson, 1972). The output from the flocculus, which is solely made up of inhibitory Purkinje neurons, projects back to neurons in the vestibular nucleus. The Flocculus is therefore anatomically placed as a side loop to direct vestibular pathways that mediate the VOR (Highstein, 1973) and receiving both visual and vestibular signals the flocculus would be ideally suited to modify vestibular signaling based on visual feedback (Ito, 1972). Should the flocculus serve such a function it would seem that lesions of this structure would somehow affect performance of the VOR. However, the contribution of floccular output to control of the VOR is unclear. Lesions of the flocculus were reported to cause a reduction of VOR gain (Keller and Precht, 1978; Ito et al., 1982a; Nagao, 1983), an increase in VOR gain (Robinson, 1976; Partsalis et al., 1995) or to have no effect on VOR gain at all (Barmack and Pettorossi, 1985). Reversible inactivation of the flocculus by local application of GABA or lidocaine did neither produce consistent results: causing a reduction of VOR gain in the rabbit (van Neerven et al., 1991), while having no effect on VOR gain in the goldfish (McElligott et al., 1998). However, one finding appears to be consistent across studies in which floccular function was blocked: impaired floccular function always resulted in an inability to adapt VOR gain in response to visuo-vestibular training

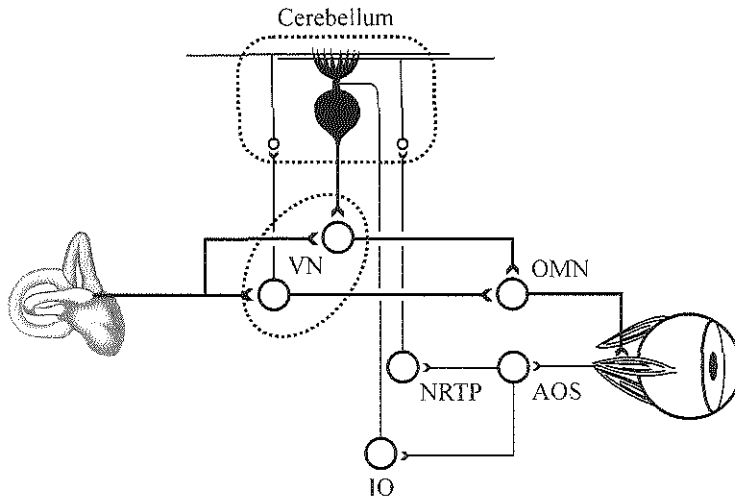


Figure 1: A schematic representation of the oculomotor pathways illustrate parallel placement of the flocculus to direct brainstem pathways that mediate the VOR. Primary vestibular afferents transmit information about head movement to the vestibular nucleus (VN). The vestibular nucleus relays this information to the cerebellar cortex via parallel fibers. Retinal slip, detected by the retina is processed by the accessory optic system (AOS) and inferior olive (IO) and is converted to a performance error signal to the Purkinje neurons via climbing fibers (Frens et al., 2001). Based on the error signal the Purkinje cell changes its contribution to floccular target neurons in the vestibular nucleus and thus acts to reduce retinal slip. OMN, oculomotor nuclei; NRTP, nucleus reticularis tegmentum pontis.

(Robinson, 1976; Zee et al., 1981; Ito et al., 1982a; Nagao, 1983; Lisberger et al., 1984; Schairer and Bennett, 1986b; McElligott et al., 1998). Intact floccular function is therefore required for VOR adaptation. Despite an unclear contribution of floccular output to the VOR in un-adapted animals, it does appear to fulfill a role as the initial storage site for a newly adapted VOR. Inactivation of the flocculus after visuo-vestibular training had been achieved returned VOR gain to its pre-training values in the goldfish and subsequent cessation of lidocaine application again restored the adapted VOR state (McElligott et al., 1998). This study reveals that at least initial storage of modifications to the VOR occurs in the flocculus. Whether the memory trace for the adapted VOR remains there in the long run is unclear in view of the variable results from the aforementioned lesion studies.

Models of cerebellar function (Marr, 1968; Albus, 1971) provided a basis for understanding how the flocculus could contribute to plasticity in the VOR (Fujita, 1982). In these models the mechanism underlying motor learning in general, and VOR adaptation specifically, was based on plasticity of the parallel fiber to Purkinje cell synapse. Although plasticity was first proposed to occur in the form of potentiation of synaptic transmission (LTP) (Marr, 1968) it was later thought to be exactly opposite: long term depression (LTD) (Albus, 1971). Single unit recordings of floccular Purkinje cells provided indirect evidence for LTD and showed that spiking activity of Purkinje neurons could indeed be depressed by pairing activation of vestibular mossy fibers to the

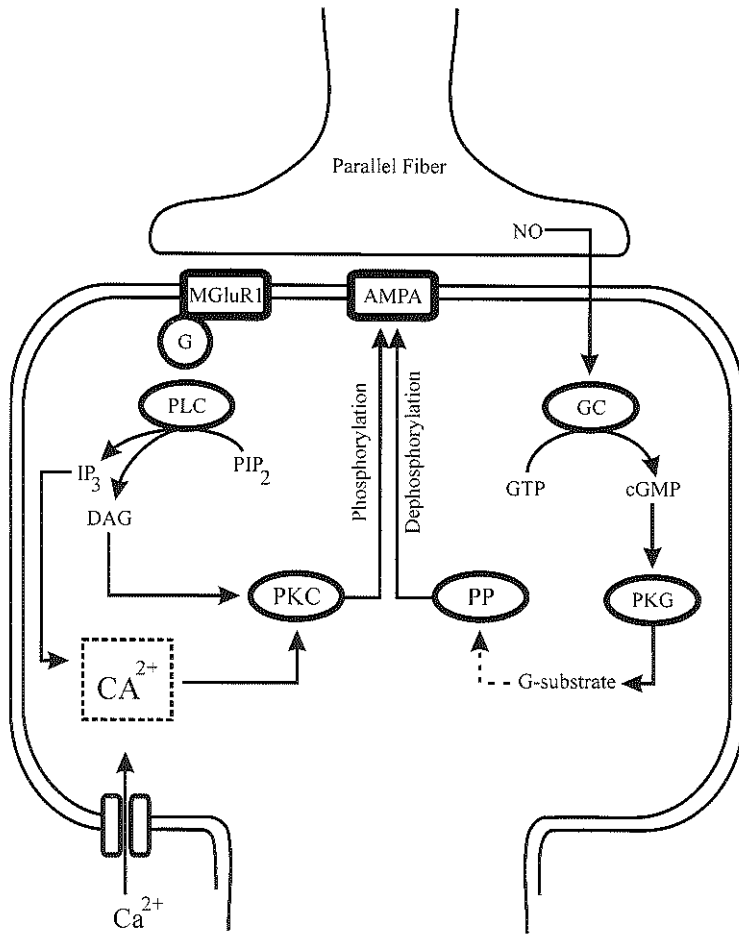


Figure 2: A simplified description of the main biochemical pathways underlying long-term depression of the parallel fiber to Purkinje cell synapse is depicted. Normal arrows represent activation while dotted arrows indicate inhibition. Phosphorylation of the AMPA receptor by PKC will cause internalization through clatherin mediated endocytosis and hence a reduction of synaptic efficacy. MgluR1, metabotropic glutamate receptor; G, g-protein; PLC, phospholipase C; PIP, phosphatidyl-inositol-phosphate; DAG, diacylglycerol; PKC, protein kinase C; PP, phosphatases; PKG, protein kinase G; GC, guanylate cyclase; NO, nitric oxide.

flocculus with stimulation of climbing fibers (Ito et al., 1982b). Confirmation of cellular plasticity in the flocculus led Ito (1982) to state his flocculus hypothesis to explain how climbing fibers, which carry retinal error signals (Maekawa and Kimura, 1974; Maekawa and Takeda, 1976), could cause depression of the appropriate parallel fiber inputs to keep the VOR calibrated (Ito, 1982, 1989, 1993) and hence reduce retinal error. Direct proof that parallel fiber to Purkinje cell transmission could be depressed came from

intracellular recordings in cerebellar slice (Ito and Kano, 1982). Since then many studies have shown that activation of a parallel fiber bundle in conjunction with the climbing fiber to the Purkinje neuron leads to a reduction of the excitatory post synaptic current that is normally generated by activating that same set of parallel fibers alone (Crépel and Krupa, 1988; Crépel and Jaillard, 1991; Konnerth et al., 1992; Aiba et al., 1994; Karachot et al., 1994).

Molecular mechanisms of cerebellar LTD have been largely elucidated and will be briefly summarized (for extensive reviews see (Linden and Connor, 1995; Daniel et al., 1998; Ito, 2001) (Fig. 2). Three postsynaptic events are required for LTD to occur: activation of metabotropic glutamate receptor mGluR1, activation of the ionotropic, α -Amino-3-hydroxy-5-methylisoxazolopropionate (AMPA) receptor and a raise in intracellular free Ca^{2+} (Linden and Connor, 1995). Climbing fiber activation leads to a massive depolarization of the Purkinje cell and to large increase in intracellular free Ca^{2+} through voltage-gated calcium channels. Parallel fiber activation of mGluR1 receptors leads to a G-protein coupled activation of phospholipase C (PLC). PLC produces the second messengers Dia-acyl-glycerol (DAG) and inositol-tri-phosphate (IP_3). IP_3 adds to the accumulation of intracellular free calcium by activating IP_3 receptors that release Ca^{2+} from intracellular calcium stores in the endoplasmatic reticulum. DAG and Ca^{2+} are both required for the activation of protein kinase C (PKC). PKC activation is thought to underlie the final pathway for expression of cerebellar LTD since inhibition of this enzyme prevents LTD from occurring (Crépel and Jaillard, 1990; Linden and Connor, 1991; Hartell, 1994; Freeman et al., 1998), while exogenous activation of PKC induces LTD (Crépel and Krupa, 1988). PKC belongs to a family of protein kinases that phosphorylate serine or threonine residues in a variety of substrates. More than 10 subspecies of PKC have been identified (Nishizuka, 1992), but PKC γ is the most likely isoform for induction of cerebellar LTD because of its abundant presence in the Purkinje cell dendritic tree (Nishizuka, 1986; Hidaka et al., 1988). PKC acts on AMPA receptors by phosphorylating a serine residue (ser-880) on the intracellular c-terminal end of GluR2/3 subunits. In GluR2/3 subunits, the target serine residue is located in a PDZ domain. This domain, named after the first three proteins in which it was first found, contains a protein-protein interaction motif (Hata et al., 1998) allowing it to associate with other proteins that possess this motif. Glutamate receptor interacting protein (GRIP) is one of the proteins that contains such a PDZ domain and as its name suggests, is associated with the glutamate receptor channel AMPA (Braithwaite et al., 2000). GRIP binds the GluR2 and GluR3 subunits of the AMPA receptor and aggregates the receptors to the postsynaptic membrane in the synapse (Dong et al., 1997; Dong et al., 1999). Phosphorylation of the AMPA receptor subunits by PKC prevents proper interaction of the receptor with GRIP facilitating internalization of the receptor, possibly because GRIP no longer stabilizes the postsynaptic localization of AMPA (Matsuda et al., 1999; Matsuda et al., 2000). Internalization of the receptor then occurs by means of clathrin-mediated endocytosis (Wang and Linden, 2000). Thus, Purkinje cells reduce the contribution of selected parallel fibers by reducing their synaptic weight through removal of AMPA receptors from the postsynaptic membrane.

A second pathway, which is mediated by nitric oxide (NO), has also been implicated in the induction of LTD. Evidence for NO involvement is threefold. First, application of NO to Purkinje cells produced LTD in a slice preparation (Daniel et al.,

1993; Lev-Ram et al., 1995). Second, blocking NO-synthetase (NOS), the enzyme that catalyzes the production of NO from L-arginine, effectively blocked induction of LTD (Crépel and Jaillard, 1990; Shibuki and Okada, 1991; Daniel et al., 1993; Lev-Ram et al., 1995). Third, LTD could not be induced in Purkinje cells of mice that lacked the gene coding for neuronal NOS (Lev-Ram et al., 1997; c.f. Linden et al., 1995). NO acts on soluble guanylyl-cyclase, which is an enzyme that produces cGMP from GTP. cGMP causes, via activation of protein kinase G, phosphorylation of g-substrate. Phosphorylated g-substrate is a potent inhibitor of two types of serine/threonine-specific protein phosphatases: protein phosphatases 1 and protein phosphatases 2A. The dephosphorylating action of protein phosphatases could possibly counteract the phosphorylating activity of PKC. Indeed, inhibition of phosphatase activity in slice has been shown to induce LTD in combination with stimulation of granule cell axons (Ajima and Ito, 1995). Phosphorylation status of AMPA receptors could therefore be envisioned as the outcome of a chemical balance between the activity of PKC on the one hand and phosphatases on the other. LTD induction would shift the equilibrium by increasing PKC and decreasing phosphatase activity.

At this point it may be prudent to note that the existence of synaptic plasticity in the cerebellum does not in itself prove that the flocculus hypothesis is correct. A few studies have attempted to directly address this question by studying the relation between LTD and VOR adaptation in vivo. Blocking the NO-dependent pathway of LTD induction through application of the NO-scavenger hemoglobin (Nagao and Ito, 1991) or the NOS inhibitor L-NMMA (Li et al., 1995) to the peri-floccular area indeed prevented adaptation of the VOR. Unfortunately, carefully designed local application of substances will never be limited to Purkinje cells only and therefore may affect more than just LTD at the parallel fiber to Purkinje cell synapse. This kind of specificity can be obtained by using genetic techniques that disrupt LTD in Purkinje cells only. Using the L7 vector De Zeeuw et al. (1998) have been able to generate transgenic mice that selectively express a pseudosubstrate PKC inhibitor protein in Purkinje cells. Purkinje cells from these transgenic mice were no longer able to show LTD and the transgenic animals were no longer able to increase the gain of their VOR in response to 1 hour of visuo-vestibular training (De Zeeuw et al., 1998). Therefore evidence exists that LTD is indeed important for VOR adaptation. However, lack of LTD in L7-PKC_i transgenic mice did not lead to any detectable impairment of motor behavior in general or oculomotor behavior specifically. Such deficits could be expected in view of the complete absence of motor learning in these animals and the question therefore arises whether cerebellar LTD is the only mechanism through which learning can occur.

Brainstem hypothesis

In search of evidence that learning occurred at floccular Purkinje neurons, the spiking behavior of these neurons during the vestibular stimulation was recorded before and after VOR adaptation had occurred. Changes in neuronal response were found to correlate nicely with training induced changes in eye movement (Dufosse et al., 1978; Miles et al., 1980b; Watanabe, 1984; Lisberger and Pavelko, 1988; Lisberger et al., 1994). However, direct interpretation of Purkinje cell modulation during normal VOR was hampered by the fact that these neurons not only receive vestibular inputs but also an efference copy of

the motor command signal (Lisberger, 1994). Any change in modulation of these neurons due to adaptation may therefore reflect normal transmission of a changed efference copy signal rather than a changed sensitivity to vestibular inputs. The isolated vestibular component of the Purkinje cell neuronal responses was therefore investigated using a vestibular cancellation paradigm. In such a cancellation condition the animal would view a visual surround that moved exactly in phase and at the same amplitude as the applied vestibular rotation. Under cancellation conditions there would be vestibular stimulation but no eye movement and the efference copy signal would be nought. The change in vestibular sensitivity as measured during cancellation before and after VOR adaptation had occurred was found to be in the wrong direction to be the sole cause for learning in the VOR (Miles et al., 1980a; Lisberger et al., 1994). In monkeys adapted to increase VOR gain a concomitant increase of head velocity sensitivity was found in Purkinje neurons. Due to the inhibitory nature of Purkinje neurons the increased head velocity sensitivity was hard to reconcile with an increase in VOR gain. To account for changes in responsiveness of Purkinje cells a new hypothesis was formulated that did not recognize the flocculus as primary site of plasticity. This hypothesis stated that changes in the response of brainstem vestibular neurons were the primary location for modifications to the VOR. Altered vestibular sensitivity of floccular Purkinje cells occurred secondary to changes in the brain stem and reflected the necessity for Purkinje cells to balance the changed efference copy signal by changing their sensitivity to head velocity (Miles and Lisberger, 1981; Lisberger, 1994; Hirata and Highstein, 2001).

Further evidence for the involvement of the vestibular nucleus in VOR adaptation came from the investigation of short latency ocular responses to steps in head velocity. After induction of VOR adaptation changes in amplitude of eye movement following a step in head velocity were found to occur at latencies that were deemed too short for the change in response to be mediated by the cerebellum. Short latency changes in the VOR therefore had to reflect plasticity in brainstem pathways (Lisberger, 1984; Khater et al., 1993; Pastor et al., 1994). In addition, disrupting floccular output by lesioning or reversibly inactivating this structure did not fully abolish the learned response in goldfish and cat (Luebke and Robinson, 1994; Pastor et al., 1994) and recording floccular target neurons in an adapted monkey after floccular output was blocked, confirmed that target neurons retained at least part the learned response (Partsalis et al., 1995; Zhang et al., 1995).

The role of the flocculus within the brainstem hypothesis of VOR adaptation would be to generate an appropriate error signal that could guide plasticity in the vestibular nucleus. Capability of the vestibular nucleus to undergo plasticity is clearly demonstrated by adaptive mechanisms that occur after unilateral labyrinthectomy. Labyrinthectomy deprives the vestibular nucleus on the side ipsilateral to the lesion from its main source of excitatory input, creating a severe imbalance in activity between left and right vestibular nuclei. The imbalanced activity results in oculomotor and postural disturbances that subside in the course of a few days, a process known as vestibular compensation (Curthoys and Halmagyi, 1995; Dieringer, 1995). Cellular correlates underlying vestibular compensation encompass changes in intrinsic excitability of vestibular nucleus neurons (Darlington et al., 1989; Smith and Curthoys, 1989; Vibert et al., 1999) as well as regulation of the neuron's sensitivity to GABA mediated neurotransmission (Cameron and Dutia, 1997; Yamanaka et al., 2000; Graham and Dutia,

2001; Johnston et al., 2001). Cellular processes observed in such an extreme condition as vestibular compensation could play an analogous role during adaptation of the VOR and changes in cellular excitability of vestibular neurons have been hypothesized to underlie VOR adaptation in the vestibular nucleus (du Lac, 1996; Smith et al., 2002). Additional mechanisms for information storage in the vestibular nucleus may also involve plasticity at the synapse of primary vestibular afferents to the vestibular nuclear neuron (Capocchi et al., 1992; Grassi et al., 1996).

1.3.3 Optokinetic Reflex

The optokinetic system acts in concert with the vestibulo-ocular system to maintain stability of images on the retina over a broad range of head movements. While the VOR compensates high frequency head movements using signals from the semi circular canals, the OKR compensates for low-frequency disturbances using visual feedback. Visual feedback defines the OKR as a closed loop negative feedback system, in which the output, i.e. eye movement, minimizes the error signal that provides its input, i.e. retinal slip. At low stimulus frequencies the feedback organization of the OKR drives the gain to one, but as stimulus frequency increases gain declines reflecting low pass character of the system (Collewijn, 1969; Nagao, 1983; Marsh and Baker, 1997). The OKR is severely non-linear in that reflex gain is not solely determined by frequency content of the stimulus but depends heavily on stimulus velocity (Collewijn, 1969). Velocity dependence of the OKR is caused by saturation occurring at its input stage (Oyster et al., 1972). In the rabbit about a quarter of all retinal ganglion cells are sensitive to a pattern moving in a preferred direction. These direction selective retinal ganglion cells fall into two categories 'on' type cells and 'on-off' type cells based on their receptive field maps. The on type neurons were most sensitive to stimulus velocities between 0.1-2 °/sec, which agrees well with peak stimulus velocities that best elicited an OKR in the rabbit. At higher stimulus velocities the response of these neurons fell, much like total OKR gain and it was thought that limited sensitivity of retinal ganglion cells to slip velocity would underlie the velocity dependent nature of the entire OKR (Collewijn, 1972). The foveate optokinetic system essentially is a low velocity system that acts to supplement the fast-acting VOR, particularly in natural conditions, where the VOR produces a near perfect compensation, and thus the velocities of any residual retinal slip are low. (Collewijn, 1969; Hess et al., 1985; Keng and Anastasio, 1997)

The velocity storage mechanism that was previously described in relation to the VOR also functions in the optokinetic system. Its presence in the OKR is revealed by a slow rise in eye velocity after sudden onset of full field visual motion at constant angular velocity. Full field visual motion in one direction elicits an ocular nystagmus at 75-100 ms latency that follows a biphasic time course in almost all species studied (Cohen et al., 1977; Cohen et al., 1981; Maioli and Precht, 1984; Hess et al., 1985; Keng and Anastasio, 1997). The biphasic profile consists of an initial jump followed by a slow rise in eye velocity. In foveate species the initial jump in eye velocity is very pronounced and has a gain of 0.6 with respect to stimulus velocity. It is thought to be largely mediated by the pursuit system (Cohen et al., 1977; Lisberger et al., 1981). In foveate species the initial response is much smaller and saturates at ± 10 °/sec (Collewijn, 1969; Hess et al., 1985). The ensuing slow rise in eye velocity is mediated by the velocity storage

mechanism that slowly charges in the presence of constant velocity visual input (Cohen et al., 1977; Cohen et al., 1981; Maioli and Precht, 1984; Hess et al., 1985). The optokinetic response to a constant velocity visual stimulus reflects activity that is mediated through a fast acting, direct pathway, which mediates the initial jump in eye velocity and a slower acting velocity storage mechanism (Cohen et al., 1977; Lisberger et al., 1981). Suddenly turning off the light in the presence of constant velocity, full field, optokinetic stimulation reveals a continued nystagmus (OKAN) that reflects the discharge properties of a charged velocity storage mechanism that is deprived of its input. Because of its slow acting properties the velocity storage mechanism contributes to the OKR at low frequency stimuli, and using sinusoidal stimuli at frequencies higher than 0.1 Hz one mostly evaluates the functional importance of the fast, direct pathway.

1.3.4 OKR adaptation

In afoveate animals, which have an OKR gain smaller than unity, OKR gain is not fixed but can be increased by prolonged visual stimulation in the presence of sufficient retinal slip. Intuitively, plasticity in the OKR seems strange considering that when OKR gain is below unity the animal should experience retinal slip and therefore already increase OKR gain to maximum in its normal environment. The answer to this seeming contradiction may lie with the fact that full field visual motion alone is a very experimental stimulus. In a more natural situation full field visual motion will likely occur in combination with vestibular stimulation due to movement of the animal through its environment. When stimulated with a combination of visual and vestibular stimulation eye movements of the rabbit proved very stable across a range of frequencies (Baarsma and Collewijn, 1974; Batini et al., 1979). It could thus be argued that untrained afoveate animals possess an OKR that is sufficient to complement their VOR to obtain some desired stability during VVOR. However, when OKR is tested in isolation there is no longer a vestibular component that would drive eye movement at higher stimulus frequencies and the increased retinal slip would prompt the animal to increase OKR gain. Additionally OKR gain in laboratory animals may be optimized to the rather limited visual contrast of their cages, subjecting them to contrast rich stimuli in the experimental setup may induce a general improvement of OKR gain.

Because the OKR and VOR pathways converge in flocculus and vestibular nucleus, it has been proposed that changes in one of these systems may transfer to the other. Such transference of learning has been shown for OKR adaptation, which caused not only an increase in OKR gain but also in VOR gain (Collewijn and Grootendorst, 1979; Schairer and Bennett, 1986a; Marsh and Baker, 1997). Collewijn (1979) explained this phenomenon very elegantly by hypothesizing that changes in VOR gain were not guided by a comparison between retinal slip and head movement, but rather between retinal slip and eye movement. Using sinusoidal stimuli he deduced that when retinal slip was in phase with eye movement VOR gain would increase and when slip was in the direction opposite to eye movement VOR gain would decrease. Under this assumption stimulation with visual stimulus alone invoked the same learning rule as a stimulus that rotated the visual surround in the opposite direction from the vestibular stimulus. The induction of changes in the VOR by visual stimulation thus results from the neural

learning rule that is implemented rather than from the presence of a common gain element shared by visual and vestibular systems.

Visuo-vestibular training paradigms meant to change VOR gain are also effective in changing OKR gain. Both VOR adaptation aimed at increasing VOR gain as well as adaptation aimed at decreasing VOR gain result in an increase of OKR gain (Collewijn and Grootendorst, 1979; Nagao, 1983). Intuitively, an increase in OKR gain is equally advantageous in these vestibular training conditions since an improvement in OKR performance will always serve to reduce retinal slip during training.

Changes in OKR gain, which occur after either optokinetic or visuo-vestibular sinusoidal training, are context specific and are largely limited to the training frequency (Collewijn and Grootendorst, 1978; Schairer and Bennett, 1986a; Nagao, 1989; Iwashita et al., 2001). Such frequency specificity of OKR adaptation is reminiscent of VOR adaptation and implies that learning in this reflex occurs via a similar if not the same mechanism. Cerebellar LTD has therefore been implicated to underlie VOR as well as OKR adaptation and lesions of the flocculus indeed prevent OKR adaptation (Kawato and Gomi, 1992; Katoh et al., 1998). However, data obtained from flocculus lesion is a little hard to interpret since these lesions cause a severe reduction of OKR gain and a differential contribution of the flocculus to learning in the OKR is therefore difficult to assess (Ito et al., 1982a; Nagao, 1983; Barmack and Pettorossi, 1985; Van Neerven et al., 1989). Several studies have attempted to confirm the importance of cerebellar LTD in OKR adaptation by studying mice that were genetically altered and no longer expressed cerebellar LTD *in vitro* (Katoh et al., 2000; Shutoh et al., 2002). These studies unfortunately lacked the cellular specificity to fully attribute observed deficits in OKR adaptation to LTD of the parallel fiber to Purkinje cell synapse.

1.4 Contribution of this thesis

In summary, multiple steps of processing contribute to the generation of compensatory eye movements and each step appears to possess some measure of plasticity. This omnipresent plasticity allows the organism to optimize almost every aspect of its oculomotor system. The most prominent and most frequently studied form of oculomotor plasticity is VOR gain adaptation, which appears to be a network property that may require adaptive sites in both cerebellum and vestibular nucleus. However, irrespective of where or in what order neuronal changes occur during VOR adaptation, a major goal remains to elucidate the link between VOR adaptation and cellular mechanisms of plasticity that are observed *in vitro*. A multidisciplinary approach involving molecular biology, cellular physiology and behavioral/systems physiology may be pre-eminently suited to address this question. The use of genetic techniques may, if not now then in the future, allow us to target, cell specifically, mechanisms that are proposed to underlie learning and behaviorally assess whether and, if so, how these mechanisms contribute to VOR adaptation. This thesis tries to realize such an integrated approach, by first of all describing a feasible technique for recording eye movements in mice and then applying this technique to study the effect of genetic manipulations and mutations on oculomotor control.

References

- Aiba A, Kano M, Chen C, Stanton ME, Fox GD, Herrup K, Zwingman TA, Tonegawa S (1994) Deficient cerebellar long-term depression and impaired motor learning in mGluR1 mutant mice. *Cell* 79:377-388.
- Ajima A, Ito M (1995) A unique role of protein phosphatases in cerebellar long-term depression. *Neuroreport* 6:297-300.
- Albus JS (1971) A theory of cerebellar function. *Math Biosci* 10:25-61.
- Baarsma E, Collewijn H (1974) Vestibulo-ocular and optokinetic reactions to rotation and their interaction in the rabbit. *J Physiol* 238:603-625.
- Balkema GW, Mangini NJ, Pinto LH, Vanable JW, Jr. (1984) Visually evoked eye movements in mouse mutants and inbred strains. A screening report. *Invest Ophthalmol Vis Sci* 25:795-800.
- Balkema GW, Jr., Pinto LH, Drager UC, Vanable JW, Jr. (1981) Characterization of abnormalities in the visual system of the mutant mouse pearl. *J Neurosci* 1:1320-1329.
- Balogh SA, McDowell CS, Stavnezer AJ, Denenberg VH (1999) A behavioral and neuroanatomical assessment of an inbred substrain of 129 mice with behavioral comparisons to C57BL/6J mice. *Brain Res* 836:38-48.
- Baloh RW, Henn V, Jager J (1982) Habituation of the human vestibulo-ocular reflex with low-frequency harmonic acceleration. *Am J Otolaryngol* 3:235-241.
- Barnack NH, Pettorossi VE (1985) Effects of unilateral lesions of the flocculus on optokinetic and vestibuloocular reflexes of the rabbit. *J Neurophysiol* 53:481-496.
- Batini C, Ito M, Kado RT, Jastreboff PJ, Miyashita Y (1979) Interaction between the horizontal vestibulo-ocular reflex and optokinetic response in rabbits. *Exp Brain Res* 37:1-15.
- Becker W, Klein HM (1973) Accuracy of saccadic eye movements and maintenance of eccentric eye positions in the dark. *Vision Res* 13:1021-1034.
- Braithwaite SP, Meyer G, Henley JM (2000) Interactions between AMPA receptors and intracellular proteins. *Neuropharmacology* 39:919-930.
- Brink MF, Bishop MD, Pieper FR (2000) Developing efficient strategies for the generation of transgenic cattle which produce biopharmaceuticals in milk. *Theriogenology* 53:139-148.
- Buettner UW, Buttner U, Henn V (1978) Transfer characteristics of neurons in vestibular nuclei of the alert monkey. *J Neurophysiol* 41:1614-1628.
- Cameron SA, Dutia MB (1997) Cellular basis of vestibular compensation: changes in intrinsic excitability of MVN neurones. *Neuroreport* 8:2595-2599.
- Cannon SC, Robinson DA (1987) Loss of the neural integrator of the oculomotor system from brain stem lesions in monkey. *J Neurophysiol* 57:1383-1409.
- Capocchi G, Della Torre G, Grassi S, Pettorossi VE, Zampolini M (1992) NMDA receptor-mediated long term modulation of electrically evoked field potentials in the rat medial vestibular nuclei. *Exp Brain Res* 90:546-550.
- Carpenter RHS (1972) Cerebellectomy and the transfer function of the vestibulo-ocular reflex in the decerebrate cat. *Proc R Soc Lond B* 181:353-374.
- Cheron G, Godaux E (1987) Disabling of the oculomotor neural integrator by kainic acid injections in the prepositus-vestibular complex of the cat. *J Physiol* 394:267-290.

- Chu L, Kaneko CR (1995) Do the saccadic system and the vestibulo-ocular reflex of monkeys share a common neural integrator? *Neurosci Lett* 187:193-196.
- Cohen B, Matsuo V, Raphan T (1977) Quantitative analysis of the velocity characteristics of optokinetic nystagmus and optokinetic after-nystagmus. *J Physiol (Lond)* 270:321-344.
- Cohen B, Henn V, Raphan T, Dennett D (1981) Velocity storage, nystagmus, and visual-vestibular interactions in humans. *Ann N Y Acad Sci* 374:421-433.
- Cohen H, Cohen B, Raphan T, Waespe W (1992) Habituation and adaptation of the vestibuloocular reflex: a model of differential control by the vestibulocerebellum. *Exp Brain Res* 90:526-538.
- Collewijn H (1969) Optokinetic eye movements in the rabbit: input-output relations. *Vision Res* 9:117-132.
- Collewijn H (1972) An analog model of the rabbit's optokinetic system. *Brain Res* 36:71-88.
- Collewijn H (1977) Eye- and head movements in freely moving rabbits. *J Physiol* 266:471-498.
- Collewijn H (1981) *The oculomotor system of the rabbit and its plasticity*, 1 Edition. Berlin: Springer-Verlag.
- Collewijn H, Grootendorst AF (1978) Adaptation of the rabbit's vestibulo-ocular reflex to modified visual input: importance of stimulus conditions. *Arch Ital Biol* 116:273-280.
- Collewijn H, Grootendorst AF (1979) Adaptation of optokinetic and vestibulo-ocular reflexes to modified visual input in the rabbit. *Prog Brain Res* 50:771-781.
- Collewijn H, Winterson BJ, van der Steen J (1980) Post-rotary nystagmus and optokinetic after-nystagmus in the rabbit linear rather than exponential decay. *Exp Brain Res* 40:330-338.
- Collewijn H, Martins AJ, Steinman RM (1983) Compensatory eye movements during active and passive head movements: fast adaptation to changes in visual magnification. *J Physiol* 340:259-286.
- Crawford JD, Cadera W, Vilis T (1991) Generation of torsional and vertical eye position signals by the interstitial nucleus of Cajal. *Science* 252:1551-1553.
- Crawley JN, Belknap JK, Collins A, Crabbe JC, Frankel W, Henderson N, Hitzemann RJ, Maxson SC, Miner LL, Silva AJ, Wehner JM, Wynshaw-Boris A, Paylor R (1997) Behavioral phenotypes of inbred mouse strains: implications and recommendations for molecular studies. *Psychopharmacology (Berl)* 132:107-124.
- Crépel F, Krupa M (1988) Activation of protein kinase C induces a long-term depression of glutamate sensitivity of cerebellar Purkinje cells. An in vitro study. *Brain Res* 458:397-401.
- Crépel F, Jaillard D (1990) Protein kinases, nitric oxide and long-term depression of synapses in the cerebellum. *Neuroreport* 1:133-136.
- Crépel F, Jaillard D (1991) Pairing of pre- and postsynaptic activities in cerebellar Purkinje cells induces long-term changes in synaptic efficacy in vitro. *J Physiol (Lond)* 432:123-141.
- Curthoys IS (1982) The response of primary horizontal semicircular canal neurons in the rat and guinea pig to angular acceleration. *Exp Brain Res* 47:286-294.

- Curthoys IS, Halmagyi GM (1995) Vestibular compensation: a review of the oculomotor, neural, and clinical consequences of unilateral vestibular loss. *J Vestib Res* 5:67-107.
- Daniel H, Levenes C, Crépel F (1998) Cellular mechanisms of cerebellar LTD. *Trends Neurosci* 21:401-407.
- Daniel H, Hemart N, Jaillard D, Crépel F (1993) Long-term depression requires nitric oxide and guanosine 3':5' cyclic monophosphate production in rat cerebellar Purkinje cells. *Eur J Neurosci* 5:1079-1082.
- Darlington CL, Smith PF, Hubbard JI (1989) Neuronal activity in the guinea pig medial vestibular nucleus in vitro following chronic unilateral labyrinthectomy. *Neurosci Lett* 105:143-148.
- De Zeeuw CI, Wylie DR, Stahl JS, Simpson JI (1995) Phase Relations of Purkinje Cells in the Rabbit Flocculus During Compensatory Eye Movements. *J of Neurophysiol* 74:2051-2063.
- De Zeeuw CI, Hansel C, Bian F, Koekkoek SK, van Alphen AM, Linden DJ, Oberdick J (1998) Expression of a protein kinase C inhibitor in Purkinje cells blocks cerebellar LTD and adaptation of the vestibulo-ocular reflex. *Neuron* 20:495-508.
- Demer JL, Robinson DA (1983) Different time constants for optokinetic and vestibular nystagmus with a single velocity-storage element. *Brain Res* 276:173-177.
- Dieringer N (1995) 'Vestibular compensation': neural plasticity and its relations to functional recovery after labyrinthine lesions in frogs and other vertebrates. *Prog Neurobiol* 46:97-129.
- Dockstader CL, van der Kooy D (2001) Mouse strain differences in opiate reward learning are explained by differences in anxiety, not reward or learning. *J Neurosci* 21:9077-9081.
- Dong H, Zhang P, Liao D, Huganir RL (1999) Characterization, expression, and distribution of GRIP protein. *Ann N Y Acad Sci* 868:535-540.
- Dong H, O'Brien RJ, Fung ET, Lanahan AA, Worley PF, Huganir RL (1997) GRIP: a synaptic PDZ domain-containing protein that interacts with AMPA receptors. *Nature* 386:279-284.
- Dow ER, Anastasio TJ (1999) Analysis and modeling of frequency-specific habituation of the goldfish vestibulo-ocular reflex [In Process Citation]. *J Comput Neurosci* 7:55-70.
- Drager UC, Olsen JF (1981) Ganglion cell distribution in the retina of the mouse. *Invest Ophthalmol Vis Sci* 20:285-293.
- du Lac S (1996) Candidate cellular mechanisms of vestibulo-ocular reflex plasticity. *Ann N Y Acad Sci* 781:489-498.
- Dufosse M, Ito M, Jastreboff PJ, Miyashita Y (1978) A neuronal correlate in rabbit's cerebellum to adaptive modification of the vestibulo-ocular reflex. *Brain Res* 150:611-616.
- Eccles JC, Ito M, Szentagothai J (1967) *The cerebellum as a neuronal machine*. Berlin-heidelberg-New York: springer.
- Fan J, Sun H, Unoki H, Shiomi M, Watanabe T (2001) Enhanced atherosclerosis in Lp(a) WHHL transgenic rabbits. *Ann N Y Acad Sci* 947:362-365.

- Fernandez C, Goldberg JM (1971) Physiology of peripheral neurons innervating semicircular canals of the squirrel monkey. II. Response to sinusoidal stimulation and dynamics of peripheral vestibular system. *J Neurophysiol* 34:661-675.
- Festing MFW (1992) In: *Techniques for the genetic analysis of brain and behavior: Focus on the mouse* (Goldowitz D, Wahlsten D, Wimer RE, eds), pp 17-38: Elsevier.
- Freeman JH, Jr., Scharenberg AM, Olds JL, Schreurs BG (1998) Classical conditioning increases membrane-bound protein kinase C in rabbit cerebellum. *Neuroreport* 9:2669-2673.
- Frens MA, Mathoera AL, van der Steen J (2001) Floccular complex spike response to transparent retinal slip. *Neuron* 30:795-801.
- Fujita M (1982) Simulation of adaptive modification of the vestibulo-ocular reflex with an adaptive filter model of the cerebellum. *Biol Cybern* 45:207-214.
- Fukuda Y (1977) A three-group classification of rat retinal ganglion cells: histological and physiological studies. *Brain Res* 119:327-334.
- Fukushima K, Kaneko CR, Fuchs AF (1992) The neuronal substrate of integration in the oculomotor system. *Prog Neurobiol* 39:609-639.
- Fuller JH (1980) Linkage of eye and head movements in the alert rabbit. *Brain Res* 194:219-222.
- Gerlai R (1996) Gene-targeting studies of mammalian behavior: is it the mutation or the background genotype? [see comments] [published erratum appears in *Trends Neurosci* 1996 Jul;19(7):271]. *Trends Neurosci* 19:177-181.
- Godaux E, Cheron G (1993) Testing the common neural integrator hypothesis at the level of the individual abducens motoneurons in the alert cat. *J Physiol* 469:549-570.
- Gossen M, Bujard H (1992) Tight control of gene expression in mammalian cells by tetracycline-responsive promoters. *Proc Natl Acad Sci U S A* 89:5547-5551.
- Gossen M, Freundlieb S, Bender G, Muller G, Hillen W, Bujard H (1995) Transcriptional activation by tetracyclines in mammalian cells. *Science* 268:1766-1769.
- Graham BP, Dutia MB (2001) Cellular basis of vestibular compensation: analysis and modelling of the role of the commissural inhibitory system. *Exp Brain Res* 137:387-396.
- Grassi S, Pettorossi VE, Zampolini M (1996) Low-frequency stimulation cancels the high-frequency-induced long-lasting effects in the rat medial vestibular nuclei. *J Neurosci* 16:3373-3380.
- Harrison RE, Baker JF, Isu N, Wickland CR, Peterson BW (1986) Dynamics of adaptive change in vestibulo-ocular reflex direction. I. Rotations in the horizontal plane. *Brain Res* 371:162-165.
- Hartell NA (1994) cGmp acts within cerebellar Purkinje cells to produce long term depression via mechanisms involving Pkc and Pkg. *Neuroreport* 5:833-836.
- Hasegawa T, Kato I, Harada K, Ikarashi T, Yoshida M, Koike Y (1994) The effect of uvulonodular lesions on horizontal optokinetic nystagmus and optokinetic after-nystagmus in cats. *Acta Otolaryngol Suppl* 511:126-130.
- Hata Y, Nakanishi H, Takai Y (1998) Synaptic PDZ domain-containing proteins. *Neurosci Res* 32:1-7.
- Hess BJ, Savio T, Strata P (1988) Dynamic characteristics of optokinetically controlled eye movements following inferior olive lesions in the brown rat. *J Physiol* 397:349-370.

- Hess BJ, Precht W, Reber A, Cazin L (1985) Horizontal optokinetic ocular nystagmus in the pigmented rat. *Neuroscience* 15:97-107.
- Hidaka H, Tanaka T, Onoda K, Hagiwara M, Watanabe M, Ohta H, Ito Y, Tsurudome M, Yoshida T (1988) Cell type-specific expression of protein kinase C isozymes in the rabbit cerebellum. *J Biol Chem* 263:4523-4526.
- Highstein SM (1973) Synaptic linkage in the vestibulo-ocular and cerebello-vestibular pathways to the VIth nucleus in the rabbit. *Exp Brain Res* 17:301-314.
- Hirata Y, Highstein SM (2001) Acute adaptation of the vestibuloocular reflex: signal processing by floccular and ventral parafloccular purkinje cells. *J Neurophysiol* 85:2267-2288.
- Hughes A (1971) Topographical relationships between the anatomy and physiology of the rabbit visual system. *Doc Ophthalmol* 30:33-159.
- Igarashi M, Miyata H, Kato Y, Wright WK, Levy JK (1975) Optokinetic nystagmus after cerebellar uvulonodectomy in squirrel monkeys. *Acta Otolaryngol* 80:180-184.
- Ito M (1972) Neural design of the cerebellar motor control system. *Brain Res* 40:81-84.
- Ito M (1982) Cerebellar control of the vestibulo-ocular reflex--around the flocculus hypothesis. *Annu Rev Neurosci* 5:275-296.
- Ito M (1984) *The cerebellum and neural control*: Raven Press, New York.
- Ito M (1989) Long-term depression. *Annu Rev Neurosci* 12:85-102.
- Ito M (1993) Synaptic plasticity in the cerebellar cortex and its role in motor learning. *Can J Neurol Sci* 20:S70-74.
- Ito M (2001) Cerebellar long-term depression: characterization, signal transduction, and functional roles. *Physiol Rev* 81:1143-1195.
- Ito M, Kano M (1982) Long-lasting depression of parallel fiber-Purkinje cell transmission induced by conjunctive stimulation of parallel fibers and climbing fibers in the cerebellar cortex. *Neurosci Lett* 33:253-258.
- Ito M, Jastreboff PJ, Miyashita Y (1979) Adaptive modification of the rabbit's horizontal vestibulo-ocular reflex during sustained vestibular and optokinetic stimulation. *Exp Brain Res* 37:17-30.
- Ito M, Jastreboff PJ, Miyashita Y (1982a) Specific effects of unilateral lesions in the flocculus upon eye movements in albino rabbits. *Exp Brain Res* 45:233-242.
- Ito M, Sakurai M, Tongroach P (1982b) Climbing fibre induced depression of both mossy fibre responsiveness and glutamate sensitivity of cerebellar Purkinje cells. *J Physiol* 324:113-134.
- Iwashita M, Kanai R, Funabiki K, Matsuda K, Hirano T (2001) Dynamic properties, interactions and adaptive modifications of vestibulo-ocular reflex and optokinetic response in mice. *Neurosci Res* 39:299-311.
- Johnston AR, Him A, Dutia MB (2001) Differential regulation of GABA(A) and GABA(B) receptors during vestibular compensation. *Neuroreport* 12:597-600.
- Jones GM, Davies P (1976) Adaptation of cat vestibulo-ocular reflex to 200 days of optically reversed vision. *Brain Res* 103:551-554.
- Juliusson B, Bergström A, Röhlich P, Ehinger B, van Veen T, Szel A (1994) Complementary cone fields of the rabbit retina. *Invest Ophthalmol Vis Sci* 35:811-818.

- Kaneko CR (1992) Effects of ibotenic acid lesions of nucleus prepositus hypoglossi on optokinetic and vestibular eye movements in the alert, trained monkey. *Ann N Y Acad Sci* 656:408-427.
- Karachot L, Kado RT, Ito M (1994) Stimulus parameters for induction of long-term depression in in vitro rat Purkinje cells. *Neurosci Res* 21:161-168.
- Katoh A, Kitazawa H, Itohara S, Nagao S (1998) Dynamic characteristics and adaptability of mouse vestibulo-ocular and optokinetic response eye movements and the role of the flocculo-olivary system revealed by chemical lesions. *Proc Natl Acad Sci U S A* 95:7705-7710.
- Katoh A, Kitazawa H, Itohara S, Nagao S (2000) Inhibition of nitric oxide synthesis and gene knockout of neuronal nitric oxide synthase impaired adaptation of mouse optokinetic response eye movements. *Learn Mem* 7:220-226.
- Kawato M, Gomi H (1992) The cerebellum and VOR/OKR learning models [see comments]. *Trends Neurosci* 15:445-453.
- Keller EL, Precht W (1978) Persistence of visual response in vestibular nucleus neurons in cerebellectomized cat. *Exp Brain Res* 32:591-594.
- Keng MJ, Anastasio TJ (1997) The horizontal optokinetic response of the goldfish. *Brain Behav Evol* 49:214-229.
- Khater TT, Baker JF, Peterson BW (1990) Dynamics of adaptive change in human vestibulo-ocular reflex direction. *J Vestib Res* 1:23-29.
- Khater TT, Quinn KJ, Pena J, Baker JF, Peterson BW (1993) The latency of the cat vestibulo-ocular reflex before and after short- and long-term adaptation. *Exp Brain Res* 94:16-32.
- Konnerth A, Dreesen J, Augustine GJ (1992) Brief dendritic calcium signals initiate long-lasting synaptic depression in cerebellar Purkinje cells. *Proc Natl Acad Sci U S A* 89:7051-7055.
- Kramer PD, Shelhamer M, Zee DS (1995) Short-term adaptation of the phase of the vestibulo-ocular reflex (VOR) in normal human subjects. *Exp Brain Res* 106:318-326.
- Langer T, Fuchs AF, Scudder CA, Chubb MC (1985) Afferents to the flocculus of the cerebellum in the rhesus macaque as revealed by retrograde transport of horseradish peroxidase. *J Comp Neurol* 235:1-25.
- Lathe R (1996) Mice, gene targeting and behaviour: more than just genetic background. *Trends Neurosci* 19:183-186; discussion 188-189.
- Leigh RJ, Zee DS (1991) *The neurology of eye movements*, 2 Edition. Philadelphia: F.A. Davis company.
- Lev-Ram V, Makings LR, Keitz PF, Kao JP, Tsien RY (1995) Long-term depression in cerebellar Purkinje neurons results from coincidence of nitric oxide and depolarization-induced Ca²⁺ transients. *Neuron* 15:407-415.
- Lev-Ram V, Nebyelul Z, Ellisman MH, Huang PL, Tsien RY (1997) Absence of cerebellar long-term depression in mice lacking neuronal nitric oxide synthase. *Learn Mem* 4:169-177.
- Li J, Smith SS, McElligott JG (1995) Cerebellar nitric oxide is necessary for vestibulo-ocular reflex adaptation, a sensorimotor model of learning. *J Neurophysiol* 74:489-494.

- Linden DJ, Connor JA (1991) Participation of postsynaptic PKC in cerebellar long-term depression in culture. *Science* 254:1656-1659.
- Linden DJ, Connor JA (1995) Long-term synaptic depression. *Annu Rev Neurosci* 18:319-357.
- Linden DJ, Dawson TM, Dawson VL (1995) An evaluation of the nitric oxide/cGMP/cGMP-dependent protein kinase cascade in the induction of cerebellar long-term depression in culture. *J Neurosci* 15:5098-5105.
- Lisberger SG (1984) The latency of pathways containing the site of motor learning in the monkey vestibulo-ocular reflex. *Science* 225:74-76.
- Lisberger SG (1994) Neural basis for motor learning in the vestibuloocular reflex of primates. III. Computational and behavioral analysis of the sites of learning. *J Neurophysiol* 72:974-998.
- Lisberger SG, Pavelko TA (1988) Brain stem neurons in modified pathways for motor learning in the primate vestibulo-ocular reflex. *Science* 242:771-773.
- Lisberger SG, Miles FA, Optican LM (1983) Frequency-selective adaptation: evidence for channels in the vestibulo-ocular reflex? *J Neurosci* 3:1234-1244.
- Lisberger SG, Miles FA, Zee DS (1984) Signals used to compute errors in monkey vestibuloocular reflex: possible role of flocculus. *J Neurophysiol* 52:1140-1153.
- Lisberger SG, Miles FA, Optican LM, Eighmy BB (1981) Optokinetic response in monkey: underlying mechanisms and their sensitivity to long-term adaptive changes in vestibuloocular reflex. *J Neurophysiol* 45:869-890.
- Lisberger SG, Pavelko TA, Bronte-Stewart HM, Stone LS (1994) Neural basis for motor learning in the vestibuloocular reflex of primates. II. Changes in the responses of horizontal gaze velocity Purkinje cells in the cerebellar flocculus and ventral paraflocculus. *J Neurophysiol* 72:954-973.
- Luebke AE, Robinson DA (1994) Gain changes of the cat's vestibulo-ocular reflex after flocculus deactivation. *Exp Brain Res* 98:379-390.
- Maekawa K, Simpson JI (1972) Climbing fiber activation of Purkinje cells in the flocculus by impulses transferred through the visual pathway. *Brain Res* 39:245-251.
- Maekawa K, Kimura M (1974) Inhibition of climbing fiber responses of rabbit's flocculus Purkinje cells induced by light stimulation of the retina. *Brain Res* 65:347-350.
- Maekawa K, Takeda T (1976) Electrophysiological identification of the climbing and mossy fiber pathways from the rabbit's retina to the contralateral cerebellar flocculus. *Brain Res* 109:169-174.
- Maioli C, Precht W (1984) The horizontal optokinetic nystagmus in the cat. *Exp Brain Res* 55:494-506.
- Malleret G, Haditsch U, Genoux D, Jones MW, Bliss TV, Vanhoose AM, Weitlauf C, Kandel ER, Winder DG, Mansuy IM (2001) Inducible and reversible enhancement of learning, memory, and long-term potentiation by genetic inhibition of calcineurin. *Cell* 104:675-686.
- Mandl G, Melvill Jones G, Cynader M (1981) Adaptability of the vestibulo-ocular reflex to vision reversal in strobe reared cats. *Brain Res* 209:35-45.
- Mansuy IM, Winder DG, Moallem TM, Osman M, Mayford M, Hawkins RD, Kandel ER (1998) Inducible and reversible gene expression with the rtTA system for the study of memory. *Neuron* 21:257-265.

- Marr D (1968) A theory of cerebellar cortex. *J Physiol* 202:437-470.
- Marsh E, Baker R (1997) Normal and adapted visuocolomotor reflexes in goldfish. *J Neurophysiol* 77:1099-1118.
- Maruta J, Simpson JI, Raphan T, Cohen B (2001) Orienting otolith-ocular reflexes in the rabbit during static and dynamic tilts and off-vertical axis rotation. *Vision Res* 41:3255-3270.
- Matsuda S, Mikawa S, Hirai H (1999) Phosphorylation of serine-880 in GluR2 by protein kinase C prevents its C terminus from binding with glutamate receptor-interacting protein. *J Neurochem* 73:1765-1768.
- Matsuda S, Launey T, Mikawa S, Hirai H (2000) Disruption of AMPA receptor GluR2 clusters following long-term depression induction in cerebellar Purkinje neurons. *Embo J* 19:2765-2774.
- McElligott JG, Beeton P, Polk J (1998) Effect of cerebellar inactivation by lidocaine microdialysis on the vestibuloocular reflex in goldfish. *J Neurophysiol* 79:1286-1294.
- Mettens P, Godaux E, Cheron G, Galiana HL (1994) Effect of muscimol microinjections into the prepositus hypoglossi and the medial vestibular nuclei on cat eye movements. *J Neurophysiol* 72:785-802.
- Miles FA, Eighmy BB (1980) Long-term adaptive changes in primate vestibuloocular reflex. I. Behavioral observations. *J Neurophysiol* 43:1406-1425.
- Miles FA, Lisberger SG (1981) Plasticity in the vestibulo-ocular reflex: a new hypothesis. *Annu Rev Neurosci* 4:273-299.
- Miles FA, Braitman DJ, Dow BM (1980a) Long-term adaptive changes in primate vestibuloocular reflex. IV. Electrophysiological observations in flocculus of adapted monkeys. *J Neurophysiol* 43:1477-1493.
- Miles FA, Fuller JH, Braitman DJ, Dow BM (1980b) Long-term adaptive changes in primate vestibuloocular reflex. III. Electrophysiological observations in flocculus of normal monkeys. *J Neurophysiol* 43:1437-1476.
- Mitchiner JC, Pinto LH, Vanable JW, Jr. (1976) Visually evoked eye movements in the mouse (*Mus musculus*). *Vision Res* 16:1169-1171.
- Nagao S (1983) Effects of vestibulocerebellar lesions upon dynamic characteristics and adaptation of vestibulo-ocular and optokinetic responses in pigmented rabbits. *Exp Brain Res* 53:36-46.
- Nagao S (1989) Role of cerebellar flocculus in adaptive interaction between optokinetic eye movement response and vestibulo-ocular reflex in pigmented rabbits. *Exp Brain Res* 77:541-551.
- Nagao S, Ito M (1991) Subdural application of hemoglobin to the cerebellum blocks vestibuloocular reflex adaptation. *Neuroreport* 2:193-196.
- Nishizuka Y (1986) Studies and perspectives of protein kinase C. *Science* 233:305-312.
- Nishizuka Y (1992) Intracellular signaling by hydrolysis of phospholipids and activation of protein kinase C. *Science* 258:607-614.
- Oberdick J, Smeyne RJ, Mann JR, Zackson S, Morgan JI (1990) A promoter that drives transgene expression in cerebellar Purkinje and retinal bipolar neurons. *Science* 248:223-226.
- Oyster CW, Takahashi E, Collewijn H (1972) Direction-selective retinal ganglion cells and control of optokinetic nystagmus in the rabbit. *Vision Res* 12:183-193.

- Partsalis AM, Zhang Y, Highstein SM (1995) Dorsal Y group in the squirrel monkey. II. Contribution of the cerebellar flocculus to neuronal responses in normal and adapted animals. *J Neurophysiol* 73:632-650.
- Pastor AM, de la Cruz RR, Baker R (1994) Cerebellar role in adaptation of the goldfish vestibuloocular reflex. *J Neurophysiol* 72:1383-1394.
- Precht W (1978) *Neuronal operations in the vestibular system*. New York: Springer-Verlag.
- Provis JM (1979) The distribution and size of ganglion cells in the retina of the pigmented rabbit: a quantitative analysis. *J Comp Neurol* 185:121-137.
- Raphan T, Matsuo V, Cohen B (1979) Velocity storage in the vestibulo-ocular reflex arc (VOR). *Exp Brain Res* 35:229-248.
- Reisine H, Raphan T (1992) Unit activity in the vestibular nuclei of monkeys during off-vertical axis rotation. *Ann N Y Acad Sci* 656:954-956.
- Robinson DA (1964) The mechanics of human saccadic eye movement. *J Neurophysiol* 174:245-264.
- Robinson DA (1965) The mechanics of human smooth pursuit eye movement. *J Physiol (Lond)* 180:569-591.
- Robinson DA (1974) The effect of cerebellectomy on the cat's vestibulo-ocular integrator. *Brain Res* 71:195-207.
- Robinson DA (1976) Adaptive gain control of vestibuloocular reflex by the cerebellum. *J Neurophysiol* 39:954-969.
- Rodriguez F, Salas C, Vargas JP, Torres B (2001) Eye-movement recording in freely moving animals. *Physiol Behav* 72:455-460.
- Schairer JO, Bennett MV (1986a) Changes in gain of the vestibulo-ocular reflex induced by sinusoidal visual stimulation in goldfish. *Brain Res* 373:177-181.
- Schairer JO, Bennett MV (1986b) Changes in gain of the vestibulo-ocular reflex induced by combined visual and vestibular stimulation in goldfish. *Brain Res* 373:164-176.
- Schmid R, Jeannerod M (1985) Vestibular habituation: an adaptive process? *Rev Oculomot Res* 1:113-122.
- Shibuki K, Okada D (1991) Endogenous nitric oxide release required for long-term synaptic depression in the cerebellum. *Nature* 349:326-328.
- Shutoh F, Katoh A, Kitazawa H, Aiba A, Itohara S, Nagao S (2002) Loss of adaptability of horizontal optokinetic response eye movements in mGluR1 knockout mice. *Neurosci Res* 42:141-145.
- Skavenski AA, Robinson DA (1973) Role of abducens neurons in vestibuloocular reflex. *J Neurophysiol* 36:724-738.
- Smith MR, Nelson AB, Du Lac S (2002) Regulation of firing response gain by calcium-dependent mechanisms in vestibular nucleus neurons. *J Neurophysiol* 87:2031-2042.
- Smith PF, Curthoys IS (1989) Mechanisms of recovery following unilateral labyrinthectomy: a review. *Brain Res Brain Res Rev* 14:155-180.
- Stahl JS, Simpson JJ (1995) Dynamics of rabbit vestibular nucleus neurons and the influence of the flocculus. *J Neurophysiol* 73:1396-1413.
- Steinhausen (1933) Über die beobachtung der cupula in den bogengangsampullen des labyrinth der lebenden Hecht. *Pflügers Arch Ges Physiol* 232:500-512.

- Szél A, Lukáts A, Fekete T, Szepessy Z, Röhlich P (2000) Photoreceptor distribution in the retinas of subprimate mammals. *J Opt Soc Am A Opt Image Sci Vis* 17:568-579.
- Takemori S, Cohen B (1974) Loss of visual suppression of vestibular nystagmus after flocculus lesions. *Brain Res* 72:213-224.
- Takemori S, Suzuki M (1977) Cerebellar contribution to oculomotor function. *ORL J Otorhinolaryngol Relat Spec* 39:209-217.
- Ter Braak JWG (1936) Investigations on optokinetic Nystagmus. In: The oculomotor system of the rabbit and its plasticity (Collewijn H, ed), pp 180-237. New york: Springer Verlag.
- Tiao YC, Blakemore C (1976) Regional specialization in the golden hamster's retina. *J Comp Neurol* 168:439-457.
- Tiliket C, Shelhamer M, Roberts D, Zee DS (1994) Short-term vestibulo-ocular reflex adaptation in humans. I. Effect on the ocular motor velocity-to-position neural integrator. *Exp Brain Res* 100:316-327.
- Uemura T, Cohen B (1972) Vestibulo-ocular reflexes: effects of vestibular nuclear lesions. *Prog Brain Res* 37:515-528.
- Uemura T, Cohen B (1973) Effects of vestibular nuclei lesions on vestibulo-ocular reflexes and posture in monkeys. *Acta Otolaryngol Suppl* 315:1-71.
- Van Neerven J, Pompeiano O, Collewijn H (1989) Depression of the vestibulo-ocular and optokinetic responses by intrafloccular microinjection of GABA-A and GABA-B agonists in the rabbit. *Arch Ital Biol* 127:243-263.
- van Neerven J, Pompeiano O, Collewijn H (1991) Effects of GABAergic and noradrenergic injections into the cerebellar flocculus on vestibulo-ocular reflexes in the rabbit. *Prog Brain Res* 88:485-497.
- Vaney DI, Hughes A (1976) The rabbit optic nerve: fibre diameter spectrum, fibre count, and comparison with a retinal ganglion cell count. *J Comp Neurol* 170:241-251.
- Vibert N, Bantikyan A, Babalian A, Serafin M, Muhlethaler M, Vidal PP (1999) Post-lesional plasticity in the central nervous system of the guinea-pig: a "top-down" adaptation process? *Neuroscience* 94:1-5.
- Voogd J, Gerrits NM, Ruigrok TJ (1996) Organization of the vestibulocerebellum. *Ann N Y Acad Sci* 781:553-579.
- Waespe W, Henn V (1977a) Vestibular nuclei activity during optokinetic after-nystagmus (OKAN) in the alert monkey. *Exp Brain Res* 30:323-330.
- Waespe W, Henn V (1977b) Neuronal activity in the vestibular nuclei of the alert monkey during vestibular and optokinetic stimulation. *Exp Brain Res* 27:523-538.
- Waespe W, Cohen B, Raphan T (1983) Role of the flocculus and paraflocculus in optokinetic nystagmus and visual-vestibular interactions: effects of lesions. *Exp Brain Res* 50:9-33.
- Wang YT, Linden DJ (2000) Expression of cerebellar long-term depression requires postsynaptic clathrin-mediated endocytosis. *Neuron* 25:635-647.
- Watanabe E (1984) Neuronal events correlated with long-term adaptation of the horizontal vestibulo-ocular reflex in the primate flocculus. *Brain Res* 297:169-174.
- Westheimer G, Blair SM (1973) Oculomotor defects in cerebellectomized monkeys. *Invest Ophthalmol* 12:618-621.

- Westheimer G, Blair SM (1974) Function Organization of primate oculomotor system revealed by cerebellectomy. *Exp Brain Res* 21:463-472.
- Westheimer G, McKee SP (1975) Visual acuity in the presence of retinal-image motion. *J Opt Soc Am* 65:847-850.
- Wilson VJ, Melvill Jones G (1979) *Mammalian vestibular physiology*. New York: Plenum Press.
- Winterson BJ, Collewijn H, Steinman RM (1979) Compensatory eye movements to miniature rotations in the rabbit: implications for retinal image stability. *Vision Res* 19:1155-1159.
- Yamanaka T, Him A, Cameron SA, Dutia MB (2000) Rapid compensatory changes in GABA receptor efficacy in rat vestibular neurones after unilateral labyrinthectomy. *J Physiol* 523 Pt 2:413-424.
- Zee DS, Yamazaki A, Butler PH, Gucer G (1981) Effects of ablation of flocculus and paraflocculus of eye movements in primate. *J Neurophysiol* 46:878-899.
- Zee DS, Tusa RJ, Herdman SJ, Butler PH, Gucer G (1987) Effects of occipital lobectomy upon eye movements in primate. *J Neurophysiol* 58:883-907.
- Zhang Y, Partsalis AM, Highstein SM (1995) Properties of superior vestibular nucleus flocculus target neurons in the squirrel monkey. II. Signal components revealed by reversible flocculus inactivation. *J Neurophysiol* 73:2279-2292.
- Zuber BL (1968) Eye movement dynamics in the cat: the final motor pathway. *Exp Neurol* 20:255-260.
- Zuidam I, Collewijn H (1979) Vergence eye movements of the rabbit in visuomotor behavior. *Vision Res* 19:185-194.

CHAPTER 2

CHARACTERIZATION OF COMPENSATORY OCULAR REFLEXES IN C57BL/6 MICE

2.1 THE DYNAMIC CHARACTERISTICS OF THE MOUSE HORIZONTAL VESTIBULO-OCULAR AND OPTOKINETIC RESPONSE

A.M. van Alphen, J.S. Stahl, C.I. De Zeeuw

Van Alphen AM, Stahl JS, De Zeeuw CI (2001) Brain. Res. 890:296-305.

Abstract

In the present study the optokinetic reflex, vestibulo-ocular reflex and their interaction were investigated in the mouse, using a modified subconjunctival search coil technique. Gain of the ocular response to sinusoidal optokinetic stimulation was relatively constant for peak velocities lower than 8 °/sec, ranging 0.7-0.8. Gain decreased proportionally to velocity for faster stimuli. The vestibulo-ocular reflex acted to produce a sinusoidal compensatory eye movement in response to sinusoidal stimuli. The phase of the eye movement with respect to head movement advanced as stimulus frequency decreased, the familiar signature of the torsion pendulum behavior of the semicircular canals. The first-order time constant of the vestibulo-ocular reflex, as measured from the eye velocity decay after a head velocity step, was 660 ms. The response of the vestibulo-ocular reflex changed with stimulus amplitude, having a higher gain and smaller phase lead when stimulus amplitude was increased. As a result of this nonlinear behavior, reflex gain correlated strongly with stimulus acceleration over the 0.1-1.6 Hz frequency range. When whole body rotation was performed in the light the optokinetic and vestibular system combined to generate nearly constant response gain (approximately 0.8) and phase (approximately 0 degrees) over the tested frequency range of 0.1-1.6 Hz. We conclude that the compensatory eye movements of the mouse are similar to those found in other afoveate mammals, but there are also significant differences, namely shorter apparent time constants of the angular VOR and stronger non-linearities.

Introduction

In genetics studies, the mouse is probably the most important mammalian model, reflecting its technical advantages of short gestation, availability of embryonic stem cells that can be readily manipulated, and the large number of genetic probes already developed for use in this animal. Our knowledge of its ocular motor behavior, however, is still rudimentary, owing to the technical difficulty of recording eye movements in such a small animal. In the past eye movement recordings in mice have been attempted by electro-oculography (Grusser-Cornehls and Bohm, 1988), video oculography (Mitchiner et al., 1976; Balkema et al., 1984; Mangini et al., 1985; Katoh et al., 1998) or via the magnetic search coil technique, using temporary coils placed upon the eye at the time of the experiment (Koekkoek et al., 1997; De Zeeuw et al., 1998b; De Zeeuw et al., 1998a). The electro-oculography and older video oculography studies were flawed by calibration strategies based upon unrealistic assumptions that the gain of the optokinetic reflex (OKR) was unity at low stimulus velocities, while the more recent video study (Katoh et al., 1998) failed to account for the anatomic parameters of the eye when geometrically converting measurements of pupil displacement to angular rotation of the eye (see Discussion). Within the past two years, the magnetic search coil technique of eye movement recording (Robinson, 1963) has been adapted for use in the mouse in our laboratory (Koekkoek et al., 1997; De Zeeuw et al., 1998b; De Zeeuw et al., 1998a). The recordings in our previous studies were performed using a relatively large coil (3 mm in diameter) encircling the optical axis of the eye. While this technique was sufficient for the purposes of those studies, the relatively bulky coil may have distorted the normal ocular motor behavior. Indications of the potential problem were the low gain of the

OKR (Koekoek et al., 1997) and the occurrence of a large phase lead during the vestibulo-ocular reflex (VOR) (De Zeeuw et al., 1998b).

If valid quantitative comparisons between the ocular motor behavior of the mouse and larger species are to be made, a less invasive coil technique is necessary. We now introduce such a technique for the mouse, using a chronically implanted mini-coil (1 mm in diameter). The new method confirms the qualitative similarities between compensatory eye movements in the mouse and those of larger avoate mammals, but also suggests novel characteristics, including higher degrees of non-linearity and unusually short time constants.

Methods

All animal procedures described below were carried out under an animal care protocol that was approved by the local ethical committee of Erasmus University Rotterdam.

Animal care and surgical procedures

Seventeen C57BL/6 mice were tested. The C57BL/6 strain is thought to perform well in behavioral tests and therefore the most commonly used strain for knockout and transgenic manipulations (Gerlai, 1996). In order to assure alertness of the animals during experiments, the light-dark cycle of the animals was shifted by 12 hours.

Animals were anesthetized with a mixture of O₂, N₂O and 2% halothane. An acrylic head fixation pedestal was formed and fixed to the skull by 5 screws (M1, 1.5 mm). Screws were implanted on the frontal, parietal and interparietal bone plates. After completion of the construct, the head was positioned in a 70-degree roll so the eye could be easily approached. A small incision was made in the conjunctiva on the temporal side of the eyeball. A pocket was bluntly dissected anterior to the insertion of the lateral rectus muscle. A copper wire coil (1 mm outside diameter, 60 turns, 1.0 mg) was placed in the pocket. The coil was fixed to the sclera with 2 sutures (10/0 nylon, Ethicon®). The sutures were approximately aligned in the equatorial plane of the eye (Fig. 1). The conjunctiva was closed over the coil with an additional suture. The leads of the coil were carefully tunneled underneath the conjunctiva and the skin to a miniature coaxial MMCX connector that was attached to the top of the acrylic head pedestal. Full recovery from the surgery was not achieved until five days after implantation. The recovery could be monitored as an increase in gain to optokinetic stimuli. In three mice the response of the OKR was monitored starting three days after implantation of the search coil. The OKR was elicited by a sinusoidal stimulus of 8 °/sec at 0.4 Hz. Gain of the eye movement increased from 0.63 ±0.07 on day three to 0.76±0.06 on the 6th postoperative day (p<0.05, paired student t-test) (Fig. 2). Based on this recovery curve full recording sessions were not started until 6 days after coil implantation. In two cases it was necessary to include data that was recorded at postoperative day 5, to construct a three-day average for the animal.

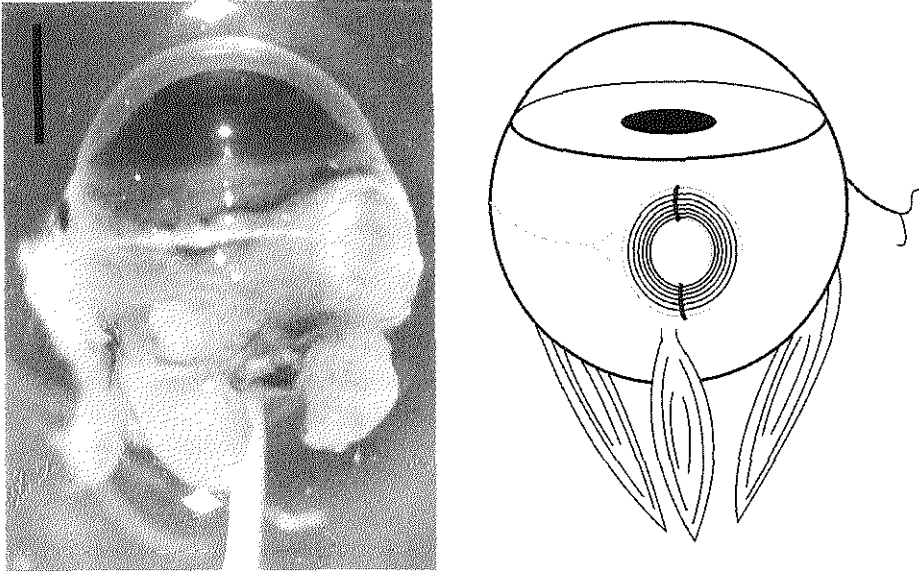


Figure 1: The figure shows a schematic drawing of the eye and a picture of a prepared mouse eye (ventral view). The scleral search coil is placed on the lateral surface of the left eye. The coil is attached to the sclera with two sutures. The conjunctiva is closed over the coil, so both the coil and its lead are located underneath the conjunctiva. The scale bar indicates 1 mm.

Eye movement recordings

Mice were immobilized in a custom-made restrainer incorporating an aluminum plate to which the mouse's head fixation pedestal was bolted. The front paws were left free. The restraint assembly was then mounted within magnetic field coils (CNC Engineering, Seattle, USA) atop a vertical-axis turntable (Biomedical Engineering Co., Thornwood, NY, USA). The midpoint of the interaural line was placed in the center of rotation for the optokinetic drum and the turntable. In order to maximize linearity of the eye movement transduction, the field coils were oriented about the mouse so that the horizontal magnetic field lines were approximately parallel to the surface of the eye-coil. Calibration was then achieved by rotating the field coils over ± 10 degrees about this optimum position while the animal maintained a stationary eye position. Thus, zero eye position corresponded to the animal's eye position at the time of calibration, and our recordings reflect eye position with respect to this resting position. Since our recordings (see below) suggest that the mouse, like the rabbit (Collewijn, 1970), tends to restrict eye eccentricity to a relatively limited range, this arbitrary zero position is probably no more than a few degrees from the center of the animal's preferred ocular motor range.

Optokinetic stimuli were delivered with a striped drum (width of bars was 4 deg). The drum had a diameter of 26 centimeters and enclosed the animal from zenith to 45 degrees below the horizon. To test the performance of the optokinetic system two different approaches were used. First, the frequency response of the OKR was tested by rotating the drum at frequencies of 0.1, 0.2, 0.4, 0.8 and 1.6 Hz with a peak velocity of

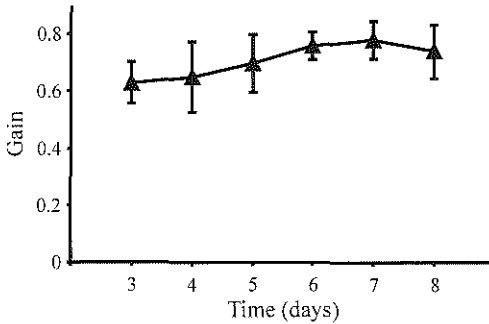


Figure 2: The recovery from surgery was monitored in three animals. As a measure of recovery the response to an optokinetic stimulus of 0.4 Hz was taken (8 °/sec peak velocity). Gain of the response was averaged across animals and plotted against time, starting on the third day after implantation of the coil. The errorbars show one standard deviation.

8 °/sec. The effect of peak velocity on gain of the OKR was evaluated by using sinusoidal stimuli at 0.4 Hz and peak velocities of 2, 4, 8, 16, and 32 °/sec. In addition, the drum was rotated at a constant velocity to elicit an optokinetic nystagmus. The optokinetic nystagmus was measured at the same stimulus velocities as the sinusoidal OKR. Velocity step stimuli (6 °/sec) were also delivered, by randomly alternating -3 and 3 °/sec constant velocity rotation.

The VOR was evaluated during sinusoidal, whole body rotation in the dark. Sinusoidal stimulation was performed at 0.1, 0.2, 0.4, 0.8, and 1.6 Hz and stimulus amplitudes of 5 or 10 deg. Velocity steps were delivered by alternating table velocity from -15 to 15 °/sec at a rate of 0.1 Hz. Peak acceleration of the turntable during a velocity step was 400°/sec². The visually enhanced vestibulo-ocular reflex (VVOR) was tested using the VOR stimulus parameters, while the animal viewed the illuminated, earth-fixed drum. The OKR, VOR and VVOR in response to sinusoidal stimuli were tested in 6 mice. The stimuli were delivered in three sessions on consecutive days at least five days after surgery. Each session consisted of three trials per stimulus. OKR, VOR and VVOR trials were randomly alternated within the session. Optokinetic and head velocity step stimuli were delivered to 11 and 10 animals respectively.

Data analysis

All recorded signals were filtered on-line at 20 Hz using a 4th order Bessel filter (Axon Instruments, Foster City, CA) and digitized at 500 Hz with 32-bit precision (CED, Cambridge, UK). Eye, head and drum position were differentiated off-line, using a 3-point software algorithm. Sinusoidal data was digitally filtered at a frequency of 20 Hz using a software Butterworth filter. Fast phases were identified and excised from the eye velocity data using combined velocity and acceleration criteria. The gain and phase of the response were calculated from the remaining slow-phase portions of the velocity signal by fitting a sine wave using least-square optimization. In this analysis the fundamental frequency of the eye movement was assumed to equal the stimulus frequency. Gain and phase values were combined per trial to yield session averages. Session averages were again averaged to yield final gain and phase values per mouse. All values reported are mean±sd, weighting each mouse equally.

The eye movement recordings obtained after optokinetic stimulation with a constant velocity were treated in the same way as sinusoidal traces. After fast phases were excised from the time base, steady state eye velocity was measured as the average slow phase eye velocity. Average slow phase eye velocity was calculated across all remaining samples spanning a time period from 10 seconds after the onset of eye movement to the moment the light was extinguished.

The latency of the optokinetic response to a velocity step was determined by measuring the onset of change in eye velocity in response to a velocity step of the drum. After data was differentiated it was filtered at 60 Hz. At least 35 step responses in each direction were averaged, aligned upon the onset of stimulus transition. We excluded any trials in which a fast phase occurred within 1 second before or after the stimulus transient. The averaged velocity curves for clockwise and counterclockwise stimuli were each referenced to the mean pre-step eye velocity and then superimposed. We defined the onset of the response to the velocity step as the last point of intersection between the re-referenced averaged eye velocity curves. Latency was measured as the difference between this point of divergence and the onset of drum movement.

We determined the dominant time constant of the VOR from the averaged responses to at least 20 velocity steps of the turntable. Eye velocity ($E'(t)$) was again obtained by differentiation of eye position traces and filtered at 60 Hz. We fitted a single exponential curve ($E'(t)=Ae^{(-t/\tau)}+B$) by least-square optimization to the epoch spanning 0.2-1.2 sec. after the reversal of turntable direction. In this equation τ was taken as the time constant for the VOR.

All statistical analyses were performed using a commercially available package (Prism, GraphPad Software, Inc., San Diego, USA).

Results

General findings

At the beginning of each recording session mice were allowed to habituate to the restrainer for 15 minutes. During this period eye position was recorded. Spontaneous gaze-shifting eye movements (saccades) rarely occurred, and when they did, they were small. Thus, eye-in-orbit positions generally remained within ± 7 degrees of the arbitrary zero position defined during calibration (see Methods). The rarity of saccades might indicate that mice, like other avoate mammals, normally use combined eye-head saccades to explore their environment (Fuller, 1981). When spontaneous saccades were made, the new eye position was never held very long before the eye was returned toward the central position by a centripetal saccade or a smooth drift. In order to determine if the eye drift was due to leakage of the velocity-to-position (neural) integrator, gaze holding ability was evaluated in 10 mice. In these mice the eye was brought to an eccentric position by slowly moving the turntable in the illuminated environment. After a new position in the orbit was reached the light was turned off and the time constant of the decay back to resting position was measured by fitting a single exponential ($E(t)=Ae^{(-t/\tau)}+B$) (Fig. 3). This procedure yielded an average time constant of 2.1 ± 0.7 sec for the neural integrator. The maximal eye deviation that could be reached in this manner ranged 5-9 degrees. Beyond this range, centripetal fast phases occurred. There was little

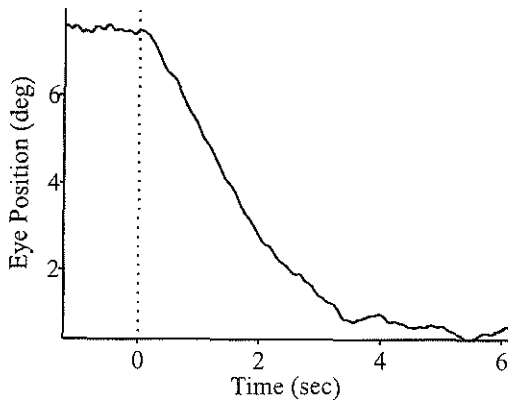


Figure 3: An example of the gaze holding ability of the mouse in the dark is shown. The eye was brought to an eccentric position by slowly rotating the animal in the light. The consequent VVOR resulted in a displacement of the eye approximately 7 degrees from the rest position. At the dotted line the light was extinguished. The eye decayed back to its resting position with an approximately exponential time course.

variation in the final resting position (B in the equation above) between trials. Averaged across animals, the standard deviation of B was only 1 degree, confirming that the arbitrary zero position as defined was very close to the true neutral eye position, and demonstrating how narrow the range of preferred resting positions was.

Optokinetic responses

When the optokinetic drum was rotated sinusoidally, eye movement responses were virtually sinusoidal, indicating the linear behavior of the optokinetic response (OKR) at low stimulus velocities. Figure 4a shows a representative response to a stimulus of 0.2 Hz, 8 °/sec peak velocity (6.3 deg amplitude). At higher peak-velocities responses tended to become distorted, evincing a more triangular profile. Such responses have been described for other afoveate animals (Collewyn, 1969; Keng and Anastasio, 1997) and reflect velocity saturation in the optokinetic system. Sinusoids were fit to the data to determine the gain and phase at the fundamental frequency of the response. Gain was constant at 0.77 ± 0.02 for stimulus velocities of 8 °/sec and smaller, but decreased at higher velocities (Fig. 4b).

Because of the obvious velocity dependence of the OKR, the frequency response of the OKR was evaluated at a constant velocity of 8 °/sec. Gain was 0.70 ± 0.07 at 0.1 Hz, 0.74 ± 0.06 at 0.8 Hz, and 0.57 ± 0.07 at 1.6 Hz (Fig. 4c). Eye velocity progressively lagged drum velocity as stimulus frequency increased. At 0.1 Hz, eye velocity lagged drum velocity by 0.5 ± 1.3 deg; at 1.6 Hz the lag had increased to 61.8 ± 6.7 deg (Fig. 4d).

The phase of the optokinetic response reflects a combination of the system's fixed delay and dynamic terms. In order to distinguish these two components, we determined the latency of the optokinetic pathway by averaging the eye velocity response to random velocity steps (Fig. 5). The system delay measured 70 ± 12 ms.

The OKR was also evaluated during constant velocity stimulation. The response to sudden illumination of the rotating drum consisted of a rapid initial rise in eye velocity followed by a slow build-up to a steady state (Fig. 6a). The size of the initial rise in

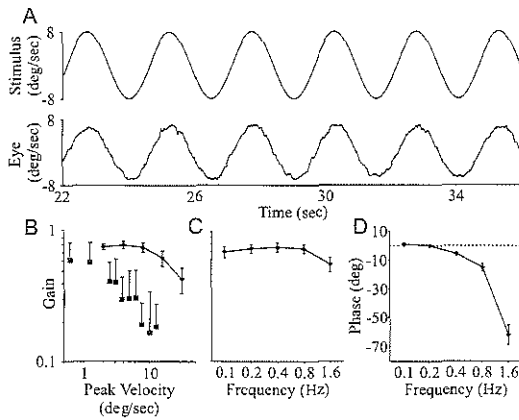


Figure 4: A. An example of a response to a sinusoidal optokinetic stimulus at 0.2 Hz and peak velocity 8 °/sec. B. Average gain of 6 animals, of the OKR to 0.4 Hz sinusoidal stimuli plotted against peak velocity of the stimulus (◆). Error bars indicate one standard deviation. Gain of the response remained constant around 0.8 for velocities lower than 8 °/sec. For comparison, earlier data obtained using the large coil (diameter: 3 mm), is also plotted (■). C. Average gain of the OKR to 8 °/sec (peak velocity) sinusoidal stimuli, plotted against the frequency of the stimulus. D. Phase of eye velocity relative to drum velocity, plotted against stimulus frequency (8 °/sec peak velocity). A negative value indicates a phase lag with respect to the stimulus.

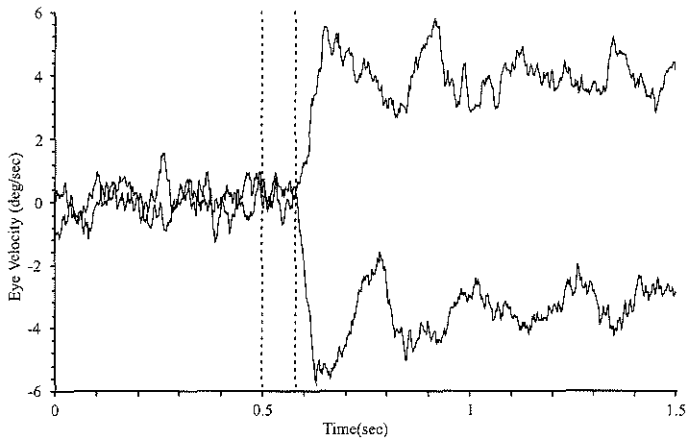


Figure 5: Average of 61 responses to a 6 °/sec (-3 °/sec to 3 °/sec) velocity step of the drum. The upper trace shows the average response for a step in clockwise direction, while the lower trace shows the response to a step in counter clockwise direction. The eye velocity traces were shifted so that the average eye velocity was 0 °/sec over the 500 ms prior to the onset of stimulus turn around. The first dotted line indicates the onset of stimulus turn around. The second dotted line indicates the last point of intersection between the traces of clockwise and counterclockwise eye movement. The distance between the two points was taken as the latency of the optokinetic response (77 ms in the graph).

slow-phase eye velocity was dependent on stimulus velocity (Fig. 6b). A single exponential could be fitted to the data, showing that eye velocity saturated at 9.8 °/sec for higher stimulus velocities ($r^2=0.98$). Saturation of initial eye velocity is in reasonable agreement with the results from sinusoidal stimulation, which indicated that steady-state

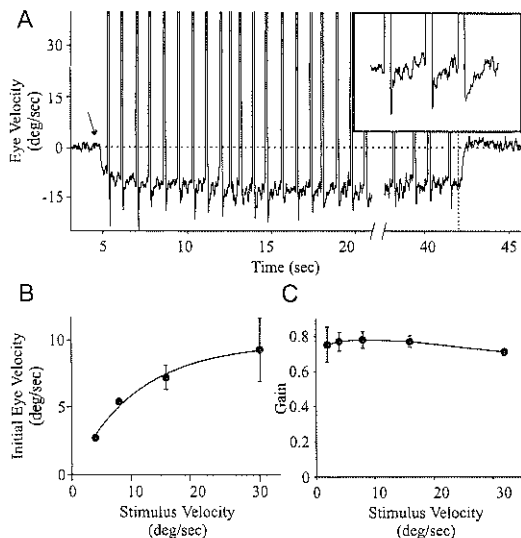


Figure 6: A. An example of the OKR to a constant 16 °/sec leftward rotation of the drum. After light was turned on (arrow), a quick initial rise in eye velocity occurred, which was followed by a gradual increase in slow phase eye velocity until a steady state was reached. Steady state eye velocity was maintained for at least 15 seconds, after which the light was turned off (vertical dotted line). Hardly any OKAN was observed. The inset shows a magnification of three beats of optokinetic nystagmus. Note the decrease of eye velocity during each slow phase. B. The amplitude of the quick initial raise in eye velocity was plotted against stimulus velocity. An exponential was fitted to the data (solid line). C. The steady state gain of the OKR in response to constant velocity stimulation was plotted against stimulus velocity. Error bars show one standard deviation.

sinusoidal gain saturates at peak stimulus velocities of approximately 8 °/sec. The steady-state constant velocity gain ranged from 0.75 ± 0.10 at 2 °/sec to 0.71 ± 0.02 at 32 °/sec (Fig. 6c).

We attempted to elicit optokinetic after nystagmus (OKAN) by extinguishing the lights at least 35 seconds after the onset of eye movement. Under our conditions, a classic sustained OKAN was rarely observed. Following a 32 °/sec stimulus, one or two beats of OKAN occasionally occurred, but the duration of this nystagmus was never long enough to allow a time constant to be measured. The lack of OKAN, the frequent departure of the slow buildup from an exponential profile, and the relatively large phase leads of VOR at low stimulus frequencies (see below) all suggest that velocity storage in the mouse is minimal under our stimulus conditions.

Vestibular responses

Horizontal VOR was elicited by whole body rotation of the animal in the dark. Unlike the OKR, which became distorted at high stimulus frequencies/velocities, vestibular eye movements were uniformly sinusoidal for all stimulus parameters we employed. At low frequencies (0.1 Hz) no response could be obtained and gain was consequently assumed to be 0. While this finding could indicate a threshold effect, it is also possible that a response was present but could not be detected in the system noise (which measured 0.2 degrees peak-to-peak with the animal at rest). In all animals a systematic effect of stimulus amplitude on gain and phase was seen. Therefore, average values are reported

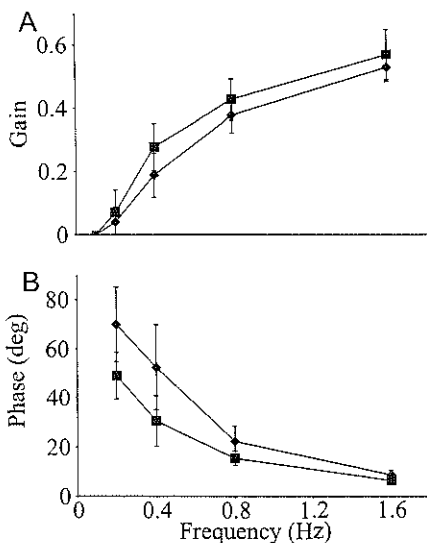


Figure 7: Gain (A) and phase (B) of the VOR were plotted against frequency for 5 deg (◆) and 10 deg (■) amplitude. Positive phase values indicate a phase lead of eye velocity with respect to head velocity. No response could be detected at 0.1 Hz for either amplitude. Note the dependence of both VOR gain and phase upon stimulus amplitude.

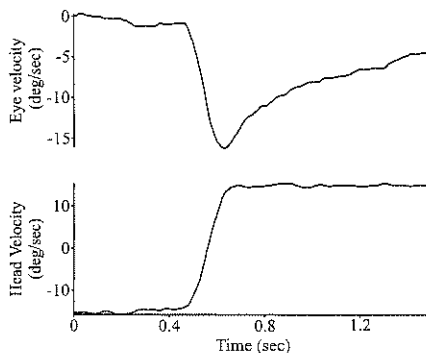


Figure 8: An average of 20 eye velocity responses (upper trace) to a velocity step of the turn table (lower trace). The size of the velocity step was 30 °/sec (-15 to 15 °/sec). Eye velocity decayed back to 0 °/sec with an approximately exponential time course.

separately for different stimulus amplitudes.

For all amplitudes the VOR showed properties of a high-pass filter in that gain increased and phase lead decreased as frequency was increased (Fig. 7a,b). For stimulus amplitudes of 10 deg, gain rose from 0 ± 0 to 0.57 ± 0.08 as frequency was increased from 0.1 Hz to 1.6 Hz. At 5 deg amplitude the curve reached its maximum value of 0.53 ± 0.05 at 1.6 Hz. Eye movement led head movement at all tested frequencies and amplitudes. Phase lead decreased with increasing frequency, from 49.0 ± 9.5 deg at 0.2 Hz to 6.4 ± 1.4 deg at 1.6 Hz (10 deg stimulus amplitude).

In the range of tested frequencies, the amplitude of the stimulus also affected gain and phase (Fig. 7a, b). A two-way ANOVA was performed on the average gain and phase data. The effect of amplitude on both gain and phase proved to be significant ($p=0.0065$ and $p<0.0001$, respectively).

Under the assumption that the low frequency behavior of the average VOR phase curve was determined by first order high-pass characteristics, the data was fitted with a single-pole transfer function ($\text{Phase} = (180/\pi) * \text{atan}(\omega^{-1} \tau^{-1})$). This calculation yielded values of 370 ± 40 and 690 ± 50 ms for the VOR time constant at 5 and 10 degrees amplitudes. The correlation coefficients for the fits to the phase curves were 0.77 and 0.85, respectively. It should be noted that, even at 10 degrees, the calculated time

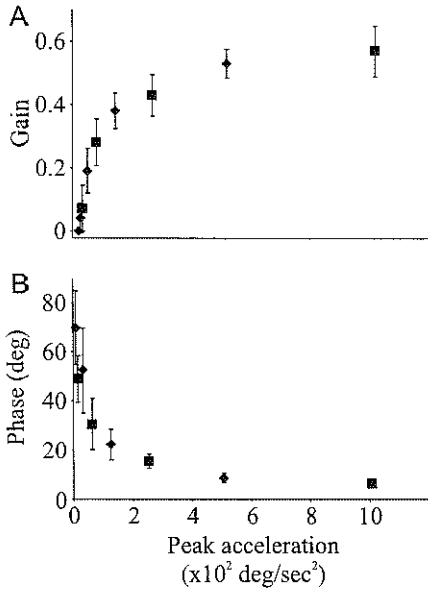


Figure 9: Gain (A) and phase (B) of the VOR were plotted against peak acceleration of the head. Symbols depict 5 deg (\blacklozenge) and 10 deg (\blacksquare) amplitude. The results from all stimulus amplitudes lie upon a single curve.

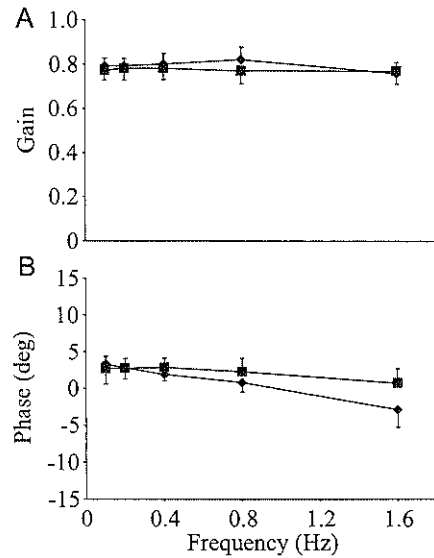


Figure 10: Average gain (A) and phase (B) of the VVOR were plotted against frequency for 5 deg (\blacklozenge) and 10 deg (\blacksquare) amplitude. These indices of VVOR performance were roughly constant across the entire tested frequency range.

constant is still exceptionally low by comparison to other animals (Robinson, 1976; Buettner et al., 1978; Raphan et al., 1979). Therefore, we validated the value by measuring it in another fashion - by analyzing the eye velocity response to a whole body velocity step in the dark. After a step of $30^\circ/\text{sec}$, eye velocity decayed with an approximately exponential time course. A single exponential was fitted to obtain the time constant of the decay (Fig. 8). The average time constant was thus estimated to be 660 ± 280 msec.

The influence of amplitude on both phase and gain of the VOR reflects a non-linearity in the vestibular system of the mouse. In fact, plotting gain and phase against peak acceleration instead of frequency collapsed the family of curves shown in figure 7 to a single curve (Fig. 9a,b). If the VOR was solely dependent on frequency, then separate curves should emerge in such a plot, for each set of frequencies. As the figure shows this separation does not occur and therefore the most important factor that determines the gain in the studied frequency range appears to be peak acceleration.

Visuo-vestibular interaction

VVOR gain was 0.78 ± 0.02 over the entire frequency range tested. Amplitude of the stimulus signal had no influence on gain (Fig 10a). Phase of the eye movement was close

to zero at all stimuli (Fig. 10b). Phase lead decreased slightly when frequency was increased, changing to a moderate phase lag at 1.6 Hz.

Discussion

The present experiments have yielded the most detailed description of compensatory eye movements in the mouse to date. In many respects optokinetic and vestibular eye movements in this species were similar to those of other afoveate species, such as the rabbit. Eye movements could be elicited by rotation of a surrounding striped drum or by whole body rotation. The horizontal frequency response of the optokinetic system was found to be essentially low pass, in that its gain fell and phase lag increased as frequency increased. Similar characteristics have been shown for the OKR in numerous species (Collewijn, 1969; Godaux et al., 1983; Paige, 1983; Hess et al., 1985). Gain at low peak velocities was relatively constant in the mouse (ranging 0.7-0.8), and comparable to values reported for the rabbit (0.7-0.8) (Collewijn, 1969; Nagao, 1983; De Zeeuw et al., 1995) and the rat (0.7-0.9) (Hess et al., 1985). When peak stimulus velocity was increased, gain of the response declined proportionally. The form of the OKR velocity-tuning curve reflects a saturation occurring in the visual pathways above stimulus velocities of 8-9 °/sec in the closed-loop condition. In the cat this value has been reported to be 6 °/sec (Godaux et al., 1983) and in the rabbit 1 °/sec (Collewijn, 1969).

The response of the mouse to constant velocity optokinetic stimuli exhibited the familiar biphasic profile seen in other species (Collewijn, 1969; Cohen et al., 1977; Paige, 1983; Maioli and Precht, 1984; Hess et al., 1985). An initial fast rise in eye velocity was followed by a slower build-up to a final steady state. In foveate species the initial acceleration is very prominent. It has a gain between 0.55 and 0.65 for stimuli of 30 °/sec and higher in monkeys (Cohen et al., 1977) and is thought to reflect in large part the cortically mediated smooth pursuit system. In afoveate species, which lack smooth pursuit, the initial component is smaller and is thought to reflect more direct subcortical pathways, perhaps involving the accessory optic system. The magnitude of the initial response in the mouse (9 °/sec) was comparable to other afoveate species, in which initial OKR eye velocities around 10 °/sec are reported (Collewijn, 1969; Hess et al., 1985; Keng and Anastasio, 1997).

The neural integrator is less prominent in the mouse

The velocity-to-position (neural) integrator generates a desired eye position command from the velocity-encoded premotor signals (Skavenski and Robinson, 1973; Godaux and Cheron, 1993). A number of lines of evidence suggest that the neural integrator is comparatively weak in mice. First, fast phases of vestibular and optokinetic nystagmus were often followed by backwards drifts. These decays, which are consistent with reduced neural integration, became more pronounced at lower stimulus velocities when fewer fast phases occurred. Second, direct tests of eye stability following step-, vestibularly-evoked displacements revealed an integrator time constant of only 2.1 ± 0.7 . This value is very low compared to 20 seconds in cat (Robinson, 1974) and monkey (Cannon and Robinson, 1987). Third, we measured a transport delay of 70 msec. for the mouse optokinetic system. OKR phase in lateral eyed mammals has been said to be

dictated by this delay in the optokinetic system (Collewijn, 1969; Hess et al., 1985). However, at stimulus frequencies below 1.0 Hz, a 70 msec. delay would cause a larger phase lag than was actually observed. This result would be explained by the weaker neural integrator which, by producing less than the usual amount of phase lag, would simulate the presence of a lead element, and so counter the phase lag produced by the visual system's pure delay element. Of note, at frequencies above 1.0 Hz, phase lag became larger than the value predicted by a fixed delay. This result may reflect additional low-pass dynamic characteristics of the optokinetic system, which become dominant at higher frequencies where the lead-producing effects of the leaky neural integrator fall off. Fourth and finally, the short time constant of the VOR provides additional evidence for a comparatively weak neural integrator.

VOR dynamics have been generally explained in terms of the mechanical properties of the peripheral organ (Steinhausen, 1933), which is modeled as an overdamped torsion pendulum. In the absence of velocity storage (which we find to be weak in the mouse, see below) the time constant of the VOR should mirror that of the cupula (Skavenski and Robinson, 1973). Based upon allometric considerations, that cupular time constant should be approximately 3 sec in the mouse (Jones and Spells, 1963). Primary vestibular afferents have not been recorded in the mouse, but in the rat their time constant measures 3.4 sec (Curthoys, 1982). The mouse VOR has the expected high pass characteristics, i.e. gain increases and phase lead decreases with increasing frequency. However, we calculated the mouse VOR time constant from both frequency- and time-domain methods to be around 690 ms, well below the probable cupular time constant. This low time constant is also consistent with the relative phase-leading effects of a weak velocity to position integration.

The integrator time constant could be affected by the presence of a scleral search coil. Placement of a search coil may change the viscoelastic properties of the oculomotor plant in a way that would mimic a reduced time constant for the neural integrator. However, such an effect of the minicoil cannot fully account for the behavior of the mouse oculomotor system since rapid centripetal decays following fastphases have also been observed using video recording (Stahl, personal communication). These findings support our measurements of short integrator time constants, and argue that the short time constants are not an artifact of search coil implantation.

Velocity storage is impaired in the mouse

The velocity storage mechanism serves to store velocity of the visual surround to stabilize gaze during constant velocity motion of the world (Cohen et al., 1977). When a constant velocity optokinetic stimulus is presented eye velocity typically exhibits a delayed, exponential increase towards a steady state. This build-up reflects charging of the velocity storage mechanism. In the mouse build-up of eye velocity differed from that described in other species. It was smaller and had a more variable profile. Thus velocity storage appears to be weak in the mouse, at least under the current stimulus conditions. In support of this conclusion, extinction of the lights following prolonged unidirectional optokinetic stimulation never elicited a well developed, optokinetic after nystagmus (OKAN).

Non-linear aspects of the VOR in the mouse

Previous studies have focused on the degree to which linear systems analysis could explain vestibular data. Some of these (Baarsma and Collewijn, 1974; Collewijn et al., 1980; Paige, 1983) observed non-linearities. Non-linearities were found at high frequencies, where an amplitude dependence of gain arose because of cutoff of cell activity in the primary vestibular afferents (Paige, 1983). In afoveate animals, non-linearities have also been reported at lower frequencies. In the rabbit, phase lead and gain of the vestibular response was found to be mildly dependent on stimulus amplitude (Baarsma and Collewijn, 1974; Collewijn et al., 1980). However, this amplitude dependence was not as pronounced in the rabbit as it was in the mouse. The present results suggest that the amplitude dependence of gain and phase arises because of the strong acceleration dependence of both quantities.

It is conceivable that the amplitude dependence of the VOR is partly caused by the presence of the scleral search coil. A possible way in which amplitude dependent changes in gain could arise due to the coil, would be when a dead zone was present between movement of the eye and displacement of the coil. Such a dead zone would cause recorded eye movement to be smaller than the actual eye movement and would thus depress gain with respect to the actual performance of the animal. Recorded amplitude of the eye would always reflect the real amplitude of the eye minus the amplitude of the dead zone and thus the relative contribution of the dead zone would decrease as the real amplitude of the eye is increased. Therefore, depression of gain would be more pronounced at smaller stimulus amplitudes causing an amplitude dependence of the system. However, the effect of a dead zone in coil movement would be the same under all stimulus conditions. Therefore any such amplitude dependence should also be present in the VVOR. Figure 10 clearly shows this is not the case; gain of the VVOR is the same for both tested amplitudes.

Although backlash between the coil and the eye did not occur, the amplitude dependence of the VOR may still be partly caused by a dead zone. This dead zone could be in the form of a threshold within the VOR circuitry. Such a threshold was observed in the present experiments, since we were unable to elicit a VOR response for accelerations below $8^\circ/\text{sec}^2$. However, It is possible that the response was simply undetectable within the combined noise of the mouse ocular motor system and our recording system. This explanation is supported by previous studies, which have argued against the presence of thresholds. In rabbits eye movements were recorded to vestibular stimuli with amplitudes as small as 2.5 min arc at 0.22 Hz (Winterson et al., 1979); no apparent threshold could be detected.

Relationship of current study to past recordings in the mouse

There have been earlier attempts at recording eye movements in mice. The current study improves on these older investigations in a number of respects. Grüsser-Cornehls and Böhm (1988) recorded eye movements using electro-oculography. The authors reported that the animals needed to be sedated to record compensatory eye movements and that responses could only be elicited in 50% of the tested animals. In contrast, we found robust optokinetic responses in all animals and sedation was never necessary. In

addition, electro-oculography did not allow for accurate quantification of the eye movements since calibration was based upon the assumption that the gain of the OKR is unity at low stimulus velocities. Our data disprove this assumption; the gain of the OKR is no greater than 0.8 at low peak velocities. Calibration was also a problem in a more recent mouse study using video oculography (Katoh et al., 1998). Katoh et al. (1998) measured motion of the mouse pupil, and converted it to angular rotation of the eye based upon an assumption of an eye radius of 1.6 mm. In calculating the distance of the pupil to the geometric center of the eye, they failed to deduct the depth of the anterior chamber (about 0.55 mm in the mouse). Finally, the present recordings also demonstrate the limitations of our own, previous investigations, using a larger search coil temporarily placed upon the eye (Koekkoeck et al., 1997; De Zeeuw et al., 1998b; De Zeeuw et al., 1998a). Based on current recordings with the smaller, chronically implanted, subconjunctival minicoil, we now suspect that the larger coil, which surrounded the entire limbus of the eye, distorted the compensatory eye movements because it impeded the free motion of the eye. In comparison to previous results, optokinetic and vestibular gains were considerably higher in the current study. The VOR gain at 0.8 Hz -10 deg. amplitude was 0.43 when measured with a minicoil, compared to 0.25 using the larger coil (De Zeeuw et al., 1998b; De Zeeuw et al., 1998a)

We have also undertaken experiments to record eye movements using an improved video calibration strategy (Stahl et al., 2000). Although the use of a minicoil greatly improved on the results from previous coil recordings in mice (Koekkoeck et al., 1997; De Zeeuw et al., 1998a), video recordings revealed that ocular motility was still slightly affected by coil placement. Gain of the VVOR was marginally smaller after animals had been implanted with a search coil. No effect of the coil on the phase of the eye movement with respect to head movement could be found (Stahl et al., 2000). Despite the effect the minicoil has on eye movement, there remain a number of advantages in using coil oculography. First, it is more difficult to precisely calibrate the video recordings. To calibrate the video, recorded pixel displacement needs to be converted into degrees of rotation. Any calculation of the angular displacement relies on accurate measurement of the pupil radius. Second, contrary to coil recordings the video technique is subject to artifacts like blinks and loss of pupil detection due to interference from the illuminating light; therefore video tracking the eye requires continuous attention. Maintaining a good quality video recording means, at least in some animals, occasionally adjusting the illumination and software tracking parameters. Thus, in neurophysiology studies where eye movement is only one of the variables being tracked, the more robust coil recording may be preferable.

References

- Baarsma E, Collewijn H (1974) Vestibulo-ocular and optokinetic reactions to rotation and their interaction in the rabbit. *J Physiol* 238:603-625.
- Balkema GW, Mangini NJ, Pinto LH, Vanable JW, Jr. (1984) Visually evoked eye movements in mouse mutants and inbred strains. A screening report. *Invest Ophthalmol Vis Sci* 25:795-800.
- Buettner UW, Buttner U, Henn V (1978) Transfer characteristics of neurons in vestibular nuclei of the alert monkey. *J Neurophysiol* 41:1614-1628.

- Cannon SC, Robinson DA (1987) Loss of the neural integrator of the oculomotor system from brain stem lesions in monkey. *J Neurophysiol* 57:1383-1409.
- Cohen B, Matsuo V, Raphan T (1977) Quantitative analysis of the velocity characteristics of optokinetic nystagmus and optokinetic after-nystagmus. *J Physiol (Lond)* 270:321-344.
- Collewijn H (1969) Optokinetic eye movements in the rabbit: input-output relations. *Vision Res* 9:117-132.
- Collewijn H (1970) The normal range of horizontal eye movements in the rabbit. *Exp Neurol* 28:132-143.
- Collewijn H, Winterson BJ, van der Steen J (1980) Post-rotary nystagmus and optokinetic after-nystagmus in the rabbit linear rather than exponential decay. *Exp Brain Res* 40:330-338.
- Curthoys IS (1982) The response of primary horizontal semicircular canal neurons in the rat and guinea pig to angular acceleration. *Exp Brain Res* 47:286-294.
- De Zeeuw CI, Wylie DR, Stahl JS, Simpson JI (1995) Phase Relations of Purkinje Cells in the Rabbit Flocculus During Compensatory Eye Movements. *J of Neurophysiol* 74:2051-2063.
- De Zeeuw CI, van Alphen AM, Koekkoek SK, Buharin E, Coesmans MP, Morpurgo MM, van den Burg J (1998a) Recording eye movements in mice: a new approach to investigate the molecular basis of cerebellar control of motor learning and motor timing. *Otolaryngol Head Neck Surg* 119:193-203.
- De Zeeuw CI, Hansel C, Bian F, Koekkoek SK, van Alphen AM, Linden DJ, Oberdick J (1998b) Expression of a protein kinase C inhibitor in Purkinje cells blocks cerebellar LTD and adaptation of the vestibulo-ocular reflex. *Neuron* 20:495-508.
- Fuller JH (1981) Eye and head movements during vestibular stimulation in the alert rabbit. *Brain Res* 205:363-381.
- Gerlai R (1996) Gene-targeting studies of mammalian behavior: is it the mutation or the background genotype? [see comments] [published erratum appears in *Trends Neurosci* 1996 Jul;19(7):271]. *Trends Neurosci* 19:177-181.
- Godaux E, Cheron G (1993) Testing the common neural integrator hypothesis at the level of the individual abducens motoneurons in the alert cat. *J Physiol* 469:549-570.
- Godaux E, Gobert C, Halleux J (1983) Vestibuloocular reflex, optokinetic response, and their interactions in the alert cat. *Exp Neurol* 80:42-54.
- Grusser-Cornehls U, Bohm P (1988) Horizontal optokinetic ocular nystagmus in wildtype (B6CBA^{+/+}) and weaver mutant mice. *Exp Brain Res* 72:29-36.
- Hess BJ, Precht W, Reber A, Cazin L (1985) Horizontal optokinetic ocular nystagmus in the pigmented rat. *Neuroscience* 15:97-107.
- Jones GM, Spells KE (1963) A theoretical and comparative study of the functional dependence of the semicircular canal upon its physical dimensions. *Proc Roy Soc Lond* 157:403-419.
- Katoh A, Kitazawa H, Itohara S, Nagao S (1998) Dynamic characteristics and adaptability of mouse vestibulo-ocular and optokinetic response eye movements and the role of the flocculo-olivary system revealed by chemical lesions. *Proc Natl Acad Sci U S A* 95:7705-7710.
- Keng MJ, Anastasio TJ (1997) The horizontal optokinetic response of the goldfish. *Brain Behav Evol* 49:214-229.

- Koekkoek SK, v. Alphen AM, v.d. Burg J, Grosveld F, Galjart N, De Zeeuw CI (1997) Gain adaptation and phase dynamics of compensatory eye movements in mice. *Genes Funct* 1:175-190.
- Maioli C, Precht W (1984) The horizontal optokinetic nystagmus in the cat. *Exp Brain Res* 55:494-506.
- Mangini NJ, Venable JW, Jr., Williams MA, Pinto LH (1985) The optokinetic nystagmus and ocular pigmentation of hypopigmented mouse mutants. *J Comp Neurol* 241:191-209.
- Mitchiner JC, Pinto LH, Venable JW, Jr. (1976) Visually evoked eye movements in the mouse (*Mus musculus*). *Vision Res* 16:1169-1171.
- Nagao S (1983) Effects of vestibulocerebellar lesions upon dynamic characteristics and adaptation of vestibulo-ocular and optokinetic responses in pigmented rabbits. *Exp Brain Res* 53:36-46.
- Paige GD (1983) Vestibuloocular reflex and its interactions with visual following mechanisms in the squirrel monkey. I. Response characteristics in normal animals. *J Neurophysiol* 49:134-151.
- Raphan T, Matsuo V, Cohen B (1979) Velocity storage in the vestibulo-ocular reflex arc (VOR). *Exp Brain Res* 35:229-248.
- Robinson DA (1963) A method of measuring eye movement using a scleral search-coil in magnetic field. *IEEE Trans Biomed Eng* 10:137-145.
- Robinson DA (1974) The effect of cerebellectomy on the cat's vestibulo-ocular integrator. *Brain Res* 71:195-207.
- Robinson DA (1976) Adaptive gain control of vestibuloocular reflex by the cerebellum. *J Neurophysiol* 39:954-969.
- Skavenski AA, Robinson DA (1973) Role of abducens neurons in vestibuloocular reflex. *J Neurophysiol* 36:724-738.
- Stahl JS, van Alphen AM, De Zeeuw CI (2000) A comparison of video and magnetic search coil recordings of mouse eye movements [In Process Citation]. *J Neurosci Methods* 99:101-110.
- Steinhausen (1933) Über die beobachtung der cupula in den bogengangampullen des labyrinth der lebenden Hecht. *Pflügers Arch Ges Physiol* 232:500-512.
- Winterson BJ, Collewijn H, Steinman RM (1979) Compensatory eye movements to miniature rotations in the rabbit: implications for retinal image stability. *Vision Res* 19:1155-1159.

2.2 A COMPARISON OF VIDEO AND MAGNETIC SEARCH COIL RECORDINGS OF MOUSE EYE MOVEMENTS

J.S. Stahl, A.M. van Alphen, and C.I. De Zeeuw

Stahl JS, van Alphen AM, De Zeeuw CI (2000) J. Neurosci. Methods. 99:101-110.

Abstract

Interest in connecting molecular biology and behavior is motivating research into the eye movements of mice. Unfortunately, recording eye movements in this diminutive animal is technically difficult. We present the first method for obtaining calibrated video oculography, and contrast the results with simultaneously obtained scleral search coil recordings in C57Bl/6 pigmented mice. We determined the distance of the pupil from the center of corneal curvature, based upon relative motions of the pupil and corneal reflections during camera movements, and used the distance to convert subsequent video measurements of pupil motion to eye rotation. We recorded responses during sinusoidal rotation (0.1-1.6 Hz) in the light, by video prior to search coil implantation, and by video and search coil simultaneously following implantation. Pre-implantation, video-derived gains ranged from 0.86 ± 0.03 (mean \pm sd) at 0.1 Hz to 0.95 ± 0.03 at 0.8 Hz. Phase progressed monotonically from $-3.1 \pm 2.6^\circ$ (eye leads head) at 0.1 Hz to $+5.9 \pm 1.1^\circ$ at 1.6 Hz. Coil implantation reduced the range of video-derived gains to 0.64-0.79. This reduction reflects disruption of normal behavior by the coil. Coil data confirmed the video results. Video and search coil techniques each have advantages. Specific precautions are required when designing and interpreting experiments using the coil technique.

Introduction

Recent months have seen an upsurge in the number of laboratories engaged in the study of mouse eye movements. This activity is driven by three factors - an interest in linkages between molecular biology and brain function, the primacy of the laboratory mouse in genetic research, and the fact that the ocular motor system is one of the best understood neural systems.

Unfortunately, this direction of research is complicated by the technical difficulty of recording eye movements in this small mammal. To date, only a handful of methodologically problematic studies have been published. Among these, two early studies of optokinetic nystagmus (one based on video, and the other upon the relatively imprecise EOG recording technique) calibrated their eye movement recordings based upon the unsupported assumption that in the mouse, eye velocity equals optokinetic drum velocity at low stimulus speeds (Grusser-Cornehls and Bohm, 1988; Mitchiner et al., 1976). Two other video studies converted the measured translation of the mouse pupil to rotation angle based on a simple model in which the pupil rotates about a radius equal to the radius of the roughly spherical eye (Katoh et al., 1998; Mangini et al., 1985). In fact, the pupil does not lie upon the surface of the eye, but rather is displaced toward the center by the depth of the anterior chamber. In the mouse, the difference is considerable; in the pure strain C57Bl6/J, the radius of the eyeball (based upon the half distance from corneal surface to anterior choroid) is 1.69 mm, while the distance of the pupil to the same central point is only 1.14 mm (Remtulla and Hallett, 1985). Alone, this error would lead to a significant underestimation of rotation angle, but it was partly (and inadvertently) offset by a second error. As is demonstrated in this study (see discussion of figure 5), the eye does not rotate about the center of curvature of the cornea. It rotates about a point

somewhat behind its center, so the effective radius is longer than the anatomical measurement.

The magnetic search coil technique has several advantages over video and EOG, not the least of which is the ease with which the recordings can be calibrated in an untrained afoveate, head-fixed mammal, i.e., by measuring the output of the recording system during rotations of the field or reference coils about the animal over known angles. This method is rendered practical by the observation, well documented in the rabbit (Fuller, 1980; Fuller, 1992), that afoveates move their eyes only rarely when the head is stationary and fixed. An initial search coil study in the mouse reported unexpectedly low gains and large phase lags (for example, 0.34 and 36° for 0.8 Hz sinusoidal rotation in the light) (Koekkoek et al., 1997). Recently the search coil technique has been modified by the use of a 1 mm diameter, 60-turn coil fixed to the sclera at the temporal side of the eye. This smaller coil and a less invasive implantation procedure led to more physiologic performance (van Alphen et al., 1999). Presumably the improvement in behavior reflects the reduced mechanical impediments of the smaller coil. This result, however, begs the question – would gains improve still more with a completely non-invasive recording technique? Clearly, a study employing a video recording technique would address this question, but better calibration methods are required.

This study addresses this question by introducing a method of calibrating video oculography in the untrained afoveate mammal. We used this video technique to record mouse eye movements before search coil implantation, and then we employed both video and search coil techniques simultaneously after search coil implantation.

Methods

We performed combined video/search coil recordings in six adult mice of the inbred pigmented C57Bl/6 strain. A set of coil-only experiments directed at a specific question were subsequently conducted on an additional five mice. All animal procedures described were carried out under animal care protocols approved by the Institutional Animal Care and Use Committees of Case Western Reserve University and the Erasmus University Rotterdam.

Surgical procedures

All surgical procedures were performed under halothane/nitrous oxide anesthesia. The mouse head was restrained during recording sessions by an acrylic pedestal. After induction of general anesthesia, the scalp was incised and five stainless steel screws (M1x1.5 mm) were implanted in the calvarium and then encased in dental acrylic. This mass was then fused by application of additional acrylic to a pre-made piece of acrylic bearing two M2 nuts. Care was taken to position the nut-bearing piece so that, when later fixed to the restraint device by the pedestal, the mouse head would be held in an approximately neutral roll and yaw position, with a natural-appearing pitch angle. After completion of the pedestal, the animal was allowed to recover from anesthesia.

Scleral search coils were implanted upon one eye after completion of the initial series of video-only eye movement recordings. The animals were re-anesthetized and placed in a rolled position so the eye could be easily approached. A small incision was made in the conjunctiva on the temporal side of the eyeball. A pocket was bluntly dissected anterior to the insertion of the lateral rectus muscle. A copper wire coil (1 mm outside diameter, 60 turns, 1.0 mg) was placed in the pocket. The leads of the coil were carefully tunneled subconjunctivally around the inferior margin of the eye, and then out of the medial superior aspect of the orbit to a miniature coaxial MMCX connector that was attached to the top of the acrylic head pedestal. The coaxial connector prevents errors in the recorded eye movement signal due to induction of currents at the connection site, a potential problem when using tiny search coils. The superior rim of the coil was then fixed to the sclera with 1 suture (10/0 nylon, Ethicon®), and the conjunctiva was closed over the coil with an additional suture. In an additional set of experiments (motivated by the analysis of the simultaneous video/coil results), coils were attached to the sclera with two sutures, aligned in the horizontal plane. Animals were allowed to recover for several days until the eye was well open before the first postoperative recordings were made. In practice, a 3-5 day recovery period was required.

Video eye movement recording apparatus

Figure 1 shows a schematic of the video recording setup, as viewed from above. The animal's body was restrained within a short acrylic tube, which incorporated a rigid plastic bar to which the head fixation pedestal was bolted. The restraint assembly was mounted upon a rotating platform (theta axis), which in turn was mounted upon an X-Y platform, which in turn was mounted atop the extended shaft of a custom-designed servo-controlled motor. The extended shaft also carried the miniature video camera of the video oculography system. The camera was joined to the turntable shaft in such a way as to allow it to be yawed about the turntable axis over a precise $\pm 10^\circ$ during calibration procedures, or locked to the shaft in a central position during recording. The X-Y platform was oriented so that, with the camera locked in its central position, the mouse eyeball could be translated left-right (X-axis) or near-far from the camera (Y-axis).

Video oculography in the mouse is particularly challenging due to the extreme curvature of the cornea and the fact that there is no visible sclera in this animal. Both factors tend to reduce luminance values at the edges of the picture, causing automated pupil detection products (such as the ISCAN system we used) to become confused as to the location of the pupil. This problem was resolved using a distributed illumination system consisting of 6 infra-red emitters (IRLEDs) (maximum output 24 mW, dispersion angle 20°) arranged as two banks of three, located approximately 3 cm from the mouse eye, to left and right of the optical axis of the video camera. Each IRLED was mounted upon a short flexible stalk, allowing optimal positioning. In practice, after the initial alignment, we rarely needed to adjust any but the outermost IRLED on either side, even as we switched between different mice. The IRLEDs lay below the horizontal plane passing through the mouse eyes, displacing their intense corneal reflections well below the pupil. Proper interpretation of the video recording also requires that a single reference corneal reflection (CR) be tracked. To produce this reference CR, we mounted

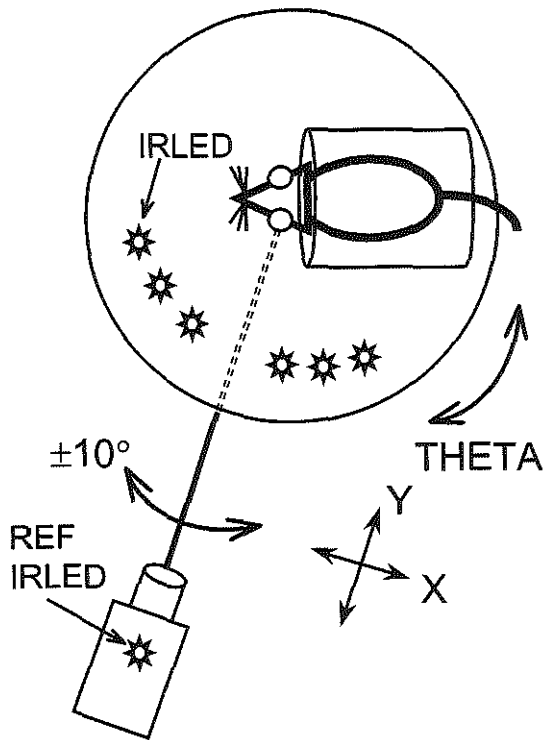


Figure 1: Schematic of experimental setup, as viewed from above. The camera is supported by an arm from the turntable axis, and turns with the animal during recording. The X-Y axis permits movement of the animal left-right and in-out with respect to the camera, while the theta axis, which rides upon the X-Y axis, allows for rotation of the animal with respect to the camera.

a single IRLED upon a rigid stalk above the camera, aligning it horizontally with the camera's optical axis. This IRLED produced a single, small CR just above the pupil.

The video eye tracking system is a commercial model designed for use in trained primates (ETL-200, ISCAN, Burlington, MA), modified only by substitution of a small macro lens that provides a horizontal field of view of approximately 4.2 mm at its working distance of 100 mm. The camera incorporates a CCD element, which generates a 512 x 256 (H x V) pixel image. The linearity of the conversion of object position to pixel position is excellent; regressing pixel position versus actual position of a tiny object mounted upon a vernier caliper yielded a correlation coefficient of 0.999 over a 4 mm horizontal range, with no evidence of systematic patterning of the regression residuals.

The ISCAN system uses proprietary algorithms to track the centers of the pupil and reference CR with 1/3 and 1/10 pixel accuracy in the horizontal and vertical directions, respectively. The video system introduces a delay in the eye movement signal measuring approximately 30 msec. For the purposes of this experiment, we sampled at 60 samples/sec (each channel), and we collected only the horizontal pupil and CR positions.

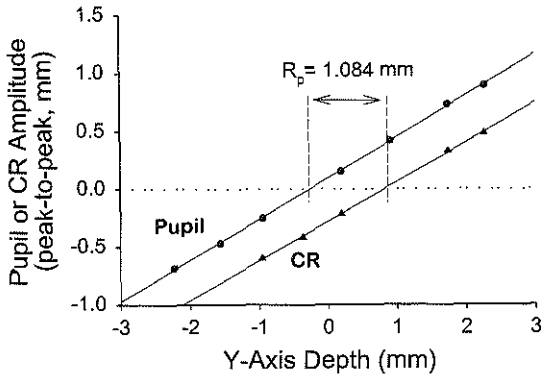


Figure 2: Results from the First method of calculating R_p , the distance of the pupil from the center of corneal curvature. Peak-to-peak amplitude of the apparent motions of pupil and corneal reflection are plotted as functions of position of the Y-axis of the table mount. Since pupil motion is nulled when the pupil is over the camera axis, and corneal reflection motion is nulled when the center of corneal curvature is over the axis, the difference in X-intercepts yields R_p .

Video eye movement calibration

The ISCAN video system outputs signals proportional to the linear positions of the pupil and reference CR. These translation positions must be converted to angular rotation of the eyeball. Translational motion of the pupil image is actually due to combinations of rotation and translation of the eyeball. Subtraction of the CR position from the pupil position yields the component of pupil motion due to rotation alone (DiScenna et al., 1995). The ability to track the CR is built into commercial video eye trackers such as the ISCAN ETL-200 for the purpose of negating any relative translation of the camera with respect to the subject's eye. However, in the current context, it is also useful for correcting for any differences between the axis of rotation of the eye and the center of corneal curvature, as well as any difference between the axis of the eyeball and the rotation axis of the video camera (see below).

Conversion of the video pupil (P) and CR linear positions to angular position of the eye E is based upon the equation:

$$E = \arcsin\{(CR-P)/R_p\} \quad (1)$$

We determined R_p , the radius of rotation of the pupil, by two different methods. In each method, the camera was unlocked from the shaft and rotated over its $\pm 10^\circ$ range as pupil and CR were tracked. The mouse eye was assumed to remain stationary during these manipulations. In practice, any eye movements were visible in the video record, and measurements only performed over regions of the record that were free of movement. Prior to video calibration the mouse was mounted in the restraint device, left/right positioned so that the pupil was roughly centered in the video image, and the light sources, video thresholds, and other video discrimination variables adjusted to produce robust pupil and CR tracking.

In the first calibration method, the $\pm 10^\circ$ camera rotation was repeated several times at various positionings of the mouse along the Y-axis (depth with respect to the camera), ranging from a position that put the center of curvature of the corneal surface in front of the axis of camera rotation, to a position that put the plane of the pupil behind the

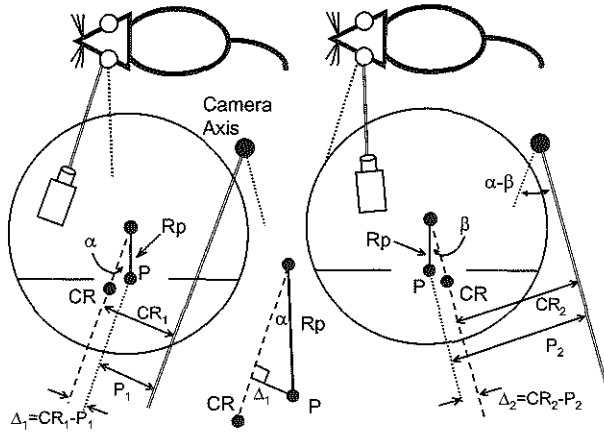


Figure 3: Top-view diagram of video calibration method 2. Left half of figure shows the geometric relations with camera rotated rightward with respect to the animal (see overlaid schematic of camera and animal). Left half of figure shows geometry with camera rotated to animal's left. The small inset triangle (center) is an enlargement of the geometry for the rightward camera position, and demonstrates that $\Delta_1 = R_p \sin \alpha$. Optical axis of camera shown as double line. It rotates about the camera axis, which for the purposes of this example was deliberately placed outside the eye. Abbreviations: P=pupil. CR=reference corneal reflection. P₁, P₂=Horizontal distances from camera optical axis to pupil in initial and final camera positions. CR₁, CR₂=distances to corneal reflections. Δ_1 , Δ_2 = initial and final horizontal distances between P and CR.

axis of camera rotation. The amplitudes of apparent motion of the pupil and reference CR were measured and correlated with Y-axis depth. Over the small range of distances employed, these amplitudes should be linear functions of depth, the pupil amplitude passing through zero when the pupil is exactly over the axis of rotation of the camera, and the CR amplitude passing through zero when the center (origin) of curvature of the cornea is over the camera axis. Figure 2 plots the pupil and CR amplitudes as functions of Y-axis position. R_p, the distance from the plane of the pupil to the center of curvature of the cornea, is simply the difference in the X-intercepts of the two curves.

The previously described method of determining R_p was laborious and devised primarily as a method of confirming the second method, which was the one actually used to calibrate the data collected for Bode analysis. The second method of establishing R_p is detailed in figure 3. Note that a corneal reflection is a virtual image of the light source, appearing (if the CR IRLED is aligned horizontally with the optical axis of the camera) on the eyeball radius that is parallel to the optical axis of the camera, at one half radius from the center of corneal curvature. Prior to calibration, we rotated the animal on the theta axis so that the horizontal positions of the reference CR and pupil were roughly aligned, when the eye was in the center of its range. This alignment was necessary so that the average angular deviation between the pupil and reference CR was within the range where $\sin \theta \approx \theta$. We then adjusted the Y-axis to place the center of corneal curvature over the camera/table axis. By this adjustment we standardized the distance from the animal's eye to the camera, and consequently the optical magnification factor and the

conversion of video pixel to position. This positioning was easily achieved by continuously oscillating the camera about the animal and moving the Y-axis until CR motion was nulled. Note that neither positioning is critical (see below).

After these alignments were complete, we recorded the pupil and CR as the camera was moved multiple times through its $\pm 10^\circ$ range. We determined Δ_1 and Δ_2 , the values of the CR-P difference taken at the two extremes of camera position. As shown graphically in the figure,

$$\Delta_1 = R_p \sin\alpha \quad \Delta_2 = R_p \sin\beta \quad (2a,2b)$$

and thus

$$\Delta_1 - \Delta_2 = R_p (\sin\alpha - \sin\beta) \quad (3)$$

For small angles measured in radians, $\sin\theta \approx \theta$, and thus:

$$\Delta_1 - \Delta_2 = R_p (\alpha - \beta) \quad (4)$$

As is evident from figure 3, $\alpha - \beta$ is equal to the camera swing of 20° (note that the signs of $\alpha - \beta$ oppose, so the difference is actually the sum of the angles as they appear in the figure), and thus, the above equation (incorporating a conversion from degrees to radians), reduces to:

$$R_p = (\Delta_1 - \Delta_2)/(20\pi/180) \quad (5)$$

Comparison of the denominator in the above equation to the denominator without the $\sin\theta \approx \theta$ assumption shows that the R_p measurement above is accurate within 5% provided that the center of the camera swing is within 17° of the 0 angle, defined as the point where the pupil and the reference CR are aligned.

Figure 3 was constructed to demonstrate that the calibration method does not depend upon the eye being perfectly centered over the camera axis, although large displacements would cause R_p to deviate from its anatomical value because distance between the camera and the eyeball affects the linear magnification of the image, and thus the conversion of video pixels to millimeters. However, the effect in our system is small, having a slope of only 1.6% per mm change in depth. In practice, it was easy to obtain a reproducibility of better than 0.3 mm when adjusting the Y-axis by simply qualitatively nulling the CR motion. Just as figure 3 demonstrates that alignment of the camera axis with the corneal center need not be perfect, it is easy to redraw the figure to demonstrate that the eye itself need not rotate about the center of corneal curvature. If the actual axis lies elsewhere, then the motion of the pupil is attributable to a component of rotation about the center of corneal curvature, and a component of translation about the true center of rotation. The CR-P subtraction isolates the component of pupil motion related to the rotation.

Search coil apparatus and calibration

Magnetic search coil recordings of horizontal eye movements were obtained using a phase-angle (rotating magnetic vector) system with 1.2-meter field coils (CNC

Engineering, Seattle, Washington). The field coils were mounted upon a 2-axis gimbal. The conversion factor from phase detector output voltage to eye angle was based upon the recorded signal as the field coils were rotated over a 15° range about the mouse. The mouse was surrounded by a cylinder during the calibration procedure so that the optokinetic stimulus produced by motion of the field coils would not cause eye movements. Since the field coils remain stationary during vestibular stimulation, this system reports eye angle with respect to the earth-stationary reference (gaze angle). Eye-in-head position was determined by subtracting turntable angle from gaze angle.

The 0 position of the coil recording was defined as the zero position of the video signal, i.e., the eye angle at which the reference CR and pupil center were aligned. As noted above, when the mouse was mounted in the apparatus with the camera locked in its recording position, the theta axis of the table was rotated until the pupil and reference CR were horizontally aligned when eye position was near the center of the animal's preferred range. Since the mouse, like the rabbit, tends to keep its eye near a particular rest position (it does not readily maintain eccentric eye positions), the 0 angle so defined was close to the animal's preferred rest position.

Stimuli

Animals were rotated sinusoidally in the light at 0.1 Hz 10° (0-peak) amplitude, 0.2 Hz 10°, 0.4 Hz ~10°, 0.8 Hz ~9.2°, 0.8 Hz ~4.6°, and 1.6 Hz ~3.9°. During rotation the animal viewed the surrounding laboratory and the earth-stationary field coils. The sequence of stimuli was repeated 3-4 times in a recording session. Each animal was recorded no more than once per day. Three sessions were recorded prior to search coil implantation, and 2-3 sessions following coil implantation.

Data collection and analysis

Horizontal pupil and CR position, head position, and coil-derived gaze position were filtered through identical 100 Hz low pass Bessel filters, digitized with 16-bit precision at 200 samples/second, and acquired to a Pentium™ computer using a custom-designed acquisition program. Overall system noise (prior to any software smoothing) measured 0.23° for the video system and 0.09° for the coil system, based upon the average standard deviation of simultaneously-acquired video and search coil signals during 4-6 second epochs (one for each of 4 animals), during which the eye was nominally stationary.

Digitized pupil and CR position signals were individually pre-processed, removing any brief dropouts by linear interpolation from the surrounding data points. The signals were then subtracted, and converted to angular position based upon equation 1. Eye velocity (both video and coil-derived) and head velocity were determined by differentiating the position signals, followed by slight smoothing using a Blackman window with a cutoff frequency of 40 Hz.

Data was analyzed to obtain response gains and phase within each record. Record duration varied from 100 seconds for the 0.1 Hz stimulus, to 25 seconds for the 1.6 Hz stimulus. Fast phase eye movements were detected interactively by their departures from the slow phase data in plots of eye velocity versus head velocity. The fast phases were

then removed by linear interpolation from the surrounding slow phase data. This fast phase removal procedure was performed separately on the video- and coil-derived eye movement data. “De-saccaded” data was then reviewed, and segments of the data excluded if necessary (e.g., due to loss of the video signal, chewing/sniffing artifact in either eye movement signal, or failure to construct a clean slow-phase signal due to excessive numbers of fast phases). Intact cycles of stimulus and response (i.e., no regions of excluded data in either eye movement signal) were then averaged.

Standard (not fast) Fourier analysis was performed upon the averaged eye and table velocity records to obtain the amplitude and phase at the fundamental (stimulus) frequency. Gain was calculated as the ratio of response to stimulus amplitudes, and relative phase as response phase minus stimulus phase. Negative phase values denote response leading the stimulus. Average gain and phase curves (with respect to stimulus frequency) were determined for each animal. Pre-coil and post-coil sessions were then averaged separately, and finally, the pre- and post-coil average curves for each animal were averaged to generate grand average pre- and post-coil curves for the 6 animals.

Results

Measurement of pupil radius

The radius of the pupil (R_p , the distance from the plane of the pupil to the center of curvature or the cornea) was measured by two procedures as described in Methods. Table 1 shows the results for the six animals studied by combined video and coil techniques. Method 1 is based upon the differences in the Y-axis depths at which pupil and CR motion are nil during rotation of the camera about the eye. Method 2 is based upon the amplitude of the motion of the pupil with respect to the CR at the Y-axis depth at which the corneal curvature center is over the axis of camera rotation. The results in the Method 1 and Method 2 “pre-coil” columns were obtained in the same pre-coil recording sessions, and represent the average of three sessions for each animal. The Method 2 (post-coil) column contains the average values of R_p obtained from the 2-3 post-coil sessions. There was no significant difference between the pre-coil Method 1 and Method 2 results (2-tailed paired t -test, $p=0.77$), or between the pre- and post-coil Method 2 results ($p=0.40$). For consistency, we used the Method 2 R_p values to convert linear CR-pupil values to eye angle, even in sessions in which both values were available. Note that animal ‘a’, which had the largest R_p measurements, was older and heavier (4 months, 29 gm) than the other experimental animals, as well as the only male.

Validation of video calibrations

The video calibration method was validated directly in two mice. After placement of the mice in the recording apparatus, the animals were deeply anesthetized in situ by intraperitoneal injection of Avertin (tribromoethanol-amylene hydrate). R_p was determined (method 2, above) and then the animal was rotated upon the theta axis over

Table 1

Animal	Method	Method	Method
	1 (pre-coil)	2 (pre-coil)	2 (post-coil)
a	1.091 mm	1.078 mm	1.112 mm
b	1.027	1.011	0.976
c	1.035	1.032	1.078
d	1.041	1.032	1.076
e	1.038	1.079	1.083
f	0.997	1.014	0.997

$\pm 13^\circ$ in measured steps. Due to the deep anesthesia, there were no reflex or spontaneous eye movements during these rotations, so eye angle with respect to the camera was equal to the known theta-axis angle. Correlating recorded and actual eye angles yielded average slopes of 1.02 and 0.98 for the two animals (a slope of 1.0 would indicate perfect correspondence). Figure 4 plots recorded versus actual angles for one trial in one animal.

Responses to sinusoidal rotation

All mice generated robust compensatory eye movements during sinusoidal rotation in the light. Figure 5 shows an example of the response to rotation at 0.2 Hz, taken from a session in which both video and coil-derived eye movements were recorded. Angular eye and head position traces are plotted with the same vertical scale to facilitate comparison of amplitudes. The figure also includes the translational position traces for CR and pupil. Note that the scale of the CR trace is 2.5 times that of the pupil. The CR moved sinusoidally in phase with the pupil, indicating that the eye actually rotated about a point that lay behind the center of corneal curvature.

Figure 6 shows the Bode plots for the average results from all animals. Each animal is equally weighted (i.e., the data for multiple sessions was first averaged within animals before creating the all-animal averages). For all animals, pre-coil gains were high, consistent (note the small standard deviation error bars), and fairly independent of stimulus frequency in the tested frequency band. The pre-coil video-derived gain did run through a shallow maximum at 0.8 Hz, which was a consistent finding in all animals. Gain values were virtually identical for the two different stimulus amplitudes ($\sim 9.2^\circ$ and $\sim 4.6^\circ$) used at 0.8 Hz. The coil implantation produced a marked decline in gain, particularly at low stimulus frequencies. Variability of the results across animals was also enhanced (note the larger error bars). Surprisingly, at all stimulus frequencies, the gain values measured with the coil were significantly lower than the gain values simultaneously obtained with the video system ($p < 0.01$ or better, 1-way ANOVA at each

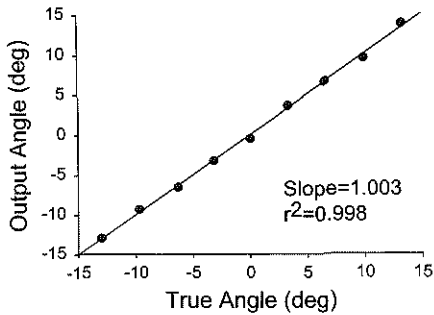


Figure 4: Validation of video calibrations. Recorded angle of the pupil with respect to the camera is plotted against actual angle, during measured rotations of the deeply anesthetized mouse. Regression slope is 1.003, indicating that the average correspondence across the $\pm 13^\circ$ range is nearly perfect.

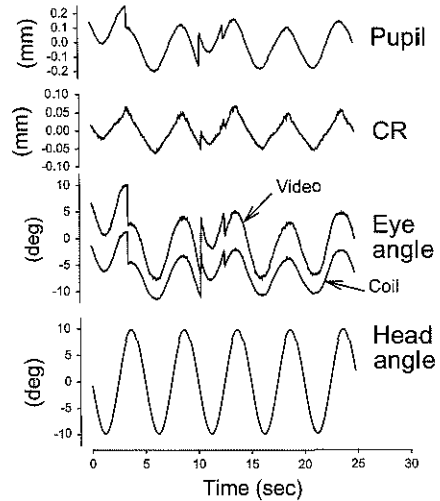


Figure 5: Example of recorded response during 0.2 Hz rotation in the light. Top traces are linear position of pupil and CR in millimeters. Note that scale of CR is expanded in comparison to pupil, and head position is inverted to facilitate its comparison to eye position. Upward deflections indicate rightward eye movements. Video- and coil-derived eye movements are arbitrarily offset for graphic clarity.

frequency). The average phase curve is representative of the curves for individual animals. All animals exhibited a small phase lead at low frequencies, progressing monotonically to a small lag at higher frequencies. The coiling procedure used for these experiments produced a slight increase in phase lead at all stimulus frequencies. Post-implantation video- and coil-derived phase measurements were very similar, except at the highest frequencies, where they diverged by 4° . Note that there is some uncertainty in the video phase at higher frequencies, since the correction factor for propagation delay through the video system is only an approximate value (the exact value varies with the complexity of the video image) and the effect of any inaccuracy in the value (which we measured to be 30 msec) upon phase assumes an increasing importance as stimulus frequency increases. While changes in stimulus amplitude at 0.8 Hz had no effect upon gain, the change to lower amplitudes did affect phase, reducing the lead by approximately 3° .

Effect of securing the search coil with two sutures

The likely cause for the lower coil-derived gains was twisting of the search coil (as a unit) relative to the eye during eye movements (see Discussion). Such twisting was

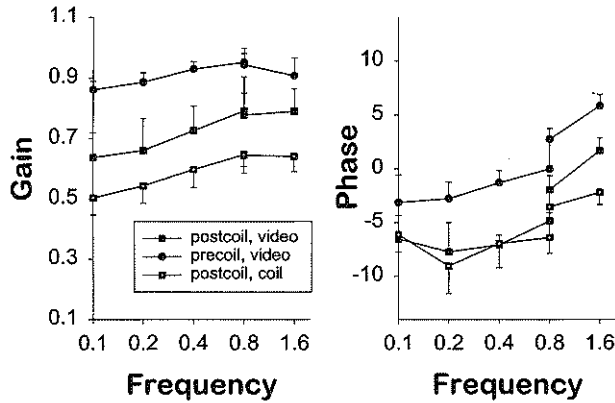


Figure 6: Average Bode plots for the 6 animals. Error bars denote 1 SD. Filled symbols denote video-derived data, open symbols denote coil-derived data. Following coil implantation, gains were decreased and phase lead increased. Coil-derived gains were uniformly smaller than video-derived gains.

theoretically possible, since coils were sutured at only one point (although gross inspection at time of implantation suggested that they tracked the eye well). To test this explanation, an additional five animals were implanted using a modified technique in which the coil was attached by two sutures. One suture was placed just behind the limbus, and the other at the exact opposite side of the coil. This “equatorial” placement would reduce the tendency of the coil to twist away from the globe during rotations in the horizontal plane. Consistent with our predictions, gains obtained with the two-suture coil increased, to 0.774 ± 0.024 , averaged across the six stimulus frequencies/amplitudes. This value differs significantly ($p=0.0004$, 2-tailed t -test) from the comparable average value obtained using the single-suture technique (0.597 ± 0.061), but is similar to the average post-implantation value obtained with video (0.769 ± 0.070 , $p=0.88$).

Discussion

We have demonstrated a method of obtaining calibrated video eye movement recordings in the mouse, compared the recordings to simultaneously obtained scleral search coil data, and highlighted the importance of technique when using the search coil method. The video results indicate that prior to search coil implantation, mice have an excellent visually-enhanced vestibulo-ocular reflex (VVOR), with gains in the vicinity of 0.9. These values slightly exceed those obtained by the invasive search coil method in the best-studied afoveate mammal, the rabbit (Collewijn, 1981; De Zeeuw et al., 1995; Stahl and Simpson, 1995). Placement of the scleral search coil significantly reduced VVOR gain, slightly increased phase lead with respect to the stimulus, and increased performance variability across the tested range of stimulus frequencies. The degradation of performance following coil implantation likely reflects either post-surgical ocular discomfort, or mechanical hindrance of free eye rotation by the coil. It was obvious from inspection of the video images that in most animals the eye never returned to its

preoperative state; the palpebral fissure remained slightly narrowed, even 10 days after the implantation procedure.

Comparison of video- and coil-derived measurements

Coil-derived and video-derived eye movement records evinced essentially identical phase behavior. The gain versus frequency curves paralleled each other, but the coil-derived movements were always smaller in the original set of animals in which the coils had been attached to the sclera with a single suture. This result could have reflected inaccuracy of either the video or the coil measurements. Several lines of evidence argued that the video recordings were accurate. Determination of R_p , the distance from the pupil to the center of corneal curvature, was the linchpin of the video calibration strategy. The two independent methods produced equivalent results. Moreover, the R_p values we obtained by the two methods (1.038 and 1.041 mm, respectively) corresponded fairly well with the value of 0.972 derived from anatomical measurements in mice of the same strain (Remtulla and Hallett, 1985). It should be noted that R_p would be consistently underestimated if the second method of determining R_p were applied when the eye was rotated away from the zero angle (the angle at which pupil and reference CR are aligned). Underestimating R_p would lead to overestimating gain. However, as noted in Methods, the misalignment must exceed 17° for the error in R_p to exceed 5%. Finally, our experiments in which two deeply anesthetized animals were rotated by known angles demonstrated that the video recording produced accurate measurements.

Given the accuracy of the video measurements, the disparity between gains indicated that the coil recording was underestimating eye rotation. The fault did not lie in the coil calibration procedure. In a procedure analogous to that used in figure 4, search coils (identical to those implanted in the mice) mounted upon a protractor jig and calibrated in the usual fashion were able to accurately measure subsequent rotations of the protractor. Therefore the most probable explanation for the lower search coil gain was a loose coupling between the search coil and the eye, allowing the coil to rotate less than the eyeball. In the combined coil/video experiments, the coil was attached to the sclera by a single suture at its superior margin. The interval between implantation and recording was too short for scar tissue to bond the coil and sclera at other points. Thus it is conceivable that the rigid coil rotated slightly about its single attachment as the eye rotated. The absolute size of this counterrotation would be quite small. Given a 10° amplitude stimulus, a video-derived gain of 0.65, a coil-derived gain of 0.53, and a coil of 1 mm diameter, then the outer edge of the coil would only need to move away from the eye by 0.01 mm at the peak eye position. Since the phase curves for post-coil video and coil-derived eye movements were essentially identical at 0.1-0.4 Hz, the coupling between the coil and eyeball must have possessed predominantly elastic (as opposed to viscoelastic) properties, at least at the timescale probed by our stimulus frequencies. The elastic structures influencing the position of the coil upon the eye included the coil lead, the single nylon suture, and the sclera itself.

This train of logic led to the additional experiments in which the coil was fixed to the eye by a pair of sutures, aligned to resist the forces that would be applied to the coil during rotation of the eye in the horizontal plane. As predicted, the measured gains

increased substantially using the 2-suture method, although they still remained well below the gains obtained by the video method prior to coil implantation.

Significance of findings for further work in the mouse

The video and search coil oculographic techniques possess distinct sets of advantages and disadvantages. Because video is entirely non-invasive, preparation time is reduced (making this technique particularly advantageous when high-throughput experiments are necessary) and there are no concerns regarding hindrance to normal eye movements. Video has already, in the current study, played a role in improving the coil technique. The disadvantages, however, are several. The head must be fixed with respect to the camera, making head-free experiments impossible. Spatial resolution is limited by the size of the video pixel, and as a consequence, noise levels tend to be high. Resolution can be improved somewhat by enlarging the percentage of the video image occupied by the pupil, but only to a limit, since the field of view must remain large enough to contain the pupil at all times. Temporal resolution is also limited. The current video data was obtained at a rate of 60 samples/sec. The ISCAN system can be operated up to 240 samples/sec. However, the higher frame rates are achieved by splitting the video image, and thus the field of view is reduced. It is generally not practical to use the 240 samples/sec setting, as the field of view is too narrow to reliably contain the pupil. It is also difficult to perform video oculography in the dark in this species. Unless pretreated with a meiotic drug, the mouse pupil becomes enormous in darkness, rendering detection of the pupil center unreliable. Finally, although the calibration method we have presented is an improvement over prior video techniques, it entails a number of simplifications, including the assumptions that the eye rotates about a single point in space and the corneal surface is spherical. Another assumption is that R_p is independent of pupil diameter. In fact, as the pupil enlarges R_p diminishes, because the plane of the pupil recedes as the border of the iris tracks the strongly curved surface of the lens. A more accurate video recording would require that pupil diameter be taken into account when converting pupil displacement to eye rotation.

Search coil oculography remains attractive in that it can be performed with the head free, it has superior spatial and temporal resolution, there are no problems with recording in darkness, and there are fewer assumptions/approximations associated with the calibration process. An inescapable disadvantage of the improved search coil technique is that the temporal placement of the miniature coil allows for recording in yaw and pitch axes only. Coil oculography also entails a delicate surgical procedure, and the experimental "window" is limited as the current coils tend to break a few weeks after implantation. Finally, coil implantation led to significant alterations in gain and phase of the VVOR (compare the pre- and post-implantation video data in figure 6). Thus the presence of the coil distorts performance, which might be expected to influence certain types of experiments, such as those investigating the relationships between neuronal firing rates and eye position.

The current results underscore the critical dependence of the coil oculography in the mouse upon instrumentation and surgical technique. The change to a 1 mm, laterally placed coil resulted in significant improvements in gain and phase of eye movements in

comparison to those obtained using the larger perilimbic coil (Koekkoek et al., 1997). The simple change from one suture to two sutures improved the recordings further. These results suggest the need for precautions when assessing coil-derived data. Laboratories reporting results of experiments in abnormal animals (for example, mutants) must have demonstrated proficiency with the technique in normal animals. In addition, the data must be gathered from enough animals to exclude the possibility that the abnormal results reflect a single suboptimal coiling procedure. The ideal coil study is one that investigates changes in performance due to an experimental manipulation (such as adaptation of gain), in which conclusions are drawn from comparison of pre- and post-manipulation data in the same animals (such as De Zeeuw et al., 1998). Second, since the current coil technique still leads to an alteration in performance gain, coil studies should be designed so that the conclusions are relatively insensitive to absolute eye movement amplitude. An example of a problematic experiment would be to use coil-derived eye movements to calculate the eye position sensitivity (k) of motor neuron firing rates, and then to compare these values to those obtained in other species. However, a coil study comparing k values in different vestibular nucleus neuron types within mice would be reasonable.

References

- Collewijn H. The Oculomotor System of the Rabbit and Its Plasticity. Springer-Verlag: New York, 1981. 240 pages.
- De Zeeuw CI, Hansel C, Bian F, Koekkoek SKE, van Alphen AM, Linden DJ and Oberdick J. Expression of a protein kinase C inhibitor in Purkinje cells blocks cerebellar LTD and adaptation of the vestibulo-ocular reflex. *Neuron*, 1998; 20: 495-508.
- De Zeeuw CI, Wylie DR, Stahl JS and Simpson JJ. Phase relations of Purkinje cells in the rabbit flocculus during compensatory eye movements. *J. Neurophysiol.*, 1995; 74: 2051-2064.
- DiScenna A, Das V, Zivotofsky A, Seidman S and Leigh R. Evaluation of a video tracking device for measurement of horizontal and vertical eye rotations during locomotion. *J. Neurosci. Meth.*, 1995; 58: 89-94.
- Fuller J. Linkage of eye and head movements in the alert rabbit. *Brain Res.*, 1980; 194: 219-222.
- Fuller JH. Comparison of head movement strategies among mammals. In: Berthoz A, Graf W and Vidal PP, editors. *The Head-Neck Sensory Motor System*. Oxford University Press: New York, 1992; pp. 101-112.
- Grusser-Cornehls U and Bohm P. Horizontal optokinetic ocular nystagmus in wildtype (B6CBA+/+) and weaver mutant mice. *Exp. Brain Res.*, 1988; 72: 29-36.
- Katoh A, Kitazawa H, Itohara S and Nagao S. Dynamic characteristics and adaptability of mouse vestibulo-ocular and optokinetic response eye movements and the role of the flocculo-olivary system revealed by chemical lesions. *Proc Natl Acad Sci USA*, 1998; 95: 7705-10.
- Koekkoek SKE, Alphen AM, van der Burg J, Grosveld F, Galjart N and De Zeeuw CI. Gain adaptation and phase dynamics of compensatory eye movements in mice. *Genes and Function*, 1997; 1: 175-190.

- Mangini N, Venable JJ, Williams M and Pinto L. The optokinetic nystagmus and ocular pigmentation of hypopigmented mouse mutants. *J. Comp. Neurol.*, 1985; 241: 191-209.
- Mitchiner J, Pinto L and Venable JJ. Visually evoked eye movements in the mouse (*Mus musculus*). *Vision Res.*, 1976; 16: 1169-71.
- Remtulla S and Hallett PE. A schematic eye for the mouse, and comparisons with the rat. *Vision Res.*, 1985; 25: 21-31.
- Stahl JS and Simpson JJ. Dynamics of abducens nucleus neurons in the awake rabbit. *J. Neurophysiol.*, 1995; 73: 1383-1395.

CHAPTER 3

USE OF EYE MOVEMENT RECORDINGS IN THE EVALUATION OF PERIPHERAL VESTIBULAR PATHOLOGY

3.1 CIRCLING BEHAVIOR IN ECL-MOUSE IS CAUSED BY LATERAL SEMICIRCULAR CANAL DEFECTS

Kim Cryns*, Michiel P. Van Spaendonck*, Arjan M. van Alphen*, Kris Flothmann, Paul H. Van de Heyning, Jean-Pierre Timmermans, Chris I. De Zeeuw and Guy Van Camp

* These authors contributed equally to this paper

Abstract

The *Epistatic circler* mouse (*Ecl*-mouse) is a naturally occurring mutant, which displays a circling behavior and hyperactivity. It has been shown that the circling phenotype in this mutant shows a complex inheritance pattern but the vestibular pathology has not been studied. The present study deals with the morphological and functional basis responsible for the circling behavior in the *Ecl*-mouse. Morphological examination of the inner ears revealed a bilateral malformation of the horizontal (lateral) semicircular canal and a modest fusion of the cristae of the superior and lateral canal. No cochlear abnormalities were detected and auditory brainstem response (ABR) measurements indicated that the auditory system is not affected. Investigation of the vestibulo-ocular reflex (VOR) in *Ecl*-mice showed that their horizontal VOR on stimulation is virtually absent, which correlates with the morphological findings. The present study shows for the first time that the horizontal and vertical vestibular system of a mouse mutant can be differently and specifically affected.

Introduction

The inner ear develops from the otic vesicle, which eventually transforms into the sensory organs for balance (vestibulum) and hearing (cochlea). The vestibular apparatus is composed of two sets of structures: the otolith organs and three semicircular canals. The canals detect angular acceleration of the head about three roughly orthogonal axes, whereas otolith organs are sensitive to linear acceleration. Damage to the vestibular system severely impairs gaze and postural stabilization, leading to dizziness and imbalance. Several mouse mutants exist that show developmental deficits in inner ear development (Deol, 1966). Such mutant mouse strains provide useful model systems to study otic development. The relatively short gestation time of this species makes it feasible to obtain a sufficiently large pedigree to identify genes that contribute to the mouse mutation and are thus assumed to underlie otic development. In most cases, the inner ear defects are caused by mutations in a single gene and are not limited to the vestibular part of the labyrinth but include deficits in cochlear and hindbrain development (Deol, 1966; Rogers et al., 1999; Alavizadeh et al., 2001).

The *Epistatic circler* mouse (*Ecl*-mouse) is a naturally occurring mouse mutant that shows rapid bi-directional circling behavior and is generally hyperactive. According to Doolittle (Doolittle 1963), the *Epistatic circler* mice circled both to the left and to the right, showed no head tremor, did not appear to be deaf and swam well. He indicated that the circling behavior results from the X-yy genotype where X is the dominant *Ecl*-gene, derived from *C57L/J*, and y the recessive *Ecs*-gene, derived from *SWR/J* (Doolittle, 1963). On the other hand, Taylor suggested that the circling behavior of *Epistatic circler* mice is caused by the simultaneous homozygosity for two recessive genes (Taylor, 1976). After out-crossing *AKXL* recombinant inbred lines to *SWR/J*, Taylor found that the circling behavior in the F2-progenies showed concordant inheritance with the hexose-6-phosphate dehydrogenase locus on chromosome 4 in eight recombinant inbred lines, suggesting that the *Ecl*-gene is localized on chromosome 4. However, since Taylor used a different strain combination than Doolittle, it cannot be excluded that the different models are due to the strain combinations used. No detailed genetic investigation of the

Epistatic circler mouse has been performed and in the present study we used the model proposed by Taylor as starting point to perform mapping studies.

The underlying structural and functional deficits, leading to the circling behavior in this mouse mutant, are largely unknown. In the present study we have therefore investigated labyrinthine function in *Ecl*-mouse. The morphology of the inner ear defect was studied by standard light and electron microscopy as well as by a new high-resolution computer tomographic scanning method (Sasov and Van Dyck, 1998) with 3D reconstruction. Investigation of the angular vestibulo-ocular reflex (VOR) in both horizontal and vertical plane verified our morphological findings, which constituted defects in the lateral semicircular canal. To exclude generalized labyrinthine pathology, auditory brainstem responses (ABR) to pure tones were measured ensuring that cochlear function was unaffected in *Ecl*-mouse.

Methods

C57L/J and *SWR/J* mice were purchased from the Jackson laboratory (Bar Harbor, ME) and IFFA CREDO (Charles River Company, France), respectively. Mouse care and experimental treatment were conducted in compliance with institutional and EU laws and policies. *C57L/J* mice were mated with *SWR/J* mice and an intercross was set up between the F1-progeny. 3662 F2-progeny were recovered and their circling phenotype was assessed at the age of 3 weeks. Actively circling animals were scored as affected, and a small piece of their tail was cut off for DNA preparation. 115 mice were scored as affected which corresponds to 1 in 32. Affected, as well as unaffected F2-animals were fertile. Affected mice also showed hyperactivity without head bobbing. An additional backcross was set up between affected F2-animals and mice from the *SWR/J* strain. 411 N2-progeny were recovered and tested for circling behavior (1 in 23).

Microtomography and three-dimensional reconstructions

A desktop X-ray microtomograph (Skyscan®, Aartselaar, Belgium) was used to obtain high-resolution tomographic images from the inner ears from *SWR/J*-mice, *C57L/J* mice, F1-mice and F2-circlers (Sasov and Van Dyck, 1998; Van Spaendonck et al., 2000). The inner ear was first positioned in a longitudinal orientation and then scanned at maximal resolution. 3D-images were reconstructed on the basis of segmented 2D tomographic images using Surfdriver 2.5.5® software. Segmentation was performed on the outer limits of the bony labyrinth along the contours of the fluid filled space (perilymphatic and endolymphatic) inside the bony labyrinth. After scanning, the bony labyrinths were further processed for light microscopy.

Light and electron microscopy

The temporal bones studied by light microscopy were, after fixation in paraformaldehyde, decalcified in 5% EDTA (1 week), followed by dehydration of the specimen in a graded alcohol series, and embedding in paraffin. Subsequently, serial sections (10µm-thick) were cut parallel to the modiolus and the sections were stained with hematoxylin-eosin.

After fixation (glutaraldehyde) and postfixation (OsO₄), the samples used for electron microscopy were transferred to 70% alcohol, in which they were dissected. The membranous labyrinth was dissected from the vestibule by carefully removing the surrounding bone. For scanning electron microscopy, the cristae of the semicircular canals and the maculae utriculi and sacculi were exposed by removing the covering epithelium at the opposing side of the membranous labyrinth. Subsequently, representative parts of the organ of Corti were dissected. After critical-point-drying, the tissues were mounted on stubs and sputtercoated with gold. The specimens were viewed in a Philips SEM 505 scanning electron microscope. For transmission electron microscopy, the vestibular structures of the membranous labyrinths were dissected from the bony structures by removing the bony walls of the vestibule, after which they were embedded in Durcupan. The tissues were cut using glass knives, contrasted and viewed in a Philips EM10 transmission electron microscope.

Hearing assessment

Hearing in mice was assessed by a modified ABR-technique. Under general anaesthesia (1 part O₂, 2 parts N₂O, and 2% Fluothane at a flow of 1.5 l/min) a stainless steel screw was inserted in the parietal bone, next to the midline, serving as midline electrode. Anterolaterally, a similar screw serving as ground electrode was positioned. Two platinum electrodes were placed laterally through the occipital bones in the vicinity of the inner ears. All electrodes were attached to a connector on a pedestal built on the cranium by means of additional stainless steel screws and dental cement. The pedestal also contained two nuts to immobilize the animal in a restrainer with two bolts. The pedestal with the electrodes did not seem to affect the health or behavior of the mice. The mice were positioned in front of a high-frequency loudspeaker (Radio Shack Super Tweeter, Cat No 40-1310B; 5-40kHz) by means of a restrainer, their heads being fixed in position by two bolts fitting the nuts on the pedestal. As a consequence of the fixed head position, there was no need to anesthetize the mice during the tests.

Stimuli consisted of 1 ms tone-bursts at frequencies of 3, 6, 12 and 24 kHz, and intensity of the stimulus was changed in steps of 5 dB. Hearing thresholds were determined manually and defined as the lowest stimulus intensity at which a reproducible field potential could be detected.

Eye movement recordings

Eye movements were recorded with the use of a search coil for mice as previously described by Van Alphen et al. (2001). Two copper wire coils with a diameter of 1 mm

were positioned on the eyeball of the mice. The coils were fixed on the sclera with two 10-0 Ethilon monofilament sutures each. The first coil was positioned on the lateral side of the left eyeball to study eye movements around the yaw-axis, while the second coil was placed atop the right eye to measure movement around the roll axis.

The scleral coils were soldered to connectors that were attached to the head fixation pedestal, which was fixed to the cranium by small screws and dental cement. Vestibular stimuli were delivered using a servo-controlled turntable, while a vertically striped optokinetic drum was rotated around the animal to elicit the optokinetic reflex (OKR). All tests were performed at frequencies ranging from 0.1 Hz to 1 Hz. The amplitude of the optokinetic stimulus was 10° ($-5^\circ/+5^\circ$), while the amplitude of the vestibular stimulus was kept constant at 20° ($-10^\circ/+10^\circ$). The OKR and the VOR were measured with the animal positioned in either a horizontal, which measured the response around the yaw axis or with the animal oriented nose up, which measured the response around the roll axis.

Genetic linkage analysis

A small piece of the tip of the tail of mice was cut off using sharp scissors. The tail tip was incubated overnight at 37°C in a $655\ \mu\text{l}$ lysis solution containing 10 mM Tris, 400 mM NaCl, 2 mM EDTA-di-Na, $1\ \mu\text{g}/\mu\text{l}$ proteinase K and 0.6% SDS. The solution was phenol/chloroform extracted and genomic DNA precipitated with ethanol. After re-dissolving the DNA, DNA concentrations were determined by spectrophotometry and samples were diluted to $100\ \text{ng}/\mu\text{l}$. For DNA samples used in the DNA pooling experiment, a second spectrophotometric reading was taken to confirm the concentration.

For the genome scan the Mouse MAPPAIRS™ Genome-Wide Screening Set was purchased from Research Genetics Inc. This set contains 410 selected markers (developed by the Whitehead/MIT Center for Genome Research) with an average inter-marker distance of 3.5 cM.

Prior to PCR, forward primers were radioactively labeled with [$\gamma^{32}\text{P}$] ATP using T4 polynucleotide kinase. PCR reaction mixtures included 100 ng genomic DNA, $0.15\ \mu\text{M}$ of each primer, $275\ \mu\text{M}$ dNTPs, 0.35 U Taq polymerase and $1.3\ \mu\text{l}$ 10X PCR buffer containing 2M Tris (pH 8), 3 M KCl, 100 mM MgCl_2 , 1% (V/V) Triton X-100 and 0.1% (W/V) gelatin. PCR conditions were as follows: initial denaturation of 3 min at 92°C was followed by 25 cycles of 15 sec at 92°C , 1 min at 55°C and 1 min at 72°C . A final extension step consisted of 7 min at 72°C . The denaturated PCR products were run on a 6% polyacrylamide, 8 M urea sequencing gel. Polymorphic bands were visualized by autoradiography. Extra markers for regions of interest were chosen from Mouse MAPPAIRS™ Genome-Wide Screening Set or from the Whitehead/MIT map (<http://carbon.wi.mit.edu:8000/cgi-bin/mouse>) if no suitable markers were available from the screening set. The extra markers were *D3Mit22*, *D3Mit142*, *D4Mit148*, *D4Mit251*, *D13Mit186* and *D13Mit213*. For markers that were not present in the 'mouse MAPPAIRS™ genome-wide screening set', one of the primers was designed with an M13 sequence at the 5'-end. A 5'-IRD (800nm) M13 primer was included in the PCR reaction, thus labeling the PCR product. Gel electrophoresis and pattern visualization was performed using a LI-COR model 4200 DNA analyzer (NEN). For primers with an

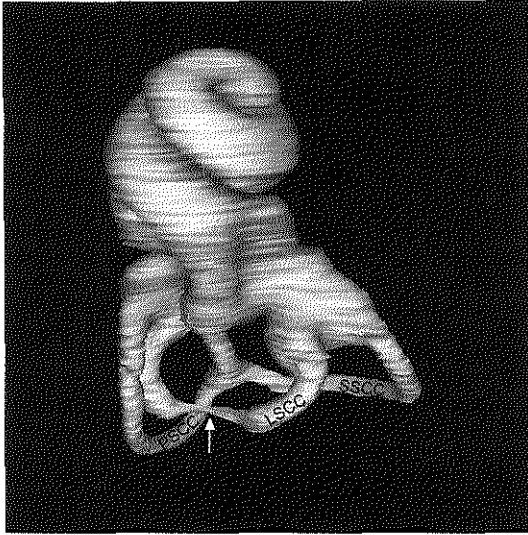


Figure 1: The figure shows a 3D reconstruction made with high resolution CT-scanning of the bony labyrinth taken from an *Ecl*-mouse. The arrow indicates the severe narrowing of the lateral semicircular canal (LSCC). The superior (SSCC) and the posterior (PSCC) semicircular canals have normal dimensions.

M13 sequence, different PCR conditions were used: PCR reaction mixtures included 100 ng genomic DNA, 0.05 μ M of each primer, 170 μ M dNTPs, 0.43 μ M M13 primer, 0.35 U Taq polymerase and 1 μ l 10X PCR buffer. PCR conditions were as follows: initial denaturation of 3 min at 95°C was followed by 40 cycles of 1 min at 95°C, 1 min at 58°C and 1 min at 72°C. A final extension step consisted of 20 min at 72°C.

MLINK two-point linkage analysis using the LINKAGE software package version 5.1 (Lathrop and Lalouel, 1984) was performed between the *Ecs*-gene and the markers which suggested linkage, based on the results of the homozygosity mapping strategy. The frequency of the *Ecs*-gene was set at 0.0001. Equal recombination frequencies between males and females were assumed. Lod scores of 3.3 were considered as significant linkage (Lander and Kruglyak, 1995). Since the LINKAGE software has limitations for the number of sibs in a pedigree, we were not able to calculate lod score values for the genome scan for the *Ecl*-genes. We therefore calculated Chi-square values on the basis of observed and expected values for the 3 genotypes (homozygous for the allele from *C57L/J*, heterozygous, homozygous for the allele from *SWR/J*). The expected values were based on the theoretically expected frequencies (1:2:1) for the 3 genotypes. P-values smaller than 10^{-4} were considered as significant for a genome wide search (Lander and Kruglyak, 1995).

Results

Histopathological examination and 3D reconstruction of the inner ear

Histological examination of the inner ears in both parental strains by means of desktop X-ray microtomography and light and electron microscopy revealed that the auditory portion of the inner ear was entirely normal in both F2-circlers and control animals.

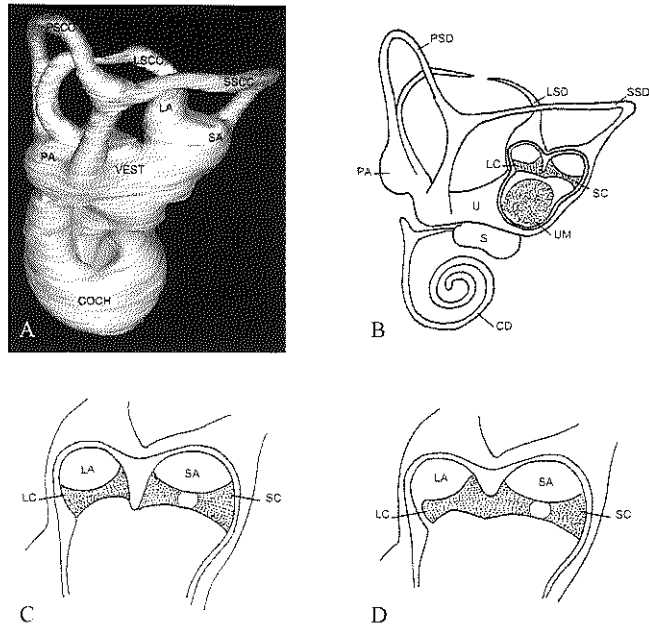


Figure 2: The schematic representation shows morphological abnormalities in the labyrinth of an *Ecl*-mouse. A: 3D reconstruction for comparison. B: Membranous labyrinth of an *Ecl*-mouse. The lateral semicircular duct is interrupted. Opening through the utricular wall shows site and orientation of the utricular macula and the superior and lateral cristae. Detail of the superior and lateral cristae is given in c and d. C: Normal situation. The lateral crista is completely separated from the superior crista. D: Abnormally fused superior and lateral cristae in an *Ecl*-mouse. Abbreviations: CD, cochlear duct; COCH, cochlea; LA, lateral ampula; LC, lateral crista; LSCC, lateral semicircular canal; LSD, lateral semicircular duct; PA, posterior ampula; PSSC, posterior semicircular canal; PSD, posterior semicircular duct; S, sacculus; SA, superior ampula; SC, superior crista; SSCC, superior semicircular canal; SSD, superior semicircular duct; U, utriculus; UM, utricular macula; VEST, vestibulum.

Micro-CT-scanning and subsequent 3D reconstruction showed that all circling F2-animals had prominent defects of their lateral semicircular canals (Fig. 1). The severity of the malformation was variable among animals and between both ears within one animal. The aberrations ranged from a narrowed canal to a complete interruption, but always included the lateral semicircular canals of both ears. Scanning electron microscopy additionally showed an incomplete separation between the lateral and superior crista in some circlers (Fig. 2). The aberrant configuration of the superior crista could underlie possible functional deficits in the vertical vestibular system. Gross anatomy of the otolith organs proved normal in circling animals and none of the labyrinthine deficits were observed in either of the parental strains, F1-offspring or unaffected F2-control animals.

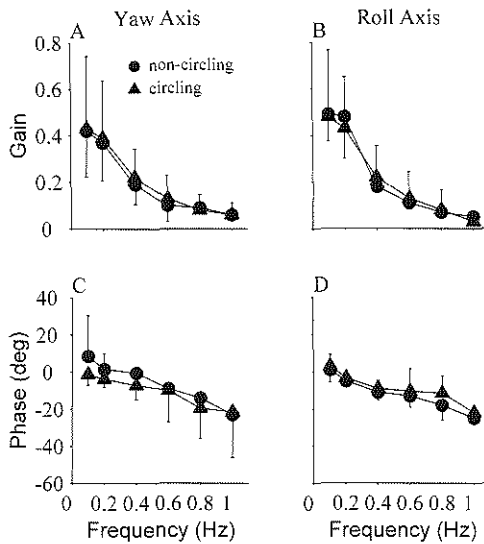


Figure 3: Response of the OKR is plotted for rotation of a visual pattern around the animals yaw (A, C) and roll (B, D) axis. OKR gain (A, B) and phase (C, D) are plotted against frequency in circling (triangles) and non-circling (circles) F2-mice. The error bars indicate S.E.M. There are no significant differences between circling and non-circling F2-mice.

Systems physiology of Ecl mice

We investigated the gain during sinusoidal optokinetic and vestibular stimulation at frequencies ranging from 0.1 Hz to 1 Hz. We tested the OKR and VOR to sinusoidal rotation around the yaw and roll axis of 5 F2-circlers and 3 unaffected littermates. OKR gain and phase showed their familiar relation to stimulus frequency of reducing gain and progressive phase lag as stimulus frequency was increased (Fig. 3). No significant differences in OKR were observed between circling and control animals.

In contrast, VOR in response to both yaw and roll vestibular stimulation showed significant differences ($p=0.002$ 2-way repeated measures ANOVA in both cases) between F2-circlers and their non-circling littermates (Fig. 4). The horizontal VOR was nearly absent in circling animals and only two animals showed small responses at 0.8 and 1 Hz. Vertical VOR in response to roll vestibular stimulation was clearly present in circling animals but were smaller than that of their non-circling littermates. In circling animals, gain increased from 0.05 ± 0.01 at 0.2 Hz to 0.11 ± 0.02 at 1 Hz, while in control animals gain increased from 0.14 ± 0.06 to 0.17 ± 0.02 at the same stimulus frequencies. Phase of the vertical eye movement with respect to table movement was not significantly different between circling and control animals ($p=0.17$; two-way repeated measures ANOVA) measuring $53\pm 15^\circ$ and $48\pm 10^\circ$ at 0.2 Hz for circling and control animals respectively and decreasing to $18\pm 11^\circ$ and $8\pm 4^\circ$ at 1 Hz.

We tested hearing in circling animals to verify that the anatomically intact cochlea was also functional. ABRs were measured in 3 circling animals and 3 non-circling littermates, which all were 2 months of age. Mean auditory thresholds were measured in steps of 5 dB. The lowest response threshold occurred at 12 kHz measuring 20 ± 10 dB and 10 ± 15 dB for circling and non-circling animals respectively (Table 1). The highest threshold was found at 3 kHz measuring 35 ± 5 dB in circling and 40 ± 10 dB in

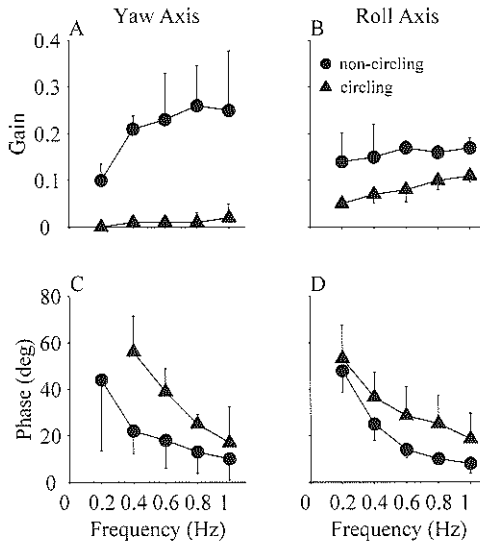


Figure 4: Response of the VOR is plotted to forced whole body rotation in the dark around the animals yaw (A, C) and roll (B, D) axis. VOR gain (A, B) and phase (C, D) are plotted against frequency in circling (triangles) and non-circling (circles) F2-mice. The error bars indicate S.E.M. VOR gain was significantly different between circling and non-circling animals for both directions of rotation. Phase lead of the eye movement with respect to stimulus movement was not significant for rotation around the roll axis. Phase the eye movement could only be calculated in 2 circling animals because VOR gain was often 0.

Stimulus Frequency	Detection threshold circling animals	Detection threshold non-circling animals
3 kHz	35±5 dB	40±10 dB
6 kHz	25±5 dB	25±10 dB
12 kHz	20±10 dB	10±15 dB
24 kHz	30±10 dB	30±15 dB

Table 1: ABR was measured at 4 different frequencies, in circling and non-circling animals. Levels could only be detected in steps of 5 dB. No significant differences were observed between circling animals and non-circling littermates, which shows that cochlear function is not affected by the circling mutation.

non-circling animals. Thresholds were not significantly different between circling and non-circling littermates ($P > 0.1$, student-t test, at all frequencies) indicating that cochlear function was not affected by the circling mutation.

Genetic mapping of *Ecl* and *Ecs* genes

On the basis of segregation analysis, Taylor (Taylor 1976) suggested that the circling behavior is due to two recessive genes. We used this model as a starting point for linkage analysis and used a DNA-pooling strategy to rapidly identify the chromosomal regions that carry recessive *Ecl*- and/or *Ecs*-genes. Pooling DNA samples has proven a very

efficient approach to map both Mendelian and complex traits (Taylor and Rowe, 1989; Asada et al., 1994; Alfred et al., 1997). The technique is based on reducing the number of PCR reactions and subsequent gel runs through analysis of a DNA sample that is taken in equal amounts from a number of affected animals. We first determined which markers from the Mouse MAPPAIRS™ Genome-Wide Screening Set were polymorphic between C57L/J and SWR/J mice. 240 out of 340 tested markers showed different alleles between the parental strains. These 240 markers were dispersed over the entire autosomal portion of the genome and were identified in a DNA sample taken from 17 circling animals. To make sure that the distance between 2 markers was no more than 20 cM, 8 additional markers were chosen from the Whitehead/MIT map. Of all 248 markers tested on the DNA pool from circling animals, two (D14Mit 120 and D14Mit 141) were solely derived from SWR/J alleles. Both markers were located in the same chromosomal region, suggesting that the Ecs-gene was located on chromosome 14. To confirm our finding, we analyzed these two markers in the 17 separate DNA samples that were pooled in the previous experiment. All 17 F2-circlers were homozygous for the SWR/J allele of this marker. Chi-square testing gave a P-value below 10^{-11} for both markers, where a point-wise P-value below 10^{-4} has been suggested as significant linkage for genome wide studies in the mouse (Lander and Kruglyak, 1995). Lod score calculations for both markers gave identical maximum LOD scores of 10.2 where a LOD-score of 3.3 is generally accepted as a genome-wide significance limit (Lander and Kruglyak, 1995). D14Mit44, a marker proximal to D14Mit120, and D14Mit32, which is a marker located distal to D14Mit141, showed both alleles from C57L/J and SWR/J in the DNA pool. These results place the Ecs-locus in a 24 cM region on chromosome 14 (based on the Whitehead/MIT map). None of the 248 informative markers were selectively linked to a C57L/J allele and no markers were therefore linked to the Ecl-locus, which indicated that the Ecl-gene is not recessive.

To confirm that Ecl gene is not a recessive gene, we set up an additional cross between F2-circlers and SWR/J mice. Offspring from this cross (N2) should never be homozygous for the mutant Ecl-gene since it is derived from C57L/J. Consequently, if any circling animals arise in N2-offspring they will invariably be heterozygous for the mutant Ecl-gene, definitely excluding the possibility of recessive Ecl-genes. 18 out of 411 N2-progeny showed circling behavior confirming the non-recessive character of the Ecl-gene. To localize this gene, we separately genotyped 46 N2-circling animals using 87 polymorphic markers dispersed over the entire autosomal portion of the genome. Again we included the same 8 additional markers that were used for mapping Ecs-gene and were located in regions with the largest between-marker distances. Of all markers tested, 22 markers showed a P-value of 0.05 or less. Five of these markers were localized on chromosome 14, confirming the linkage to the Ecs-locus previously found by means of the DNA pooling strategy. With the exception of the chromosome 14 markers, the other 17 markers were tested on 43 additional samples. Only 7 markers showed significant linkage ($P \leq 10^{-4}$, with all samples pooled $n=89$). These markers were located on chromosome 3, 4 and 13 and to distinguish between them these loci are labelled Ecla, Eclb and Eclc. The most frequent allele was in each case derived from the C57L/J strain. For the localization on chromosome 3, 4 and 13, two nearby markers were identified to confirm linkage of these loci to the circling phenotype. All these additional markers were

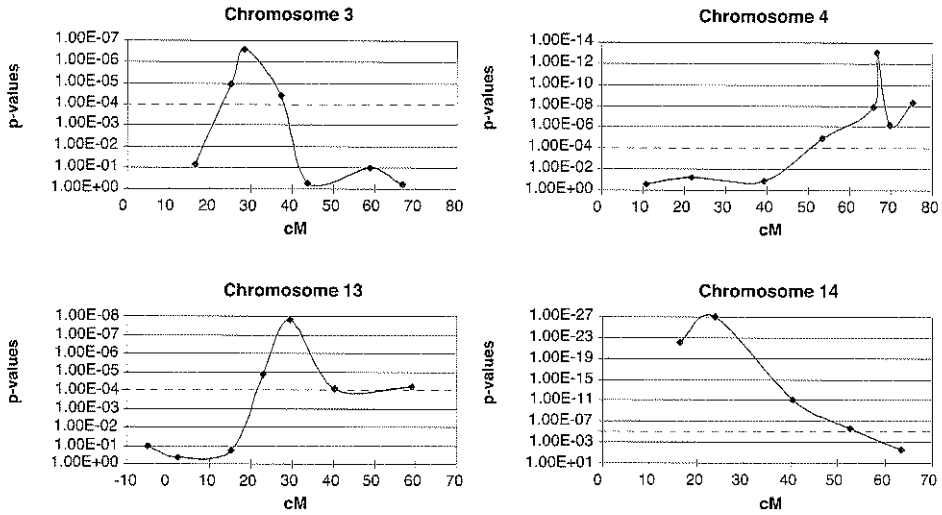


Figure 5: The significance of linkage between markers (dots) and the circler phenotype is represented graphically. Distance to the centromere is expressed in cM. One cM is defined as distance between two locations on a chromosome that have a 1% probability of being separated during recombination in a single generation (approximately 10^6 basepairs in humans). Threshold for a marker, which is significantly linked to the phenotype, is 10^{-4} . Note that the ordinate has been inverted, showing the lowest p-values as a peak in the curve. A smaller P-value situates a marker closer to the locus that is linked to the phenotype. Chromosomes 3,4 and 13 represent the Ecla, Eclb and Eclc loci respectively, while chromosome 14 carries the recessive Ecs locus.

significantly linked at P-values of 10^{-4} or less. Figure 5 presents a graphical interpretation of the P-values from chromosomes 3, 4, 13 and 14.

Liability assessment

Since the Ecs-gene is necessary but not sufficient to cause circling, we wanted to define a liability scale to investigate the contribution of the Ecl-genes. We determined the presence of the recessive Ecs-gene in 243 non-circlers from the F2 offspring. Fifty of these unaffected animals inherited both copies of the mutant Ecs-gene. In a next stage, we genotyped 47 of these selected animals for a genetic marker close to each of the 3 Ecl-genes (on chromosome 3, 4 and 13) and we counted the number of risk Ecl-alleles. For genotyping, we choose markers with the most significant P-value (D3Mit230, D4Mit251 and D13Mit191). Table 2 gives an overview of the distribution of different genotypes at the three Ecl-loci. Note that animals that show 2 Ecla-risk alleles (chromosome 3) and 1 Eclc-risk allele (chromosome 13) but no Eclb-risk allele (chromosome 4) are unaffected. This genotype was never found in affected animals while 8.5% of the unaffected animals displayed this genotype. Only 1 affected animal did not inherit an Eclb-risk allele. Figure 6 presents a graphical overview of these results

Number of risk alleles	Ecla (chrom 3)	Eclb (chrom 4)	Eclc (chrom 13)	# circling mice (% animals)	# non-circling mice (% animals)
6	AA	BB	CC	11 (12%)	1 (2%)
5	Aa	BB	CC	14 (15%)	1 (2%)
	AA	BB	Cc	12 (13%)	1 (2%)
	AA	Bb	CC	7 (7%)	2 (4%)
4	Aa	Bb	CC	11 (12%)	2 (4%)
	Aa	BB	Cc	10 (10%)	2 (4%)
	AA	Bb	Cc	4 (4%)	0 (0%)
	AA	BB	cc	3 (3%)	2 (4%)
	aa	BB	CC	3 (3%)	1 (2%)
	AA	bb	CC	0 (0%)	0 (0%)
3	aa	Bb	CC	4 (4%)	2 (4%)
	aa	BB	Cc	3 (3%)	1 (2%)
	Aa	Bb	Cc	3 (3%)	4 (8.5%)
	AA	Bb	cc	2 (2%)	4 (8.5%)
	Aa	BB	cc	1 (1%)	4 (8.5%)
	AA	bb	Cc	0 (0%)	4 (8.5%)
	Aa	bb	Cc	0 (0%)	0 (0%)
2	AA	bb	cc	1 (1%) ^(*)	1 (2%)
	Aa	Bb	cc	1 (1%)	0 (0%)
	aa	BB	cc	1 (1%)	3 (6%)
	aa	Bb	Cc	0 (0%)	4 (8.5%)
	Aa	bb	Cc	0 (0%)	3 (6%)
	aa	bb	CC	0 (0%)	1 (2%)
1	Aa	bb	cc	0 (0%)	3 (6%)
	aa	Bb	cc	0 (0%)	1 (2%)
	aa	bb	Cc	0 (0%)	0 (0%)
0	aa	bb	cc	0 (0%)	0 (0%)

Table 2: Table 2 shows the distribution of risk alleles in circling and non-circling animals. Non-circling mice represent a selected group that shows homozygosity for the recessive *Ecs*-gene. Upper cases represent risk-alleles derived from *C57L/J* and lower cases represent non-risk alleles derived from *SWR/J*. (*) This is the single circling mouse that did not inherit a copy of the *Eclb*-risk allele for the neighbouring marker. A recombination between the marker and the risk conferring mutation may have occurred in this animal.

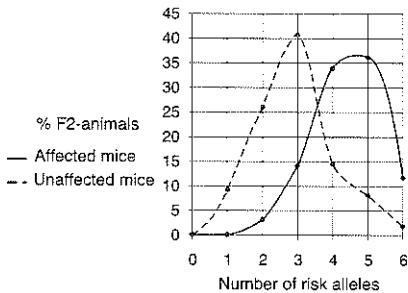


Figure 6: The number of *Ecl* risk alleles was counted in a pool of 47 animals that were homozygous for the recessive *Ecs* allele. Since there were three *Ecl* loci, each animal could have a maximum of 6 risk alleles. Although the number of risk alleles is higher in circling animals, it does not fully predict whether an animal will be affected.

for a model of equal and additive contribution of the three *Ecl*-genes. Although there is a shift in the number of risk alleles between unaffected and affected F2-animals, there is no complete separation between affected and unaffected animals, and a clear threshold cannot be determined.

Discussion

In this paper we report on the morphological and functional properties of the *Ecl*-mouse, a pre-existing mutant with a previously unstudied vestibular pathology. Morphological examination of the inner ears of affected animals revealed a bilateral malformation of the lateral semicircular canal. Furthermore, the cristae of the superior and lateral canals were sometimes fused, supporting the hypothesis that these two sensory structures have a common origin (Morsli et al., 1998). The morphological findings are supported by performance of the VOR, which was virtually absent when the animal was rotated around the vertical axis and clearly attenuated when tested around the animals roll axis. A genome search revealed that circling behavior in *Epistatic circler* mutants is under control of more than 2 genes. Next to the recessive *Ecs*-gene on chromosome 14, we found three modifying *Ecl*-genes localized on chromosomes 3, 4 and 13, which we respectively labeled *Ecl*a, *Ecl*b and *Ecl*c.

Relation of functional and morphological deficits

One of the main functions of the semicircular canals is to provide information about angular acceleration of the head. These accelerations elicit compensatory eye movements that stabilize gaze. The nearly absent horizontal VOR in the *Ecl*-mouse is directly linked to the malformation of the lateral semicircular canal. Only at high stimulus frequencies a small response could be elicited, which likely reflects the fact that orientation of the lateral semicircular canals was not perfectly orthogonal to the plane of stimulation. A proportional component of angular head rotation is therefore sensed by the other semicircular canals and contributes to the VOR in the plane of stimulation. Remaining function of the lateral semicircular canal cannot be fully ruled out since some circling animals possessed a narrowed rather than an interrupted canal. Nevertheless, horizontal VOR gain in circling animals was always lower than in their non-circling littermates.

Vertical VOR gain was also reduced in circling animals compared to control animals. Obviously the same reasoning used to explain the residual horizontal VOR may be applied in this case. In the roll position the canals are not so perfectly aligned as to put the axis of stimulation exactly in the plane of the lateral semicircular canal. This means that in normal animals the lateral semicircular canal may constitute part of the input to the vertical VOR. Eliminating this input could cause a reduction in vertical VOR gain. However, orientation of the lateral semicircular canal is certainly far from the orientation in which it is maximally sensitive and it seems disproportionate that omitting this signal would cause almost 50% reduction in vertical VOR gain. The fact that malformations occur in the crista of the superior semicircular canal may add to the reduction in vertical VOR gain. It is possible that fusion of the anterior and lateral cristae impairs proper

function of the superior semicircular canal and that reduced vertical VOR gain in circling animals is a result of this defect.

In contrast to the VOR, the OKR retrieves information from the visual system to generate eye movements. As expected, the OKR in horizontal and vertical direction is normal in circling animals, indicating that their visual system is not affected. These control experiments demonstrate that the impaired VOR responses are not due to some deficit in the oculomotor output system or in central parts of the nervous system that produce this output. We also tested the hearing of *Ecl*-mice by ABR and found normal thresholds. These findings are in line with the absence of cochlear abnormalities.

Genotype underlying the functional and morphological deficits

Genetic linkage studies revealed two important facts. First, we never found circling animals that were not homozygous for the *Ecs*-gene, which indicates that 2 risk alleles for *Ecs* are needed to produce the phenotype. Second, we could identify only 1 affected animal that was homozygous for the non-risk allele of the *Eclb*-gene. As the exact genetic distance between the marker used for genotyping and the *Eclb*-gene is unknown, a recombination between these two may have occurred in this animal. Under this assumption, all affected animals should have at least 1 risk allele for *Eclb* to produce circling behavior. The fact that *Ecla* and *Eclc* are clearly not obligatory suggests an epistatic interaction between *Ecs* (recessive) and *Eclb* (non-recessive), with additive effects of *Ecla*, *Eclc* and possibly the second allele of *Eclb*. A simple model of equal and additive effects for the *Ecl*-genes is represented in figure 6. The fact that we were not able to determine a clear threshold in the number of risk *Ecl*-alleles to produce circling indicates that this model is not entirely correct. Functional inequality between the 3 *Ecl*-genes may be an explanation as well as involvement of additional genetic or environmental factors. Despite possible involvement of other genes or environmental factors, it is clear that the *Ecs*-, *Ecla*-, *Eclb*- and *Eclc*-genes are important contributors to vestibular dysfunction in the *Epistatic circler* mouse.

We mapped the *Ecl*-gene on chromosome 4 where also the *Wheels* (*Whl*) mutation has previously been mapped (Nolan et al., 1995). The *Whl*-mutation displays a complex phenotype, which includes hyperactive circling. The map location of the *Eclb*-gene on chromosome 4, at 66 cM distal to the centromere, allowed us to rule out the possibility that the *Eclb*- gene is allelic to the *Whl*-mutation, which is localized within the 0-8 cM region distal to the centromere of chromosome 4 (Nolan et al., 1995). *Whirler* (Lane, 1963) and *Jerker* (Eicher et al., 1977) are other candidate genes, localized in this region of chromosome 4. Both these mouse mutants show circling behavior in addition to deafness. The *Whirler* mutation is located at 31.4 cM distal to the centromere and *Jerker* maps at 80.1 cM distal to the centromere. Haplotypes of the *Eclb*-candidate region will have to be constructed to indicate if one of these genes is located in the *Eclb*-candidate region.

In conclusion, the circling behavior in the *Epistatic circler* mouse is controlled by a necessary recessive *Ecs*-gene and a necessary *Eclb*-gene, in combination with several facultative modifying *Ecl*-genes. Identification of the individual genes in the *Ecs* and *Ecl* loci and how exactly they interact to produce vestibular dysfunction remains to be

determined. This study illustrates how the horizontal and vertical vestibular system of a mouse mutant can be differently affected and how genetic determinants of such complex and multigenic pathology can be identified using modern molecular genetic tools.

References

- Alavizadeh A, Kiernan AE, Nolan P, Lo C, Steel KP, Bucan M (2001) The Wheels mutation in the mouse causes vascular, hindbrain, and inner ear defects. *Dev Biol* 234:244-260.
- Alfred JB, Rance K, Taylor BA, Phillips SJ, Abbott CM, Jackson IJ (1997) Mapping in the region of Danforth's short tail and the localization of tail length modifiers. *Genome Res* 7:108-117.
- Asada Y, Varnum DS, Frankel WN, Nadeau JH (1994) A mutation in the Ter gene causing increased susceptibility to testicular teratomas maps to mouse chromosome 18. *Nat Genet* 6:363-368.
- Deol MS (1966) Influence of the neural tube on the differentiation of the inner ear in the mammalian embryo. *Nature* 209:219-220.
- Doolittle DP (1963) Two-gene circling in the mouse. *Genetics* 48:887.
- Eicher EM, Reynolds S, Southard JL (1977) Linkage of Gpd-1 and of je. *Mouse News Lett* 56:42.
- Lander E, Kruglyak L (1995) Genetic dissection of complex traits: guidelines for interpreting and reporting linkage results. *Nat Genet* 11:241-247.
- Lane PW (1963) A recessive behaviour mutation in linkage group VIII. *J Hered* 54:263-266.
- Lathrop GM, Lalouel JM (1984) Easy calculations of lod scores and genetic risks on small computers. *Am J Hum Genet* 36:460-465.
- Morsli H, Choo D, Ryan A, Johnson R, Wu DK (1998) Development of the mouse inner ear and origin of its sensory organs. *J Neurosci* 18:3327-3335.
- Nolan PM, Sollars PJ, Bohne BA, Ewens WJ, Pickard GE, Bucan M (1995) Heterozygosity mapping of partially congenic lines: mapping of a semidominant neurological mutation, Wheels (Whl), on mouse chromosome 4. *Genetics* 140:245-254.
- Rogers MJ, Fleming J, Kiernan BW, Mburu P, Varela A, Brown SD, Steel KP (1999) Genetic mapping of the whirler mutation. *Mamm Genome* 10:513-519.
- Sasov A, Van Dyck D (1998) Desktop X-ray microscopy and microtomography. *J Microsc* 191:151-158.
- Taylor BA (1976) Epistatic circling gene of C57L/J. *Mouse News Lett* 55:17.
- Taylor BA, Rowe L (1989) A mouse linkage testing stock possessing multiple copies of the endogenous ecotropic murine leukemia virus genome. *Genomics* 5:221-232.
- van Alphen AM, Stahl JS, De Zeeuw CI (2001) The dynamic characteristics of the mouse horizontal vestibulo-ocular and optokinetic response. *Brain Res* 890:296-305.
- Van Spaendonck MP, Cryns K, Van De Heyning PH, Scheuermann DW, Van Camp G, Timmermans JP (2000) High resolution imaging of the mouse inner ear by microtomography: a new tool in inner ear research. *Anat Rec* 259:229-236.

3.2 ORIGIN OF VESTIBULAR DYSFUNCTION IN USHER SYNDROME TYPE 1B

John C. Sun*, Adriaan M. van Alphen*, Mariette Wagenaar, Patrick Huygen, Casper C. Hoogenraad, Tama Hasson, Sebastiaan K.E. Koekkoek, Barbara A. Bohne and Chris I. De Zeeuw

* These authors contributed equally to this paper

Sun JC, van Alphen AM, Wagenaar M, Huygen P, Hoogenraad CC, Hasson T, Koekkoek SK, Bohne BA, De Zeeuw CI (2001) *Neurobiol Dis* 8:69-77.

Abstract

It is still debated to what extent the vestibular deficits in Usher patients are due to either central vestibulocerebellar or peripheral vestibular problems. Here, we determined the origin of the vestibular symptoms in Usher 1B patients by subjecting them to compensatory eye movement tests and by investigating the shaker-1 mouse model, which is known to have the same mutation in the *myosin-VIIa* gene as Usher 1B patients. We show that Myosin-VIIa is not expressed in the human or mouse cerebellum and that the vestibulocerebellum of both Usher 1B patients and shaker-1 mice is functionally intact in that the gain and phase values of their optokinetic reflex are normal. In addition, Usher 1B patients and shaker-1 mice do not show an angular vestibulo-ocular reflex even though eye movement responses evoked by electrical stimulation of the vestibular nerve appear intact. Finally, we show histological abnormalities in the vestibular hair cells of shaker-1 mice at the ultrastructural level, while the distribution of the primary vestibular afferents and the vestibular brainstem circuitries are unaffected. We conclude that the vestibular dysfunction of Usher 1B patients and shaker-1 mice is peripheral in origin.

Introduction

Usher syndrome is the most frequent cause of deaf-blindness in humans (Boughman et al., 1983). Usher syndrome type 1 is an autosomal recessive disorder characterized by sensorineural hearing loss, balance problems and retinitis pigmentosa. Usher 1B accounts for 75% of Usher 1 patients. Mutations in the *myosin-VIIa* gene are responsible for the deficits in Usher 1B patients (Weil et al., 1995). Hallgren (1959) was the first to describe the vestibular dysfunction of Usher syndrome patients as "vestibulocerebellar ataxia". Others later provided radiographic evidence for cerebellar abnormalities in Usher 1 patients (Bloom et al., 1983; Lynch et al., 1994; Tamayo et al., 1996; Schaefer et al., 1998). These findings included cerebellar atrophy and a diminished level of circulation in the cerebellar vermis and lateral hemispheres. In line with these studies Kumar et al. (Kumar et al., 1984) found in part of his Usher patients retro labyrinthine signs such as vestibular decruitment and spontaneous vertical or horizontal nystagmus. However, these studies diverge with other clinical investigations such as those of Möller and colleagues (Möller et al., 1989), who propagated that the vestibular deficits in Usher patients are not due to central but peripheral problems.

A central vestibular abnormality has also been implicated in shaker-1 mice (Deol, 1956), which suffer from the same mutation in the *myosin-VIIa* gene (Gibson et al., 1995). The shaker-1 (sh1) mouse mutant was first described in 1929 by Lord and Gates (Lord and Gates, 1929) as possessing several presumably central behavioral abnormalities including hyperactivity, head-tossing and circling. In 1969, Tan Creti (1969) found gliosis in the medial vestibular nucleus of shaker-1 mice, again suggesting a central vestibular lesion. However, more recent morphological investigations and localization studies of Myosin-VIIa did not provide unequivocal answers yet as to whether both central and peripheral defects may contribute to the vestibular deficits. For example, Gibson et al. (Gibson et al., 1995) showed that Myosin-VIIa is present in the murine brain, but it is still unknown whether it is also expressed in the human or murine cerebellum. Similarly, Hasson et al. (1997b) demonstrated that Myosin-VIIa is present in

vestibular hair cells of the frog, but so far no ultrastructural abnormalities have been described for the vestibular hair cells of the semicircular canals in shaker-1 mice. Therefore, the controversy concerning the origin of the vestibular dysfunction in Usher 1 patients and shaker-1 mice is still unresolved. In the present multidisciplinary study we have attempted to elucidate to what extent the peripheral vestibular and/or the central cerebellar components each contribute to the general vestibular deficits in Usher 1B patients and shaker-1 mice.

Methods

Immunohistochemistry

Cerebellar sections were immunoreacted with antisera against Myosin-VIIa and for control against Myosin-VI (Avraham et al., 1995). Sections of human cerebellum were obtained from non-demented normal adult subjects, while sections of the mouse cerebellum were obtained from adult C57BL/6 mice. The immunostaining procedure was performed as described by De Zeeuw et al. (1997). Rabbit-affinity-purified anti-human Myosin-VIIa was used at a concentration of 20 µg/ml, while rabbit affinity purified anti-porcine Myosin-VI was used at a concentration of 10 µg/ml (Hasson and Mooseker, 1994; Hasson et al., 1997a). All sections were counterstained with cresyl violet.

Western blot

To confirm the immunohistological analyses described above we made western blots of the human and mouse cerebellum with the use of the same antisera. Fresh non-fixed frozen human cerebellum was obtained from non-demented adults (Hersenbank, Dutch Brain Institute NIH). Fresh mouse brains and kidneys were obtained from 3 month-old control +/sh-1 mice after cervical dislocation. Protein samples were prepared by homogenization in phosphate buffered saline (+1%Triton) in the presence of protease inhibitors (Boehringer Mannheim), sonicated and boiled in sodium dodecyl sulphate sample buffer in the presence of dithiothreitol. Ten µg of total protein was loaded per lane, separated by electrophoresis and immunoblotted as described by De Zeeuw et al. (1997). Antibodies were diluted as follows: rabbit-affinity-purified anti-human Myosin-VIIa was used at a concentration of 5 µg/ml (Hasson et al., 1997a); rabbit affinity purified anti-porcine Myosin-VI was used at a concentration of 1 µg/ml (Hasson and Mooseker, 1994); and goat-anti-rabbit antibodies coupled to alkaline phosphatase was diluted 1:2000 (Sigma). Enzymatic detection of bound antibody was carried out using Sigma Fast BCIP/NBT system.

Eye movement recordings

We recorded the eye movements of Usher 1B patients and shaker-1 mice as well as control subjects and littermates. Fifteen Usher 1B patients (age 9-35 years) and 28 age-matched normal subjects were tested and included in the analyses. All selected patients

were confirmed to have the USH1B genotype (W. Kimberling, personal communication 1999). We excluded the three oldest Usher 1B patients who had considerable degree of visual acuity loss and visual field loss due to progressive pigmentary retinopathy. The compensatory eye movements were recorded with Toennies recording equipment (Freiburg im Breisgau, Germany). Velocity step stimulation (90°/sec) was used to evaluate the angular vestibulo-ocular reflex (VOR). The optokinetic reflex (OKR) tests were performed at constant velocities of 40°/sec and 60°/sec.

The original shaker-1 (SH1/LeS1) mutant strain was obtained from Jackson Laboratory (Bar Harbor, ME). Eight homozygous shaker-1 mice (sh1/sh1) and seven heterozygous mice (+/sh1) control littermates with ages ranging from one to two months were tested. Eye movements were recorded with the use of the scleral search coil method for mice (De Zeeuw et al., 1998). After general anesthesia was induced and maintained with halothane (1 part O₂, 2 parts N₂O, and 2% Fluorane), a minicoil was placed underneath the conjunctiva and lateral to the cornea using standard procedures in our laboratory (Koekkoek et al., 1997; De Zeeuw et al., 1998). Sinusoidal stimulation was used to measure the gain and phase of the eye movements in awake mice. The OKR and VOR tests were performed at frequencies and peak velocities ranging from 0.1 Hz to 1.2 Hz and 1.3°/sec to 37.7°/sec, respectively. The eye movement and stimulus traces were sampled with a 32b A-D converter at a frequency of 500 Hz (CED Ltd., Cambridge, UK). All data was analyzed offline using a custom-made analysis program for Windows (De Zeeuw et al., 1995).

Electrical stimulation experiments

Eye movements of shaker-1 mutants were recorded following electrical stimulation of their vestibular apparatus or vestibular nerve. After general anesthesia was induced and maintained with halothane, electrode implants made of Teflon-insulated platinum-iridium wire (25 µm) were placed into the horizontal semicircular canals or vestibular nerve of four 1-month-old shaker-1 mice and four control littermates on the side contralateral to their eye coils. The ground electrode was soldered to a screw, which was placed in the skull. Galvanic stimulation with a single pulse (pulse width = 0.4 msec) of negative current (300 µA) was applied to the canal, and eye movements were recorded at a sampling rate of 5 kHz. Traces were digitally differentiated and latencies were measured at the onset of the first change in eye velocity.

Vestibular nerve tracing and immunostaining of vestibular afferents and efferents

To visualize the vestibular afferents and efferents we employed both anterograde and retrograde vestibular nerve tracing and immunohistochemistry. The vestibular nerves were traced with the use of wheat germ agglutinin conjugated to horse radish peroxidase (WGA-HRP; Sigma, St. Louis, MO; 7% volume in 1 µl saline), which was injected into the perilymph and endolymph of the horizontal semicircular canal of shaker-1 mice and control littermates. The holes were sealed with bone wax. After a survival time of 48 hours, the brainstem was processed for HRP according to standard procedures in our laboratory. In some experiments neuronal tracing was combined with vestibular nerve

stimulation; in these cases 50 μ A of negative current was applied to the semicircular canal. The vestibular nerve was stimulated for 1 hour immediately after injection and 1 hour prior to sacrifice of the mouse, at 48 hours post-injection. Immunostaining of the vestibular fibers was performed with the use of antisera against calretinin (1:6,000 rabbit polyclonal antibody; Chemicon, Temecula, CA) according to standard procedures in our laboratory (Kevetter, 1996; De Zeeuw et al., 1997).

Electron microscopy

To find out whether a mutation of *myosin-VIIa* induces a morphological aberration in vestibular hair cells, which are known to express this protein (Hasson et al., 1997b), we performed an ultrastructural analysis of these cells in the shaker-1 mutant. Three 1-month-old shaker-1 mice and three control littermates were processed according to the protocol described by Bohne and Harding (Bohne and Harding, 1997). In short, the temporal bone was dissected and the bony labyrinth surrounding the cristae ampullaris was removed by hand using a steel pick and razor blades after plastic embedding and prior to ultrathin sectioning in order to avoid any artifacts secondary to decalcification. Thin sections of cristae ampullaris were made perpendicular to the endolymphatic surface of the sensory epithelium. The sections were examined with a Philips CM100 transmission electron microscope.

Results

Expression of Myosin-VIIa in Human and Mouse Cerebellum

In view of the cerebellar abnormalities observed in radiographs of Usher 1 patients, we first determined whether Myosin-VIIa is expressed in the human cerebellum. Sections of human cerebellum were immunostained with an antibody against Myosin-VIIa, and as a positive control with an antibody against Myosin-VI, a different class of the Myosin isozyme, which has been shown to be expressed in the murine brain (Avraham et al., 1995). Our results showed that the Purkinje cell bodies of the human cerebellum were positively labeled for Myosin-VI (Fig. 1a), but not for Myosin-VIIa (Fig. 1b). This result also held true for the mouse sections (data not shown). The immunocytochemical data were corroborated by Western blot analysis, which showed that neither the human nor mouse cerebellum expressed Myosin-VIIa (Fig. 1d). In contrast, Myosin-VI was found at high levels in both the human and mouse cerebellum (Fig. 1c).

Eye Movement Recordings in Usher 1B Patients and Shaker-1 Mice

To determine the cerebellar function of Usher 1B patients and shaker-1 mice at the behavioral level we investigated their OKR, which is known to be controlled by the flocculus of the vestibulocerebellum (Ito et al., 1982; Rambold et al., 2002). None of the Usher 1B patients showed any spontaneous nystagmus. The OKR gains of both Usher 1B

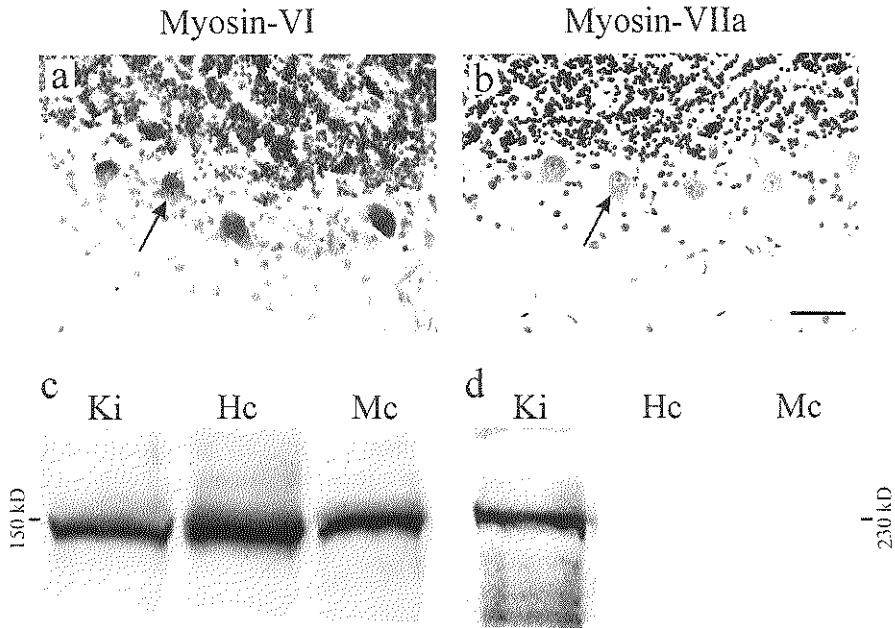


Figure 1: Expression of myosin-VIIa in human and mouse cerebellum. Human cerebellum immunostained with an antibody against (a) myosin-VI and (b) myosin-VIIa. Western blot of mouse kidney (Ki), human cerebellum (Hc) and mouse cerebellum (Mc) labeled with an antibody against (c) myosin-VI and (d) myosin-VIIa. Arrows in (a, b) indicate Purkinje cell bodies. Scale bar is 50 μ m.

patients and shaker-1 mice were not significantly different from those of normal age-matched subjects and heterozygous littermate mice, respectively (Fig. 2a, b). The OKR phase values were also not significantly different from their controls (data not shown).

To assess the vestibular function in Usher 1B patients and shaker-1 mice, the gain of their VOR was also investigated. Both Usher 1B patients and shaker-1 mice had no VOR response. Nystagmic responses to velocity step stimulation were lacking (Fig. 2c). To determine the site of the lesion in their VOR pathway, we investigated the eye movement response of shaker-1 mice following direct electrical stimulation of their primary vestibular afferents thereby bypassing the vestibular hair cells. Unilateral stimulation of the horizontal semicircular canal evoked contralateral horizontal eye movements in both the shaker-1 mice and control littermates (Fig. 3). Latencies of the eye-movement response in the shaker-1 mice were not significantly longer than those in controls. In fact, the mean latency value was 3.6 ms for the shaker-1 mice as opposed to 3.9 ms for the controls. Interestingly, electrical stimulation of the cochlea in the deafness mouse, a mutant with cochlear hair cell degeneration, has also been reported to have a slightly shorter latency of its central brainstem response (Bock et al., 1985).

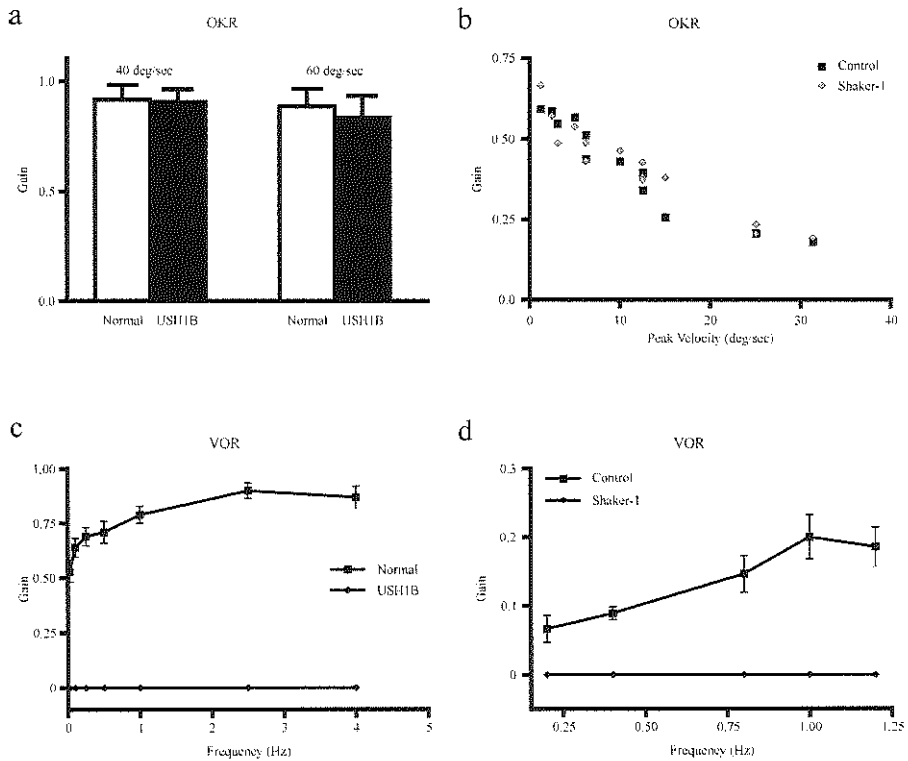


Figure 2: Eye movement recordings in Usher 1B patients and shaker-1 mice. (a) OKR gain values of normal controls and Usher 1B patients were not significantly different, p value = 0.57 at 40°/sec and p value = 0.11 at 60°/sec (unpaired t-test). (b) OKR gain values of control littermates and shaker-1 mice were also not significantly different, p value = 0.31 for all peak velocities (two-way ANOVA). VOR gain values of (c) normal controls and Usher 1B patients, and (d) control littermates and shaker-1 mice. The gain values of Usher 1B patients and shaker-1 mice during VOR in the dark were zero for all frequencies tested.

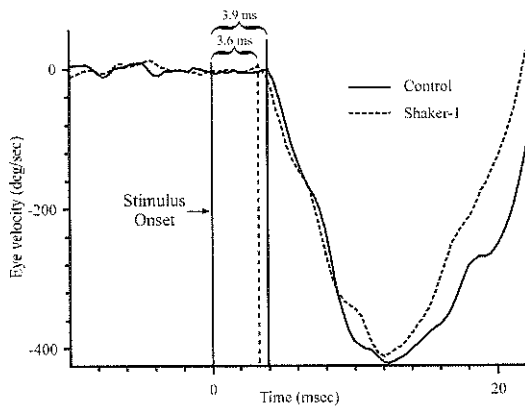


Figure 3: An example is shown of the horizontal eye movements that are elicited by electrical stimulation of the lateral canal in one control and one shaker mouse. The trace represents an average of 11 electrical stimulations.

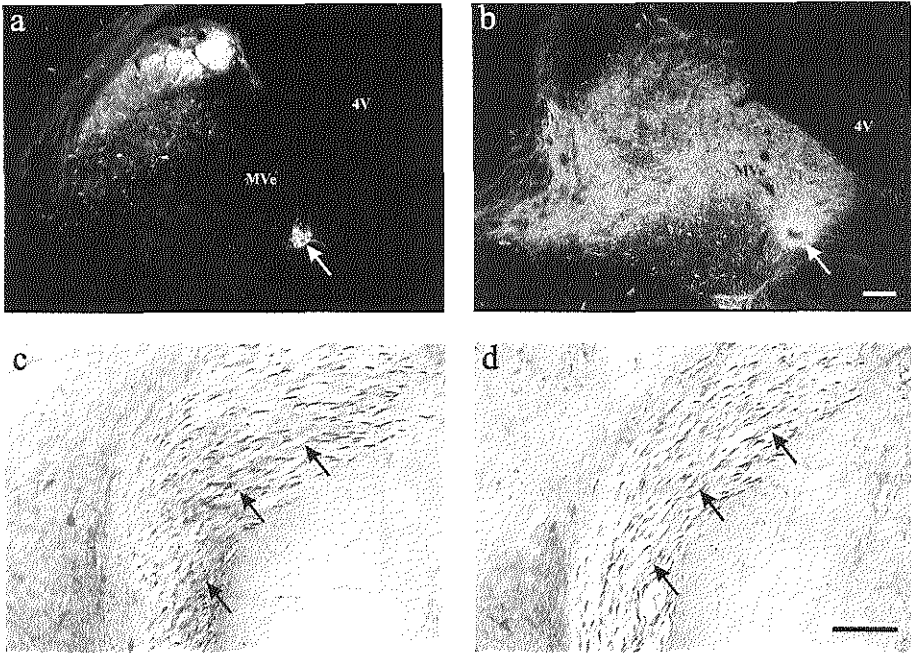


Figure 4: WGA-HRP tracing and immunocytochemistry of the central vestibular pathway. WGA-HRP neuronal tracing of central vestibular pathway of shaker-1 mice (a) without brainstem stimulation and (b) with stimulation. Photomicrographs (a,b) are darkfield coronal sections through the medial vestibular nucleus (MVe) of the shaker-1 mice brainstems. Arrows indicate retrograde labeled vestibular neuronal cell bodies that provide the efferents to the vestibular apparatus. 4V=fourth ventricle. Immunostaining of primary vestibular afferent fibers (arrows) at their entrance of the brainstem labeled with an antibody against calretinin in (c) control littermates and (d) shaker-1 mice. Scale bars are 100 μm .

Vestibular Nerve Tracing and Immunostaining of Vestibular Afferents and Efferents

To support our electrophysiological data described above, we confirmed histologically that the central vestibular pathway of the shaker-1 mouse is intact. When we injected WGA-HRP into the horizontal semicircular canal of shaker-1 mice and control littermates, we found that the shaker-1 mice showed retrograde transport of WGA-HRP, but no anterograde transport (Fig. 4a), whereas the control littermates showed both retrograde labeling of their vestibular efferents and anterograde labeling of their vestibular afferents (not shown). However, when the vestibular nerve of shaker-1 mice was stimulated with electrical current, anterograde transport did occur (Fig. 4b). Immunolabeling of the primary vestibular afferents with the use of an antibody against calretinin also showed that the primary vestibular afferents are present in shaker-1 mice, and that they have the same distribution as in their control littermates (Fig 4c, d). Thus,

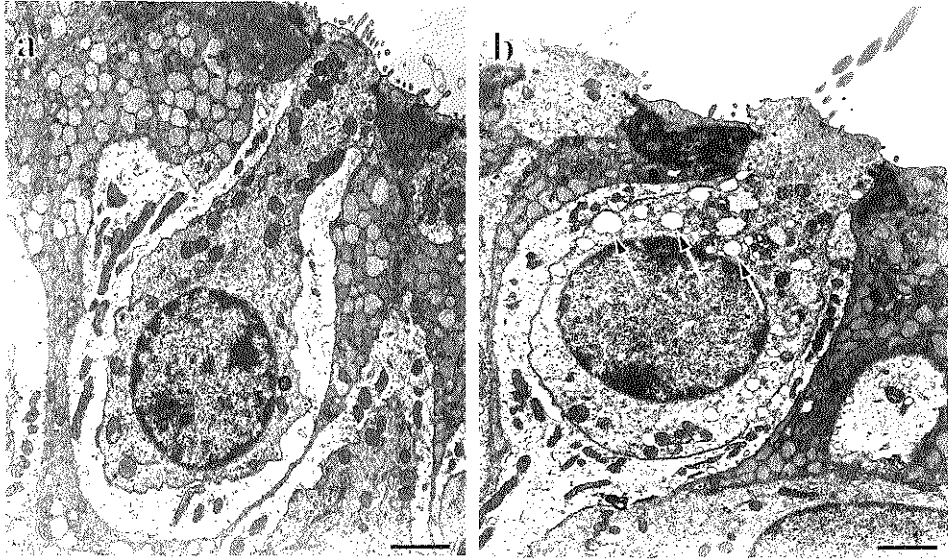


Figure 5: Transmission electron microscopy of vestibular hair cells. Type I vestibular sensory hair cell in the cristae ampullaris of (a) a control littermate and (b) a shaker-1 mouse. Note the presence of numerous vacuoles (arrows) in the hair cells of the shaker-1 mouse. Scale bars are 2 μm .

together the data presented above indicate that the vestibular fibers are normally developed in the shaker-1, but that their transport of neuronal tracers can be hampered by reduced activity in the hair cells.

Transmission Electron Microscopy of Vestibular Hair Cells

To understand the mechanism of dysfunction in the vestibular hair cells of shaker-1 mice, we analyzed their hair cells by transmission electron microscopy. In shaker-1 mice numerous large vacuoles were found in the cytoplasm of the hair cells, while vacuoles were rarely found in controls (Fig. 5a, b). The vacuoles were present in both type I and type II vestibular hair cells. Contrary to our expectation, the stereocilia and kinocilium of the vestibular hair cells in the shaker-1 mice did not show any abnormality even though such deficits have been demonstrated in the cochlear hair cells of the shaker-1 mice by our group (unpublished data) and others (Self et al., 1998).

Discussion

The major topic of the present paper was to elucidate to what extent peripheral deficits in the vestibular apparatus and/or central deficits in the vestibulocerebellum may contribute to the vestibular symptoms in Usher 1B patients and shaker-1 mice. We have employed a large variety of different techniques and all experiments indicate that the primary cause

of the vestibular disorders following mutations in the *myosin-VIIa* gene is in essence a peripheral and not a central defect.

Several pieces of evidence indicate that the function of the vestibular apparatus in Usher 1B patients and/or shaker-1 mice is not intact. First, the VOR in both Usher 1B patients and shaker-1 mice was totally absent. Central vestibular deficits can impair the VOR in several ways, but to our best knowledge a total blockage of the VOR has never been reported to be caused by a pure central deficit due to a genetic disorder. Second, the cytology of the vestibular hair cells was abnormal. The present electron microscopic analysis demonstrated that large numbers of vacuoles accumulate in these cells. Since Myosin-VIIa, which is present in hair cells (Hasson et al., 1997b), may play a role in intracellular organelle targeting and membrane trafficking (Richardson et al., 1997; Liu et al., 1998), these ultrastructural results suggest that transport of membranous organelles inside the hair cells is impaired. Third, anterograde transport of neuronal tracers was strongly reduced or absent following injection in the unstimulated vestibular apparatus of shaker-1 mice, while the same process was normally present in unstimulated control littermates and in shaker-1 mutants that were electrically stimulated in their vestibular apparatus. Apparently, the vestibular hair cells in the shaker-1 mutants are normally not sufficiently active to allow uptake and/or transport of tracers by the primary vestibular afferents. In conjunction, the findings described above strongly point towards a severe peripheral problem that impairs signal transduction from the hair cells to the second-order vestibular neurons.

In contrast, other pieces of evidence indicate that function of the central vestibulocerebellar system in Usher 1B patients and/or shaker-1 mice is intact and not directly affected by a mutation in the *myosin-VIIa* gene. First, both the immunocytochemical studies and the western blots indicated that Myosin-VIIa is not expressed in the cerebellum. Second, both the tracing studies and the immunocytochemical calretinin studies showed that the vestibular efferents as well as the primary vestibular afferents, which also project to the vestibulocerebellum, are normally developed and intact. Third, the finding that eye movements could be evoked by electrical stimulation of the vestibular apparatus at normal latencies also indicates that the vestibular brainstem pathways and connections are functionally intact. Finally, our eye movement recordings in Usher 1B patients and shaker-1 mutants showed that a mutation in the *myosin-VIIa* gene is compatible with normal OKR gain and phase values. These latter results indicate that the function of the vestibulocerebellum is intact because aberrations in this function will lead to a gain reduction and phase lag of the OKR (Fetter et al., 1994; De Zeeuw et al., 1995; Koekkoek et al., 1997; Wessel et al., 1998).

Together the data presented above allow us to conclude that vestibular dysfunction due to mutations in the *myosin-VIIa* gene is probably caused by peripheral deficits. This conclusion raises the question as to how the cerebellar pathology that has been documented in radio-imaging studies of Usher 1 patients comes about (Bloom et al., 1983; Lynch et al., 1994; Tamayo et al., 1996; Schaefer et al., 1998). One explanation is that the cerebellar atrophy is secondary to the peripheral defect and the concomitant change in motor behavior. This explanation would be in line with the fact that the cerebellar MRI abnormalities associated with Usher syndrome type I occur only in 50% of the cases and that the exact site and size of the atrophy can vary substantially (Tamayo et al., 1996). Another possibility is that the previously documented Usher 1 patients were

not all Usher 1B patients. Because the *myosin-VIIa* gene was only recently cloned, the Usher 1 patients of previous studies were not, in contrast to those of the present study, genetically screened. The present conclusion about the origin of the vestibular dysfunctions in Usher 1B patients and shaker-1 mice may have some positive impact on the mode of future therapy. With the belief that the CNS may be involved in the vestibular dysfunction of Usher 1B patients, researchers have not been too optimistic about finding a treatment. The present findings might revive research to develop local peripheral treatment for the balance problems in Usher 1B patients using for example virally mediated vectors to efficiently transfer candidate genes into hair cells (see e.g. Kelley, 1997).

References

- Avraham KB, Hasson T, Steel KP, Kingsley DM, Russell LB, Mooseker MS, Copeland NG, Jenkins NA (1995) The mouse Snell's waltzer deafness gene encodes an unconventional myosin required for structural integrity of inner ear hair cells. *Nat Genet* 11:369-375.
- Bloom TD, Fishman GA, Mafee MF (1983) Usher's syndrome. CNS defects determined by computed tomography. *Retina* 3:108-113.
- Bock GR, Horner K, Steel KP (1985) Electrical stimulation of the auditory system in animals profoundly deaf from birth. *Acta Otolaryngol Suppl* 421:108-113.
- Bohne BA, Harding GW (1997) Processing and analyzing the mouse temporal bone to identify gross, cellular and subcellular pathology. *Hear Res* 109:34-45.
- Boughman JA, Vernon M, Shaver KA (1983) Usher syndrome: definition and estimate of prevalence from two high- risk populations. *J Chronic Dis* 36:595-603.
- De Zeeuw CI, Wylie DR, Stahl JS, Simpson JI (1995) Phase Relations of Purkinje Cells in the Rabbit Flocculus During Compensatory Eye Movements. *J of Neurophysiol* 74:2051-2063.
- De Zeeuw CI, Hoogenraad CC, Goedknecht E, Hertzberg E, Neubauer A, Grosveld F, Galjart N (1997) CLIP-115, a novel brain-specific cytoplasmic linker protein, mediates the localization of dendritic lamellar bodies. *Neuron* 19:1187-1199.
- De Zeeuw CI, Hansel C, Bian F, Koekkoek SK, van Alphen AM, Linden DJ, Oberdick J (1998) Expression of a protein kinase C inhibitor in Purkinje cells blocks cerebellar LTD and adaptation of the vestibulo-ocular reflex. *Neuron* 20:495-508.
- Deol M (1956) The anatomy and development of the mutants pirouette, shaker-1 and waltzer in the mouse. *Proc Roy Soc Lond* 145.
- Fetter M, Klockgether T, Schulz JB, Faiss J, Koenig E, Dichgans J (1994) Oculomotor abnormalities and MRI findings in idiopathic cerebellar ataxia. *J Neurol* 241:234-241.
- Gibson F, Walsh J, Mburu P, Varela A, Brown KA, Antonio M, Beisel KW, Steel KP, Brown SD (1995) A type VII myosin encoded by the mouse deafness gene shaker-1. *Nature* 374:62-64.
- Hallgren B (1959) Retinitis pigmentosa combined with congenital deafness; with vestibulo-cerebellar ataxia and mental abnormality in a proportion of cases: a clinical and genetic statistic study. *Acta Psychiatr Scand* 34:5-101.

- Hasson T, Mooseker MS (1994) Porcine myosin-VI: characterization of a new mammalian unconventional myosin. *J Cell Biol* 127:425-440.
- Hasson T, Walsh J, Cable J, Mooseker MS, Brown SD, Steel KP (1997a) Effects of shaker-1 mutations on myosin-VIIa protein and mRNA expression. *Cell Motil Cytoskeleton* 37:127-138.
- Hasson T, Gillespie PG, Garcia JA, MacDonald RB, Zhao Y, Yee AG, Mooseker MS, Corey DP (1997b) Unconventional myosins in inner-ear sensory epithelia. *J Cell Biol* 137:1287-1307.
- Ito M, Jastreboff PJ, Miyashita Y (1982) Specific effects of unilateral lesions in the flocculus upon eye movements in albino rabbits. *Exp Brain Res* 45:233-242.
- Kelley MW (1997) Cellular commitment and differentiation in the cochlea: potential advances using gene transfer. *Audiol Neurootol* 2:50-60.
- Kevetter GA (1996) Pattern of selected calcium-binding proteins in the vestibular nuclear complex of two rodent species. *J Comp Neurol* 365:575-584.
- Koekkoek SK, v. Alphen AM, v.d. Burg J, Grosveld F, Galjart N, De Zeeuw CI (1997) Gain adaptation and phase dynamics of compensatory eye movements in mice. *Genes Funct* 1:175-190.
- Kumar A, Fishman G, Torok N (1984) Vestibular and auditory function in Usher's syndrome. *Ann Otol Rhinol Laryngol* 93:600-608.
- Liu X, Ondek B, Williams DS (1998) Mutant myosin VIIa causes defective melanosome distribution in the RPE of shaker-1 mice. *Nat Genet* 19:117-118.
- Lord EM, Gates WH (1929) Shaker, a new mutation in the house mouse (*mus musculus*). *American Naturalist* 63:435-442.
- Lynch SG, Digre K, Rose JW (1994) Usher's syndrome and multiple sclerosis. Review of an individual with Usher's syndrome with a multiple sclerosis-like illness. *J Neuroophthalmol* 14:34-37.
- Möller CG, Kimberling WJ, Davenport SL, Priluck I, White V, Biscone-Halterman K, Odkvist LM, Brookhouser PE, Lund G, Grissom TJ (1989) Usher syndrome: an otoneurologic study. *Laryngoscope* 99:73-79.
- Rambold H, Churchland A, Selig Y, Jasmin L, Lisberger SG (2002) Partial Ablations of the Flocculus and Ventral Paraflocculus in Monkeys Cause Linked Deficits in Smooth Pursuit Eye Movements and Adaptive Modification of the VOR. *J Neurophysiol* 87:912-924.
- Richardson GP, Forge A, Kros CJ, Fleming J, Brown SD, Steel KP (1997) Myosin VIIA is required for aminoglycoside accumulation in cochlear hair cells. *J Neurosci* 17:9506-9519.
- Schaefer GB, Bodensteiner JB, Thompson JN, Jr., Kimberling WJ, Craft JM (1998) Volumetric neuroimaging in Usher syndrome: evidence of global involvement. *Am J Med Genet* 79:1-4.
- Self T, Mahony M, Fleming J, Walsh J, Brown SD, Steel KP (1998) Shaker-1 mutations reveal roles for myosin VIIA in both development and function of cochlear hair cells. *Development* 125:557-566.
- Tamayo ML, Maldonado C, Plaza SL, Alvira GM, Tamayo GE, Zambrano M, Frias JL, Bernal JE (1996) Neuroradiology and clinical aspects of Usher syndrome. *Clin Genet* 50:126-132.

- Tan Creti DM (1969) Neuropathology of mutant mice with auditory and/or vestibular deficiencies. *J Neuropathol Exp Neurol* 28:159.
- Weil D, Blanchard S, Kaplan J, Guilford P, Gibson F, Walsh J, Mburu P, Varela A, Levilliers J, Weston MD, et al. (1995) Defective myosin VIIA gene responsible for Usher syndrome type 1B. *Nature* 374:60-61.
- Wessel K, Moschner C, Wandinger KP, Kompf D, Heide W (1998) Oculomotor testing in the differential diagnosis of degenerative ataxic disorders. *Arch Neurol* 55:949-956.

CHAPTER 4

CEREBELLAR CONTRIBUTION TO PLASTICITY IN THE VOR

4.1 MOTOR PERFORMANCE AND MOTOR LEARNING IN LURCHER MICE

A.M. Van Alphen, T. Schepers and C.I. De Zeeuw

Van Alphen AM, Schepers T, De Zeeuw CI (2002) Ann. N. Y. Accad. Sci. (*in press*).

Abstract

In adult Lurcher mice virtually all cerebellar Purkinje cells have degenerated as a direct consequence of mutant gene action, providing a natural model for studying the effect of cerebellar cortical lesions on the generation of compensatory eye movements. Lurcher mice possessed both optokinetic (OKR) and vestibular (VOR) compensatory reflexes. However, clear differences were observed in control of the OKR consisting of a large reduction in gain and a moderate increase in phase lag. Minor differences were also observed in the VOR in that gain and phase lead of the reflex were both increased in Lurcher animals. Subjecting Lurcher animals to 8 days of visuo-vestibular training tested the assumption that increased VOR gain reflected an adaptive mechanism within remaining brainstem oculomotor pathways to compensate for the reduced OKR. Contrary to control animals, Lurcher animals were unable to modify either VOR or OKR in the course of training and therefore confirmed that an intact cerebellum is indispensable for the implementation of adaptive modifications to the oculomotor system.

Introduction

Oculomotor reflexes like the optokinetic reflex (OKR) and the vestibulo-ocular reflex (VOR) reduce slip of visual images across the retina by generating eye movements that are compensatory to head motion or movement of the visual surround. Both reflexes are mediated by a neural network that is largely located in the brain stem (Szentágothai, 1950; Zee et al., 1981; Barmack and Pettorossi, 1985) supported by a parallel pathway through the cerebellum. The cerebellar side loop has been deemed particularly necessary for maintaining accuracy of compensatory ocular reflexes (Robinson, 1976; Ito, 1982), a process referred to as motor learning.

With the discovery of Purkinje cell specific gene-promoters it has become possible to switch individual genes on or off at will, allowing us to study cerebellar information processing and motor learning in a controlled way at the level of individual proteins (Barski et al., 2000; Kitayama et al., 2001). As a reference against which to compare such specific molecular modifications, it seems prudent to quantify in mice the worst intervention possible, i.e. complete ablation of the cerebellar cortex. Rather than attempting extensive surgical procedures, we chose to use Lurcher mice, a strain of mutant mice that completely lack cerebellar Purkinje cells making their deficit equivalent to a complete cerebellar cortical lesion. The underlying pathology of Purkinje cell death has been traced to a mutation of $\delta 2$ -glutamate receptor (GluR $\delta 2$) resulting in a gain of this receptors function that triggers apoptotic cell death of Purkinje cells in these animals (Wullner et al., 1995; Zuo et al., 1997; Doughty et al., 2000).

The Lurcher strain provides us with a model for cerebellar cortical lesions, which is highly reproducible between individual animals and it allows us to judge how ocular reflexes are controlled on a sub-cortical level. Previous studies have attempted to describe the oculomotor performance of Lurcher mice, but they failed to be quantitatively accurate due to the use of a large scleral search coil that partially impeded eye movements (Koekkoek et al., 1997; De Zeeuw et al., 1998a). We therefore extend on these previous studies by using a less invasive mini-search coil technique to investigate Lurcher oculomotor behavior over a wider range of stimulus parameters and by assessing the extent to which motor plasticity still occurs in these Purkinje cell deficient animals.

Methods

The eye movement performance of 15 Lurcher mutant mice and 13 normal control littermates was tested. The procedures for implanting a head fixation pedestal and a 'mini' search coil were identical to those previously described for this laboratory (van Alphen et al., 2001). Animals were allowed to recover for at least 3 days prior to the first recording session. The local ethical committee of the Erasmus University Rotterdam approved animal care and experimental protocols.

The optokinetic reflex (OKR) and vestibulo-ocular reflex (VOR) and visually enhanced VOR (VVOR) were measured. Two different approaches were used to test the performance of the optokinetic system. First, the frequency response of the OKR was tested by sinusoidally rotating a vertically striped (width of bars 4°) optokinetic drum around the animal at frequencies of 0.1, 0.2, 0.4, 0.8 and 1.6 Hz while peak stimulus velocity was kept constant at 8 °/sec. Second, the effect of peak velocity on gain of the OKR was evaluated by varying peak stimulus velocity between 2, 4, 8, 16, and 32 °/sec at 0.4 Hz stimulus frequency. The VOR was elicited by sinusoidal, whole body rotation in the dark. Sinusoidal stimulation was performed at 0.1, 0.2, 0.4, 0.8, and 1.6 Hz and 10° stimulus amplitude. The VVOR was tested using the VOR stimulus parameters while the animal viewed the illuminated, earth-fixed drum.

Gain of the eye movement (eye velocity/ head velocity) and phase of eye movement with respect to stimulus movement were calculated by fitting a sine wave to the average response using least-square optimization. When eye movement lagged stimulus movement, phase was expressed with a negative sign. Phase relations of VOR were shifted by 180° making the phase angle zero for perfectly compensatory responses. All values reported are mean and standard error, weighting each mouse equally. All Signal analysis was done with MATLAB (Mathworks Inc., Natick, USA.).

A VOR reversal paradigm was used to test VOR adaptation. In this paradigm the animal had to learn to reverse the natural direction of the VOR. Reversal training lasted for 8 days and began by rotating the optokinetic drum in phase, i.e. 0° phase difference, with table rotation at 5° amplitude. In the following five days amplitude of the optokinetic drum was increased by 1 °/day until it was 10° on day 6. At this point the optokinetic drum was rotating in phase with table rotation but at twice the amplitude. Amplitude of the optokinetic drum remained 10° from day 6 on. Every day the VOR was checked before training to monitor progression of VOR change.

Differences between Lurcher and control animals in gain or phase of OKR, VOR and VVOR were tested for statistical significance using a two way, repeated measures ANOVA. The effect of visuo-vestibular training on OKR and VOR was tested for each mouse separately using a one way, repeated measures ANOVA. Statistical analysis was performed, using a commercial software package called SAS-6.12 (SAS institute inc., Cary, NC, USA).

Results

Motor performance

Lurcher mice were easily distinguished from control littermates by their ataxic behavior, which was visible as a wobbly, lurching gate. Oculomotor control of Lurcher mice was considerably less accurate than that of normal control animals, as reflected by a large decrease in OKR gain across all tested peak velocities (Fig. 1A, $p < 0.001$). While OKR gain of normal animals remained fairly constant at 0.7 for stimulus velocities smaller than 8 deg/sec and decreased for higher peak velocities, that of Lurcher animals was already considerably smaller at 2 %/sec and declined immediately when peak stimulus velocity was increased. The increased dependence of Lurcher OKR on peak velocity was reflected in the 2-way ANOVA by a significant interaction ($p < 0.001$) between the two independent factors: animal type and peak stimulus velocity. Performance of the OKR was also tested against stimulus frequency while peak stimulus velocity was kept constant at 8 %/sec. OKR gain in Lurcher animals again showed a significant depression over the entire range of tested frequencies when compared to control animals (Fig. 1B, $p < 0.001$). Again interaction between animal type and stimulus frequency proved significant ($p < 0.001$) in the analysis, reflecting the fact that OKR gain remained relatively constant up to 0.8 Hz in control animals but showed no such stability in Lurcher animals. The reduced OKR gain of Lurcher animals was accompanied by an increase in phase lag of the eye movement with respect to stimulus movement. Eye movements of Lurcher mice generally lagged stimulus movement more than those of control animals (Fig. 1D, $p = 0.03$). Phase Lag was significantly different at all tested frequencies ($p < 0.01$, two tailed t-test with Bonferroni correction) except 1.6 Hz. The stronger dependence of OKR gain on frequency and the increased phase lag indicate that the absence of cerebellar cortical output in Lurcher animals has changed the low pass filter characteristics of the OKR in the closed loop situation by an apparent reduction of the overall time constant.

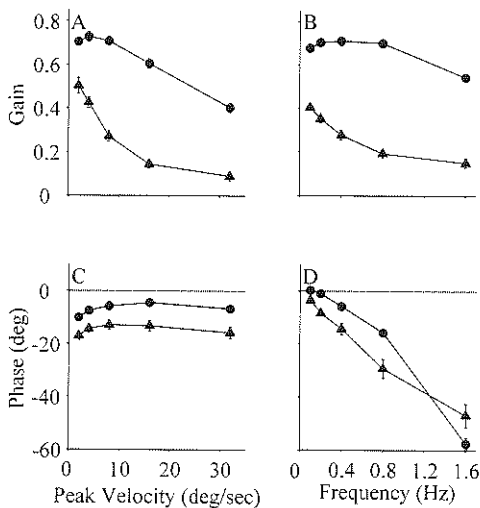


Figure 1: The OKR of Lurcher (triangles) and control (circles) animals is presented in Bode-plots relating gain and phase of the response to peak stimulus velocity (1 A, C) and stimulus frequency (1 B, D). Lurcher OKR gain was found to be smaller than that of control animals across all stimulus conditions. In addition to a reduced OKR gain Lurcher animals also showed increased phase lag of eye velocity with respect to stimulus velocity. Phase lag at 1.6 Hz was not significantly different from that of control animals ($p = 0.14$). The error bars indicate 1 S.E.M.

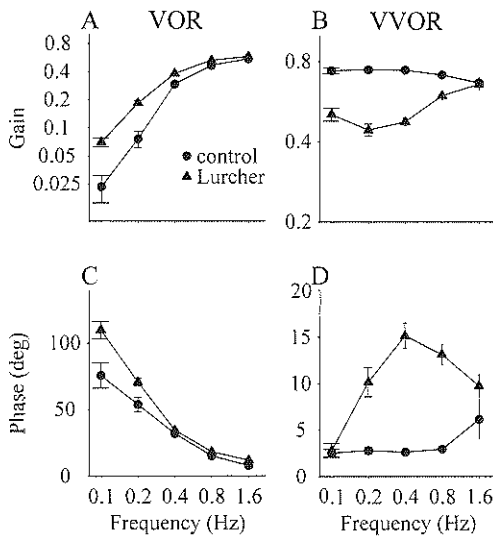


Figure 2: Bode plots for Lurcher (triangles) and control (circles) animals are shown of the VOR (Fig. 2 A, C) and VVOR (Fig. 2 B, D). VOR gain increased with increasing stimulus frequency for both transgenic and control animals. The interaction of VOR and OKR provided a stable VVOR in control animals across the tested frequency range. VVOR gain and phase were more variable in Lurcher animals reflecting the inability of their severely impaired OKR system to complement VOR.

The VOR of Lurcher animals was similar to that of control animals in that VOR gain increased with frequency, measuring 0.07 ± 0.008 and 0.59 ± 0.02 at 0.1 Hz and 1.6 Hz respectively (Fig. 2A). The relation of gain with frequency was complemented by a reduction in phase lead for increasing stimulus frequencies. At 0.1 Hz Phase lead measured $110 \pm 6.5^\circ$ and decreased to $12 \pm 1.2^\circ$ at 1.6 Hz (Fig. 2B). In normal animals VOR gain increased from 0.02 ± 0.009 to 0.55 ± 0.02 and VOR phase decreased from $75 \pm 9.5^\circ$ to $7.8 \pm 0.7^\circ$ at 0.1 Hz and 1.6 Hz respectively. Both VOR gain and Phase curves were significantly different between Lurcher and control animals ($p < 0.01$). A post hoc t-test with Bonferroni correction for multiple comparisons pinpointed the differences between Lurcher and control animals at 0.1, 0.2 and 0.4 Hz. At these three frequencies VOR gain of Lurcher mice was significantly larger ($p < 0.05$) than that of control animals, while phase lead of the VOR in Lurcher mice was significantly larger than that of control animals ($p < 0.05$) at 0.1 and 0.2 Hz. Because both phase lead and gain of the Lurcher VOR increased, the difference between control and Lurcher animals cannot be solely attributed to a different overall VOR time constant between Lurcher and control animals. In fact a decrease in the dominant time constant of the VOR could be expected in Lurcher mutants, but such a decrease would result in a concomitant decrease in VOR gain at low frequencies. From the present results we witness the exact opposite: VOR gain is relatively increased in Lurcher animals at low stimulus frequencies.

One of the functions assigned to the flocculus is that it provides the site of direct interaction between OKR and VOR (Ito, 1982), in such a way that the OKR would supplement VOR to provide a stable, combined response. In control animals the VVOR indeed proved stable across the range of tested frequencies. Gain was 0.74 ± 0.02 at 0.1 Hz and 0.67 ± 0.03 at 1.6 Hz, while phase measured 2.5 ± 0.4 and 6.1 ± 2.1 at the same frequencies (Fig. 2C,D). The VVOR response of Lurcher mice was more variable, gain first declined from 0.51 ± 0.03 at 0.1 Hz to 0.44 ± 0.02 at 0.2 Hz and then increased again to

0.66±0.03 at 1.6 Hz. VVOR phase followed a similar change in Lurcher mice, measuring 3±0.8° and 10±1.2° at 0.1 and 1.6 Hz respectively, and reaching a peak of 15±1.4° at 0.4 Hz. The variable response of Lurcher mice can be reasonably well explained from a linear addition of VOR and OKR. Since, VVOR is a combination of both vestibular and optokinetic inputs, the response at high stimulus frequency is largely driven by the VOR while that at low stimulus frequency will be relatively more dependent on the OKR. The OKR of Lurcher animals did not extend far enough into the higher frequency range to complement VOR and achieve a stable VVOR across all tested frequencies. The validity of explaining differences in VVOR between Lurcher and controls from a defect in Lurcher OKR may be illustrated by a linear reconstruction of the VVOR at 0.4 Hz using separately measured OKR and VOR responses.

By vectorially subtracting VOR of Lurcher mice from the VVOR-stimulus the residual vector that drives the optokinetic system can be estimated. At 0.4 Hz this estimate comes to a residual optokinetic stimulus of 18 °/sec at 162° phase angle with ipsilateral head velocity. Figure 1A can now be used as a look-up table that maps the response of the OKR at 0.4 Hz for different peak stimulus velocities. OKR gain and phase at 18 °/sec can be read from the curve at 0.15 and -14°, with respect to stimulus movement. Converting these values to the VVOR coordinate system yields an eye velocity of 2.7 °/sec at a phase lag of -32° with ipsilateral head velocity. Vectorially adding the estimated eye velocity vector for optokinetic component with vestibular component yields a VVOR gain of 0.44 and a phase lead of 21° with ipsilateral head velocity. These values are close enough to the real values (0.48 and 15° respectively) to assume that deficits in Lurcher VVOR are largely caused by a normal integration of an impaired OKR and VOR.

Motor Learning

Visuo-vestibular adaptation was tested in 4 Lurcher mice and 5 control animals. Both Lurcher and control animals displayed a VVOR during training that was different from their normal VOR at the same vestibular stimulus, indicating that visual information was used to guide the eye movements during training. Control animals responded to the training stimulus by slowly decreasing VOR gain at 0.6 Hz from 0.30±0.03 on the first to 0.13±0.02 on the 6th day and then slightly increasing VOR gain again to 0.16±0.03 on day 8 (Fig. 3A). Changes in VOR gain were accompanied by a slow rise in phase of the eye movement with respect to turntable movement, measuring 30±5°, 111±26° and 115±31° on the same days (Fig. 3B). No changes were observed in Lurcher mice. VOR gain measured 0.37±0.1 before and 0.42±0.03 after training, while phase of the eye movement with respect to table movement was 30±2° before and 28±4° after training. In control animals phase lead changed so much that direction of the VOR actually reversed from out of phase with table rotation to in phase. In order to accentuate the actual reversal of direction we calculated an adaptation index (AI) according to the equation: $AI = G \cdot \cos(\theta)$. In this equation G equals VOR gain and θ is the phase angle of the eye movement with respect to table movement. As phase lead of the eye movement with respect to table movement increased to values larger than 90° AI became negative, indicating that VOR had reversed direction. Fig. 3E shows AI, normalized to its initial value, for all animals at the training frequency (0.6 Hz). As expected control animals

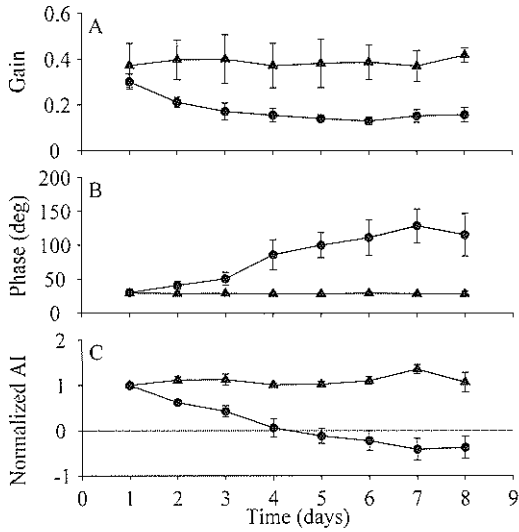
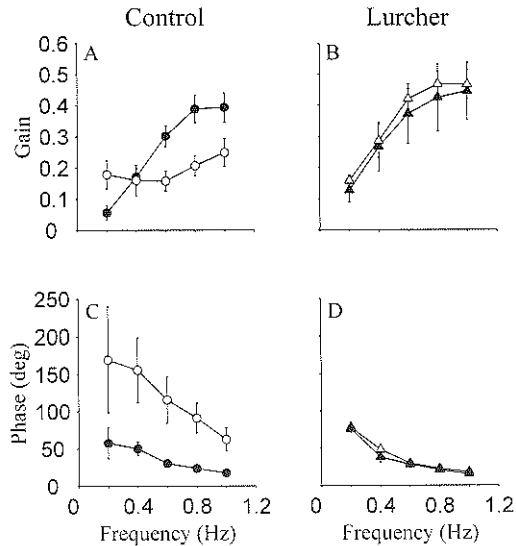


Figure 3: Change in properties of the VOR at 0.6 Hz in response to visuo-vestibular training is plotted against time. A). Absolute VOR gain for Lurcher (triangles) and control animals (circles) is presented against time. VOR in control animals is reduced with training while that of Lurcher animals doesn't change. Error bars indicate S.E.M. B) Phase of the eye movement with respect to table movement is plotted in the same way as gain. Control animals show a pronounced advance in phase lead with training reflecting a change in direction of the VOR. C) Normalized adaptation index is shown, to outline two distinct features. First, VOR reverses direction as phase lead is larger than 90° and the adaptation index changes sign. Second, normalizing the data of each animal to their initial performance clearly shows that the Lurcher animals do not adapt their VOR.

Figure 4: Change in properties of the VOR in control (Fig. 4 A, C) and Lurcher (Fig. 4 B, D) animals is presented in the form of BODE plots. Closed symbols represent data before and open symbols after 8 days of visuo-vestibular training. Error bars indicate S.E.M.



differed significantly from Lurcher animals ($p=0.002$, two way ANOVA with repeated measures), in that control animals showed a steady decrease of AI, while Lurcher animals showed no change in AI throughout the entire 8 days of training. In addition to the training frequency VOR was also tested for 4 other frequencies centered about the training frequency (fig. 4). Although training was performed exclusively at 0.6 Hz changes in VOR of control animals were not limited to the training frequency but

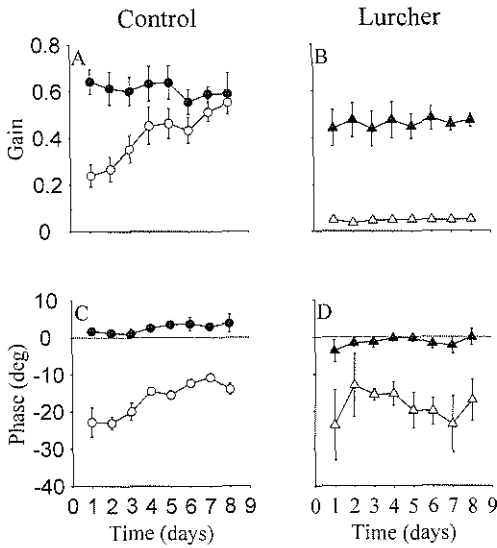
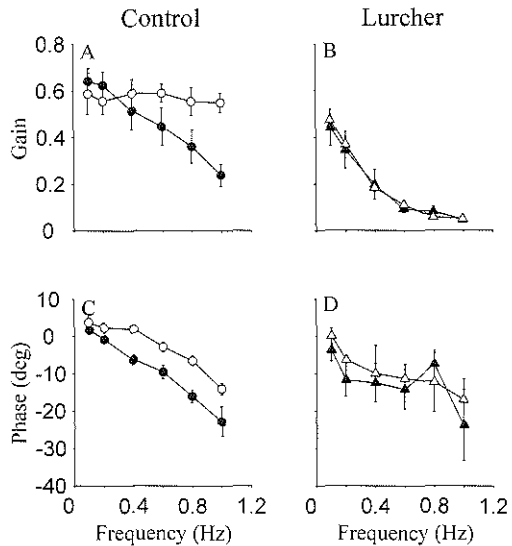


Figure 5: The progression of OKR changes in time is presented for control (Fig. 5 A, C) and Lurcher (Fig. 5 B, D) animals. Only data taken at 0.1 Hz (closed symbols) and 1 Hz (open symbols) are shown, because those data represent the smallest and largest effect of training on OKR respectively.

Figure 6: Changes in OKR due to visuo-vestibular training are represented in the form of BODE plots for control (Fig. 6 A, C) and Lurcher (Fig. 6 B, D) animals. Closed symbols represent data before and open symbols after 8 days of training. Bode plots of the OKR before training differ from those shown in FIG.1 because a constant stimulus amplitude was used to assess the OKR during training. Because of the constancy of stimulus amplitude peak stimulus velocity increased as frequency was increased. Stimulus frequencies of 0.4, 0.8 and 1.2 correspond to peak stimulus velocities of 12.6, 25.1 and 37.7 %/sec respectively.



encompassed the entire tested spectrum. AI changed significantly at all frequencies in control animals ($p < 0.001$ at all frequencies) while in Lurcher animals it did not change at any of the tested frequencies ($p > 0.05$ at all frequencies).

After visuo-vestibular training behavioral changes in control animals were not limited to the VOR but also included the OKR. Every day the OKR was tested at the

same amplitude (5°) and frequencies as the VOR with the addition of 0.1 Hz. The experimental protocol to monitor progression of learning in the OKR therefore differed from that described earlier in that peak stimulus velocity increased as frequency was increased. During visuo-vestibular training OKR gain progressively increased and phase lag decreased in control animals (Fig 5 A,C). At 1 Hz (31 $^\circ$ /sec peak stimulus velocity) OKR gain increased from 0.24 ± 0.05 to 0.55 ± 0.04 ($p=0.007$) and phase lag decreased from $-24 \pm 9^\circ$ to $-14 \pm 2^\circ$ ($p=0.006$). In Lurcher animals neither OKR gain nor phase changed during training (Fig. 5 B, D). Adaptive changes of the OKR in control animals were limited to higher stimulus frequencies. Changes in gain proved significant at 0.6, 0.8 and 1 Hz ($p=0.02$, $p<0.001$ and $p<0.001$) while changes in phase were significant at all frequencies except 0.1 Hz ($p=0.03$ at 0.2 Hz and $p<0.001$ for all other frequencies). In Lurcher mice the OKR remained unchanged at all tested frequencies. An intact cerebellar cortex is therefore required both for adaptation of the VOR as well as for adaptation of the OKR.

Discussion

The oculomotor performance of Lurcher mice is largely dominated by an impaired OKR. Closed loop OKR gain is severely reduced and phase lag of the eye movement with respect to stimulus movement is increased compared to control animals. Lurcher OKR, like that of control animals, is clearly non-linear, rendering accuracy of the OKR not only dependent on stimulus frequency but also on stimulus velocity. This non-linear relation of the OKR appeared more pronounced in Lurcher animals as reflected by the stronger dependence of OKR gain on peak stimulus velocity. Control animals showed a stable OKR gain for sinusoidal stimuli with a peak velocity smaller than 9 $^\circ$ /sec, while Lurcher mice did not exhibit any such plateau response. In relation to frequency the OKR (peak velocity 8 $^\circ$ /sec) both Lurcher and control animals revealed typical low pass characteristics of declining gain and increased phase lag with increasing stimulus frequency. However, in addition to a severely reduced OKR gain, phase lag was also larger in Lurcher mice than in control animals. Changes in the OKR of Lurcher mice may be explained by considering the OKR, in its reduced form, to be a low pass system within a negative feed back loop. The internal filter element can be expressed as the Laplace transfer function $g_{int}/(s\tau+1)$ in which g_{int} represents the internal gain, s denotes complex frequency and τ represents the time constant. Placing such an element inside a negative feed back loop result in a systems performance $E'/D' = (g_{int}/g_{int}+1)/(s(\tau/1+g_{int})+1)$. A reduction in the internal gain of the system would therefore result in a reduction of both the closed-loop OKR gain and time constant. The result of such a deficit was present in Lurcher animals as reduced OKR gain and increased phase lag with respect to control animals. In addition to explaining the increased phase lag this interpretation of a reduced internal gain could also explain the more pronounced dependence of Lurcher OKR on stimulus velocity, since a reduction of the internal gain would emphasize the effect of a saturation element in the system. Saturation is known to occur in the optokinetic system at the level of the accessory optic system involving the detection of retinal slip (Collewyn, 1969; Oyster et al., 1972). The nature of the deficits observed in Lurcher mice hint at the possibility that cerebellar output is necessary in mice

to partially compensate for the non-linear nature of the OKR by boosting internal gain of the system.

Assigning a role to the cerebellum in gain control is definitely not new (Ito, 1982; Nagao et al., 1991). The cerebellum has been assigned a short term role in oculomotor control concerned with directly fine-tuning VOR based on optokinetic information (Ito, 1982) but also a long term role in which vestibular and optokinetic interaction would shape dynamics of the underlying VOR (Robinson, 1976; Ito, 1982; Lisberger et al., 1984). In this respect it was striking that in Lurcher mice no severe impairments emerged in either VOR alone or in the ability to combine VOR and OKR. VVOR gain was reduced in Lurcher mice, but this impairment is attributable to the obvious OKR deficit. Lack of a functional cerebellum did not appear to prevent normal integration of optokinetic and vestibular signals into a VVOR.

VOR of Lurcher mice was similar to that of control animals and only differed significantly at 0.2 and 0.4 Hz. Contrary to expectation (Keller and Precht, 1978; Ito et al., 1982; Van Neerven et al., 1989), at these low frequencies Lurcher mice perform better, i.e. they have a higher VOR gain, than normal animals and show an increased phase lead of the eye movement with respect to stimulus movement. An increased phase lead of the VOR has been described before in Lurcher (Stahl, 2002) and PCD (Killian and Baker, 2002) mice and can be attributed to a reduced function of the velocity to position neural integrator (Skavenski and Robinson, 1973), the function of which depends on cerebellar output (Robinson, 1974). However, an isolated reduction in performance of the neural integrator would invariably lead to a reduction in VOR gain at low stimulus frequencies. Contrary to a reduction we observed an increased VOR gain in Lurcher animals, which is comparable to that reported in previous studies of Purkinje cell deficient mutants (Killian and Baker, 2002; Stahl, 2002). It is unclear whether increased VOR gain in cerebellar mutant mice is a primary effect of the cerebellar lesion or a secondary compensatory mechanism that allows the animals to achieve a reasonable performance of the VVOR despite an impaired OKR. Lesion studies provide no unequivocal answer to this question since lesions of the flocculus have been reported to cause both a decrease (Keller and Precht, 1978; Ito et al., 1982; Nagao, 1983; Van Neerven et al., 1989) or increase (Robinson, 1976; Partsalis et al., 1995) of VOR gain, and some studies report no effect at all (Ito et al., 1982; Barmack and Pettorossi, 1985). The same conflicting results have been reported for lesions of the nodulus, ascribing both an increasing (Nagao, 1983; Killian and Baker, 2002) and decreasing (Barmack et al., 2002) influence on angular VOR gain to the lesion. Rather than adding to this list of lesion studies we asked whether Lurcher animals might have retained some adaptive capacity in the remaining, extra cerebellar circuitry that would allow them to adapt VOR gain.

The extent to which Lurcher and control animals were able to adapt their VOR was investigated by subjecting both groups to a vision reversal paradigm. In this paradigm control animals responded by an initial drop of VOR gain followed by an increase in phase lead. Changes in VOR were paralleled by an increased OKR gain and reduced phase lag of the OKR. Lurcher animals proved incapable to adapt their VOR or OKR, demonstrating once more the necessity of an intact cerebellum to express these forms of plasticity (Robinson, 1976; Ito et al., 1982; Nagao, 1983; Lisberger et al., 1984). Though cerebellar involvement in adaptation of the VOR and OKR is evident, long-term

depression of the parallel fiber to Purkinje cell synapse (Ito, 1982) does not appear to be an absolute prerequisite to express the adaptive behavior, since L7-PKCi transgenic animals, in which LTD was selectively disrupted, did show attenuated adaptation when subjected to the same adaptation protocol (unpublished observations). The present data differ from previous adaptation studies (Collewijn and Grootendorst, 1978; Nagao, 1983; Schairer and Bennett, 1986; De Zeeuw et al., 1998b) in that in control mice neither VOR adaptation nor OKR was frequency specific. The different findings are possibly caused by differences in experimental protocols. Particularly the fact that we extended training to eight consecutive days may have prevented us from seeing any frequency specific changes.

In view of absent oculomotor plasticity it is unlikely that increased VOR gain in Lurcher mice reflects a compensatory mechanism that complements the reduced OKR to ensure a stable VVOR. It rather seems that the cerebellum has a general depressing influence on the mouse VOR, and that this influence is removed in Lurcher animals. Such an inhibition could be advantageous for the mouse to suppress responses that would otherwise not be compensatory due to extreme phase leads.

References

- Barmack NH, Pettorossi VE (1985) Effects of unilateral lesions of the flocculus on optokinetic and vestibuloocular reflexes of the rabbit. *J Neurophysiol* 53:481-496.
- Barmack NH, Errico P, Ferraresi A, Fushiki H, Pettorossi VE, Yakhnitsa V (2002) Cerebellar nodulectomy impairs spatial memory of vestibular and optokinetic stimulation in rabbits. *J Neurophysiol* 87:962-975.
- Barski JJ, Dethleffsen K, Meyer M (2000) Cre recombinase expression in cerebellar Purkinje cells. *Genesis* 28:93-98.
- Collewijn H (1969) Optokinetic eye movements in the rabbit: input-output relations. *Vision Res* 9:117-132.
- Collewijn H, Grootendorst AF (1978) Adaptation of the rabbit's vestibulo-ocular reflex to modified visual input: importance of stimulus conditions. *Arch Ital Biol* 116:273-280.
- De Zeeuw CI, van Alphen AM, Koekkoek SK, Buharin E, Coesmans MP, Morpurgo MM, van den Burg J (1998a) Recording eye movements in mice: a new approach to investigate the molecular basis of cerebellar control of motor learning and motor timing. *Otolaryngol Head Neck Surg* 119:193-203.
- De Zeeuw CI, Hansel C, Bian F, Koekkoek SK, van Alphen AM, Linden DJ, Oberdick J (1998b) Expression of a protein kinase C inhibitor in Purkinje cells blocks cerebellar LTD and adaptation of the vestibulo-ocular reflex. *Neuron* 20:495-508.
- Doughty ML, De Jager PL, Korsmeyer SJ, Heintz N (2000) Neurodegeneration in Lurcher mice occurs via multiple cell death pathways. *J Neurosci* 20:3687-3694.
- Ito M (1982) Cerebellar control of the vestibulo-ocular reflex--around the flocculus hypothesis. *Annu Rev Neurosci* 5:275-296.
- Ito M, Jastreboff PJ, Miyashita Y (1982) Specific effects of unilateral lesions in the flocculus upon eye movements in albino rabbits. *Exp Brain Res* 45:233-242.
- Keller EL, Precht W (1978) Persistence of visual response in vestibular nucleus neurons in cerebellectomized cat. *Exp Brain Res* 32:591-594.

- Killian JE, Baker JF (2002) Horizontal Vestibuloocular Reflex (VOR) Head Velocity Estimation in Purkinje Cell Degeneration (pcd/pcd) Mutant Mice. *J Neurophysiol* 87:1159-1164.
- Kitayama K, Abe M, Kakizaki T, Honma D, Natsume R, Fukaya M, Watanabe M, Miyazaki J, Mishina M, Sakimura K (2001) Purkinje cell-specific and inducible gene recombination system generated from C57BL/6 mouse ES cells. *Biochem Biophys Res Commun* 281:1134-1140.
- Koekkoek SK, v. Alphen AM, v.d. Burg J, Grosveld F, Galjart N, De Zeeuw CI (1997) Gain adaptation and phase dynamics of compensatory eye movements in mice. *Genes Funct* 1:175-190.
- Lisberger SG, Miles FA, Zee DS (1984) Signals used to compute errors in monkey vestibuloocular reflex: possible role of flocculus. *J Neurophysiol* 52:1140-1153.
- Nagao S (1983) Effects of vestibulocerebellar lesions upon dynamic characteristics and adaptation of vestibulo-ocular and optokinetic responses in pigmented rabbits. *Exp Brain Res* 53:36-46.
- Nagao S, Yoshioka N, Hensch T, Hasegawa I, Nakamura N, Nagao Y, Ito M (1991) The role of cerebellar flocculus in adaptive gain control of ocular reflexes. *Acta Otolaryngol Suppl* 481:234-236.
- Oyster CW, Takahashi E, Collewijn H (1972) Direction-selective retinal ganglion cells and control of optokinetic nystagmus in the rabbit. *Vision Res* 12:183-193.
- Partsalis AM, Zhang Y, Highstein SM (1995) Dorsal Y group in the squirrel monkey. II. Contribution of the cerebellar flocculus to neuronal responses in normal and adapted animals. *J Neurophysiol* 73:632-650.
- Robinson DA (1974) The effect of cerebellectomy on the cat's vestibulo-ocular integrator. *Brain Res* 71:195-207.
- Robinson DA (1976) Adaptive gain control of vestibuloocular reflex by the cerebellum. *J Neurophysiol* 39:954-969.
- Schäirer JO, Bennett MV (1986) Changes in gain of the vestibulo-ocular reflex induced by combined visual and vestibular stimulation in goldfish. *Brain Res* 373:164-176.
- Skavenski AA, Robinson DA (1973) Role of abducens neurons in vestibuloocular reflex. *J Neurophysiol* 36:724-738.
- Stahl JS (2002) Calcium Channelopathy Mutants and Their Role in Ocular Motor Research. *Ann N Y Acad Sci* 956:64-74.
- Szentágothai J (1950) The elementary vestibulo-ocular reflex arc. *J Neurophysiol* 13:395-407.
- van Alphen AM, Stahl JS, De Zeeuw CI (2001) The dynamic characteristics of the mouse horizontal vestibulo-ocular and optokinetic response. *Brain Res* 890:296-305.
- Van Neerven J, Pompeiano O, Collewijn H (1989) Depression of the vestibulo-ocular and optokinetic responses by intrafloccular microinjection of GABA-A and GABA-B agonists in the rabbit. *Arch Ital Biol* 127:243-263.
- Wullner U, Loschmann PA, Weller M, Klockgether T (1995) Apoptotic cell death in the cerebellum of mutant weaver and lurcher mice. *Neurosci Lett* 200:109-112.
- Zee DS, Yamazaki A, Butler PH, Gucer G (1981) Effects of ablation of flocculus and paraflocculus of eye movements in primate. *J Neurophysiol* 46:878-899.

Zuo J, De Jager PL, Takahashi KA, Jiang W, Linden DJ, Heintz N (1997)
Neurodegeneration in Lurcher mice caused by mutation in delta2 glutamate
receptor gene. *Nature* 388:769-773.

4.2 CEREBELLAR LTD FACILITATES BUT IS NOT ESSENTIAL FOR LONG-TERM ADAPTATION OF THE VESTIBULO-OCULAR REFLEX

A.M. van Alphen and C.I. De Zeeuw

Van Alphen AM, De Zeeuw CI (2002) Eur. J. Neurosci. *(in press)*.

Abstract

The induction of cerebellar long-term depression at the parallel fiber – Purkinje cell synapse (LTD) is selectively blocked in L7-PKCi transgenic mice, rendering these mice unable to adaptively modify their vestibulo-ocular reflex (VOR) during visuo-vestibular training for a few hours. Despite this deficit, their eye movement performance as well as their general motor behavior appears unaffected. This combination suggests that, in the long-term, remaining forms of plasticity in the vestibulo-cerebellar circuitry can compensate for the absence of cerebellar LTD. To find out whether LTD-deficient mice exhibit motor learning in the long run, we subjected L7-PKCi transgenic mice to visuo-vestibular training paradigms that were aimed at either increasing or decreasing the VOR response in the course of 8 consecutive days. During the increasing paradigm VOR gain of transgenic mice increased significantly, while VOR gain decreased and VOR phase lead increased during the decreasing paradigm. The impact of these long training periods on the VOR was significantly smaller in LTD-deficient mice than in wild type littermates. Thus, while LTD may be necessary for short-term VOR adaptation, it facilitates but is not required for long-term adaptation of the VOR.

Introduction

The vestibulo-ocular reflex (VOR) generates compensatory eye movements in response to head movements. Head motion is detected by the semicircular canals and translated into adequate motor commands via a well-defined neural network located in the brainstem (Lorente de Nó, 1933; Szentágothai, 1950; Ito et al., 1977). This reflex can adapt to external requirements or changes in its internal components that would otherwise render it inaccurate. Such adaptive modifications are guided by visual input and represent a well-defined example of motor learning (Gonshor & Jones, 1973; Miles & Fuller, 1974). The cerebellum is involved in this form of motor learning since impairment of cerebellar function by physical lesions prevents its occurrence (Robinson, 1976; Zee et al., 1981).

Based on theories of cerebellar function (Marr, 1968; Albus, 1971), Ito (1982), was the first to propose that long-term depression (LTD) at the parallel fiber - Purkinje cell synapse in the cerebellar flocculus could act as one of the major mechanisms underlying adaptation of the VOR (see also Ito et al., 1982). Miles & Lisberger (1981) obtained evidence that vestibular nuclei neurons are also actively involved in these plastic modifications, although the cellular mechanisms underlying these changes remain to be established. Comparative analyses of electrical activity from Purkinje cells in the flocculus and floccular target neurons in the vestibular nuclei supports the emerging notion that sites for formation and storage of modifications to the VOR are distributed over both brainstem and cerebellum (Lisberger, 1994; Partsalis et al., 1995; Lisberger, 1998; Hirata & Highstein, 2001).

Recent studies of transgenic mice in which we selectively blocked the induction of LTD at the parallel fiber - Purkinje cell synapse provided evidence that LTD may indeed be involved in adaptation of the VOR (De Zeeuw et al., 1998; Goossens et al., 2001). These mutants were created by inserting an inhibitory peptide that affects various isoforms of protein kinase C (PKCi) into the Purkinje cell specific L7-vector (Oberdick et al., 1990; Linden & Connor, 1993). When we subject L7-PKCi transgenic animals to a

visuo-vestibular training paradigm for two hours they show no adaptation of their VOR (De Zeeuw et al., 1998). On the one hand this phenotype allows us to conclude that the deficit in motor learning is not caused by impaired motor performance, but on the other hand it raises the question as to how these animals can achieve normal motor performance while they lack the ability to learn. We have therefore proposed that other plastic processes may compensate for the absence of LTD in the Purkinje cells of L7-PKCi mice and that the behavioral effects of these processes may only become apparent when the animals are exposed to longer training periods as occur in daily life. To find out whether such mechanisms may exist and to find out whether LTD may facilitate these processes, we subjected L7-PKCi mutants to a long-term training period of 8 consecutive days. The training included visuo-vestibular mismatch paradigms aimed at either increasing or decreasing VOR responses.

Methods

Surgical procedure

We used heterozygous L7-PKCi transgenic mice and normal control littermates (3 to 10 months old) that had been bred on a C57BL/6 background for at least 7 generations. Mice were anaesthetized with a mixture of halothane, nitrous oxide and oxygen. The procedures for implanting a head fixation pedestal and a 'mini' search coil were identical to those previously described for this laboratory (van Alphen et al., 2001). Animals were allowed to recover for at least 3 days prior to the first recording session. The local ethical committee of the Erasmus University Rotterdam approved animal care and experimental protocols.

Behavioral testing

To assess differences in performance between L7-PKCi transgenic mice and control littermates prior to training, we took baseline measurements for their optokinetic reflex (OKR) and VOR. The OKR in response to sinusoidal movement of the drum was tested at 6 different frequencies including: 0.1 Hz, 0.2 Hz, 0.4 Hz, 0.6 Hz, 0.8 Hz, and 1 Hz. Amplitude of the drum was kept constant at 5° (0-peak). In this manner peak velocities ranging from 3 to 31 °/sec were obtained. VOR in response to sinusoidal whole body rotation was tested at 0.2 Hz, 0.4 Hz, 0.6 Hz, 0.8 Hz, and 1 Hz. Amplitude of the vestibular stimulus was also kept constant at 5° (0-peak) across frequencies.

After baseline recordings were completed, the animals were subjected to visuo-vestibular training for 8 days, which lasted 1.5 hrs per day. To prevent extinction of the learned response the animals were kept in the dark in between sessions. During all training sessions the amplitude of the turntable was 5°, while the amplitude of the optokinetic drum was varied depending on the day of training (see below). For both turntable and drum movement we chose a stimulus training frequency of 0.6 Hz, which is an optimal compromise to ensure both a reliable vestibular input to the VOR and a visual input with a peak velocity well within the physiological range of the mouse optokinetic system (van Alphen et al., 2001).

Animals were trained to either increase VOR gain or to reverse its direction. When visuo-vestibular training was aimed at increasing the gain of the VOR, animals were presented with 'out of phase' conflicting optokinetic and vestibular stimuli. In this paradigm the optokinetic drum was rotated in the direction opposite to that of the turntable. The amount of conflicting visual stimulus was slowly built up by increasing drum amplitude at a rate of 1°/day, until it matched table amplitude at 180° phase difference. In this manner drum amplitude was increased from 1° on the first day, 2° on the second to 5° on the 5th day. From day 6 to day 8 drum amplitude remained 5°.

The 'in phase' training protocol, which was meant to reverse direction of the VOR, was analogous to the 'out of phase' training protocol. Training began on the first day by rotating the optokinetic drum in phase, i.e. 0° phase difference, with table rotation at 5° amplitude. In the following five days, amplitude of the optokinetic drum was increased at 1°/day until it was 10° on day 6. At this point the optokinetic drum was rotating in phase with the table but at twice the amplitude. Amplitude of the optokinetic drum remained 10° from day 6 on.

Data analyses

Eye, head and drum position were differentiated off-line. All cycles in a trace were taken together to construct an average eye velocity curve. Gain of the eye movement and phase of eye movement with respect to stimulus movement were calculated by fitting a sine wave to the average response using least-square optimization. When eye movement lagged stimulus movement, phase was expressed with a negative sign. Phase relations of VOR were shifted by 180° making the phase angle zero for perfectly compensatory responses. All values reported are mean and standard error, weighting each mouse equally. Signal analysis was done with MATLAB (Mathworks Inc., USA).

To test the 0-hypothesis that the learning curve of L7-PKCi transgenic mice did not differ from that of control littermates a mixed model analysis of variance (ANOVA) was used. This analysis design allowed for repeated measures and changes in variance over time. Initial performance of each animal was included as a covariate. Missing values were adjusted for using a 'maximum likelihood' procedure. Statistical analysis was performed using a commercially available package (SAS, SAS Institute Inc., USA.).

Results

General oculomotor performance

Basic properties of OKR and VOR were assessed to verify that naïve L7-PKCi mutants (n=32) showed an oculomotor performance identical to that of their wild type littermates (n=33). No differences were found in dynamics of OKR between transgenic and control animals (Fig. 1 A1, B1). OKR gain decreased, from 0.69±0.03 at 0.1 Hz to 0.22±0.02 at 1 Hz in transgenic animals and from 0.70±0.02 to 0.20±0.01 at the same frequencies in control animals. At these frequencies phase lag increased from 0.0±0.4° to -27.5±1.6°

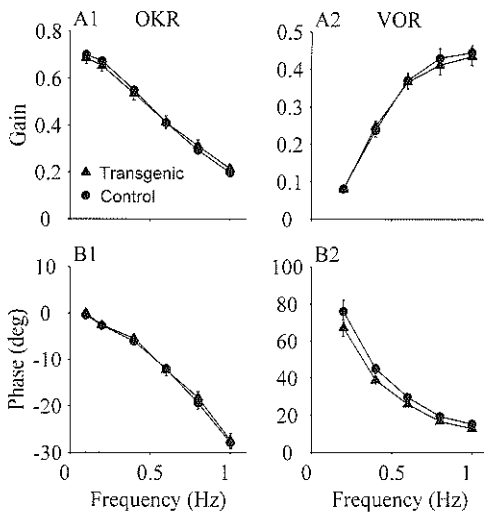


Figure 1: Normal performance of OKR (A1, B1) and VOR (A2, B2) in untrained L7-PKCi transgenic (triangles) and control animals (circles). Gain and phase values of the eye movement relative to stimulus movement were plotted against stimulus frequency. Error bars indicated SEM. Neither OKR nor VOR were statistically different.

and from $-0.4 \pm 0.3^\circ$ to $-27.9 \pm 1.3^\circ$ in transgenic and control animals, respectively. The VOR of both types of mice showed the familiar characteristics of a high-pass system in that gain increased and phase lead decreased as stimulus frequency was increased (Fig. 1 A2, B2). Gain rose from 0.08 ± 0.01 to 0.44 ± 0.02 in L7-PKCi transgenic mice and from 0.08 ± 0.01 to 0.45 ± 0.02 in control animals, when stimulus frequency was increased from 0.1 Hz to 1 Hz. Phase lead decreased from $67.2 \pm 4.5^\circ$ at 0.1 Hz to $12.9 \pm 0.5^\circ$ at 1 Hz in L7-PKCi transgenic and from $76.1 \pm 6.0^\circ$ to $15.3 \pm 0.7^\circ$ in control animals. Thus, one can conclude that baseline responses of compensatory eye movements did not differ between mutants and their wild type littermates prior to training.

Increasing the VOR response

In response to 'out of phase' visuo-vestibular training for 8 consecutive days both L7-PKCi transgenic ($n=12$) and control mice ($n=11$) responded with positive changes in VOR gain (Fig. 2 A1, A2). In control animals VOR gain increased significantly at 0.6 Hz ($P=0.03$), 0.8 Hz ($P=0.002$) and 1 Hz ($P<0.001$) (repeated measures ANOVA), while transgenic animals showed a significant increase in VOR gain at 0.8 Hz ($P=0.01$) and 1.0 Hz ($P=0.01$). At 0.8 Hz and 1 Hz the increase in VOR gain of transgenic animals was significantly smaller than that of control animals ($P<0.01$, mixed model ANOVA). Neither controls nor mutants showed any significant change in VOR phase, before and after the training (Fig. 2 B1, B2). Thus, LTD-deficient mice can increase their VOR gain by long-term visuo-vestibular 'out of phase' training, but these increases are not as pronounced as in control animals. In addition, this type of long-term training results for neither controls nor mutants in frequency specific gain changes.

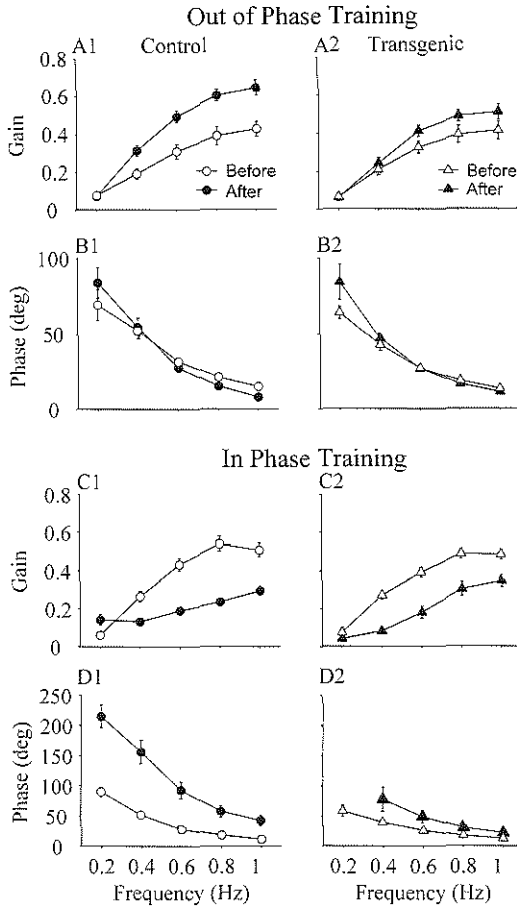


Figure 2: The effect of visual vestibular training on the VOR is shown for control animals (circles) and L7-PKCi transgenic animals (triangles). Changes in VOR gain between the first and the 8th day of 'out of phase' training are plotted against frequency for both control (A1) and L7-PKCi transgenic animals (A2). The open symbols represent VOR before training and the closed symbols after training. VOR phase after 'out of phase' training is plotted in the same manner as VOR gain (B1, B2). In response to 'out of phase' training gain increased predominantly at high frequencies (0.6-1 Hz), while phase remained unchanged. The increases in VOR gain were significantly higher in wild type animals than in mutants (see text). The effect of 'in phase' training on VOR gain (C1, C2) and phase (D1, D2) are plotted as for 'out of phase' training. 'In phase' training resulted in gain decreases across all higher frequencies (0.4-1 Hz), which were accompanied by increases in phase lead. In general, changes in phase but not in gain, were significantly different between wild types and mutants (see text). Phase is absent at 0.2 Hz in L7-PKCi transgenic animals because of the low VOR gain at this frequency. Error bars indicate SEM.

Decreasing the VOR response

In response to 'in phase' training during eight consecutive days, both L7-PKCi transgenic animals (n=8) and control animals (n=13) responded with clear changes in VOR dynamics (Fig. 2 C, D). With respect to VOR gain, L7-PKCi transgenic animals and control animals both showed significant decreases at 0.4 Hz, 0.6 Hz, 0.8 Hz and 1 Hz ($p < 0.001$) (Fig. 2 C1, C2). No significant differences in gain were observed between the two groups at any of these frequencies (mixed model ANOVA). With respect to the phase relation of the VOR, both transgenic and control animals were able to increase VOR phase lead significantly (for control animals $p < 0.001$ at 0.2 Hz, 0.4 Hz, 0.6 Hz, 0.8 Hz and 1 Hz; for transgenic animals $p < 0.01$ at 0.6 Hz, 0.8 Hz, and 1.0 Hz; 1-way ANOVA) (Fig. 2 D1, D2). However, at all these frequencies the increase in phase lead was significantly larger in control than in L7-PKCi transgenic animals (p -values equaled 0.006, 0.02, 0.02 and 0.02 at 0.4 Hz, 0.6 Hz, 0.8 Hz, and 1.0 Hz, respectively; mixed

model ANOVA). Ultimately, control animals, but not LTD-deficient mutants, were able to reverse the direction of their VOR at 0.2 Hz and 0.4 Hz. Thus, LTD-deficient mice can decrease VOR gain and increase the phase lead of their VOR in response to long-term visuo-vestibular ‘in phase’ training, but the overall change in their VOR dynamics is not as prominent as in controls.

Progression of adaptation over time

Progression of adaptation was followed by recording the VOR before each training session began. In response to ‘out of phase’ visuo-vestibular training control animals increased VOR gain in the first four days of training by $170 \pm 23\%$ (Fig. 3 A1). No significant further increase in VOR gain was observed when training was continued up to 8 days. L7-PKCi transgenic animals showed a gradual change in VOR gain when subjected to ‘out of phase’ visuo-vestibular training and by the 8th day of training transgenic animals had increased VOR gain by $125 \pm 15\%$. VOR phase changed in neither control nor L7-PKCi transgenic animals during ‘out of phase’ training (Fig. 3 B1). In response to ‘in phase’ visuo-vestibular training both transgenic and control animals showed the largest reduction in VOR gain in the first 5 days of training (Fig 3 A2). By the 5th day VOR gain had decreased to $43 \pm 6\%$ of its initial value in control animals and $53 \pm 4\%$ in L7-PKCi transgenic animals. Increase in VOR phase lead followed changes in VOR gain and showed a plateau on the 6th day of training in control animals at $326 \pm 45\%$ (Fig. 3 B2). L7-PKCi transgenic animals did not show a plateau response and continued increasing VOR phase lead to $223 \pm 30\%$ of its initial value on the 8th day of recording. Eye movement recordings were not continued beyond 8 days of training and it therefore remains possible that LTD deficient animals might ultimately reach the same level of adaptation as control animals.

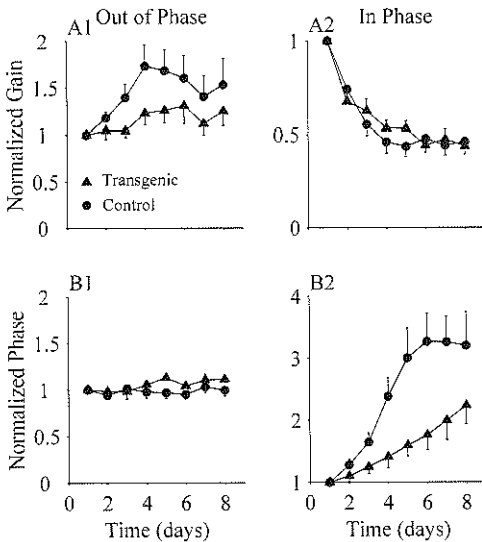


Figure 3: Progression of VOR adaptation in time is shown for the response at the training frequency (0.6 Hz). VOR gain and phase values obtained during training were normalized to the value obtained before training (day1) for each animal individually. Normalized data were then averaged across animals to obtain mean and SEM. Data from transgenic animals (triangles) and control animals (circles) are plotted together for out of phase (A1, B1) and in phase (A2, B2) training. A1 and A2 show changes in VOR gain while B1 and B2 depict changes in phase of the VOR.

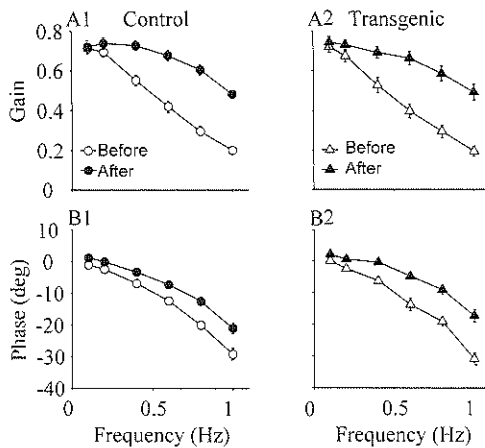


Figure 4: Changes in OKR after visuo-vestibular training in control animals (circles) and L7-PKCi transgenic animals (triangles). OKR gain values of control animals (A1) and mutants (A2) are plotted against frequency before (open symbols) and after training (solid symbols). OKR phase values of control animals and mutants (B2) are shown in B1 and B2, respectively. No differences were observed between mutants and controls. Error bars indicate SEM.

Concomitant changes of OKR responses

To find out whether the observed differences in oculomotor dynamics between LTD-deficient mutants and their control littermates after long-term visuo-vestibular training were limited to the VOR, we also investigated their OKR. Figure 4 demonstrates that OKR gain of both control and transgenic animals increased after 8 days of training and that in both groups phase lag of the eye movement with respect to stimulus movement decreased concomitantly. However, at none of the tested frequencies were changes in OKR significantly different between transgenic and control animals ($p=0.47$, mixed model ANOVA). Moreover, changes in OKR during ‘out of phase’ training did not differ from those during ‘in phase’ training (data not shown). Thus, the long-term training paradigms we used, were discriminative for the type of animal and for the polarity of the response as far as the VOR was concerned, but showed no differential effects on the OKR.

Discussion

The main finding of this study is that selectively blocking LTD at the parallel fiber - Purkinje cell synapse partially, but not totally, impairs long-term VOR adaptation. Thus, LTD may be necessary for short-term VOR adaptation and may facilitate long-term VOR adaptation, but the present data show that slow implementation of adaptive changes to the VOR remains possible even without cerebellar LTD.

The increase in VOR gain observed in the LTD-deficient mutants after ‘out of phase’ visuo-vestibular training was approximately half of that observed in wild types, while VOR phase changes were not observed in either group by this training paradigm. In contrast, the decrease in VOR gain observed in LTD-deficient mutants after ‘in phase’ visuo-vestibular training did not differ from that observed in wild types, while the increase in phase lead in mutants was approximately half of that in wild types. These

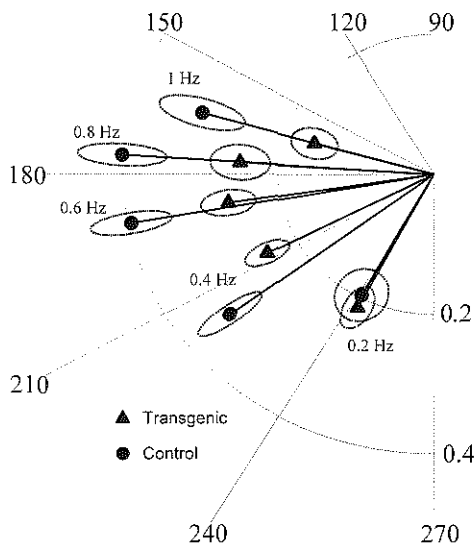


Figure 5: Change in VOR dynamics is expressed as the vectorial difference (β) between the VOR before and after 'in-phase' visuo-vestibular training. β is plotted separately for each frequency and translated to the origin for clarity. At all frequencies β is directed towards the left in both control (circles) and L7-PKCi transgenic (triangles) animals indicating the animals attempt to reverse direction of the VOR. L7-PKCi transgenic mice did not differ from control animals in the direction of vector β ($p > 0.5$, student-t test). However, magnitude of β at 0.6 Hz, 0.8 Hz and 1 Hz was smaller in L7-PKCi transgenic animals ($p < 0.05$, student-t test). Dotted oval lines delineate an area that represents one SEM around the vector tip.

differences are most likely caused by the fact that 'in phase' training differs from 'out of phase' training in that a mere change in VOR gain no longer provides sufficient compensation. A reduction in VOR gain must be accompanied by a reversal of its direction, which is accomplished by an increase in phase lead.

Despite apparently differential deficits of L7-PKCi transgenic animals in the two adaptation paradigms, absence of LTD may affect long-term learning similarly in the two protocols. To illustrate this point the overall impact of long-term training on the VOR can best be visualized by displaying VOR gain and phase in terms of vectors. The length of a vector α can represent VOR gain, while VOR phase is represented by the vector angle with the abscissa. 'In phase' training drives the VOR response vector to a gain of 1 and 180° phase angle with the abscissa. Indeed, after training the VOR is shifted towards this point in both L7-PKCi transgenic and control animals. In analogy to Robinson (1976), change in VOR can thus be expressed as an addition of a vector β to the initial VOR vector α . Figure 5 shows β for control and L7-PKCi transgenic animals after 'in phase' training. Explaining changes in VOR properties by a difference vector β reveals that transgenic animals appear to reverse their VOR in much the same way as control animals do, except that they are just not as capable in achieving their goal since the length of the added vector β is at all higher frequencies significantly smaller than it is in control animals.

The present data show that there must be additional form(s) of plasticity other than LTD of the parallel fiber – Purkinje cell synapse that are involved in long-term adaptation of the VOR. This conclusion can be drawn not only from the fact that VOR gain and phase dynamics of LTD-deficient mice and controls were identical prior to training or that the LTD-deficient mice can show a substantial level of adaptation during long-term visuo-vestibular training, but also from the fact that long-term training at one

particular frequency does not evoke a frequency specific effect as can be observed following short-term training for which parallel fiber LTD induction is essential (De Zeeuw et al., 1998). The existence of other forms of plasticity in the control of compensatory eye movements is further supported by the fact that changes in OKR of control animals during the presently used training paradigms were the same as those in LTD-deficient mutants (cf. Shutoh et al., 2002). These adaptive changes in OKR were such that the resulting eye velocity after training, exceeded the closed loop saturation level of 9.8°/s that is normal for mice under standard conditions (van Alphen et al., 2001). Thus, it may well be that multiple cellular mechanisms other than cerebellar LTD are involved in oculomotor plasticity. To what extent these processes take place up and/or downstream of the Purkinje cell and to what extent they interact with LTD are now the major questions that will have to be addressed.

References

- Albus, J.S. (1971) A theory of cerebellar function. *Math. Biosci.*, **10**, 25-61.
- De Zeeuw, C.I., Hansel, C., Bian, F., Koekkoek, S.K., van Alphen, A.M., Linden, D.J. & Oberdick, J. (1998) Expression of a protein kinase C inhibitor in Purkinje cells blocks cerebellar LTD and adaptation of the vestibulo-ocular reflex. *Neuron*, **20**, 495-508.
- Gonshor, A. & Jones, G.M. (1973) Proceedings: Changes of human vestibulo-ocular response induced by vision-reversal during head rotation. *J. Physiol.*, **234**, 102P-103P.
- Goossens, J., Daniel, H., Rancillac, A., van der Steen, J., Oberdick, J., Crépel, F., De Zeeuw, C.I. & Frens, M.A. (2001) Expression of protein kinase C inhibitor blocks cerebellar long-term depression without affecting Purkinje cell excitability in alert mice. *J. Neurosci.*, **21**, 5813-5823.
- Hirata, Y. & Highstein, S.M. (2001) Acute adaptation of the vestibuloocular reflex: signal processing by floccular and ventral parafloccular purkinje cells. *J. Neurophysiol.*, **85**, 2267-2288.
- Ito, M. (1982) Cerebellar control of the vestibulo-ocular reflex--around the flocculus hypothesis. *Annu. Rev. Neurosci.*, **5**, 275-296.
- Ito, M., Nisimaru, N. & Yamamoto, M. (1977) Specific patterns of neuronal connections involved in the control of the rabbit's vestibulo-ocular reflexes by the cerebellar flocculus. *J. Physiol.*, **265**, 833-854.
- Ito, M., Sakurai, M. & Tongroach, P. (1982) Climbing fibre induced depression of both mossy fibre responsiveness and glutamate sensitivity of cerebellar Purkinje cells. *J. Physiol.*, **324**, 113-134.
- Linden, D.J. & Connor, J.A. (1993) Cellular mechanisms of long-term depression in the cerebellum. *Curr. Opin. Neurobiol.*, **3**, 401-406.
- Lisberger, S.G. (1994) Neural basis for motor learning in the vestibuloocular reflex of primates. III. Computational and behavioral analysis of the sites of learning. *J. Neurophysiol.*, **72**, 974-998.
- Lisberger, S.G. (1998) Cerebellar LTD: A molecular mechanism of behavioral learning? *Cell*, **92**, 701-704.

- Lorente de Nó, R. (1933) Vestibulo-ocular reflex arc. *Arch. Neurol. Psychiat.*, **30**, 245-291.
- Marr, D. (1968) A theory of cerebellar cortex. *J. Physiol.*, **202**, 437-470.
- Miles, F.A. & Fuller, J.H. (1974) Adaptive plasticity in the vestibulo-ocular responses of the rhesus monkey. *Brain. Res.*, **80**, 512-516.
- Miles, F.A. & Lisberger, S.G. (1981) Plasticity in the vestibulo-ocular reflex: a new hypothesis. *Annu. Rev. Neurosci.*, **4**, 273-299.
- Oberdick, J., Smeyne, R.J., Mann, J.R., Zackson, S. & Morgan, J.I. (1990) A promoter that drives transgene expression in cerebellar Purkinje and retinal bipolar neurons. *Science*, **248**, 223-226.
- Partsalis, A.M., Zhang, Y. & Highstein, S.M. (1995) Dorsal Y group in the squirrel monkey. II. Contribution of the cerebellar flocculus to neuronal responses in normal and adapted animals. *J. Neurophysiol.*, **73**, 632-650.
- Robinson, D.A. (1976) Adaptive gain control of vestibuloocular reflex by the cerebellum. *J. Neurophysiol.*, **39**, 954-969.
- Shutoh, F., Katoh, A., Kitazawa, H., Aiba, A., Itohara, S. & Nagao, S. (2002) Loss of adaptability of horizontal optokinetic response eye movements in mGluR1 knockout mice. *Neurosci. Res.*, **42**, 141-145.
- Szentágothai, J. (1950) The elementary vestibulo-ocular reflex arc. *J. Neurophysiol.*, **13**, 395-407.
- van Alphen, A.M., Stahl, J.S. & De Zeeuw, C.I. (2001) The dynamic characteristics of the mouse horizontal vestibulo-ocular and optokinetic response. *Brain. Res.*, **890**, 296-305.
- Zee, D.S., Yamazaki, A., Butler, P.H. & Gucer, G. (1981) Effects of ablation of flocculus and paraflocculus of eye movements in primate. *J. Neurophysiol.*, **46**, 878-899.

4.3 VESTIBULAR COMPENSATION DOES NOT RELY ON LTD OF THE PARALLEL FIBER TO PURKINJE CELL SYNAPSE

M. Faulstich*, A.M. van Alphen*, S. du Lac and C.I. De Zeeuw.

* These authors contributed equally to this paper.

Abstract

Recovery from a unilateral labyrinthectomy is a clear example of plasticity in the central nervous system. To investigate the contribution of cerebellar LTD in this form of plasticity we made unilateral lesions of the labyrinth in Lurcher mice, L7-PKCi transgenic mice and control mice. Lurcher is a mutant mouse strain that is characterized by absence of cerebellar Purkinje cells in adult life and hence has no functional cerebellum. L7-PKCi transgenic animals lack a form of cellular plasticity called cerebellar long-term depression, which is a candidate cellular learning mechanism thought to underlie different forms of motor learning. Vestibular compensation following unilateral labyrinthectomy reflects a long-term adaptive process and comparison of Lurcher and control mice confirmed that this process depends on the cerebellum. However, absence of differences in VOR recovery between L7-PKCi transgenic animals and control animals shows that, although dependent on cerebellar function, recovery of the VOR does not rely on LTD of the parallel fiber to Purkinje cell synapse.

Introduction

De-afferentation of one labyrinth results in a characteristic syndrome of oculomotor and postural disorders. These disorders can be divided into two categories: dynamic and static symptoms (Smith and Curthoys, 1989; Dieringer, 1995). Static symptoms include a deviation of the eyes towards the lesioned side and spontaneous nystagmus. Dynamic symptoms encompass alterations in reflexes that derive their input from the vestibular organ, like the vestibulo ocular reflex (VOR). The VOR typically exhibits a severely reduced gain and increased phase lead following unilateral labyrinthectomy (Baarsma and Collewijn, 1975; Maioli et al., 1983; Fetter and Zee, 1988; Vibert et al., 1993). Vestibular compensation is a clear example of plasticity in the central nervous system.

Resolution of dynamic symptoms is analogous to a well-known form of motor learning, i.e. VOR adaptation. In VOR adaptation the relation between head movement and image slip is altered, for instance by placing an optical device like reversing prisms in front of the eyes, which results in a recalibration of the underlying VOR (Jones and Davies, 1976; Jones, 1977). After unilateral labyrinthectomy a recalibration of the VOR is also required because this intervention essentially halves the input to this reflex. Over time VOR gain recovers to almost normal values in monkey and man for low stimulus velocities, while at higher stimulus velocities recovery is less complete and remains asymmetric (Allum et al., 1988; Fetter and Zee, 1988; Curthoys and Halmagyi, 1995). Recalibration of the VOR following unilateral labyrinthectomy does not occur in the absence of vision (Courjon et al., 1977) and requires intact cerebellar function (Courjon et al., 1982), which lends further support to the analogy between this phenomenon and VOR adaptation.

A candidate cellular mechanism underlying VOR adaptation is long-term depression (LTD) of the parallel fiber to Purkinje cell synapse (Ito, 1982). L7-PKCi transgenic mice, in which cerebellar LTD was selectively blocked, were unable to increase VOR gain when subjected to a visuo-vestibular adaptation paradigm for one hour (De Zeeuw et al., 1998). In the present study we investigate whether vestibular compensation in the mouse is indeed dependent on the cerebellum and whether it involves the same cellular mechanism as short term VOR adaptation. Unilateral

labyrinthectomies were therefore performed in three types of mice, including L7-PKCi transgenic mice, Lurcher mice and control mice. Lurcher mutant mice effectively model a complete lesion of the cerebellar cortex since at three months of age all cerebellar Purkinje neurons have degenerated in this mutant strain.

Methods

Surgical procedures

Mice were anaesthetized with a mixture of halothane, nitrous oxide and oxygen. An acrylic head fixation pedestal was formed and fixed to the skull with small screws (M1, 1.5 mm) implanted on the frontal, parietal and interparietal bone plates. A small incision was made in the conjunctiva on the temporal side of the eyeball. A pocket was bluntly dissected anterior to the insertion of the lateral rectus muscle. A copper wire coil (1 mm outside diameter, 60 turns, 1.0 mg) was placed in the pocket. The coil was fixed to the sclera with 2 sutures (10/0 nylon, Ethicon). The sutures were approximately aligned in the equatorial plane of the eye. The conjunctiva was closed over the coil with an additional suture. The leads of the coil were carefully tunneled underneath the conjunctiva and the skin to a miniature coaxial MMCX connector that was attached to the top of the acrylic head pedestal. All animals were allowed to recover for at least 3 days before the first eye movement recordings were made.

Following recovery, 2-3 days of baseline eye movement measurements were made, after which a labyrinthectomy was performed under halothane/nitrous oxide anesthesia. A retro-auricular incision was made to expose the temporal bone and the horizontal semicircular canal. The horizontal canal was drilled open over an extent of at least 1 mm with a .5 mm burr. The endolymphatic fluid was drained passively with absorbent points (Henry Schein Inc. NY, USA). After the flow of endolymph ceased, air was flushed through the canal via a blunted 30-gauge needle connected to a 3 cc syringe. The airflow was aimed anteriorly into the canal, in the direction of the horizontal canal crista. After draining and flushing, a dental paper tip was inserted into the rostral opening of the canal and fixed in place with bone wax.

Damage to the vestibular apparatus was verified post-mortem in a subset of animals. Following transcardial perfusion, the temporal bones were embedded in resin, sectioned at 10 μ m, and stained with a mixture of toluidine blue and methylene blue (1:1; final concentration 1%). Microscopic evaluation revealed a complete loss of tectorial structure over the cristae of the semicircular canals and the utricle and saccule on the side of the lesion. As shown in Fig. 1A, all stereocilia were missing, and hair cells showed signs of degeneration. Corresponding sections of the temporal bone from the intact side showed normal hair cells and intact stereocilia and tectorial structure (Fig. 1B).

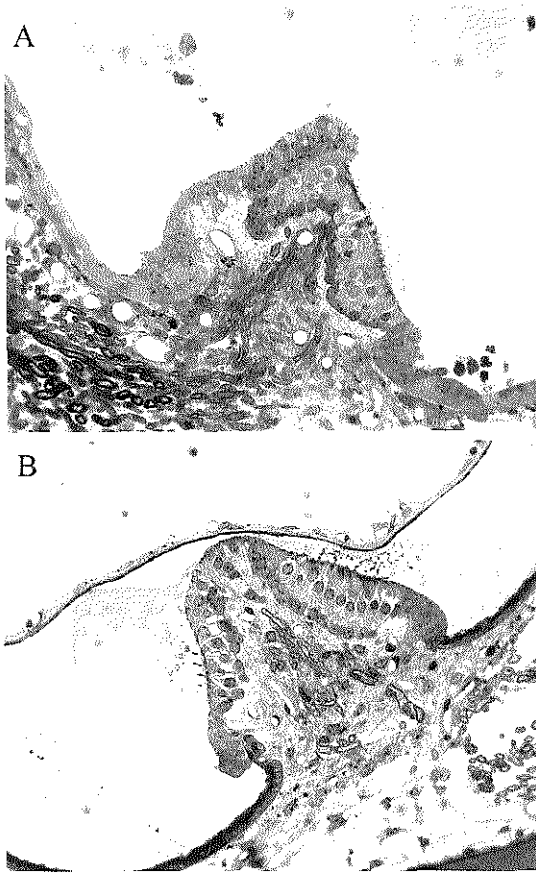


Figure 1: Histology of the crista of the horizontal canal in a canal-lesioned mouse. Sections show corresponding locations from the lesioned (A) and intact (B) side. Note in A the lack of tectorial structure, the absence of stereocilia and the degeneration of hair cells with the resulting disarray of cellular structure. Hair cells in B show the normal regular arrangement and stereocilia. Part of the tectorial structure can be seen attached to the cilia. The thin structure spanning the canal lumen just above the crista in B is the lining of the canal, which detached during histological preparation.

Behavioral testing

During eye movement measurements, mice were immobilized in a custom-made restrainer incorporating an aluminum plate to which the head fixation pedestal was bolted. The restraint assembly was mounted within magnetic field coils (CNC Engineering, Seattle, WA) atop a vertical-axis turntable (Biomedical Engineering Co., Thornwood, NY). The midpoint of the interaural axis was positioned in the center of rotation of the turntable. The field coils were attached to the turntable and moved with the animal. Optokinetic stimuli were delivered with a striped drum (bar width: 4 deg). The drum had a diameter of 26 centimeters and surrounded the animal. The vestibulo-ocular reflex (VOR) was evaluated during sinusoidal, whole body rotation in the dark. Eye position and stimulus recordings were filtered on-line at 20 Hz using a 4th order Bessel filter (Axon Instruments, Foster City, CA) and digitized at 250 Hz with 32-bit precision (CED, Cambridge, UK). Before each recording session the eye coil was calibrated by rotating the field coils around the animal. During rotation of the field coils

of 20 degrees and the resulting voltage was taken as a reference for the following recording session.

The optokinetic reflex (OKR) and vestibulo-ocular reflex (VOR) were measured in three different strains of mice: L7-PKCi (De Zeeuw et al., 1998), wildtype C57bl/6, and Lurcher. The OKR was tested with sinusoidal rotation of the striped drum at 5 different frequencies: 0.2, 0.4, 0.6, 0.8 and 1 Hz. The amplitude of the drum was constant at 5 deg (0-peak), resulting in peak velocities that ranged from 3 to 31 deg/sec. The VOR was tested by rotating the animal sinusoidally in the dark over the same frequency range as the OKR and with amplitudes of 5 and at 10 deg (0-peak). The visually enhanced VOR (VVOR) was tested in the light by whole body rotation with respect to an earth fixed drum. The order in which stimuli were delivered was randomized. Each recording session lasted approximately 30 minutes.

Data analysis

Eye, head and drum position were differentiated off-line, using a 3-point software algorithm. Fast phases were identified algorithmically whenever eye velocity exceeded 2.5 times the peak stimulus velocity. Identified fast phases were excised from the eye velocity trace with a margin of 20 ms before to 80 ms after detection. Gain and phase of eye movement with respect to stimulus movement were calculated by fitting a sine wave to the average using least-square optimization. When eye movement lagged stimulus movement, phase was expressed with a negative sign. Phase relations of VOR and VVOR were shifted by 180 deg, making the phase angle 0 for perfectly compensatory responses.

Nystagmus was analyzed by counting the number of fast phases (eye velocity > 150 deg/s) that occurred in 3 minutes when the animal was stationary in the dark.

Results

Effects of labyrinthectomy on wildtype mice

Following labyrinthectomy, mice displayed the postural symptoms of unilateral vestibular dysfunction that have been observed in other species, including head tilt, rolling, and circling. Ocular nystagmus with quick phases directed toward the side contralateral to the lesion was prominent immediately after labyrinthectomy and declined to control levels over a time course that varied from hours to days across mice. Fig 2A plots the rate of quick phases as a function of time with respect to labyrinthectomy averaged across 6 wildtype mice. In one mouse, a spontaneous nystagmus redeveloped 5-7 days following labyrinthectomy, as has been observed in monkeys (Fetter and Zee, 1988).

Labyrinthectomy impaired the ability of mice to stabilize gaze during head movements. Within a period of days, however, adaptive changes in the VOR restored gaze stabilization. Fig. 3 shows gain (A) and phase (B) of VVOR in wildtype mice as a

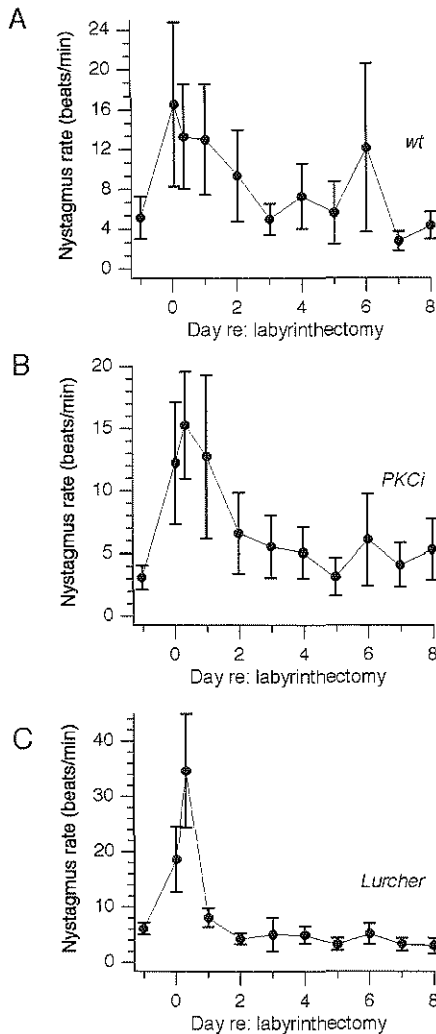


Figure 2: Timecourse of spontaneous nystagmus following labyrinthectomy. Each panel plots the mean rate of rapid (> 150 deg/s) eye movements recorded during 3 minutes in darkness in the absence of vestibular stimulation, as a function of day with respect to labyrinthectomy. A. Wildtype mice ($n=5$). B. L7-PKCi mice ($n=6$). C. Lurcher mice ($n=6$). Error bars are standard error of the mean.

function of time with respect to labyrinthectomy. Data are the mean \pm SEM of 6 animals in response to head rotation at 0.6 Hz, ± 5 deg. In control conditions, the average VVOR gain in the two days preceding the lesion was 0.77. The gain measured 8 hours after the lesion dropped to 0.46, and then increased over the subsequent three days. By the third day following the lesion, gain had increased to 0.65 and showed little change for the duration of the experiment (8 days). VVOR phase was almost perfectly compensatory in control conditions and was affected relatively little by labyrinthectomy (Fig. 3B)

To assess the relative contributions of vestibular and visual pathways to the adaptive changes in gain stabilization observed in VVOR, we analyzed recovery of VOR and OKR following labyrinthectomy. Fig. 3C shows VOR gain and Fig. 3D shows VOR

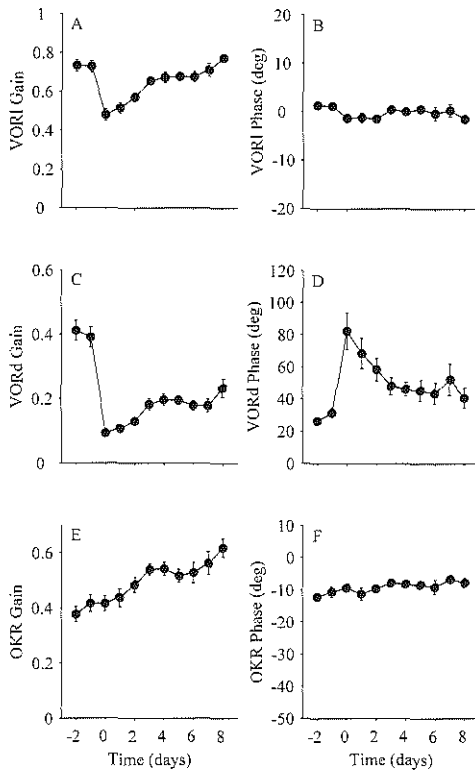


Figure 3: Effects of labyrinthectomy on evoked eye movements in wildtype mice. A and B plot gain and phase, respectively, of VOR in the light (VVOR) as a function of day with respect to labyrinthectomy. C and D plot gain and phase of VOR in the dark. E and F plot gain and phase of the OKR. Stimuli in all conditions were 0.6 Hz, ± 5 deg. Plots show averages and standard errors of data from 6 mice. Phase in B and D is shifted by 180 deg such that a phase response of 0 deg represents perfectly compensatory VOR. Positive phase indicates a phase lead with respect to compensatory.

phase at 0.6 Hz, ± 5 deg for our population of 6 wildtype mice. In control conditions VOR gain averaged 0.41, with a phase lead relative to compensatory of 33 deg. Following labyrinthectomy, VOR gain dropped to 0.09. Gain increased to 0.18 over the following 3 days, after which it remained relatively constant (ranging from 43 to 55% of control values). Labyrinthectomy resulted in a large and variable phase lead in VOR that averaged 82 deg. Within 3 days, VOR phase lead dropped to 52 deg and was relatively stable from the third to the eighth day following the lesion.

Fig. 3E shows OKR gain prior to and following labyrinthectomy. The OKR gain in control conditions was 0.4 when measured at 0.6 Hz, ± 5 deg, and eye movement phase lagged that of the visual stimulus by 13 deg. Labyrinthectomy had no immediate effect on OKR gain. During the 8 subsequent days, OKR gain increased to values that were higher than in control conditions. OKR phase remained relatively constant throughout the testing period (Fig 3F).

Adaptive increases in VOR gain following labyrinthectomy were evident across all but the lowest frequency that we tested. Fig. 4A plots VOR gain prior to, 8 hours following, and 6-8 days following labyrinthectomy as a function of stimulus frequency. In control mice, VOR gain depended on frequency, increasing to a plateau level from 0.2

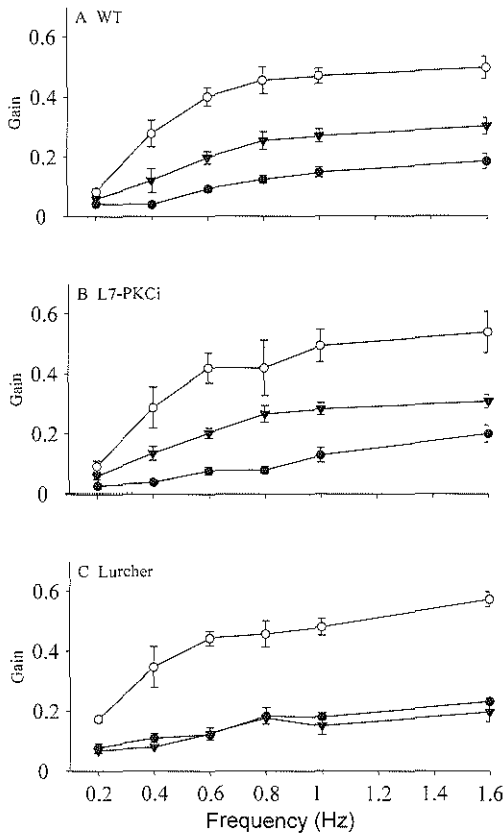


Figure 4: Frequency-dependence of adaptive increases in VOR gain. The gain of VOR in the dark is plotted as a function of rotation frequency in control conditions (open circles), 8 hours following labyrinthectomy (filled circles), and 6-8 days following labyrinthectomy (filled triangles). Plots indicate the mean and standard error of 6 mice; stimulus amplitude was ± 5 deg. Panel A shows data from wildtype mice; B shows L7-PKCi mice, and C. shows Lurcher mice.

Hz to 0.8 Hz, as has been reported previously. Following labyrinthectomy, gain dropped to 48% of control levels when tested at 0.2 Hz and to between 16 and 32% at higher stimulus frequencies. No significant change in gain was observed after 6-8 days in response to head rotations at 0.2 Hz. The largest increases in gain were observed in response to head rotations at 1.6 Hz, the highest frequency that we tested. Following labyrinthectomy, eye movements directed away from the side of the lesion were slightly greater than those oppositely directed; however, these differences were not statistically significant (paired t-test, $p > .05$ at all frequencies, $n=6$ animals).

L7-PKCi mice show normal adaptive gain increases following labyrinthectomy

To determine whether cerebellar long term depression (LTD) is required for the adaptive increases in VOR gain that are induced by unilateral damage to the vestibular periphery, we analyzed eye movements in transgenic mice in which an inactivating peptide of

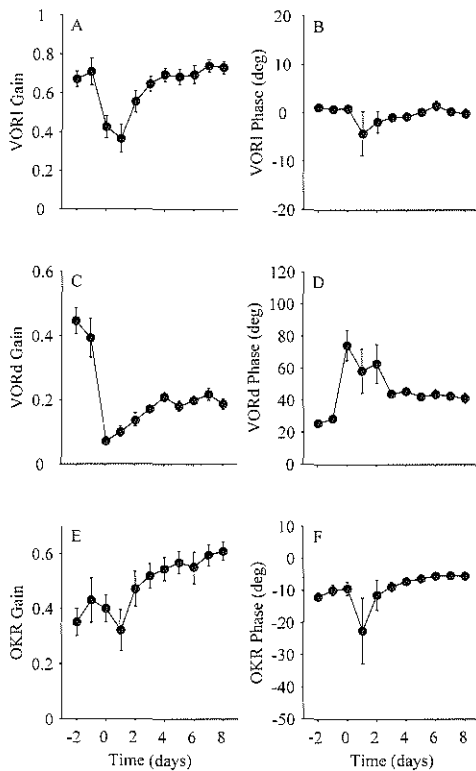


Figure 5: Effects of labyrinthectomy on evoked eye movements in L7-PKCi mice. A and B plot gain and phase, respectively, of VOR in the light (VVOR) as a function of day with respect to labyrinthectomy. C and D plot gain and phase of VOR in the dark. E and F plot gain and phase of the OKR. Stimuli in all conditions were 0.6 Hz, ± 5 deg. Plots show averages and standard errors of data from 6 mice. Phase in B and D is shifted by 180 deg such that 0 phase represents perfectly compensatory VOR. Positive phase indicates a phase lead with respect to compensatory.

protein kinase C was expressed under control of the Purkinje cell promotor L7. Previous studies have shown that L7-PKCi mice do not exhibit cerebellar LTD, either in culture (De Zeeuw et al., 1998) or in brain slices (Goossens et al., 2001). As described previously (De Zeeuw et al., 1998), we found that under control conditions, eye movements are normal in L7-PKCi mice; at 0.6 Hz ± 5 deg, VVOR gain averaged 0.70, VOR gain averaged 0.42, and OKR gain averaged 0.39. Although L7-PKCi mice are unable produce rapid adaptive increases in VOR gain following an hour of visual-mismatch training (De Zeeuw et al., 1998), they exhibited gain increases following labyrinthectomy that were indistinguishable from those in wildtype mice. Fig. 5A shows VVOR prior to and during the 8 days following unilateral labyrinthectomy in 6 L7-PKCi mice. Labyrinthectomy induced an initial drop in VVOR gain to 0.43, which was followed by increases in gain over the subsequent 3-4 days. Gain reached plateau values of 0.69-0.74 between days 4 and 8. As in wildtype animals, after labyrinthectomy, the phase of VVOR remained nearly perfectly compensatory (Fig. 5B). L7-PKCi mice showed adaptive increases in VOR, as seen in Fig 5C. The gain of VOR dropped to 0.16 within 8 h following labyrinthectomy and recovered to a plateau value of 0.28 within 4

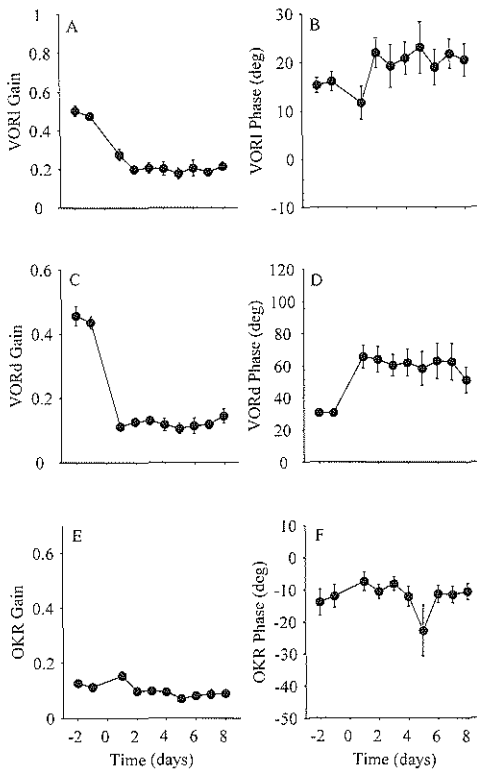


Figure 6: Effects of labyrinthectomy on evoked eye movements in Lurcher mice. A and B plot gain and phase, respectively, of VOR in the light (VVOR) as a function of day with respect to labyrinthectomy. C and D plot gain and phase of VOR in the dark. E and F plot gain and phase of the OKR. Stimuli in all conditions were 0.6 Hz, ± 5 deg. Plots show averages and standard errors of data from 6 mice. Phase in B and D is shifted by 180 deg such that 0 phase represents perfectly compensatory VOR. Positive phase indicates a phase lead with respect to compensatory.

days. As shown in Fig. 5B Labyrinthectomy resulted in large and variable phase lead over the first 2 post-lesion days. By the third post-lesion day VOR phase a value of 44 deg, which remained stably and significantly elevated over control conditions during the subsequent 5 days.

These adaptive increases in VOR gain were not significantly different from those in wildtype mice on any of the days tested ($p > .20$; unpaired t-tests). As in wildtype mice, OKR gain in L7-PKCi mice increased following labyrinthectomy (Fig. 5E), and OKR phase was unaffected by labyrinthectomy (Fig. 5F). The patterns of gain changes across frequency were similar in L7-PCKi and wildtype mice (Fig. 4B).

Impaired VOR plasticity in Lurcher mice

The results described above indicate that PKC expression in Purkinje cells is not required for adaptive increases in VOR gain following unilateral loss of the vestibular periphery. To investigate whether labyrinthectomy-induced gain increases depend on intact cerebellar function, we measured eye movements in the Lurcher strain of mice, in which

Purkinje cells degenerate by the sixth postnatal week (Caddy and Biscoe, 1979; Wetts and Herrup, 1982).

Labyrinthectomy produced a pronounced nystagmus in Lurcher mice that returned to control values within 2 days (Fig. 2C). In contrast with wildtype and L7-PKCi mice, Lurcher mice did not show long-lasting adaptive increases in gaze stabilization following unilateral vestibular dysfunction. One day after labyrinthectomy, VVOR gain in Lurcher mice dropped to approximately one-half of the control value and remained depressed for the subsequent 7 days tested (Fig 6A). Labyrinthectomy had relatively little effect on VVOR phase (Fig. 6B).

VOR gains did not show adaptive changes following labyrinthectomy (Fig. 6C). VOR gain dropped to 23% of control conditions within one day and remained at depressed levels of between 21% and 32% of control over the subsequent 7 days. VOR gains in Lurchers were significantly lower than those in both wildtype and L7-PKCi mice from the third through the eighth day following labyrinthectomy ($p < .05$; unpaired t-test). No recovery of VOR gain was observed at any frequency tested (Fig 4C). VOR phase lead increased from 30 to 69 following labyrinthectomy and remained elevated for the subsequent testing period (Fig. 6D). Neither OKR gain nor phase, were significantly affected by labyrinthectomy in Lurcher mice (Fig 6E and F).

Discussion

This study analyzed a form of long-term plasticity of the VOR in mice that is induced by damage to the peripheral vestibular endorgan. Following unilateral labyrinthectomy, VOR gains in wildtype mice dropped and then increased over the course of about a week. To determine whether the mechanisms of these adaptive gain increases are similar to those underlying short-term plasticity of the VOR, we analyzed the consequences of labyrinthectomy in L7-PKCi transgenic mice that express a peptide inhibitor of protein kinase C in cerebellar Purkinje cells. Although these mice are impaired in both short-term plasticity of the VOR and cerebellar long-term depression (De Zeeuw et al., 1998; Goossens et al., 2001), they exhibited VOR gain increases following unilateral labyrinthectomy that were indistinguishable from those in wildtype mice. These adaptive gain increases depend on the integrity of the cerebellum, since they were absent in Lurcher mice, which lack functional Purkinje cells. These findings indicate that cerebellar-dependent long and short-term gain increases in the VOR are mediated by distinct mechanisms.

Although the method that we used to damage the vestibular periphery in mice differs from those described in studies of other animals (Maioli and Precht, 1985; Fetter and Zee, 1988; Vibert et al., 1993; Gilchrist et al., 1998; Balaban et al., 1999), a number of lines of evidence indicate that vestibular hair cells suffered permanent damage and thus could not signal information related to head motion. Histological analyses of the inner ears in lesioned animals revealed complete loss of tectorial structure, damage to hair cells, and loss of stereocilia, as would be expected from the combination of endolymph loss and physical shearing due to perfusion of the canal with air. Some of the increases in VOR gain following physical plugging of the semicircular canal have been attributed to peripheral rather than central processes (Hess et al., 2000). The fact that

Lurcher mice did not show increases in VOR gain indicates that the plasticity we measured in this study resulted from central rather than peripheral adaptive mechanisms.

The consequences of a peripheral vestibular lesion for the gain of the VOR were qualitatively similar between mice and other species (Maioli and Precht, 1985; Fetter and Zee, 1988; Vibert et al., 1993) but showed some quantitative differences. Following the lesion, VOR gains dropped to about 20% of control values in mice, whereas they dropped to about 50% in monkeys and cats (Maioli and Precht, 1985; Fetter and Zee, 1988; Lasker et al., 2000) and to about 30-50 % of control in guinea pigs (Vibert et al., 1993). A velocity-dependent asymmetry in the VOR following peripheral damage has also been reported (Fetter and Zee, 1988; Vibert et al., 1993; Broussard et al., 1999; Lasker et al., 2000), but was not apparent with the low velocity stimuli used in the present study. VOR gain increased rapidly in mice following a peripheral lesion, recovering to 50-60% of control values within less than a week. Although most published studies do not measure VOR gain during the first week following vestibular damage, rapid increases in VOR gain following unilateral loss of vestibular inputs have been documented in monkeys and cats (Maioli et al., 1983; Fetter and Zee, 1988; Broussard et al., 1999). A slower time course of vestibular compensation appears to exist in guinea pigs (Vibert et al., 1993). Unfortunately, limitations on the durability of implanted eye coils used in this study precluded extended measurements of VOR gain following labyrinthectomy. Studies that measured eye movements with a video tracker, which are not hampered by such restrictions, indicate that following vestibular damage VOR gains in mice recover to about 70% of control values with a time constant of 5-6 days and show no further increase over many months (Faulstich and du Lac, personal communication).

Increases in VOR gain following labyrinthectomy depended on the integrity of the cerebellum, as evidenced by the lack of gain increase in Lurcher mice. Lurcher animals, named after their obviously ataxic lurching gate, have a mutation in the gene that encodes the delta-2-glutamate receptor (Zuo et al., 1997). The mutation results in postnatal Purkinje cell death and consequent degeneration of cerebellar granule cells and inferior olive neurons (Caddy and Biscoe, 1979). Degeneration of vestibular nucleus neurons or other neurons in the circuitry for the VOR due to the Lurcher mutation have not been reported. However, the fact that the VOR of intact Lurcher mice is very similar to that of wildtype mice indicates that vestibular compensation was impaired because of the defective cerebellar circuitry and not because of possible aberrations in extra-cerebellar vestibular pathways. A role for the cerebellum in vestibular compensation has been reported (Courjon et al., 1982), as has a role for inferior olive neurons in postural recovery (Llinas et al., 1975).

Persistent image motion during head movement evokes cerebellar-dependent changes in the gain of the VOR that occur over a time course of hours to days (reviewed in: du Lac et al., 1995; Raymond et al., 1996). The time course and magnitude of these adaptive gain changes appears to depend, in part, on the duration of the discrepant visual and vestibular stimuli (Raymond and Lisberger, 1996). Small changes in VOR gain that occur over 1-2 hours of forced visual/vestibular mismatch training require protein kinase C expression in cerebellar Purkinje cells, as they are abolished in L7-PKCi mice that express a PKC inhibitor (De Zeeuw et al., 1998). The finding that L7-PKCi mice show normal VOR plasticity following labyrinthectomy but show impaired plasticity during visual-vestibular mismatch training may indicate different cellular mechanisms for these

two forms of cerebellar-dependent plasticity. Given that cerebellar LTD is impaired in L7-PKCi mice (De Zeeuw et al., 1998; Goossens et al., 2001), our data suggest that LTD is not a mechanism subserving vestibular compensation following peripheral vestibular dysfunction, and that this form of plasticity can proceed independently of LTD.

Changes in PKC expression in cerebellar Purkinje cells have been observed following labyrinthectomy (Goto et al., 1997; Barmack et al., 2001). Pharmacological blockade of PKC causes an increase in spontaneous nystagmus following labyrinthectomy in guinea pigs (Sansom et al., 2000) and delays the normally rapid recovery from nystagmus in rats (Balaban et al., 1999). In contrast, we observed neither a difference in nystagmus nor in gain recovery between wildtype and L7-PKCi mice. Increases in PKC expression may be a mechanism for the earliest phases of recovery from unilateral vestibular damage. Our data indicate, however, that PKC activation in Purkinje cells is not a critical step in VOR plasticity following peripheral lesions.

In summary, our data indicate that multiple mechanisms of cerebellar-dependent adaptive gain control exist in the circuitry for the VOR. Short-term plasticity induced by visual-vestibular mismatch training requires PKC activation in Purkinje cells and may utilize LTD as a mechanism of learning. Long-term plasticity following peripheral vestibular dysfunction proceeds independently of LTD and Purkinje cell PKC activation but requires the integrity of the olivo-cerebellar circuitry. Multiple sites of cellular plasticity in cerebellar dependent motor learning have been postulated (Raymond et al., 1996). It will be intriguing to determine how different components of the circuit are responsible for plasticity that occurs over different time scales and in response to different stimulus conditions.

References

- Allum JH, Yamane M, Pfaltz CR (1988) Long-term modifications of vertical and horizontal vestibulo-ocular reflex dynamics in man. I. After acute unilateral peripheral vestibular paralysis. *Acta Otolaryngol* 105:328-337.
- Baarsma EA, Collewijn H (1975) Changes in compensatory eye movements after unilateral labyrinthectomy in the rabbit. *Arch Otorhinolaryngol* 211:219-230.
- Balaban CD, Freilino M, Romero GG (1999) Protein kinase C inhibition blocks the early appearance of vestibular compensation. *Brain Res* 845:97-101.
- Barmack NH, Qian ZY, Kim HJ, Yoshimura J (2001) Activity-dependent distribution of protein kinase C-delta within rat cerebellar Purkinje cells following unilateral labyrinthectomy. *Exp Brain Res* 141:6-20.
- Broussard DM, Bhatia JK, Jones GE (1999) The dynamics of the vestibulo-ocular reflex after peripheral vestibular damage. I. Frequency-dependent asymmetry. *Exp Brain Res* 125:353-364.
- Caddy KW, Biscoe TJ (1979) Structural and quantitative studies on the normal C3H and Lurcher mutant mouse. *Philos Trans R Soc Lond B Biol Sci* 287:167-201.
- Courjon JH, Jeannerod M, Ossuzio I, Schmid R (1977) The role of vision in compensation of vestibulo ocular reflex after hemilabyrinthectomy in the cat. *Exp Brain Res* 28:235-248.
- Courjon JH, Flandrin JM, Jeannerod M, Schmid R (1982) The role of the flocculus in vestibular compensation after hemilabyrinthectomy. *Brain Res* 239:251-257.

- Curthoys IS, Halmagyi GM (1995) Vestibular compensation: a review of the oculomotor, neural, and clinical consequences of unilateral vestibular loss. *J Vestib Res* 5:67-107.
- De Zeeuw CI, Hansel C, Bian F, Koekkoek SK, van Alphen AM, Linden DJ, Oberdick J (1998) Expression of a protein kinase C inhibitor in Purkinje cells blocks cerebellar LTD and adaptation of the vestibulo-ocular reflex. *Neuron* 20:495-508.
- Dieringer N (1995) 'Vestibular compensation': neural plasticity and its relations to functional recovery after labyrinthine lesions in frogs and other vertebrates. *Prog Neurobiol* 46:97-129.
- du Lac S, Raymond JL, Sejnowski TJ, Lisberger SG (1995) Learning and memory in the vestibulo-ocular reflex. *Annu Rev Neurosci* 18:409-441.
- Fetter M, Zee DS (1988) Recovery from unilateral labyrinthectomy in rhesus monkey. *J Neurophysiol* 59:370-393.
- Gilchrist DP, Curthoys IS, Cartwright AD, Burgess AM, Topple AN, Halmagyi M (1998) High acceleration impulsive rotations reveal severe long-term deficits of the horizontal vestibulo-ocular reflex in the guinea pig. *Exp Brain Res* 123:242-254.
- Goossens J, Daniel H, Rancillac A, van der Steen J, Oberdick J, Crepel F, De Zeeuw CI, Frens MA (2001) Expression of protein kinase C inhibitor blocks cerebellar long-term depression without affecting Purkinje cell excitability in alert mice. *J Neurosci* 21:5813-5823.
- Goto MM, Romero GG, Balaban CD (1997) Transient changes in flocculonodular lobe protein kinase C expression during vestibular compensation. *J Neurosci* 17:4367-4381.
- Hess BJ, Lysakowski A, Minor LB, Angelaki DE (2000) Central versus peripheral origin of vestibuloocular reflex recovery following semicircular canal plugging in rhesus monkeys. *J Neurophysiol* 84:3078-3082.
- Ito M (1982) Cerebellar control of the vestibulo-ocular reflex--around the flocculus hypothesis. *Annu Rev Neurosci* 5:275-296.
- Jones GM (1977) Plasticity in the adult vestibulo-ocular reflex arc. *Philos Trans R Soc Lond B Biol Sci* 278:319-334.
- Jones GM, Davies P (1976) Adaptation of cat vestibulo-ocular reflex to 200 days of optically reversed vision. *Brain Res* 103:551-554.
- Lasker DM, Hullar TE, Minor LB (2000) Horizontal vestibuloocular reflex evoked by high-acceleration rotations in the squirrel monkey. III. Responses after labyrinthectomy. *J Neurophysiol* 83:2482-2496.
- Llinas R, Walton K, Hillman DE, Sotelo C (1975) Inferior olive: its role in motor learning. *Science* 190:1230-1231.
- Maioli C, Precht W (1985) On the role of vestibulo-ocular reflex plasticity in recovery after unilateral peripheral vestibular lesions. *Exp Brain Res* 59:267-272.
- Maioli C, Precht W, Ried S (1983) Short- and long-term modifications of vestibulo-ocular response dynamics following unilateral vestibular nerve lesions in the cat. *Exp Brain Res* 50:259-274.
- Raymond JL, Lisberger SG (1996) Behavioral analysis of signals that guide learned changes in the amplitude and dynamics of the vestibulo-ocular reflex. *J Neurosci* 16:7791-7802.

- Raymond JL, Lisberger SG, Mauk MD (1996) The cerebellum: a neuronal learning machine? *Science* 272:1126-1131.
- Sansom AJ, Smith PF, Darlington CL, Lavery R (2000) The effects of protein kinase C and calmodulin kinase II inhibitors on vestibular compensation in the guinea pig. *Brain Res* 882:45-54.
- Smith PF, Curthoys IS (1989) Mechanisms of recovery following unilateral labyrinthectomy: a review. *Brain Res Brain Res Rev* 14:155-180.
- Vibert N, de Waele C, Escudero M, Vidal PP (1993) The horizontal vestibulo-ocular reflex in the hemilabyrinthectomized guinea-pig. *Exp Brain Res* 97:263-273.
- Wetts R, Herrup K (1982) Interaction of granule, Purkinje and inferior olivary neurons in lurcher chimaeric mice. I. Qualitative studies. *J Embryol Exp Morphol* 68:87-98.
- Zuo J, De Jager PL, Takahashi KA, Jiang W, Linden DJ, Heintz N (1997) Neurodegeneration in Lurcher mice caused by mutation in delta2 glutamate receptor gene. *Nature* 388:769-773.

CHAPTER 5
GENERAL DISCUSSION

In the past chapters we have presented a reliable technique to measure eye movements in mice. The eye movements of four selected mutants have been described, which included epistatic circler, Shaker, Lurcher and L7-PKCi transgenic mice. Results from our recordings in epistatic circler mice and Shaker mice have shown that morphological aberrations of the labyrinth in these animals led to a functional impairment of this structure. Eye movement recordings in Lurcher mice and L7-PKCi transgenic mice revealed that adaptation of the optokinetic reflex (OKR), adaptation of the vestibulo-ocular reflex (VOR) and recovery of the VOR following unilateral labyrinthectomy required an intact cerebellum, but that not all these forms of oculomotor plasticity relied on cerebellar long-term depression.

5.1 Technical considerations

We have discussed two different techniques for recording eye movements in mice: video oculography and mini-search coil technique. Combined video and mini-coil recordings of eye movements in the mouse revealed that implanting a coil into the eye of a mouse was not without consequence for normal generation of eye movements. A small dissociation between coil movement and actual movement of the eye was observed, which led us to modify our surgical procedure for implanting a search-coil. An additional suture was placed to more firmly attach the search-coil to the sclera. This procedure considerably improved our recordings in that gain of the eye movements was larger when the eye coil was more tightly secured to the eyeball. However, despite the improvement in our ability to detect eye movement, gain of the vVOR as measured with a scleral search coil remained smaller than when it was measured using video-oculography (Stahl et al., 2000; Stahl, 2002; Faulstich, personal communication). Video recordings therefore revealed that ocular motility was still slightly affected by coil placement.

Other groups performed OKR measurements using video oculography in C57BL/6 mice, and found gain values that were close to and even slightly lower than what we observed using the scleral search coil (Katoh et al., 1998; Iwashita et al., 2001; Shutoh et al., 2002). This set of studies by no means validates our coil recordings as a 'golden standard', but it does show that even using video techniques different labs may obtain quite different results. Differences between studies that used video oculography were attributed to erroneous assumptions on the distance of the pupil from the center of rotation of the eyeball, which led to a systematic calibration error (Katoh et al., 1998, 2000; Kitazawa et al., 2000), but correction of the calibration method did not substantially alter the results (Shutoh et al., 2002). However, the possibility that technical aspects may cause differences in absolute gain values between labs is not crucial for interpretation of the experimental results from a single lab as long as experiments were set up to compare two groups.

We used the improved coil technique to describe comparisons between mutant mice and their control littermates and hence any impediment of normal eye movement due to coil placement was equal in both experimental groups. Since all procedures were identical for both experimental groups they could not confound interpretation of our data. The only article that lacks a comparative design is part of chapter 2 and describes control of compensatory reflexes in C57BL/6 mice. Any effect of the coil on interpretation is

extensively discussed in that section and will not be repeated here. I would however like to stress that the most obvious impediment due to the coil seems to remain quantitative and reflects an overall reduction of eye movement gain.

5.2 The use of eye movement recordings as a tool to assess vestibular function

Chapter 2 describes two studies that were not primarily aimed at elucidating mechanisms of oculomotor control. In stead, the search coil technique provided one tool in a multidisciplinary attempt to confirm the labyrinthine origin of the behavioral phenotype observed in epistatic circler and Shaker mutant mice. In both types of mutant mice morphological findings indicated vestibular dysfunction but functional testing was required to confirm this hypothesis. Epistatic circler mice possessed bilateral occlusions of the lateral semi circular canals, which rendered normal function of these structures highly unlikely. In Shaker mice a mutation had occurred in the myosin VIIa gene (Gibson et al., 1995), which was expressed in vestibular and cochlear hair cells (Hasson et al., 1997). Electron microscopic images taken from the inner ear of Shaker mice revealed accumulation of large vacuoles inside hair cells, which indicated that these cells were abnormal and might not be functional. Since the VOR indirectly reflects vestibular function, absence of this reflex in both types mutants confirmed vestibular dysfunction. However, performance of the VOR is only an indirect measure of peripheral vestibular function. Possible involvement of additional central deficits therefore needs to be excluded in order to fully attribute observed behavior to peripheral vestibular pathology. Evaluation of the OKR in addition to the VOR partly achieves this task. Normal OKR performance in epistatic circler and shaker animals indicates that the final oculomotor pathway and structures involved in OKR processing, like the vestibulo cerebellum and the vestibular nucleus, are intact. In shaker animals we also confirmed that the three-neuron arc, which directly relays activity from primary vestibular afferents to oculomotor neurons (Lorente de Nó, 1933), was intact by recording short latency eye movements following electrical stimulation of the vestibular afferents. In summary, the mini-coil technique provided a reliably method for recording eye movements in these mutant mice without which we would have been unable to determine peripheral vestibular pathology as the cause of complex behavioral phenotypes.

5.3 Plasticity in the oculomotor system

In chapter 4 three different forms of behavioral adaptation that occur in the oculomotor system are described. These forms of adaptation include adaptation of the OKR, adaptation of the VOR and recovery of the VOR following unilateral labyrinthectomy. These three forms of adaptation were investigated in Lurcher and L7-PKCi transgenic mice to assess how the cerebellum contributes to these forms of motor learning and, more specifically, whether learning was implemented through long-term depression (LTD) of the parallel fiber to Purkinje cell synapse. Findings from these experiments sketch a very diverse picture that requires a more extensive discussion than is achieved in the individual sections of chapter 4.

5.3.1 VOR adaptation

L7-PKCi transgenic mice selectively express a peptide inhibitor of protein kinase C (PKC) in cerebellar Purkinje neurons. PKC is required for the induction of long-term depression (LTD) of the parallel fiber to Purkinje cell synapse (Linden and Connor, 1991, 1993), which constitutes a candidate cellular mechanism for different forms of cerebellum dependent motor learning including VOR adaptation (Ito, 1986; Thompson et al., 1997; Ito, 2001). Inhibition of PKC in L7-PKCi transgenic animals prevented LTD from occurring (De Zeeuw et al., 1998; Goossens et al., 2001) and subjecting L7-PKCi transgenic animals to visuo-vestibular training protocols for 1 hour did not result in adaptation of VOR gain (De Zeeuw et al., 1998). The oculomotor deficit in L7-PKCi transgenic animals appeared to be confined to the process of VOR adaptation and did not involve normal performance of OKR, VOR or their interaction. The idea that development of adequate compensatory ocular reflexes was at least partly learned through experience rather than pre-programmed from birth (van Hof-Van Duin, 1976; Collewijn, 1977; Favilla et al., 1984) appeared to be at odds with the normal oculomotor behavior observed in L7-PKCi transgenic animals. De Zeeuw et al. (1998) hypothesized that LTD dependent learning might not be the only form of plasticity available to the animal, but reflect a relatively fast adaptive system that acted in concert with slower learning mechanisms. These remaining, slower learning mechanisms would allow L7-PKCi transgenic animals to obtain normal ocular reflexes. The results described in chapter 4 are in agreement with this hypothesis. L7-PKCi transgenic animals are able to adapt their VOR but did so at a slower rate than normal animals. However, remaining learning in L7-PKCi transgenic animals still appears to rely on an intact cerebellum, because Lurcher animals do not show this slow acting form of VOR adaptation. The brainstem hypothesis (see introduction) would nicely explain remaining learning in L7-PKCi transgenic animals in that the mechanism for VOR adaptation could involve plasticity in vestibular nucleus that is guided by cerebellar output (Miles and Lisberger, 1981; Lisberger et al., 1984). However, plasticity in the brainstem is not the only possible explanation. In recent years many synapses in the cerebellum have been shown to be modifiable and plasticity in the cerebellar cortex is by no means limited to LTD of the parallel fiber to Purkinje cell synapse (Hansel et al., 2001). It may very well be that neural network of both cerebellar cortex and vestibular nucleus provide the stage for plasticity on which LTD of the parallel fiber to Purkinje cell synapse plays a leading role but is not the sole actor.

Irrespective of what mechanism is responsible for motor learning in L7-PKCi transgenic animals it requires cerebellar output. The absolute requirement of cerebellar output for learning in the VOR presents us with a serious contradiction. If, as we reasoned before, a normal VOR is acquired through learning and if this learning requires cerebellar output, then how did Lurcher mice obtain a relatively normal VOR? One answer lies with the possibility that Lurcher animals are able to learn but that we were not able to detect it because visual slip in our training stimulus was too high to properly induce learning in these animals. Obviously, if optokinetic stimulus velocity were too fast for Lurcher animals to track, it was unlikely to induce learning of the VOR. Judging from the response during training, Lurcher animals were able to track the visual stimulus. They showed a clear depression in the amplitude of their eye movements during visuo-vestibular training as compared to the response to the vestibular stimulus alone and one

would therefore expect to see some reduction in VOR gain after training. We therefore think that adult Lurcher animals are truly unable to modify their VOR. How to reconcile absent learning with the relatively normal VOR performance in naïve Lurcher mice? One possible answer may lie with the fact that degeneration of Purkinje neurons in Lurcher mice is not instantaneous and roughly stretches across a period of several months after birth (Caddy and Biscoe, 1979). Lurcher mice may thus have achieved a relatively normal VOR in the period before all Purkinje neurons degenerated. In support of this idea, 3 month old Lurcher animals were able to improve their performance on a complex motor task like the rotorod test, while at the age of 9 months they had totally lost this ability to learn (Hilber and Caston, 2001). Interestingly, any learning in the VOR that may have occurred early in the animal's life must have been retained in extra-cerebellar circuits since the cerebellar cortex of adult Lurcher animals can no longer contribute to the VOR.

5.3.2 Vestibular compensation

The consequences of unilateral labyrinthectomy can be divided into two distinct sets of symptoms labeled static and dynamic symptoms (Smith and Curthoys, 1989). Static symptoms include ocular nystagmus, body rolling and static head deviations. A static imbalance in background activity between the vestibular nuclei on either side due to the deafferentation of one side underlies these symptoms. Recovery of static symptoms is largely brought about by rebalancing background activity between both vestibular nuclei (Precht and Dieringer, 1985; Precht, 1986; c.f. Ris et al., 1997).

Dynamic symptoms include a reduction in VOR gain and an asymmetric response of the VOR to ipsi and contra lateral rotation of the head. Unilateral labyrinthectomy in mice caused a reduction in VOR gain to approximately 20% of normal, which recovered in the course of 8 days to 60-70% of normal. Under the assumption that lesions to the canal would maintain linear behavior of the VOR, taking out 50% of the input should result to a 50% reduction of the output. The fact that eye movement responses recover to more than 50 % of the initial value implies that sensitivity of the oculomotor output to vestibular input has been scaled up. This situation is analogous to VOR adaptation and possible entails the same neuronal mechanism.

Like VOR adaptation recovery of dynamic symptoms relies on intact cerebellar function because lesions of the flocculus prevent its occurrence (Courjon et al., 1982). Our finding that VOR gain of Lurcher mice did not recover after unilateral labyrinthectomy is in agreement with the effect of floccular lesions. However, whether the cerebellum plays the same role in vestibular compensation as it does in VOR adaptation is questionable, since control and LTD deficient animals exhibited equal recovery of VOR gain following unilateral labyrinthectomy. The amount and rate of Vestibular compensation were, unlike VOR adaptation, not related to the presence of cerebellar LTD. The presence of vestibular compensation in LTD deficient mice implies that vestibular compensation is something different from VOR adaptation.

Alternatively, the identical time course of vestibular compensation in LTD deficient and normal animals may reflect the fact that unilateral labyrinthectomy is a much stronger 'training' stimulus than our visuo-vestibular training paradigm. In our visuo-vestibular training paradigm animals were trained for 1.5 hours every day, while

after unilateral labyrinthectomy animals are essentially trained during the entire light cycle of their day (12 hours). Since LTD deficient animals are clearly capable of learning during our visuo-vestibular training paradigm the stronger drive to change VOR gain following hemi-labyrinthectomy may obscure differences between control and L7-PKCi transgenic animals. Hence, the added advantage of having LTD in the recovery process might not have been revealed. However, this interpretation does not change the fact that for recovery from unilateral labyrinthectomy LTD is apparently not essential.

5.3.3 OKR adaptation

Any form of prolonged visual stimulation in the presence of sufficient retinal slip is capable of eliciting OKR adaptation in afoveate species that have an OKR gain smaller than unity (Collewijn and Grootendorst, 1979; Schairer and Bennett, 1986; Marsh and Baker, 1997). Earlier studies investigated the role of LTD in adaptation of the OKR by studying knock out mice that either lacked the gene encoding neuronal NOS (Shutoh et al., 2002) or the gene coding for mGluR1 (Katoh et al., 2000). Both types of mice had previously been shown to lack LTD of the parallel fiber to Purkinje cell synapse in cerebellar slices (Aiba et al., 1994; Lev-Ram et al., 1997) and the ability for OKR adaptation was thus linked to the presence of cerebellar LTD. However, these studies involved global knockouts and therefore lacked the cellular specificity needed to fully attribute the observed deficit in OKR adaptation to LTD of the parallel fiber to Purkinje cell synapse. Such specificity is achieved in the L7-PKCi transgenic mouse and these animals proved equally able as control animals to adapt their OKR. Normal OKR adaptation in these L7-PKCi mice therefore rules out LTD of the parallel fiber to Purkinje cell synapse as the cellular substrate underlying this form of oculomotor plasticity.

Changes in gain of the OKR in control and L7-PKCi transgenic animals were limited to higher stimulus frequencies. All visuo-vestibular training occurred at 0.6 Hz while changes in OKR gain were relatively largest at 1 Hz, while no changes occurred at 0.1 Hz. In fact OKR adaptation did not seem to be related to any feature of the training stimulus, since 'out of phase' visuo-vestibular training, 'in phase' visuo-vestibular training and labyrinthectomy all resulted in increases in OKR gain at higher stimulus frequencies. Due to the experimental set up, in which amplitude of the stimulus was kept constant, higher stimulus frequencies coincided with higher peak stimulus velocities. Since the optokinetic system is known to be dependent on stimulus velocity (Collewijn, 1969; Maioli and Precht, 1984; Hess et al., 1985), adaptation of OKR gain at higher peak velocities could reflect a change in velocity sensitivity of the OKR. In chapter 2 we show that closed loop OKR gain in the mouse starts to fall off at peak stimulus velocities higher than 8 °/sec, an increase in this cut-off point after training would account for the observed increase in OKR gain. However, the velocity dependence of OKR gain is thought to be largely due to velocity sensitivity at its input stage (Oyster et al., 1972). It is unlikely that OKR adaptation induces changes at such an early stage of oculomotor processing. Besides, lack of OKR adaptation in Lurcher mice shows that the cerebellum mediates adaptation of the OKR.

Based on the OKR of untrained Lurcher animals we hypothesized that the flocculus would constitute the main pathway to mediate the OKR in mice. Lack of this floccular pathway in Lurcher mice caused a drastic reduction of OKR gain and made the

OKR more sensitive to velocity content of the stimulus. We explained this finding by assuming that absence of cerebellar function reflected a reduction in the open loop gain of the OKR, which would render the effect of velocity saturation at the input more pronounced. Reasoning the other way around, one could argue that increasing this central gain element in the flocculus would make the reflex less sensitive to stimulus velocity and would increase OKR gain at higher peak stimulus velocities, which in our paradigm coincide with higher stimulus frequency. However, such a mechanism is inconsistent with the lack of increased OKR gain at low stimulus frequency, which remains unchanged after visuo-vestibular adaptation.

Unfortunately, the current experimental setup predominantly addressed changes in VOR and to more clearly discriminate between frequency and velocity selective changes in the OKR, we need to test OKR performance after training across a wider range of stimuli.

In summary, we can conclude that adaptation of the VOR, adaptation of the OKR and recovery of VOR gain following unilateral labyrinthectomy all rely on intact cerebellar function. It is unlikely that cerebellar contribution to these forms of behavioral adaptation solely involves storage of the altered behavioral responses by means of long-term depression of selected parallel fibers to the Purkinje cell. LTD proved not to be essential for either OKR adaptation or recovery of VOR gain following unilateral labyrinthectomy. LTD was found to be important for adaptation of the vestibulo-ocular reflex to modified visual slip, but lack of cerebellar LTD appeared merely to retard acquisition of the modified response. Adaptation of compensatory ocular reflexes therefore seems to be mediated by a network of neurons located in both cerebellum and vestibular nucleus that utilizes cerebellar LTD as one of multiple mechanisms to recalibrate its output.

References

- Aiba A, Kano M, Chen C, Stanton ME, Fox GD, Herrup K, Zwingman TA, Tonegawa S (1994) Deficient cerebellar long-term depression and impaired motor learning in mGluR1 mutant mice. *Cell* 79:377-388.
- Caddy KW, Biscoe TJ (1979) Structural and quantitative studies on the normal C3H and Lurcher mutant mouse. *Philos Trans R Soc Lond B Biol Sci* 287:167-201.
- Collewijn H (1969) Optokinetic eye movements in the rabbit: input-output relations. *Vision Res* 9:117-132.
- Collewijn H (1977) Optokinetic and vestibulo-ocular reflexes in dark-reared rabbits. *Exp Brain Res* 27:287-300.
- Collewijn H, Grootendorst AF (1979) Adaptation of optokinetic and vestibulo-ocular reflexes to modified visual input in the rabbit. *Prog Brain Res* 50:771-781.
- Courjon JH, Flandrin JM, Jeannerod M, Schmid R (1982) The role of the flocculus in vestibular compensation after hemilabyrinthectomy. *Brain Res* 239:251-257.
- De Zeeuw CI, Hansel C, Bian F, Koekkoek SK, van Alphen AM, Linden DJ, Oberdick J (1998) Expression of a protein kinase C inhibitor in Purkinje cells blocks cerebellar LTD and adaptation of the vestibulo-ocular reflex. *Neuron* 20:495-508.

- Favilla M, Ghelarducci B, La Noce A (1984) Development of vertical vestibulo-ocular reflex characteristics in intact and flocculectomized rabbits visually deprived from birth. *Behav Brain Res* 13:209-216.
- Gibson F, Walsh J, Mburu P, Varela A, Brown KA, Antonio M, Beisel KW, Steel KP, Brown SD (1995) A type VII myosin encoded by the mouse deafness gene shaker-1. *Nature* 374:62-64.
- Goossens J, Daniel H, Rancillac A, van der Steen J, Oberdick J, Crépel F, De Zeeuw CI, Frens MA (2001) Expression of protein kinase C inhibitor blocks cerebellar long-term depression without affecting Purkinje cell excitability in alert mice. *J Neurosci* 21:5813-5823.
- Hansel C, Linden DJ, D'Angelo E (2001) Beyond parallel fiber LTD: the diversity of synaptic and non-synaptic plasticity in the cerebellum. *Nat Neurosci* 4:467-475.
- Hasson T, Walsh J, Cable J, Mooseker MS, Brown SD, Steel KP (1997) Effects of shaker-1 mutations on myosin-VIIa protein and mRNA expression. *Cell Motil Cytoskeleton* 37:127-138.
- Hess BJ, Precht W, Reber A, Cazin L (1985) Horizontal optokinetic ocular nystagmus in the pigmented rat. *Neuroscience* 15:97-107.
- Hilber P, Caston J (2001) Motor skills and motor learning in Lurcher mutant mice during aging. *Neuroscience* 102:615-623.
- Ito M (1986) Long-term depression as a memory process in the cerebellum. *Neurosci Res* 3:531-539.
- Ito M (2001) Cerebellar long-term depression: characterization, signal transduction, and functional roles. *Physiol Rev* 81:1143-1195.
- Iwashita M, Kanai R, Funabiki K, Matsuda K, Hirano T (2001) Dynamic properties, interactions and adaptive modifications of vestibulo-ocular reflex and optokinetic response in mice. *Neurosci Res* 39:299-311.
- Katoh A, Kitazawa H, Itohara S, Nagao S (1998) Dynamic characteristics and adaptability of mouse vestibulo-ocular and optokinetic response eye movements and the role of the flocculo-olivary system revealed by chemical lesions. *Proc Natl Acad Sci U S A* 95:7705-7710.
- Katoh A, Kitazawa H, Itohara S, Nagao S (2000) Inhibition of nitric oxide synthesis and gene knockout of neuronal nitric oxide synthase impaired adaptation of mouse optokinetic response eye movements. *Learn Mem* 7:220-226.
- Kitazawa H, Katoh A, Yagi T, Nagao S (2000) Dynamic characteristics and adaptability of reflex eye movements of Fyn- kinase-deficient mice. *Neurosci Lett* 280:179-182.
- Lev-Ram V, Nebyelul Z, Ellisman MH, Huang PL, Tsien RY (1997) Absence of cerebellar long-term depression in mice lacking neuronal nitric oxide synthase. *Learn Mem* 4:169-177.
- Linden DJ, Connor JA (1991) Participation of postsynaptic PKC in cerebellar long-term depression in culture. *Science* 254:1656-1659.
- Linden DJ, Connor JA (1993) Cellular mechanisms of long-term depression in the cerebellum. *Curr Opin Neurobiol* 3:401-406.
- Lisberger SG, Miles FA, Zee DS (1984) Signals used to compute errors in monkey vestibuloocular reflex: possible role of flocculus. *J Neurophysiol* 52:1140-1153.
- Lorente de Nó R (1933) Vestibulo-ocular reflex arc. *Arch Neurol Psychiat* 30:245-291.

- Maioli C, Precht W (1984) The horizontal optokinetic nystagmus in the cat. *Exp Brain Res* 55:494-506.
- Marsh E, Baker R (1997) Normal and adapted visuoculomotor reflexes in goldfish. *J Neurophysiol* 77:1099-1118.
- Miles FA, Lisberger SG (1981) Plasticity in the vestibulo-ocular reflex: a new hypothesis. *Annu Rev Neurosci* 4:273-299.
- Oyster CW, Takahashi E, Collewijn H (1972) Direction-selective retinal ganglion cells and control of optokinetic nystagmus in the rabbit. *Vision Res* 12:183-193.
- Precht W (1986) Recovery of some vestibuloocular and vestibulospinal functions following unilateral labyrinthectomy. *Prog Brain Res* 64:381-389.
- Precht W, Dieringer N (1985) Neuronal events paralleling functional recovery (compensation) following peripheral vestibular lesions. *Rev Oculomot Res* 1:251-268.
- Ris L, Capron B, de Waele C, Vidal PP, Godaux E (1997) Dissociations between behavioural recovery and restoration of vestibular activity in the unilabyrinthectomized guinea-pig. *J Physiol (Lond)* 500:509-522.
- Schäfer JO, Bennett MV (1986) Changes in gain of the vestibulo-ocular reflex induced by sinusoidal visual stimulation in goldfish. *Brain Res* 373:177-181.
- Shutoh F, Katoh A, Kitazawa H, Aiba A, Itoharu S, Nagao S (2002) Loss of adaptability of horizontal optokinetic response eye movements in mGluR1 knockout mice. *Neurosci Res* 42:141-145.
- Smith PF, Curthoys IS (1989) Mechanisms of recovery following unilateral labyrinthectomy: a review. *Brain Res Brain Res Rev* 14:155-180.
- Stahl JS (2002) Calcium Channelopathy Mutants and Their Role in Ocular Motor Research. *Ann N Y Acad Sci* 956:64-74.
- Stahl JS, van Alphen AM, De Zeeuw CI (2000) A comparison of video and magnetic search coil recordings of mouse eye movements [In Process Citation]. *J Neurosci Methods* 99:101-110.
- Thompson RF, Bao S, Chen L, Cipriano BD, Grethe JS, Kim JJ, Thompson JK, Tracy JA, Weninger MS, Krupa DJ (1997) Associative learning. *Int Rev Neurobiol* 41:151-189.
- van Hof-Van Duin J (1976) Development of visuomotor behavior in normal and dark-reared cats. *Brain Res* 104:233-241.

SUMMARY

The generation of compensatory eye movements is a relatively well-understood form of motor behavior. The behavior is based on two kinds of reflexes that derive their input either from the retina, the optokinetic reflex (OKR), or from the labyrinth, vestibulo-ocular reflex (VOR). The relative ease with which input and output of these reflexes can be measured makes the system amenable to rigorous quantitative analysis. The oculomotor system can therefore serve as a model system to evaluate the effect of genetic interventions at a behavioral level. However, since genetic techniques are largely limited to one species, the mouse, this avenue of research requires a reliable method for recording eye movements in these animals. The present work presents such a technique, which comprises a modified scleral search coil technique. In addition to the search coil technique, a method for recording mouse eye movements using video-oculography is also described. The remainder of this thesis illustrates the use of the coil technique in the analysis of 4 types of mutant mice: epistatic circler mouse, Shaker mouse, Lurcher mouse and L7-PKCi transgenic mouse.

Epistatic circler mice and Shaker mice both showed morphological aberrations in their labyrinths and we recorded compensatory eye movements of these mutants to assess the extent to which this structure was functional. Adult Lurcher animals effectively have no cerebellar cortex and comparative analysis of compensatory eye movements in this mutant strain could elucidate cerebellar contribution to generation of these movements. L7-PKCi transgenic animals were genetically modified to include an inhibitory peptide for the enzyme PKC into their genome. The inhibitory peptide was selectively expressed in cerebellar Purkinje neurons and PKC was therefore specifically blocked in these neurons. The function of PKC in cerebellar Purkinje cells has been related to the ability for motor learning and L7-PKCi transgenic animals therefore provided a model to verify involvement of PKC in this process.

Motor learning takes place in the oculomotor system, allowing compensatory eye movements to be modified based on experience. A well-known example of oculomotor learning is adaptation of the VOR, which can be achieved by placing optical devices in front of the eyes. For instance, someone wearing miniaturizing lenses would experience a reduction of visual field movement associated with movement of the head. After sufficient exposure to such a conflicting condition, vision will reduce gain of the underlying VOR. It is often assumed that learning and memory in the brain are mediated by changes in synaptic coupling of individual neurons. This is also the case in the oculomotor field where a long-standing hypothesis related adaptation of the VOR to a form of associative synaptic plasticity, called long-term depression (LTD). LTD was observed in Purkinje neurons of the cerebellum and served to reduce synaptic efficacy of selective parallel fiber inputs to the Purkinje neuron when these fibers were coactive with the climbing fiber to the same neuron. Development of L7-PKCi transgenic mice allowed us to investigate the validity of this hypothesis in an almost direct way, since the genome of L7-PKCi was genetically altered to include a peptide that disrupted LTD in Purkinje neurons. Subsequent analysis of the ability to adapt VOR gain revealed that even without LTD, transgenic animals could still learn. Learning was clearly retarded but certainly not absent. Other forms of oculomotor adaptation, which because of their absence in Lurcher mice were shown to rely on cerebellar function, were unaffected in LTD deficient animals. The analysis of mutant mice thus revealed that LTD

certainly plays a part in oculomotor plasticity but it is by no means the universal mechanism to adjust all parameters of compensatory ocular reflexes. Quite possibly plasticity in the oculomotor system is distributed over multiple locations in its neural control network and involves multiple forms of cellular plasticity.

SAMENVATTING

Dit proefschrift handelt over de oogbewegingen van muizen. De reden om juist in deze dieren de oogbewegingen te bestuderen is tweeledig. Ten eerste bestaan er veel muizenrassen waarin mutaties zijn opgetreden die neurologische afwijkingen bij deze dieren tot gevolg hebben. Sommige van deze mutaties zijn analoog aan erfelijke afwijkingen die bij mensen gevonden worden en deze dieren kunnen als model dienen om het menselijke syndroom beter te leren begrijpen. Ten tweede zijn muizen bij uitstek geschikt zijn om geselecteerde genen te manipuleren, ondermeer omdat ze zich relatief snel voortplanten. Het effect van de genetische manipulatie op het gedrag van de muis kan ons inzicht verschaffen in de mogelijke rol die een gen speelt in de normale muis. De vraag blijft dan bestaan waarom we geïnteresseerd zouden zijn in specifiek de oogbewegingen. Oogbewegingen vertegenwoordigen een relatief simpele en goed kwantificeerbare vorm van motoriek. Het betreft de beweging in één gewricht, namelijk dat van de oogbol in zijn kas, en bovendien is de kracht die geleverd moet worden om een oogbeweging te maken niet afhankelijk van externe invloeden. Waar het voor de sturing van een arm nog al wat uitmaakt of je een blaadje papier of een bureaustoel optilt, is de sturing van het oog alleen afhankelijk van de mechanische eigenschappen van het oog en het omliggende weefsel. Daarnaast zijn niet alleen de oogbewegingen zelf maar ook de stimuli die deze bewegingen opwekken relatief makkelijk te kwantificeren en te controleren. De relatie tussen stimulus-input en oogbeweging-output kan hierdoor nauwkeurig bestudeerd worden. Deze relatieve eenvoud heeft het oculomotor systeem onderwerp gemaakt van veel studie en er is derhalve veel bekend over hoe het brein oogbewegingen controleert. Doordat we al zoveel weten over de sturing van oogbewegingen, is het mogelijk om aan de hand van de veranderde bewegingen bij mutante muizen een idee te krijgen hoe neurologische processen, die aan de sturing ten grondslag liggen, zijn veranderd. Bij manipulatie of mutatie van een enkel gen kan de verandering in oogmotoriek een indicatie geven over hoe het eiwit, waarvoor dat gemuteerde gen codeert, bijdraagt aan de signaalverwerking in het brein. Door oogbewegingen te bestuderen in geselecteerde mutante en genetisch gemanipuleerde muizen hopen we dus op moleculair niveau inzicht te verwerven in informatieverwerking door het brein.

We bewegen continu onze ogen om ze te richten naar dingen in onze omgeving die om de een of andere reden de aandacht verdienen. Wanneer we de omgeving in ons opnemen, kijken we van object naar object met snelle verspringende oogbewegingen die we saccades noemen. Mochten we tijdens het rondkijken geïnteresseerd raken in een object dat beweegt, zoals een meeuw die aan ons raam voorbij vliegt, dan kunnen we met een gladde volgbeweging die meeuw volgen in zijn vlucht. Door het maken van een gladde volgbeweging zorgen we ervoor dat de projectie van de meeuw niet over ons netvlies beweegt. Beweging van het geprojecteerde beeld over het netvlies zou het beeld onscherp maken. Beweging van het visuele beeld treedt ook op wanneer het hoofd bewogen wordt. Deze situatie komt continu voor doordat we ons ten opzichte van de omgeving bewegen en zou, net als een foto die werd genomen met een bewegende camera, het beeld van de gehele omgeving onscherp maken. De oogbewegingen die gemaakt worden om te compenseren voor de bewegingen van het hoofd zijn van een

andere origine dan de gladde oogbeweging die we gebruiken om de meeuw te volgen. Het verschil tussen de compensatoire oogbeweging en de gladde oogbeweging zit hem vooral in de stimulus die de oogbeweging opwekt. In het geval van de gladde oogbeweging bestaat de stimulus uit één object dat beweegt ten opzichte van een stationaire achtergrond, bijvoorbeeld een meeuw die voor een gebouw langs vliegt, terwijl de compensatoire oogbeweging wordt uitgelokt door beweging van het hele visuele veld, zoals dat optreedt bij het bewegen van de camera tijdens het nemen van een foto. In het geval dat de oogbeweging wordt opgewekt door beweging van het hele visuele veld spreken we van een optokinetische reflex (OKR). De optokinetische reflex is niet de enige reflex die compenseert voor beweging van het hoofd. De beweging van het hoofd wordt namelijk gedetecteerd door het evenwichtsorgaan en op basis van die informatie worden ook oogbewegingen gemaakt. Oogbewegingen die gegenereerd worden door informatie uit het evenwichtsorgaan behoren tot de vestibulo-oculaire reflex (VOR). De twee compensatoire reflexen, OKR en VOR, werken samen om te voorkomen dat bewegingen van het hoofd de projectie van de visuele wereld onscherp zouden maken. Bij praktisch alle gewervelde dieren kunnen de optokinetische en vestibulo-oculaire reflexen opgewekt worden. De OKR wordt opgewekt door een proefdier voor een scherm te zetten waarop een bewegend patroon te zien is. De VOR kan worden opgewekt door het proefdier rond te draaien in het donker zodat visuele informatie niet gebruikt kan worden en alleen op basis van vestibulaire informatie oogbewegingen kunnen worden gemaakt.

In de afgelopen eeuw is men, mede dankzij proefdiermodellen, veel te weten gekomen over de controle van oogbewegingen. Een belangrijke bevinding is geweest dat de oculaire reflexen, met name de vestibulo-oculaire reflex, niet statisch zijn maar continu gekalibreerd worden om maar optimaal te compenseren voor bewegingsartefacten van het hoofd. Dit proces van continu afstemmen van de oogbeweging is belangrijk, omdat door het opeenstapelen van kleine beschadigingen gedurende ons leven de compensatoire reflexen uiteindelijk ontregeld zouden raken. Dat deze kalibratie plaatsvindt, kan onder experimentele omstandigheden worden aangetoond door aan een proefpersoon of proefdier gedissocieerde visuele en vestibulaire stimuli aan te bieden. Dissociatie van vestibulaire en visuele informatie ontstaat bijvoorbeeld wanneer een proefpersoon wordt uitgerust met een bril waarvan de lenzen links en rechts verwisselen. Met een dergelijke bril op verplaatst het visuele beeld zich niet meer naar rechts maar naar links, wanneer een hoofdbeweging naar links wordt gemaakt. Deze onnatuurlijke situatie resulteert na verloop van tijd in het omkeren van de onderliggende VOR. De proefpersoon heeft dan geleerd om de informatie uit het evenwichtsorgaan, welke onveranderd blijft, te gebruiken om de ogen naar links in plaats van rechts te bewegen, bij een naar links draaiende hoofd beweging. Deze vorm van leren is geen bewuste keuze van de proefpersoon, maar een onbewuste aanpassing van de vestibulo-oculaire reflex en wordt VOR-adaptatie genoemd. De kleine hersenen spelen een essentiële rol bij VOR-adaptatie. Het neuronale mechanisme dat aan VOR-adaptatie ten grondslag ligt, vormt waarschijnlijk ook de basis voor het leren aanpassen van andere bewegingen en reflexen. Deze vormen van leren worden gezamenlijk wel 'motorisch leren' genoemd.

Hoe het brein in staat is om te leren, vormt een van de meest interessante onderwerpen binnen het gebied van de neurowetenschappen. De meeste wetenschappers

zijn het er over eens dat informatie in het brein voor een belangrijk deel wordt opgeslagen in de verbindingen tussen neuronen, de zogenaamde synapsen. De biochemische processen die overdracht van informatie over de synaps kunnen veranderen, worden samen gevat onder de noemer 'synaptische plasticiteit'. In het cerebellum is een hele duidelijke vorm van synaptische plasticiteit gevonden, genaamd 'long term depression' (LTD). LTD is een associatieve vorm van synaptische plasticiteit die plaatsvindt in de Purkinje neuronen van het cerebellum. Elk Purkinje neuron krijgt informatie van, en heeft dus synapsen met, ongeveer 100.000 granulaire neuronen. Naast de synapsen met granulaire neuronen maakt het Purkinje neuron ook nog contact met één enkel neuron uit de nucleus oliva inferior, welke in de hersenstam gelegen is. De term LTD doelt op het proces waarbij het Purkinje neuron de effectiviteit van synapsen met specifieke granulaire neuronen verlaagt op geleide van de activiteit die het ontvangt uit de oliva inferior. De meest gangbare hypothese zegt, in gereduceerde vorm, dat het oliva neuron een foutmelding geeft aan het Purkinje neuron en dat alle granulaire cellen die op dat moment actief waren bijdragen aan de 'foute' beweging. Onderdrukking van de foute informatie door het Purkinje neuron zou dus op termijn moeten leiden tot een verbetering van de beweging. LTD is aangetoond in vitro door gelijktijdig de olivaire en granulaire vezels naar het Purkinje neuronen elektrisch te stimuleren. In de afgelopen 15 jaar is de biochemische cascade die ten grondslag ligt aan LTD in Purkinje neuronen in verregaande mate opgehelderd. Het definitieve bewijs dat deze vorm van synaptische plasticiteit in vivo ook daadwerkelijk nodig is voor motorisch leren is echter nog niet afdoende geleverd en vormt een belangrijk doel van dit proefschrift.

Om de oogbewegingen van mutante en genetisch gemanipuleerde muizen te meten, is een betrouwbare techniek vereist. Na de inleiding, worden in het tweede hoofdstuk van dit proefschrift twee technieken beschreven om oogbewegingen te meten bij muizen: de 'scleral search coil' techniek en video-oculografie. De scleral search coil techniek bestaat uit het plaatsen van een spoeltje, dat gewonden is van koperdraad, op het oog van de muis. De muis wordt vervolgens in een magnetisch veld geplaatst zodat elke beweging van het oog een inductie-spanning veroorzaakt, die aan de twee polen van het spoeltje gemeten kan worden. De grootte van de inductie-spanning is evenredig aan de gemaakte oogbeweging en geeft, mits juist gekalibreerd, het aantal graden rotatie van het oog weer. Bij video oculografie wordt het oog gevolgd met een video camera en wordt de verplaatsing van de pupil op het beeld gemeten en omgerekend naar graden rotatie. De voor- en nadelen van beide technieken worden beschreven in dit hoofdstuk.

In hoofdstuk drie wordt de toepassing van de 'scleral search coil' techniek beschreven in 'epistatic circler' muizen en 'Shaker' muizen. Beide soorten muizen hebben anatomische defecten in hun evenwichtsorgaan. Het meten van oogbewegingen in deze muizen toont aan dat deze anatomische defecten ook de functie van het evenwichtsorgaan verstoren. Door zowel de OKR als VOR te testen, is duidelijk geworden dat het defect in de oogbewegingen waarschijnlijk niet gelegen is in het brein maar primair het gevolg is van het defecte evenwichtsorgaan. De Shaker muis is met name interessant daar deze muis een mutatie heeft in hetzelfde gen als waar een mutatie voorkomt bij een erfelijke menselijke aandoening, genaamd Usher syndrome type 1B. Met behulp van dit muismodel is aannemelijk gemaakt dat de vestibulaire component van het menselijke syndroom in de eerste plaats perifeer van origine is.

Hoofdstuk vier beschrijft in hoeverre VOR-adaptatie afhankelijk is van cerebellaire LTD. Het is het belangrijkste hoofdstuk in dit proefschrift omdat het inzicht verschaft in de validiteit van een bestaande theorie over VOR-adaptatie. In het hoofdstuk worden drie typen muizen gebruikt: Lurcher muizen, L7-PKCi muizen en controle muizen. Lurcher muizen hebben geen cerebellaire Purkinje neuronen en als gevolg daarvan is de functie van het cerebellum helemaal afwezig. Deze natuurlijk voorkomende mutante muis staat model voor het effect van een totale cerebellaire laesie. Het voordeel dat deze muis heeft boven het maken van een chirurgische laesie, is dat in de mutante muis de laesie exact reproduceerbaar is van dier tot dier. De L7-PKCi transgene muis is een genetisch gemodificeerde muis waarbij één enkel enzym, dat voor LTD belangrijk is, specifiek in Purkinje neuronen geremd wordt. Hierdoor is de mogelijkheid om informatie op te slaan in deze neuronen theoretisch geblokkeerd. De L7-PKCi muis maakt een eiwit aan dat de functie van het enzym proteïne kinase C (PKC) inhibeert. Uit de experimenten met Lurcher muizen blijkt dat het cerebellum een cruciale rol speelt bij VOR adaptatie. De rol van LTD is hierbij echter niet zo essentieel als op basis van de eerder beschreven theorie verwacht zou worden. De aanwezigheid van cerebellaire LTD versnelt het proces van VOR-adaptatie. De L7-PKCi muizen, die geen cerebellaire LTD hebben, zijn zeker wel in staat om hun VOR aan te passen. Zij kunnen dit alleen niet zo goed als controle dieren. De grootte van de aanpassing is kleiner en het duurt langer om die te bereiken dan in controle dieren. De resultaten geven aan dat LTD in de Purkinje neuronen wel bijdraagt aan VOR-adaptatie en dat LTD het dier in staat stelt om snel aanpassingen te maken in zijn motoriek. Zonder LTD is de rest van het neurale systeem echter nog steeds in staat om zich aan te passen, zei het op een langere tijdschaal.

Dit proefschrift illustreert hoe de analyse van het oculomotor systeem gebruikt kan worden om de veranderingen in neurale informatieverwerking als gevolg van genetische manipulatie of natuurlijke mutatie aan te tonen op systeem fysiologisch niveau. De beschreven techniek om oogbewegingen te meten bij muizen kan een waardevolle bijdrage leveren aan de multidisciplinaire analyse die nodig is om de functie van genen op te helderen.

LIST OF PUBLICATIONS

- De Zeeuw CI, Ruigrok TJH, Hawkins R, van Alphen AM (1997) Climbing fiber collaterals contact neurons in the cerebellar nuclei that provide a GABAergic feedback to the inferior olive. *Neuroscience* 80(4):981-6.
- Koekkoek SK, v. Alphen AM, v.d. Burg J, Grosveld F, Galjart N, De Zeeuw CI (1997) Gain adaptation and phase dynamics of compensatory eye movements in mice. *Genes. Funct.* 1:175-190.
- De Zeeuw CI, van Alphen AM, Koekkoek SK, Buharin E, Coesmans MP, Morpurgo MM, van den Burg J (1998) Recording eye movements in mice: a new approach to investigate the molecular basis of cerebellar control of motor learning and motor timing. *Otolaryngol. Head. Neck. Surg.* 119:193-203.
- De Zeeuw CI, Hansel C, Bian F, Koekkoek SK, van Alphen AM, Linden DJ, Oberdick J (1998b) Expression of a protein kinase C inhibitor in Purkinje cells blocks cerebellar LTD and adaptation of the vestibulo-ocular reflex. *Neuron* 20:495-508.
- Stahl JS, van Alphen AM, De Zeeuw CI (2000) A comparison of video and magnetic search coil recordings of mouse eye movements. *J. Neurosci. Methods* 99:101-110.
- Sun JC, van Alphen AM, Bohne BA, De Zeeuw CI (2001) Shaker-1 mice show an optokinetic reflex but no vestibulo-ocular reflex. *Ann. N. Y. Acad. Sci.* 942:492.
- Sun JC[#], van Alphen AM[#], Wagenaar M, Huygen P, Hoogenraad CC, Hasson T, Koekkoek SK, Bohne BA, De Zeeuw CI (2001) Origin of vestibular dysfunction in Usher syndrome type 1B. *Neurobiol. Dis.* 8:69-77.
- Sun JC, van Alphen AM, Wagenaar M, Huygen P, Hoogenraad CC, Hasson T, Koekkoek SK, Bohne BA, De Zeeuw CI (2001) Hereditary familial vestibular degenerative diseases. *Ann. N. Y. Acad. Sci.* 942:493-496.
- van Alphen AM, Stahl JS, De Zeeuw CI (2001) The dynamic characteristics of the mouse horizontal vestibulo-ocular and optokinetic response. *Brain. Res.* 890:296-305.
- Cryns K, Van Spaendonck MP, Flothmann K, van Alphen AM, Van De Heyning PH, Timmermans JP, De Zeeuw CI, Van Camp G (2002) Vestibular dysfunction in the epistatic circler mouse is caused by phenotypic interaction of one recessive gene and three modifier genes. *Genome Res.* 12:613-617.
- Hoogenraad CC, Dortland BR, Koekkoek SKE, Akhmanova A, van Alphen AM, Kistler WM, Jaegle M, Koutsourakis M, van der Linden A, van Camp N, Krugers H, Grosveld F, De Zeeuw CI, and Galjart N. (2002) CYLN2 gene targeting links CLIP-115 haploinsufficiency to neurodevelopmental features of Williams Syndrome. *Nat. Genet.* (in press).
- van Alphen AM, De Zeeuw CI (2002) Cerebellar LTD facilitates but is not essential for LONG-TERM adaptation of the vestibulo-ocular reflex. *Eur. J. Neurosci.* (*in press*).
- van Alphen AM, Schepers T, De Zeeuw CI (2002) Motor performance and motor learning in Lurcher mice. *Ann. N. Y. Acad. Sci.* (*in press*).
- C.I. De Zeeuw, A.M. van Alphen, J. van der Steen, M.A. Frens, J. Sun, S.K.E. Koekkoek, J. Goossens, D. Jaarsma, M.P.H. Coesmans, A.L. Mathoera and N. Galjart. (2002) Gain and phase control of compensatory eye movements by the vestibulo-

cerebellar system. In: Handbook of Auditory Research (S. Highstein Ed.). (*In Press*).

Goossens HHLM, van Alphen AM, van der Steen J, Oberdick J, De Zeeuw CI, and M.A. Frens Purkinje Cells in the Flocculus of Mice Lacking Cerebellar LTD Exhibit Normal Responses in the Optokinetic Reflex (*to be submitted*).

Coemans M, Sillevs Smitt P, Linden DJ, Shigemoto R, Hirano Y T, van Alphen AM, Luo C, Frens MA, and De Zeeuw CI. Mechanisms underlying deficits in cerebellar motor coordination due to auto-antibodies against mGluR1 (*to be submitted*).

These authors contributed equally to the paper

CURRICULUM VITAE

The author of this work was born in Delft on 26 September 1974. After elementary school he attended gymnasium β at the Theresia Lyceum in Tilburg, from which he graduated cum laude in 1992. In September 1992 he started his medical studies at the Erasmus University in Rotterdam. After four years of studying at the Erasmus University a research project at the department of anatomy kindled his interest for neuroscience. For the duration of a year (1-1-1996/1-1-1997) he labored in the department of anatomy to develop a method for recording eye movements in mice. After one year his supervisor, Prof. Dr. De Zeeuw, introduced him to Prof. Dr. Simpson from New York University. As part of an ongoing collaboration between Prof. Dr. De Zeeuw and Prof. Dr. Simpson, the author spent half a year in the lab of Prof. Dr. Simpson to investigate the firing properties of putative Golgi cells located in the depths of the rabbit flocculus. In September 1997 he returned to Rotterdam to receive his 'Geneeskunde doctoraal diploma' from the Erasmus University. The author suspended his medical training and accepted a PhD. position at the department of anatomy, which was at that time headed by Prof. Dr. Voogd. The anatomy department later merged with the dept of physiology to become the department of neuroscience and the author continued his investigations of the mouse oculomotor system, under the inspiring leadership of Prof. Dr. De Zeeuw. On July 1st 2002 he completed his research project and returned to his medical studies at the Erasmus University.

DANKWOORD

Het is een uurtje of tien 's avonds. Er is voldoende Leffe in huis en er is geen Star Trek op tv. Alle ingrediënten lijken aanwezig om een fatsoenlijk dankwoord te schrijven.

Als eerste gaat mijn dank natuurlijk uit naar Chris die deze promotie mogelijk gemaakt heeft. Chris heeft door het verschaffen van een prima infrastructuur en door de vele connecties met andere laboratoria een ideale omgeving gecreëerd waarbinnen het voor mij mogelijk werd om goed onderzoek te verrichten. Bovendien is zijn ongekeerde gedrevenheid een inspiratie geweest die mijn productiviteit zeker ten goede is gekomen. Naast zijn wetenschappelijke rol waardeer ik ook het feit dat hij altijd open stond om onderwerpen van een meer persoonlijke aard te bespreken. Ik vind dat die combinatie van wetenschappelijke en persoonlijke interesse hem sieren en tot een uitstekende mentor maken.

The second person who deserves my gratitude is Jerry. I immensely enjoyed the dinners and scientific discussions I had with him. One of the first things that spring to mind when thinking of Jerry is his Blue ruler. This blue ruler is not just a device with which to measure the thickness of ones steak but has become a symbol of accuracy and humor. Jerry possesses both qualities in abundance and I believe some of it has rubbed off on me and made me a better scientist. Jerry's almost encyclopedic knowledge on the oculomotor system has been a great source of information, which has helped me to understand the field.

John Stahl deserves special thanks for his critical reviews of my manuscripts and for showing me that good data is only acquired through hard work. It's unfortunate that the time he reserved for research always seemed to include the evenings and nights, which made our collaborations exhausting but extremely productive events.

Natuurlijk wil ik de mede grondlegger van het muizen oogbewegingen lab, Bas, bedanken. Ik denk dat we door discussie van problemen met de data analyse en programmeren altijd veel aan elkaar gehad hebben. Bovendien was het mij waarschijnlijk niet gelukt een Duke-Nukem netwerk game voor 6 personen op te zetten. Naast de wetenschappelijke samenwerking waren uiteraard de kip/kerrie maaltijden aan de Zaagmolenkade en de vele avonden in Pardoën memorabel. Het wordt ook voor jou eens tijd je resultaten op te tekenen. Eén van de regels voor het promoveren zegt namelijk dat je alleen artikelen kunt gebruiken die uitgekomen zijn vijf jaar voor je promotiedatum. Dus, zoals een collega ooit heeft gezegd: "Papertjes bij elkaar, nietje erdoor en promoveren." (Ik ben er inmiddels wel achter dat dat dus volslagen onzin is; Kasper bedankt)

Michiel mede bedankt voor de avonden in Pardoën en natuurlijk de mGluR1 paper. Je moet de zaak maar snel afronden en beginnen met de PKV. Deze is, even als de applicatie tamelijk hilarisch.

Edith zo ontzettend bedankt voor de tucjes, soep, dropjes, spekjes, gepofte rijst, chocolade truffels, chocolade koekjes, 'American cookies', pinda's, scherpe nooten mix, borrelnoten, worst, knoflook soepbroodjes, tosti's en natuurlijk de Douwe Egberts (!) oploskoffie (Joan ook bedankt hè). Zonder jouw goede zorgen had de dagelijkse 16:00h dip de experimentele productie aanzienlijk verlaagd. Naast de maag, waarlangs des mans affectie altijd gewonnen wordt, wil ik ook de 'conversaties' niet vergeten waarbij, in bescheiden volume, de hele afdeling wel eens onderwerp geweest is. In dit kader moet ik uiteraard Erica aanhalen, die ook altijd bereid was om, zei het in minder bescheiden volume, haar weinig genuanceerde mening te ventileren. Daar ik er ook niet wars van ben te zeggen wat ik denk, een eigenschap die in de rol van co niet altijd gewaardeerd wordt, zal ik in de komende periode waarschijnlijk nog herhaaldelijk even stoom komen afblazen op het lab.

Bij die mensen die de olie hebben gevormd om mijn wetenschappelijke motor draaiende te houden wil ik ook ome kees niet vergeten. Kees, je weet inmiddels dat het geen kabouters zijn die in het weekend de Leffe uit de koude kamer bietsen, maar het muizen spook van kamer 1208. Zonder de Leffe-blond in het weekend waren de experimenten zeker niet zo succesvol verlopen, bedankt.

Mandy, bedankt voor de coupes, de muizen en de tails. Het was helemaal kansloos geweest als ik dat zelf had moeten doen. Ik heb twee van de drie taken op enig moment zelf nog geprobeerd te volbrengen maar van zowel de coupes als de muizen boekhouding bleek uiteindelijk weinig te kloppen.

Hans, bedankt voor de constructie van bijna alles waar ik mee gewerkt heb. Gelukkig bekijk je 'moeder natuur' met dezelfde ogen als ik, zodat er altijd genoeg interessante onderwerpen voor discussie zijn geweest. Ik begrijp overigens best dat aan jouw muur slechts foto's mogen hangen van vriendelijke jonge dames en oudere heren die hun sporen in het leven verdient hebben. Ik berust er daarom maar in dat het nog wel even zal duren voordat ik plaats mag nemen in die eregalerij.

Loes, bedankt voor het regelen van de standaardbrieven en het verzamelen van de handtekeningen.

Maarten, bedankt voor de hulp bij mijn onderzoek maar vooral ook voor de enige zinnige AIO cursus die ik in deze 5 jaar heb gedaan.

Niels, bedankt voor de uitleg dat oligo's heel erg tof zijn. Overigens ook bedankt voor die Zeer Fijne Populatie muizen waarmee het meten van oogbewegingen in deze soort begonnen is.

Luo, bedankt voor je chirurgische kwaliteiten. Het feit dat jij een deel van de coils kon implanteren heeft het mij een stuk makkelijker gemaakt. Succes met het voortzetten van de recordings.

Bakker, ik wens je succes met de neural recordings. Ik weet zeker dat John je wel even bijbrengt wat echt hard werken is. Je bent voor zover ik weet nog steeds de enige in de wereld die de activiteit van Purkinje cellen meet in de muizen flocculus, dus laat die papers maar komen.

Mochten er in mijn lijstje nog mensen ontbreken dan komt dat omdat het inmiddels wat laat geworden is. Voor hen, die niet met name genoemd zijn maar mij wel geholpen hebben de afgelopen 5 jaar, geldt alsnog een iets minder persoonlijk maar evenzogoed gemeend: "bedankt."

Ten slotte is Lieke er voor mij geweest. Zonder haar onvoorwaardelijk steun, interesse en motivering was ik nu waarschijnlijk nog steeds bezig geweest met het meten van muizensinussen. Gelukkig gaat zij nu geld verdienen en kan ik, als arme student, eens in haar buidel tasten.

Arjan van Alphen

P.S. Voor die leden van de Tang Soo Do die gedurende het afgelopen half jaar tijdens het sparring misschien ietwat te direct geconfronteerd zijn met de fysieke ontlading van mijn beroepsmatige frustraties: 'kahn sa ham ni da.'